Diploma Thesis

Biomechanical Analysis of Gait of transfemoral Amputees while using novel Prosthetic Technologies and Control Methods

submitted in satisfaction of the requirements for the degree of

Diplom-Ingenieur

of the TU Wien, Faculty of Mechanical and Industrial Engineering

---

Diplomarbeit

Biomechanische Analyse von Gangdaten oberschenkelamputierter Personen unter Nutzung neuartiger Prothesentechnologien und Steuerungsmethoden

ausgeführt zum Zwecke der Erlangung des akademischen Grades eines

Diplom-Ingenieurs

eingereicht an der Technischen Universität Wien, Fakultät für Maschinenwesen und Betriebswissenschaften

von

Rene Christoph Haslhofer, BSc

Matr.Nr.: 01326703

unter der Anleitung von

Ao. Univ.Prof. Dipl.-Ing. Dr.techn. **Heinz-Bodo Schmiedmayer**

Dipl.-Ing. Dr.-Ing. **Roland Pawlik**

Dipl.-Ing. **Dirk Seifert**

Institut für Mechanik und Mechatronik
Technische Universität Wien
Getreidemarkt 9, 1060 Wien, Österreich

Wien, im April 2022

Kurzfassung

Mit dieser Arbeit wurden zwei Ziele verfolgt: Erstens einen Algorithmus zu implementieren, der Referenz-Schritte aus mehreren aufgezeichneten Schritten automatisch erkennt und zweitens anhand einer dreidimensionalen Ganganalyse aus dem Ganglabor Veränderungen im Gangbild unter Verwendung eines aktiven Knieprothesen Prototyps im Vergleich zur Alltagsversorgung zu erkennen und statistisch auszuwerten.

Für die Erkennung eines Referenzschrittes aus einem Anwendertest wurden die internen Sensordaten des Prothesenkniegelenks herangezogen. Nachdem mehrere Algorithmen zur Erkennung eines Referenzschrittes implementiert wurden, konnte in einem Black-Box-Test für die verschiedenen Ergebnisse abgestimmt werden. Hierbei wurde Dynamic Time Warping in Kombination mit dem Median aus den aufgezeichneten Schritten als geeignetstes Verfahren ausgewählt. Implementiert wurden alle Verfahren in Python. Die Referenzkurven wurden anschließend mit Metadaten in eine Datenbank transferiert, um so bei der Weiter- und Neuentwicklung von Knieprothesen das Entwicklerteam unterstützen zu können.

Der zweite Teil beschäftigt sich mit der Ganganalyse von transfemoral amputierten Personen. Für zwei Anwender wurden Daten sowohl mit deren Standard als auch mit einer neuartigen aktiven Knieprothese für Gehen in der Ebene aufgezeichnet. Danach wurden mehrere Parameter hinsichtlich Symmetrie und Extremwerte analysiert. Bei der Auswahl der Parameter flossen unter anderem die Eigenschaften des Prototyps sowie Feedback der Anwender während der Aufzeichnung ein. Für die statistische Analyse wurde die Python Distribution von statistical parametric mapping (spm1d) verwendet, welche es erlaubt kontinuierliche Signale statistisch auszuwerten. Der Prototyp zeichnet sich durch einen aktiv unterstützenden Antrieb aus, welcher in der Lage ist Flexion und Extension des Knies aktiv zu unterstützen.

Abstract

Two main objectives were set in this thesis: Firstly, the implementation of an algorithm to detect a reference step out of multiple steps automatically and secondly, to detect changes in gait of trans-femoral amputees when using a novel active knee prosthesis prototype compared to their everyday prosthesis.

To detect the users reference step, internal sensor data of the prosthesis was used. After implementing multiple algorithms and evaluating the results in a black-box test it could be shown that a combination of dynamic time warping and the median of the steps produced the best results. All algorithms have been implemented with Python. After finding a reference step the data along with metadata was saved in a database in order to assist new and further development of knee prostheses.

The second part focusses on the gait analysis of trans-femoral amputees. Data for level ground walking was recorded for two subjects, each using the prototype and the everyday prosthesis. Subsequently multiple parameters were investigated based on symmetry or peak values. The choice of parameters that should be included in the analysis was mainly influenced by the characteristics of the prosthesis as well as the feedback of the subjects during the recording of the gait data. Statistical analysis was done with the python implementation of statistical parametric mapping (spm1d), which allows continuous signals to be evaluated statistically. The prototype features a motor that allows to assist knee flexion and extension.

Contents

1 Aim of Work **11**

2 Introduction **13**

3 Theoretical Background **14**
3.1 Human Gait . . . 14
3.1.1 Stance Phase . . . 15
3.1.2 Swing Phase . . . 17
3.1.3 Differences and Difficulties in Prosthetic Gait . . . 17
3.2 Gait Analysis and Gait Assessment . . . 19
3.2.1 Visual gait analysis and assessment . . . 20
3.2.2 Direct measurement gait analysis . . . 20
3.2.3 Motion Capture Systems . . . 23
3.3 Knee Prostheses . . . 23
3.3.1 Socket . . . 24
3.3.2 Knee Prosthesis . . . 25
3.3.3 Prosthetic Foot . . . 27

4 Reference Curves **29**
4.1 Implemented and tested Methods . . . 30
4.1.1 Median . . . 31
4.1.2 Median with Time Normalisation . . . 31
4.1.3 Percentile . . . 31
4.1.4 Percentile with Time Normalisation . . . 32
4.1.5 Dynamic Time Warping . . . 32
4.1.6 Dynamic Time Warping with Median . . . 33
4.1.7 Longest Common Subsequence . . . 33
4.2 Implemented Process . . . 34

5 Gait Analysis **37**
5.1 Method . . . 37
5.1.1 Investigated Prostheses . . . 37
5.1.2 Equipment . . . 38
5.1.3 Subjects . . . 39
5.1.4 Analysis . . . 41
5.1.5 Statistical Parametric Mapping (SPM) . . . 44
5.2 Results . . . 46
5.2.1 Walking Speed . . . 46
5.2.2 Stance Phase Duration . . . 47
5.2.3 Foot Clearance . . . 48
5.2.4 Ankle Angles . . . 50
5.2.5 Knee Angles . . . 58
5.2.6 Hip Angles . . . 64

5.2.7 SACR lateral movement . . . 68
5.2.8 SACR cranial movement . . . 74
5.2.9 SACR velocity anterior . . . 78
5.2.10 Hip Moment sagittal . . . 83
5.2.11 Hip Moment frontal . . . 89
5.2.12 Hip Power . . . 93
5.2.13 Hip Work . . . 98
5.3 Discussion . . . 103
5.3.1 Stance Phase more symmetrical . . . 103
5.3.2 Symmetry and Control of the Foot Clearance improves . . . 103
5.3.3 Symmetry in Hip, Knee and Ankle Angles improves . . . 104
5.3.4 Trunk can be held more upright / Smoother Gait . . . 107
5.3.5 Symmetry of Hip Joint Moments increases / Magnitude decreases . . . 107
5.3.6 Symmetry of Hip Power increases / Magnitude decreases . . . 108
5.3.7 Work done in the hip joint gets more symmetrical . . . 110
5.3.8 Limitations . . . 111

6 Conclusion **112**

7 Appendix **114**

Abbreviations

BW Body Weight

DTW Dynamic Time Warping

EMG Electromygraphy

GLM General Linear Model

GRF Ground Reaction Force

IMU Inertial Measurement Unit

LCSS Longest Common Subsequence

RFT Random Field Theory

RMS Root Mean Square

ROM Range of Motion

SPM Statistical Parametric Mapping

TFA Transfemoral Amputees

Chapter 1

Aim of Work

Transfemoral Amputeess (TFAs) suffer greatly from their loss of one limb. It is not only an irreversible surgery but also incorporates the loss of mobility. Walking is the most basic form of getting from A to B and can usually only be recovered partially by using walking aids such as crutches, wheelchairs or prostheses. While crutches and wheelchairs feature major disadvantages like increased energy expenditure and the dependency on elevators, respectively, prostheses allow greater freedom of movement. However, prostheses are still mostly passive devices which means that the hip of the affected leg has to compensate for lost limb functions, which is not ideal. To address this problem and associated problems like gait asymmetry, secondary physical conditions, back pain etc. so called active prostheses are being developed that allow a net positive power output to assist the subject with compensating the lost functionality.
Otto Bock HealthCare GmbH (Duderstadt, Germany) is one of the leading companies regarding prostheses for upper and lower limbs. Their most sophisticated knee prosthesis, the Genium X3®, allows a variety of activities like going backwards or ascending or descending stairs amongst scenarios featuring water, sand, dust or dirt that were not possible with its predecessor, the C-Leg®. The C-Leg and the Genium being passive microprocessor-controlled prostheses are not contributing to several gait scenarios by a positive power output. Their novel active prosthesis prototype is fitted with an electrical motor that can provide up to 60 newton meters of torque to the knee axis. It allows control of the stance flexion and of the swing phase by driving the knee directly. This prototype was tested in a gait laboratory by using a Vicon® motion capture system and the results where compared with the users everyday prosthesis. The following hypotheses were developed and are discussed in section 5.3:

1. stance phase duration more symmetrical;
2. better foot clearance due to active control of the swing phase;
3. more symmetrical in hip, knee and ankle-angles compared to a passive prosthesis;
4. smoother gait due to stance phase flexion;
5. hip joint moments more symmetrical;
6. hip power more symmetrical;
7. hip work divided into positive and negative work more symmetrical.

In the first part of the thesis gait data recorded by the sensors of the prostheses is analysed in order to find one step that is representative of that recording. In order to choose a reference step based on internal sensor data of a gait trail an algorithm had to be found that is able to identify curves that are alike consistently. Because taking the average does come with some drawbacks like the blurring of sharp edges, new approaches and methods have been tested to analyse the recordings. After successful identification of a reference step the data, along with

additional information about the test, can then be stored in a database, where it can be used for the development of new prototypes or further improvement of already existing prostheses. In the second part of this thesis the chosen algorithm is used to filter curves that are misaligned and therefore excluded from the hypothesis testing.

Chapter 2

Introduction

Human gait is the simplest method of getting from A to B. Although it requires some initial training, once mastered, humans can perform the rather difficult task of walking upright without having to concentrate on it. Walking requires no additional tools or aids in healthy humans, which makes it obvious why walking is the most frequently used means of transport in Austria. More than 70 percent of Austrians choose to walk at least once a day for distances over 250 meters [69]. Even more significant, 92 percent occasionally use walking as a type of transportation [70]. Therefore, it seems consistent, that patients that are unable to walk (or handicapped) want to be able to walk again as quickly as possible and that compensatory reactions are accepted in achieving that goal [75].

The reasons for not being able to walk properly can be found in multiple diseases like stroke, spinal cord injury, brain trauma, mixed trauma etc [75]. While all these medical conditions can have impacts of different magnitude on the way patients walk, the effect of amputation is huge. The reasons for the need of amputation can be similarly diverse. The most important ones being vascular diseases, traumas, infections or tumours [35]. However, the main cause for amputation, at least in European countries, is diabetes [7]. In Germany 67 percent of all patients in need of an amputation are simultaneously treated for diabetes. In the United Kingdom this this number is smaller, although still at an remarkable 54 percent [7]. Despite the fact that the number of major amputations has decreased slightly from 24 per 100.000 in 2010 to 21 per 100.000 in 2014 in Austria there are still a lot of people in need of aids after the loss of one or more body parts [7].

Even tough modern prosthesis are much more sophisticated than they were just years ago, prosthetic gait is still very different from normal gait and comes with lots of associated secondary physical conditions [4]. The metabolic consumption during gait increases [27] although walking speed decreases largely [42]. Another associated issue is lower back pain caused by hip hiking which is often used to advance the prosthetic limb forward [27]. Furthermore, asymmetric gait patterns like longer double stance periods, larger stride widths or decreased swing/stance ratios can be found in multiple studies [16, 42, 65, 99]. Naturally the goal for newly developed prosthesis has to be to reduce these side effects as much as possible. Not only to make walking easier by reducing metabolic consumption through new prosthetic mechanisms but also to reduce asymmetry to subsequently decrease secondary physical conditions.

This thesis focuses mainly on possible improvements in amputees gait with an active knee prosthesis prototype. This prototype should allow an increased gait symmetry in spatio-temporal, kinetic and kinematic variables as well as allow smoother gait patterns. The first part describes mechanisms to find a reference curve out of a range of gait samples based on multiple sensor data criteria while in the second part possible improvements in level walking while using an active prosthesis are compared to the subjects everyday prosthesis.

Chapter 3

Theoretical Background

3.1 Human Gait

The word gait

> describes the manner or style of walking [94, p.48]

not the act of walking itself. Therefore, the word gait is used when talking about differences between patients rather than differences in walking. Walking on the other hand is defined as an action to

> move the body forward while maintaining stance stability.[75, S. 3–4]

To maintain stability one limb acts as support for the whole body weight, while the other limb (currently in swing phase and in preparation of loading response afterwards) advances itself forward, where the roles of the limbs are reversed. This means that at least one leg is always in touch with the ground and when the weight is shifted from one leg to the other, both legs are on the ground simultaneously. This periods of double support last about ten percent of a gait cycle in normal gait, but they vary with different speeds. The higher the walking speed, the shorter these phases get until they disappear completely when humans are running [75, 94].
Human gait is a circular movement consisting of the periods called stance and swing phase which last about 60 and 40 percent of the gait cycle (see fig.3.1a). During stance phase one foot is touching the ground while during swing phase the foot is in the air. Within these phases there are times of double support, where both feet are touching the ground and periods of single support, where one foot is touching the ground (see fig.3.1a) [75, 94]. These periods can further be divided in seven phases with each phase having a distinct start and end event (see fig.3.1b). These events are initial contact, opposite toe off, heel rise, opposite initial contact, toe off, feet adjacent and tibia vertical [94]. Because the movement follows a reoccurring pattern, any of the events could be chosen as the start event for a gait cycle. However, in most cases initial contact is chosen as the beginning of the gait cycle. The seven events split the gait into seven phases, four of which happen in the stance phase and are called [54, 75, 94]:

1. Loading response
2. Mid-stance
3. Terminal stance
4. Pre-swing

Therefore the other three phases are in the swing period and are called [54, 75, 94]:

1. Initial swing
2. Mid-swing
3. Terminal swing

These gait phases can be grouped according to different tasks which have to be performed in order to move and support the body at the same time: weight acceptance, single limb support and limb advancement [75].

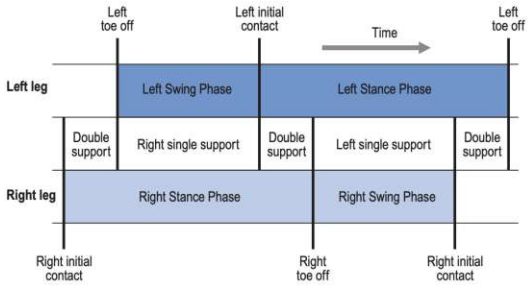

(a) Single/double support times and swing and stance phases for left and right leg in a little more than one gait cycle beginning with initial contact (Source: [94, p. 54])

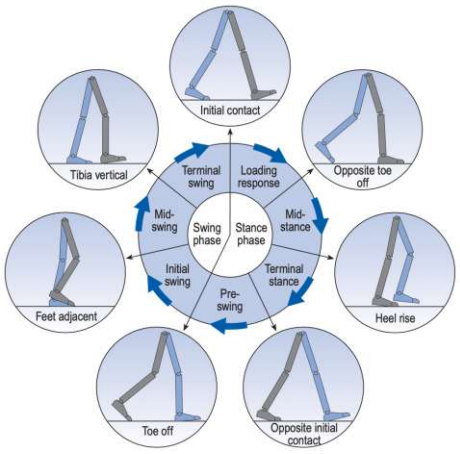

(b) Overview of the GC with events and phases (Source: [94, p. 52])

Fig. 3.1: Gait phases and events with times for single and double support

3.1.1 Stance Phase

The main characteristic in the stance phase is the fact that one foot is always touching the ground. It lasts about 60 percent of the whole GC and begins with initial contact. During stance phase weight acceptance and single limb support are the two main tasks that need to be accomplished [75].

3.1.1.1 Initial Contact

Initial contact marks the first phase in the first double support period and lasts from zero to two percent of the GC. It can be recognised by the foot establishing first contact with the ground. Together with the position of the ankle close to neutral in dorsi-/plantarflexion. This results in the heel touching the ground first. This creates an abrupt rise in magnitude of the Ground Reaction Force (GRF) vector. Despite the fact that both feet are touching the ground simultaneously, the body is falling onto the new supporting leg. The GRF is generally upwards which positions it posterior to the ankle resulting in a plantarflexion moment. The knee is in a slightly flexed position (about five degrees) which presents a stable state due to the anterior alignment of the GRF and effect of a extensor moment. The hip is in 30 degree flexion which constitutes a compromise between the danger of a foot sliding forward which would cause instability and

stabilizing the hip due to the loading of the leading limb. The trunk is positioned behind the foot which contacts the ground and is leaning towards this side as well. [75, 94]

3.1.1.2 Loading Response

In loading response the GRF vector changed its position from pointing almost vertical to upwards and backwards and its magnitude is increasing rapidly because the opposite limb is unloaded but still in contact with the ground. This means that both feet are on the ground and therefore this is the second phase of the first double support period. The GRF is positioned posterior to the ankle which creates a plantarflexion moment that lowers the foot to the ground. If this is not slowed down by the use of muscle force it results in a foot slap on the floor. The knee begins to flex to about 18 degrees to provide shock absorption because of the rapidly increasing GRF vector which peaks at around 120 percent of Body Weight (BW). The hip is in a 30 degree flexed position as it was earlier in the initial contact phase. The trunk is at its lowest vertical position. [75, 94]

3.1.1.3 Mid Stance

The opposite foot leaving the ground marks the transition from loading response to mid stance. It lasts to about 30 percent of the GC and marks the first single support period. The GRF vector moves forward across the foot reaching the knee axis at about 22 percent of the GC and continuing to move forward until the line of action of the vector is located anterior to the knee resulting in an extensor moment. A combination of the knee extending and the hip also changing from flexion to extension means that the trunk is lifted upwards in vertical direction. This can be seen as an energy conversion, because the trunk is slowing down simultaneously. That translates into a transformation of kinematic to potential energy. [75, 94]

3.1.1.4 Terminal Stance

The heel lifting of the ground is the event which starts the terminal stance phase. It lasts to 50 percent of GC and marks the beginning of the second double support period of the GC. Plantar flexion of the ankle joint shifts the GRF even more forwards which stabilizes the knee. The trunk is at its highest position due to the lift of the heel from the ground. Because of this lift there are large forces needed in the ankle and the GRF is again (like in Loading Response) larger than BW. The body's centre of gravity is now in front of the foot which increases dorsiflexion at the ankle and results in a fall forward which is the main progression force that is used in walking. [75, 94]

3.1.1.5 Pre Swing

Pre swing is the second phase in the second double support period and lasts to about 60 percent of the GC. It marks the last phase in the stance period preparing for toe off (see fig.3.1b) and the beginning of swing phase. The trunk is decreasing to its lowest position throughout the GC and as the limb is unloaded the pelvis drops creating a tilt. By the end of this phase flexion of the knee is important because it helps in providing vital ground clearance in the oncoming swing phase. This flexion is largely passive in the unloaded limb with muscle force only preventing excessive knee flexion. The ankle is in plantar flexion of approximately 20 degrees and balances the body until toe off. After that, muscle force decreases rapidly because of the absent need for stabilization. [75, 94]

3.1.2 Swing Phase

The swing phase lasts about 40 percent of the GC and is initiated by the toes leaving the ground (also called Toe off see fig.3.1b). The main task is to establish enough ground clearance to allow limb advancement while preventing it from touching the ground and preparing the limb for the next stance phase. [75]

3.1.2.1 Initial Swing

Initial swing is the first phase in the Swing phase and lasts to about 73 percent of the GC. This means that it starts with toe off and the limb being totally unloaded and stops when the feet are adjacent. The advancement of the limb is a largely passive action and results from mechanisms initiated in pre swing. Knee flexion has to increase even further up to about 60 degrees to lift the foot of the floor an provide enough ground clearance. As only the toes are touching the ground in Pre Swing and the ankle therefore being plantar flexed the ankle has to go into dorsiflexion again by mid swing which is achieved with active muscle force in the ankle. The trunk is now rising again because the weight is now supported by the stance leg. [75, 94]

3.1.2.2 Mid Swing

Mid swing is initiated when both limbs are adjacent and lasts until the tibia of the swing leg is vertical, which is at about 85 percent of the GC. This means that the foot is now clear, which reduces the need for further knee flexion resulting in passive knee extension caused by angular momentum generated at the hip and gravity. At the ankle muscle force is needed to hold the foot in a neutral position against gravity while the hip is continuing its flexion largely passively again due to momentum preservation. The trunk is losing vertical height again and the lateral displacement of the trunk onto the stance leg side is diminishing. [75, 94]

3.1.2.3 Terminal Swing

Terminal Swing is the last period in the swing phase and its main task is to prepare the previously advanced limb for the next initial contact. Therefore, the knee has to be further extended which is not longer achieved passively but requires active muscle force to lift the tibia up against gravity. Flexion of the hip ends at about 30 degrees and muscle force at the ankle ensures that the foot is in an optimal position for heel strike. Furthermore, increased muscular activity in the ankle can be seen as the foot is preparing for the high demand of weight loading. [75, 94]

3.1.3 Differences and Difficulties in Prosthetic Gait

After an amputation of the lower limb a walking aid is usually needed to ensure that the amputee will be able to walk again. These aids can be a wheelchair, crutches or a prosthesis. Using wheelchair might be a very economic way of movement, but it can be associated with problems, like not being able to climb stairs. Crutches on the other hand are not economical when used as the only walking aid after amputation. In theory prostheses allow the patient to walk again, irrespective of time, terrain, weather or speed [6]. Although modern prostheses are very good in restoring a healthy gait, there are differences to normal gait that need to be considered when evaluating prosthetic gait.

Energy consumption First of all energy consumption (see fig.3.2a) can be higher, especially when the prosthesis was not fitted properly. The higher demand of energy can be a direct

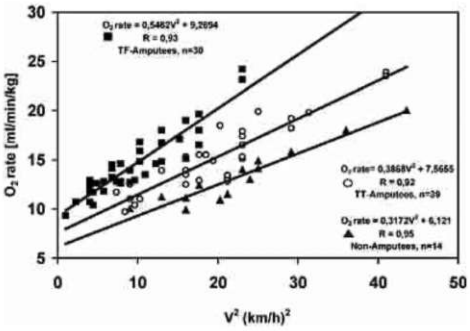

(a) Rate of oxygen consumption for transfemoral (squares), transtibial amputees (circles) and healthy subjects (triangles) with increased walking speed (Source: [86, p. 261])

	Distribution (%)
Pain frequency past 4 weeks	
Back pain present but during the past 4 weeks	2
Intermittent back pain	72
Constant back pain with variations in intensity	22
Constant back pain with little variation in intensity	4
Back pain episodes in past 4 weeks if pain was not constant	
Once a week or less	47
2–3 times/wk	28
4–6 times/wk or more	25
Duration of back pain episodes	
A few minutes	12
Several minutes to 1 hour	30
Several hours	30
One day or longer	28

(b) Secondary physical conditions in above knee amputees (n=132) (Source: [23, p. 733])

Fig. 3.2: Secondary physical conditions and increased oxygen consumption for lower limb amputees

result of compensatory movements that try to balance the body while walking [6]. But even if the prosthesis fits properly, the energy cost per meter (often measured by oxygen consumption per meter of walking) is higher in amputees. This can be explained by a general decrease in walking speed when compared to healthy subjects [92]. As the development of prostheses is improving steadily, the severity of this issue is declining, which can be seen in an decrease of oxygen consumption when wearing a state of the art prosthesis compared to a conventional one [86].

Spatiotemporal differences However, concerning spatiotemporal variables differences can be seen more clearly. As already mentioned walking speed decreases in amputees using prostheses compared to healthy individuals. Moreover, walking speed is also dependent on the height of the amputation [4, 88, 92]. Compared to healthy subjects the decrease in walking speed can be as high as 30 percent [42]. For stance and swing phase, differences in duration can be seen as well. Prosthetic gait indicates longer stance time and longer double support times which inevitable leads to more asymmetric gait [39, 42, 68]. Furthermore, a broader stride width and decreased cadence can also be found when evaluating gait [42, 77].

Biomechanical differences Because there are variances in spatiotemporal variables indicating differences compared to healthy gait, it is necessary to analyse gait from a biomechanical standpoint as well. Some of these differences are related to prosthetic boundaries. For TFA the knee joint is typically replaced with an active prosthesis, while the foot and ankle is often just a passive carbon spring. Therefore, the plantarflexion of the ankle in terminal stance (see 3.1.1.4) and pre swing (see 3.1.1.5) is not as large as in able-bodied gait [88]. Because the prosthetic knee joint is not as powerful compared to an intact leg, knee flexion in early stance (see 3.1.1.2) can not be as large as in able-bodied gait [88]. These boundaries lead to the need for compensating strategies which often lead to higher loading of the intact limb. This results in bigger hip, knee and ankle moments of the healthy leg [67, 88], but also in bigger hip flexor moments at late stance (see 3.1.1.4) in the amputated limb [88]. Other compensation strategies include a pelvic tilt on the prosthetic side [4, 77] and lateral bending of the trunk [42]. These compensating

strategies not only make it more difficult to detect improvements in gait but can also lead to secondary physical conditions [82].

Secondary physical conditions Prosthetic gait sometimes results in an increased loading of the intact limb which can lead to cartilage damage [82], joint pain or degeneration [67]. Lower back pain (see fig.3.2b) is also frequently reported, often caused by poor socket fit and poor alignment [27, 32, 83], however, also postural changes and general de-conditioning are seen regularly [32]. Significant differences for the back extensor muscles in both strength and endurance are also factors that need to be considered [27].

3.2 Gait Analysis and Gait Assessment

Evaluating gait has always been of great interest for scientists. The first known work about gait was dated 4000 years back [75] and the first known scientist to contribute to that topic was Aristotle who lived from 384-322 BC [5, 75]. After that it took until the 19th century until gait analysis became a popular research topic again and with the development of the force plate new results and a deeper understanding of gait was now possible [5]. With the development of computers gait analysis became available widely for clinical and scientific research [5].

In order to be able to assess a subjects gait, data has to be acquired and interpreted. The acquisition of this data is called gait analysis [75, 94]. It can be easily done using a trained eye, however, without knowing clinical details and the subjects history an objective evaluation is not possible [75]. Furthermore, it has to be kept in mind that gait analysis observes effects and compensation mechanisms but not causes [94]. A broader picture can only be made with gait assessment which is the combination of gait analysis data and information available from patients history and examination [81]. Walking speed is influencing gait analysis majorly, which is the reason why it would be best to limit speed by using e.g. a metronome. However, it can be shown that walking changes drastically when boundaries like speed limitations are used. The relation between step frequency and step length is lost and therefore effects duration of swing, stance and double stance phases as well [98].

The reasons to assess gait can be diverse. Athletes are typically looking for minor improvements to achieve better performance. On the contrary, amputees are mainly searching for major differences to reduce the risk of secondary physical conditions and the risk of falling. Another reason can be to regain safety in walking after an accident or illness [95]. But it is not only important to people who want to improve gait but can also be used to determine early stages of diseases like MS or Parkinson [64]. Because human gait involves complex mechanisms in limbs and arms there are lots of variables that can be recorded. The complete analysis of one body segments requires about 15 variables which includes position, linear and angular velocities and linear and angular accelerations [95]. Combined with 12 body segments (feet, legs, thighs, trunk, head, upper arms, forearms and hands) this leads to 180 variables that can be obtained if the whole body is described during gait [95]. Not all of the variables are of interest all the time, which is why it requires detailed planning of the gait analysis in order to include only as much data as necessary. There are lots of different methods available for data acquisition, which can be separated into visual, direct and motion capture systems.

3.2.1 Visual gait analysis and assessment

Visual gait analysis is the easiest way to evaluate gait. Nothing more is needed than a trained eye and the subject itself. It requires several walks up and down a walkway and an observation from both sides, from the front and the back [94]. To make evaluation even easier several questionnaires like the Wisconsin gait scale for hemiplegic gait analysis [79] or the Rancho system [75] have been developed. However, it is very hard to combine the different views of the walking trails to a big picture without having records available. If for example the leg is rotated inwards, reduced knee angle can be seen when evaluated from the sagittal plane [75]. Therefore, the use of video is recommended when visual gait analysis is performed. It not only reduces the need for multiple walks, because all planes can be recorded simultaneously, but provides also records of progress a patient made over time [94]. For recording gait, a laboratory with a minimum of 10 meters length and 4 meters width (see fig.3.3a) is recommended [94]. This should allow patients to get into their stride and therefore minimize possible variances in speed [94]. Nevertheless, even with video recordings it can be difficult to analyse gait correctly as one study showed that visual observation noticed 3.4 times less gait deviations than advanced computer aided methods [85]. For the sake of completeness, it should be mentioned that there are further aids to evaluate gait visually, like walking on glass to evaluate pressure distribution [94], using cardboard models to understand walking mechanisms [75] or walking with chalk on the feet to measure step length [94]. But as gait analysis is mostly done with the help of computers, sensors and markers nowadays, these methods are not used very often any more.

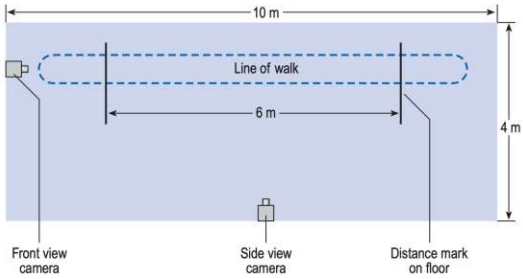

(a) Recommended layout for a small gait laboratory for visual gait analysis (Source: [94, p. 139])

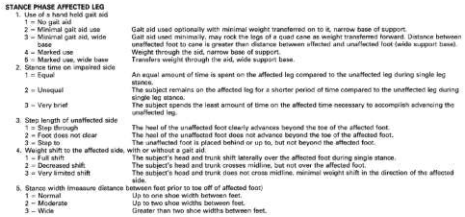

(b) Excerpt of the Wisconsin gait scale to evaluate hemiplegic gait visually (Source: [79, p. 803])

Fig. 3.3: Small Gait laboratory as proposed by [94] and and excerpt of the Wisconsin gait scale [79] to evaluate hemiplegic gait.

3.2.2 Direct measurement gait analysis

Direct measurement devices can be used to measure acceleration, pressure or muscle activation directly for a segment by attaching sensors to it. These sensors can be gyroscopes, electrogoniometers, accelerometers, electromyographic sensors and pressure sensors. Sometimes magnetometers are used to measure the magnetic field which, in combination with a gyroscope and accelerometers, allows to define a global reference systems [84].

Electrogoniometers Electrogoniometers (see fig.3.4a and 3.4b) are devices to measure angles between segments directly. It is attached to the limb segment and aligned with the joint axis [95]. However, it was not until the development of parallelogram electrogoniometers that these angles could be measured correctly in joints that are not hinge joints. The knee has a floating

instantaneous rotational centre that follows a curved path which makes it impossible to measure with normal goniometers that measure the angles on a fixed axis [26, 75]. Nevertheless, this type of sensor is a very cheap way of measuring angles and the output signal is immediately available, which is why it is often used in a clinical setting [94, 95]. However, the accuracy is not very precise which means it should be applied in tests where great precision is not of greatest interest, e.g. for analysis of Range of Motion (ROM) [43]. Other disadvantages are that instead of absolute angles, only relative angles are measured and that alignment can be difficult [95].

Accelerometers Accelerometers are used to measure acceleration by using one or multiple transducers. The acceleration vector can be split into a component normal and a component tangential to the transducer if it is not at a right angle. However, it is only possible for a transducer to record the normal, not the tangential component to it which is why triaxial accelerometers with three transducers mounted at right angles to each other, are mostly used [94, 95]. These sensors use Newtons second law to determine acceleration. With Force equals mass times acceleration $\vec{F} = m \cdot \vec{a}$ it is only necessary to measure the force exerted on a known mass to receive the acceleration [84, 95]. These sensors provide a cheap way to analyse gait, however, it has to be noted that they are sensitive to temperature and mechanical wear [60]. Another disadvantage is, that although velocity could be easily computed by integrating the sensor output, this is often difficult as there is a drift and noise in the output signals [94]. That is also the reason why these sensors are mostly used for the detection of gait phases [60, 94]. The mounting on the body can also be a possible difficulty and when large amounts of these devices are fitted lots of cable can influence the way a subject walks [60, 95]. Advantages are that the sensor is relatively cheap and a non-invasive method to measure gait [43].

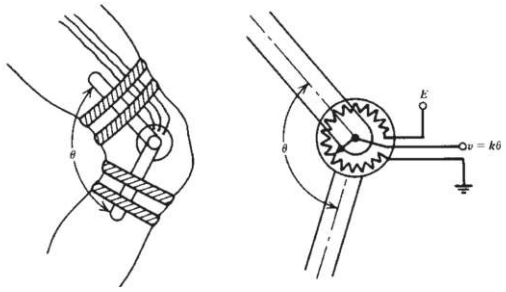

(a) Mechanical and electrical layout of a goniometer measuring relative knee angles (Source: [95, p. 49])

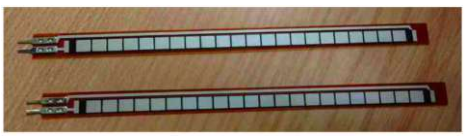

(b) Strain gauge goniometer. When bent the current has to travel a longer way through the sensor and thus the resistance increases with the angle. (Source: [64, p. 3375])

Fig. 3.4: Electrogoniometer and accelerometer used in gait analysis

Gyroscope Accelerometers measure linear and gyroscopes measure angular acceleration. Together they are often found in an Inertial Measurement Unit (IMU) [43]. Gyroscopes can also be used to measure angular velocity without the effect of gravity however, these sensors can be affected by drifts and offsets so integration has to be handled with care [84]. As for accelerometers these sensors provide a cheap way to detect gait phases when fitted to shanks thigh and foot [60].

Electromyography Electromygraphy (EMG) allows to measure muscular activity [43]. This is done with either surface (see fig.3.5a), needle or wire electrodes that measure the potential difference between each other and therefore allow prediction of muscle activation [75, 94, 95].

Surface electrodes measure signals from the muscles underneath, however, it is not possible to measure activity from muscles that lie underneath other muscles [94]. Because surface electrodes pick up signals from a wide range of sources it is best to not use them to record action from one distinct muscle but rather to detect activation of a muscle group [94]. Another method uses needles or fine wire electrodes that are inserted directly into the muscle. Their range is much narrower and allows for a more focused recording of muscle activation [75, 94, 95]. But it has to be kept in mind, that the insertion into the muscle can be quite uncomfortable and painful for the subject and therefore may lead to abnormal gait [94]. Furthermore, it is not possible to distinguish between isometric, concentric and eccentric contraction [94]. Because the change in potential is very small, amplification is needed close to the electrodes [64]. This recording mechanism is utilized to get a picture of the patients timing of muscular activity during gait [75, 94, 95]. Another application is that EMG it is able to detect movements up to 138 milliseconds earlier, which can be useful in prosthetic gait [93].

(a) Surface electrodes for electromyography (Source: [64, p. 3376])

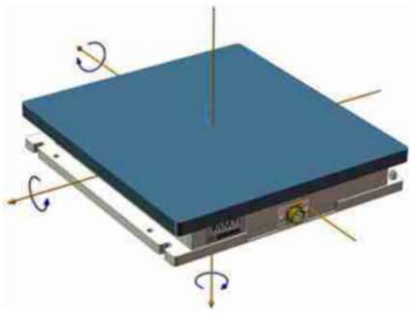

(b) Force plate illustration displaying three forces and three moments that are recorded (Source: [64, p. 3372])

Fig. 3.5: Electromyography surface electrodes and a force plate

Force Plates A force plate (see fig.3.5b) can be used to directly measure the GRF, since this force is exactly the opposite of the force exerted onto the plate (newtons third law action-reaction) [75, 94, 95]. There are basically two designs of force plates: One is supported by trans axial transducers at every corner while the other is supported by a central pillar. Both types measure the moments and forces to calculate the position and magnitude of the force vector [95]. To get a clear signal it is advised to have the complete foot on the force plate and the other one clear of it. Therefore, two force plates or a double set of force plates have been used to give greater walking freedom for the subject. This is also important, because it is possible that the patient is aiming for the device, which is not wanted either. Consequently force plates should be mounted evenly with the floor and also camouflaged in a way that they cannot be seen directly [75]. Another possibility to measure GRF is with pressure soles inside the shoe. However, this is difficult because the space inside the shoe is limited and lots of cables are needed from inside the shoe to outside [94]. Nonetheless the advantage is that it allows to monitor multiple consecutive steps, which can speed up the process of gait analysis [68].

3.2.3 Motion Capture Systems

In order to analyse the kinematics of patients gait so called motion capture systems have been developed. It started with the subject wearing black clothing with reflective stripes along their longitudinal limb axis and multiple pictures were taken onto the same single film. When the picture was printed afterwards the angles could be measured by hand [75]. Nowadays this method has advanced into using multiple cameras, segment markers and cameras that have LEDs around them that emit a stroboscopic infrared illumination that is reflected by the markers [75, 84]. The frame rate from these systems is usually 50, 60 or 200 Hz and if a marker is visible for two cameras simultaneously its position in three-dimensional space can be calculated. If that is not the case the position is usually estimated using the old value and the next available value [94]. These markers can then be used to establish joint angles, velocities and accelerations. However, it has to be kept in mind that angles have to be differentiated in order to be able to analyse the movement, which magnifies the recording errors. Therefore, the data usually has to be low-pass filtered, which eliminates high accelerations like heel strike [94]. Possible errors can still occur in marker placement. The markers are usually placed on relevant bone landmarks that are found by palpation [84] and are attached onto the skin. As the bone movement is not the same as the movement of the tissue this can lead to errors that can be up to ten millimetres translational and eight degrees rotational depended, on the segment [40]. To get rid of that error it would be necessary to drill the markers into the bone, which is not very practical but has been done to estimate these errors [40]. There are several different protocols on where to position those markers and which markers are used. Generally, there are markers that are attached directly onto the skin (see fig.3.6b) and marker pods (see fig.3.6b) that consist of three markers and are placed at each limb segment [94]. When comparing results calculated with different marker sets it has to be kept in mind that these might not be comparable directly [95]. Nevertheless, in a study by Ferrari et al [25] which compared five different protocols (Newington, Plug-in Gait, Servizio di Analisi della Funzione Locomotoria, Calibration Anatomical System Technique and Laboratorio per l'Analisi del Movimento nel Bambino) it was found that the repeatability of the results was generally very good [25]. Furthermore, the precision of the cameras are dependent on the position of the subject in space and is only very accurate in the middle of the room, but this is also dependent on the amount of cameras used (see fig.3.6a). Motion Capture Systems can be seen as the industry standard when it comes to gait analysis and are largely used in combination with force plates which provide the kinetic data to the kinematic data that allows a full assessment [94]. This produces lots of different data on gait which means that only necessary and significant variables should be analysed [94].

3.3 Knee Prostheses

Prostheses enable a human to regain some functionality after losing one or more limbs. While there are prostheses for upper limbs, this thesis solely focuses on lower limb prostheses. The amputation level for lower limbs can be divided into (see fig. 3.7a) partial ankle disarticulation, foot -, below knee -, above knee amputation and hip disarticulation. If a knee prosthesis is needed the amputation level is going to be above knee or hip disarticulation [57]. Prosthetic devices have already been used more than 2000 years ago when they were made out of wood, copper or iron and attached with leather straps. Similarly to gait analysis it was not until the renaissance until new developments could be observed [57]. Today's prostheses consist of (see fig. 3.7b) a socket, knee joint, pylon and a foot [37, 57]. To achieve that, a prosthesis has to fulfil certain requirements, like support of the body weight during stance, prevent sudden knee joint

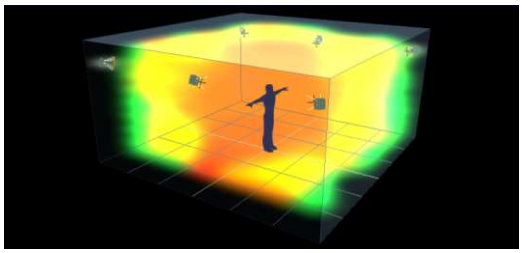

(a) Heat map of Vicon accuracy dependent on position in the room (red good accuracy, green less accurate) (Source: *https://www.vicon.com/visualization/*, accessed 06.12.2021)

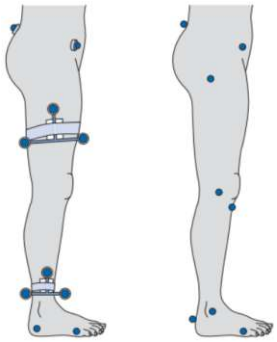

(b) Markers on pelvis and lower limb. On the left using arrays and skin mounted markers on the right. (Source: [94, p. 169])

Fig. 3.6: Heat map of a Vicon camera system and marker placement on the lower limb

flexion, duplicate normal gait as much as possible and limit undesirable pressure at the stump [49].

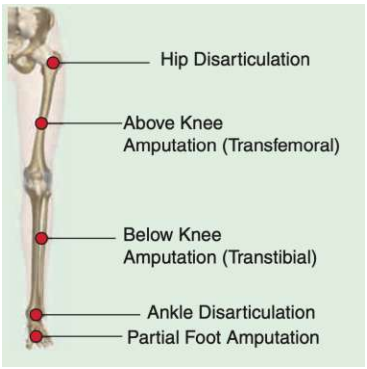

(a) Different levels of amputation for lower limb (Source: [57, p. 19])

(b) A prosthesis for TFA usually consists of socket, knee joint, pylon and a foot (Source: [57, p. 19])

Fig. 3.7: Amputation levels for lower limbs and parts of a knee prosthesis

3.3.1 Socket

After losing one limb the remaining part of the leg is called stump. The stump can be moved in a similar way like a normal leg which is necessary in order to manipulate an artificial leg. This allows for lost functionality to be regained by using a prosthesis [49]. The Socket is the direct link between the prosthesis and the user which incidentally means that it influences comfort and satisfaction substantially [57, 74]. Sockets often use lightweight materials like thermoplastics, acrylic or epoxy reinforced with fibreglass or kevlar for added strength. The fitting is usually done by a trained technician to ensure proper fit [57]. The connection between the stump and the

socket can be done with harnesses or by using a sub-atmospheric pressure system, where negative pressures within the socket creates a suction effect that holds the socket in place. However, this increases the risk of skin problems which is counteracted by the usage of liners, which is a protective cover made out of flexible cushioning materials [57, 74].

3.3.2 Knee Prosthesis

There are many different models of knee prostheses available today, which are chosen based on preconditions of the stump, safety requirements and on activity level of the patient [38]. While knee prostheses are chosen based on these parameters they can generally be classified by knee axis, securing stance or swing phase control mechanisms or active and passive devices [17].

3.3.2.1 Active and passive Prosthesis

Passive prosthesis (see fig. 3.9a - 3.9d) are devices that do not provide any net positive power output hence, can only store and release energy. These devices can be equipped with a microprocessor and several sensors like the C-Leg® or Genium® developed by Otto Bock or the RheoKnee® developed by Össur or have no electronics at all and rely on mechanics only. Passive knees are mostly lighter than their active counterparts due to the fact, that batteries are either smaller or missing totally and that there are no motors or gearboxes necessary [2].

Active prostheses (see fig. 3.9e) provide a net positive power output that is achieved by an electric motor added to the prosthesis. As a result these devices are usually heavier than their non-active counterparts. The power outputs ranges from less than 100 Watts up to 200 Watts with transmission designs ranging from directly driven to transmission gears or even belt drives [2]. Other designs couple an actively driven knee joint with an active ankle joint [58] or feature two drives in the knee joint to mimic agonist-antagonist action of the muscles in the shank [20, 62]. For drives DC, BLDC, linear step motors or pneumatic motors are the most commonly used designs [12, 14, 20, 33, 36, 58, 62]. Most designs feature a single axis knee joint, polycentric joints are seldom used [33]. However, the most difficult part of designing an active prosthesis is, that the motor has to firstly account for the weight addition caused by itself and the battery pack and secondly has to make sure that the batteries last long enough, hence the efficiency of the system has to be very good [2, 14]. Only one knee joint is available on the European market today, the Össur Power Knee®, which lasts up to seven hours with a full battery, which is less compared to its non-active counterparts that last up to 48 hours [36].

3.3.2.2 Knee Axis Configuration

The simplest design of an artificial knee joint is the hinge joint which has a single axis that allows flexion and extension of the knee. This design is very light and durable, however, without any additional stance or swing phase control it is rarely used, except when maintenance is an issue in some remote areas [17, 63]. When there is no additional break mechanism used (like a hydraulic cylinder, friction surfaces, friction clamps or differential handbrakes) the single axis knee joint is limited to the load passing in front of the knee axis and generating an extension moment that forces the knee to a fully extended position [78].

Polycentric knees (see fig. 3.9c) have floating instantaneous centres of rotation (see fig. 3.8b). These rotational centres change as the knee flexion angle changes. This is achieved by linking two or more bars (see fig. 3.8a) between the upper and the lower part of the knee [17, 78]. This allows improved stance phase stability but is less durable as a single axis knee joint [17]. Like in the single axis knee joint, the knee can only be stabilized without any additional break mechanism, if the ground reaction force passes anterior to the instantaneous centre of rotation.

The difference is, that the centre can be manipulated in a way that stance phase flexion of the knee is possible, which leads to a smoother forward progression of the body compared to a stiff knee. The 3R60® manufactured by Otto Bock allows up to 15 degrees of stance phase flexion with the rate of flexion being controlled by a spring. Another advantage of polycentric knees is that they offer increased toe clearance and controlled deceleration in swing phase [10].

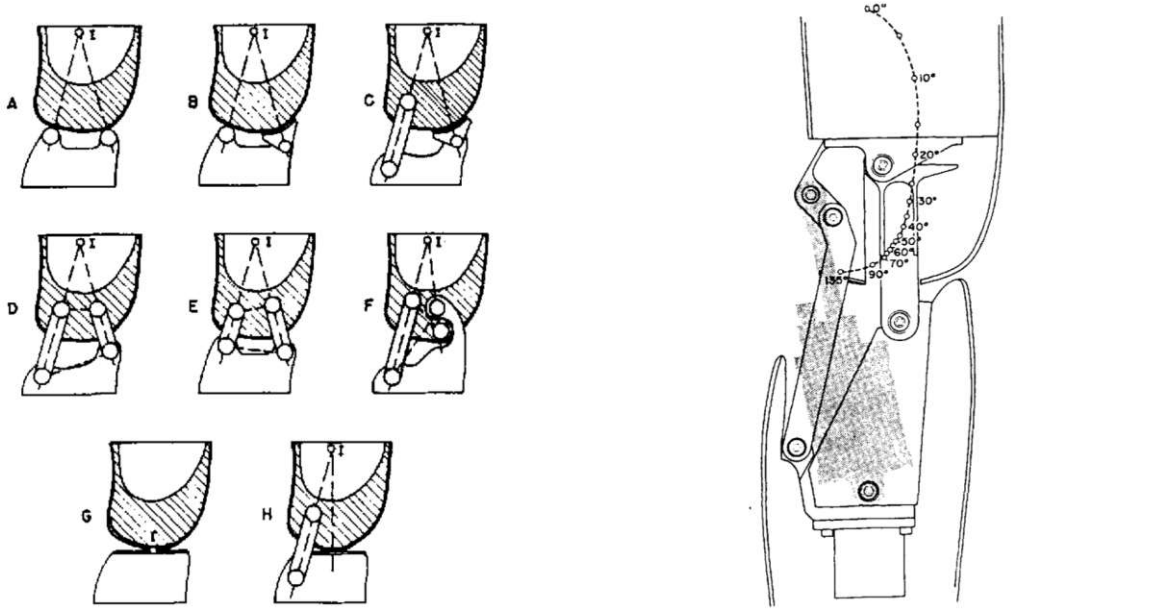

(a) Different designs of a polycentric artificial knee (Source: [78, p. 150])

(b) Instantaneous centre of rotation of a four bar linkage polycentric artificial knee (Source: [78, p. 154])

Fig. 3.8: Polycentric knee prosthesis design and instantaneous centres of rotation for a polycentric knee

3.3.2.3 Stance Phase Control Mechanisms

After a short double support phase at the beginning of the stance phase one limb has to support the whole body weight. Therefore, it is necessary to secure uncontrolled and sudden flexion of the knee. A knee flexion moment occurs, when the GRF Vector passes anterior to the knee axis or in polycentric knee prosthesis anterior to the instant centre of rotation. To ensure that there is no uncontrolled flexion, several stance phase control mechanism can be used. This can be achieved by an additional hip extension moment at the hip, which forces the vector to lie anterior to the knee axis [80]. However, this can be very exhausting for the user which is why a fully locked knee (see fig. 3.9a and fig. 3.9b), which can be released manually for seating, can be used. This method can be an advantage if long standing is required or for people with weak hip extensors or endurance problems. However, a fully locked knee provides some serious drawbacks, like no swing phase control, which begs the need for a shorter prosthetic limb, compared to the intact limb which incidentally leads to asymmetric gait patterns [17].

Other mechanisms for securing stance phase flexion can be mechanical breaks that lock automatically during stance and unlock during swing phase. This can be achieved with spring assemblies and friction mechanisms which engage based on the load. Therefore, a flexion moment which is normally present in early stance engages the locking mechanism, while an extension moment caused by foot loading and muscle activation unlocks the knee automatically [3]. Another

technique that does not utilize IMUs or additional sensors is a mechanism with a hydraulic cylinder. With this design the cylinder movement is locked by an isolator valve that is closed due to a vertical force that acts on a spring. If the force exceeds a threshold the cylinder is in locking mode while when force is below a certain limit the valve opens again and does not resist flexion of the knee to allow a controlled swing phase [51].

Another method to control stance phase is by using an electrical system with different sensors or IMUs and integrate routines that open or close valves in hydraulic or pneumatic systems, which is based on multiple parameters like knee angle, ground reaction force, accelerations or velocities. These so called microprocessor controlled knee joints (see fig. 3.9d) provide multiple improvements that lead to increased mobility and confidence of the patients, without adding additional costs to society [31, 34, 71]. The main benefits are that with an automatically adjustable damping it is possible to support multiple walking speeds and provide different settings for cycling, hiking, slope descending or stair climbing [2]. However, these devices are more expensive than their non-electronic counterparts and often not robust enough for obese patients or for usage in hazardous environments [17]. Microprocessor controlled knee joints are still passive devices that can only manipulate motorized valves to increase or decrease damping and therefore only dissipate energy [2].

Active knee joints (see fig. 3.9e) that can output net power are another possibility for securing stance phase by providing breaking by the motor. This can be done only electrically and can allow stance phase flexion to a certain extent only limited by the amount of torque the motor is able to deliver.

3.3.2.4 Swing Phase Control Mechanisms

Similarly to stance phase control there are swing phase control mechanisms as well. In the swing phase a large power generation at the hip accelerates the swinging leg forwards and flexion at the knee ensuring ground clearance. When the foot is clear the hamstrings are active to break further knee extension and hold the knee and foot in the air, preparing heel strike [75]. Swing phase control in passive knee joints can only accomplish smooth acceleration and breaking of the shank in swing phase. To achieve that, elastic webbing that stretches when the knee flexes can be used, but hydraulic or pneumatic solutions generally work best [17, 78]. With non-microprocessor prostheses, cylinders with multiple holes can be used that progressively change the rate of damping as the piston moves through the cylinder. However, microprocessor controlled devices work best as they can alter the damping automatically based on speed [78].

Active prostheses can vary the resistance to flexion and assist with powered extension to control the swing phase [36]. Other designs feature two separate drives for flexion and extension movements that mimic muscular agonist-antagonist movement [20, 62].

3.3.3 Prosthetic Foot

The most distal part of a knee prostheses, is the foot. While there are some designs for electronically controlled or even active feet in combination with knee prosthesis [59] usually the foot is a passive device. The solid ankle cushion heel (SACH) and stationary attachment flexible endoskeletal (SAFE) foot are two feet that can only absorb energy and are relatively low-cost. Other foot designs feature single or multiple axis that allow movement and help with stability in uneven terrain. Dynamic response feet are also possible which feature springs that can store energy and generate a push off effect that can help people increase their activity level [57].

(a) Simple locking knee from Össur which is mostly used for less active patients or as part of rehabilitation (Source: `https://media.ossur.com/image/upload/product-documents/de-de/PN20045/catalogs/PN20045_Locking_Knee_DE.pdf`, accessed 04.01.2022)

(b) Locking knee manufactured by Otto Bock for water activities (Source: `https://www.ottobock.de/prothesen/beinprothesen/wasserfeste-gehhilfen/aqualine/`, accessed 04.01.2022)

(c) Polycentric knee joint from Össur with pneumatic cylinders (Source: `https://media.ossur.com/image/upload/product-documents/de-de/PN20104/catalogs/PN20104_Total_Knee_2000_DE`, accessed 04.01.2022)

(d) Microprocessor controlled knee joint C-Leg® with hydraulic cylinders (Source: `https://www.ottobock.at/prothesen/beinprothesen/kniegelenke/c-leg-beinprothese/`, accessed 04.01.2022)

(e) Össur Power Knee® which includes an electric motor for better extension when standing up, descending slopes and controlled stance phase flexion (Source: `https://www.ossur.com/en-us/prosthetics/knees/power-knee`, accessed 04.01.2022)

Fig. 3.9: Collection of different knee joints from simple locking knees to power knee devices

Chapter 4

Reference Curves

For developing new prostheses or adapting control strategies for existing devices, reference curves from previous tests are considered. The goal was to provide an algorithm that chooses the reference curve from an existing recording of multiple steps based on multiple criteria, like ground reaction force, knee angle and motor current. Because gait variables can vary between consecutive gait cycles boundaries are given as well to identify steps that can still be considered as valid. All steps that are outside of the chosen boundaries are discarded because their variation is thought to be too high, compared to the other steps of the chosen trail. To achieve that, a Python (Python Software Foundation, Wilmington, USA) program has been developed and several algorithms have been written and verified with a black-box test afterwards. For the graphical user interface *Dear PyGui* (`https://dearpygui.readthedocs.io/en/latest/index.html`) was used, because the ability to draw diagrams matched the needs to achieve the desired results best.
Prostheses that are equipped with a microprocessor control are also fitted with various sensors that allow controlling the device within a gait cycle. For passive devices the control is limited to opening and closing of valves of the hydraulic cylinder but active prostheses contain a motor control as well. Otto Bock is using their own BioLeg software to record internal sensor data and provide the data as a tabulator separated text-file afterwards.
To choose the best method for finding a reference, a total of seven different algorithms were implemented. The results were presented as part of a black-box test to some of the researchers of Otto Bock. These implemented algorithms were:

1. Find the median and calculate the Root Mean Square (RMS) error for each step.
2. First normalise the time for each step to 100 percent. After that the procedure is the same as mentioned in the first item of this list.
3. Calculate the 10^{th} and 90^{th} percentile and calculate the RMS error for each step if the value is not within those boundaries
4. The steps are normalised in time to 100 percent. After that the operation is the same as in item three of this list.
5. Dynamic Time Warping (DTW) is used to calculate the warping path for each step to each of the other steps. DTW returns a matrix that can be interpreted as the cost for transforming the curve to match the reference.
6. Because DTW is a procedure that takes a lot of computing power it was accelerated by first calculating the median and then calculating the DTW matrices for each signal to the median.
7. Longest Common Subsequence (LCSS) is a procedure that is often used in speech recognition. It is a faster computing algorithm compared to DTW especially when noisy data is being

used. It calculates the longest subsequence that can be found when comparing two signals and the length can be interpreted as the distance of those signals [21].

After implementing these algorithms they where tested with six different test recordings of six different subjects. Without the researches of Otto Bock knowing which procedure they were looking at they had to identify the best and the worst results with the allowance to pick multiple methods as best or worst for each subject. After evaluating the results it was clear, that DTW with the usage of median was the best result overall followed by percentile and DTW without median (see fig. 4.1). All other methods were chosen equally often or more often as worst method, rather than best method, which excluded them from usage.

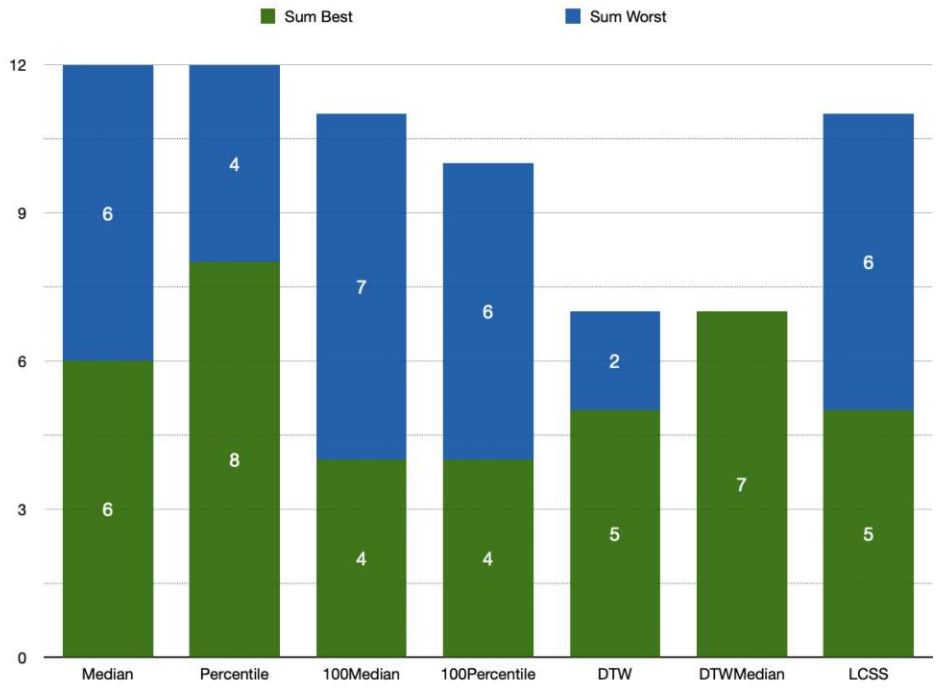

Fig. 4.1: Result of the black-box test to find the best method for selecting references. The blue bar is indicating the number of picks as the best method and the grey bar indicates the total amount of times the method was chosen as the worst method out of all methods.

4.1 Implemented and tested Methods

In this section all of the implemented methods are explained and discussed in greater detail. Because the detection of reference steps could not be achieved by investigating only one signal, the algorithm had to be able to include multiple signals of the same steps and compute the reference and boundaries based on that information. Therefore, in order to start the calculation three signals have to be chosen which should be consulted for the reference calculations. For active prostheses these usually were knee angle, ground reaction force and motor current (see fig. 4.2a) with the latter exchanged for another signal in passive devices. After calculating the distances or errors the steps were displayed in three different colours (see fig. 4.2b). Blue means that the curve is not within the established range (distance or error), white means that the step can be considered inside the range and the red step is the step with the minimum error or distance depending on the method that was used.

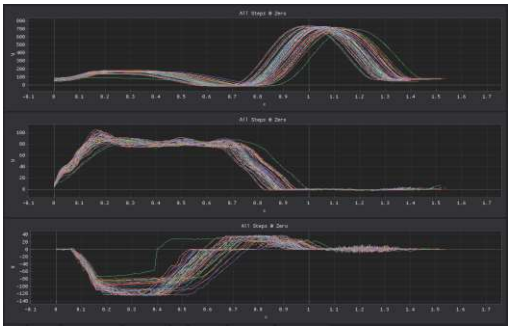

(a) Signals for knee angle, ground reaction force and motor current from one test file. A total of 48 steps are displayed.

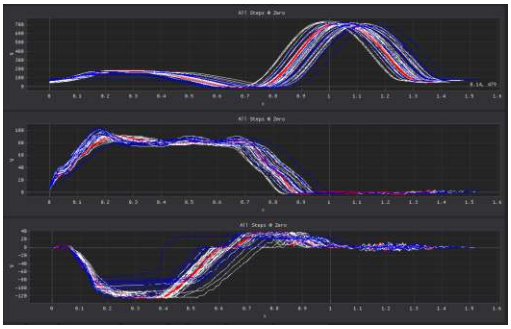

(b) Signals after DTW was calculated. The blue steps are not within the calculated range and are therefore not included. The white curves are within the average distance to the median curve with the red one being the step with the minimum distance to the median and hence identified as the reference.

Fig. 4.2: Signals before and after DTW

4.1.1 Median

Calculating the median for each point in time is a commonly known method and must not be mistaken by the mean value. The median is simply the value that is right in the middle of an array of data points. For arrays that contain an even number of elements the median is usually computed by taking the mean of the two values surrounding the middle value (e.g. 5^{th} and 6^{th} element of an array containing 10 elements). After calculating the median for each of the three different signals the squared error normalized by the maximum of the current signal was calculated and summed up for each signal. This results in three error values for each of the three signals for each step. After that the individual errors are added together to give one error figure for each step with the mean error determining the limit of inclusion and the smallest value defining the reference step.

4.1.2 Median with Time Normalisation

Because the duration of each step can vary in time in biomechanical signals, the time for one step is usually normalised to 100 percent. This ensures that each step can be compared regardless of its duration. However, it also involves approximation and thus loss of information, although the effect is usually small. In the case of the traditional algorithms like median and percentile methods time normalisation is done beforehand, but did not improve the results. After normalising, the method was the same as described in section 4.1.1.

4.1.3 Percentile

The second distinct method that was implemented was using percentiles. A ten percentile lower and a 90 percentile upper limit was calculated. This was done for each point in time to get two continuous curves for the upper and lower limit. To get the corresponding percentile value of an array, containing the values for each step at a given point in time, the array has to be sorted in ascending order first. After that the 10^{th} percentile value is found by getting the value of the element that is corresponding to 10 percent (e.g. 40 elements in an array sorted in an ascending order, the 10^{th} percentile value is the value that is corresponding to the 4^{th} element of the array).

When the upper and lower percentile curves have been found, the error is calculated and summed up for each curve. If the corresponding value of a step is inside the two boundaries, the error is estimated to be zero else the square error normalized to the maximum of the current signal is added to the sum. After all errors for the different signals and steps have been calculated the average error is taken as the limit whether the step can be seen as a reference. The step with the smallest error is determined as the reference step of the trail.

4.1.4 Percentile with Time Normalisation

As with the method using the median the percentile method was also implemented with a time normalisation before the actually algorithm. Yet again the method with time normalisation produced no better results than the standard method.

4.1.5 Dynamic Time Warping

Dynamic time warping originates in speech recognition were usually word templates are matched against continuous speech patterns. Successful recognition has to have the ability to match the word in spite the fact that the word might be spoken in different speeds [9]. If two time series are given, they usually consist of n discrete points in time. In equation 4.1 two time series A and B given with n and m data points, respectively.

$$A = a_1, a_2, ..., a_n; B = b_1, b_2, ..., b_m \tag{4.1}$$

Both signals A and B can be arranged to form a matrix W with dimensions $n \times m$. Each element $w_{i,j}$ in the matrix is now calculated using equation 4.2. $d_{i,j}$ is the distance of the i^{th} to the j^{th} element of signal A and B, respectively. The distance is simply calculated by subtracting the two values and taking the absolute value of the result. The second term adds the minimum values of the adjourning cells in the matrix to the distance calculated before. The path connecting each minimum is then called the warping path. Because the distances are accumulated it is possible to take the last entry $w_{n,m}$ as a measure of distance to the other signal if the two signals are of the same length and if $a_n = b_m$. If that is not the case the minimum value is found in the last column if columns exceed rows or vice versa.

$$w_{i,j} = d_{i,j} + min[w_{i-1,j}, w_{i-1,j-1}, w_{i,j-1}] \tag{4.2}$$

The result of two sample signals can be seen in figure 4.3a. The warping path is along the minimum values in the direction of the orange arrows. The cumulative distance of both signals to each other in that instance is calculated to be 10. In figure 4.3b the difference between an euclidean distance and DTW can be seen. After calculating the matrix for each signal with each

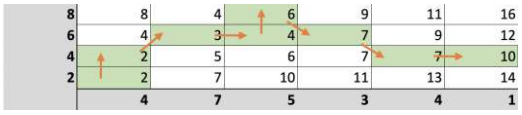

(a) Dynamic time warping matrix with warping path of two signals $A = [2, 4, 6, 8]$ and $B = [4, 7, 5, 3, 4, 1]$. Warping path follows the orange arrows through the matrix. The cumulative distance between the two signals is calculated to be 10.

(b) Difference between an euclidean distance and dynamic time warping. DTW allows a 1:n match for each point in contrast to euclidean where each point is matched 1:1. ([53, p. 369])

Fig. 4.3: Signals before and after DTW

other signal (if k steps were identified then this adds up to k-times calculating k-1 matrices of size n x m for all of the three different variables) the cumulative distances are summed up for each. The reference step is the step which has the minimum summed up cumulative distances from all steps in the trail. Steps are included if their distance is below the average distance calculated. This method was also tried with a normalisation to the maximum of the signal. However, it did not produce better results than without a normalisation. Because no normalisation to the maxima of the different signals where included, it acts as a natural weighting of the signals based on their amplitude. In the case of knee angle, ground reaction force and motor current the weighting is leaning towards the knee angle and ground reaction force, which did produce the wanted results.

4.1.6 Dynamic Time Warping with Median

Because DTW is a time consuming algorithm it was also implemented by combining the median with DTW. Therefore, only the distance to the median of the signals were calculated. This did not only increase speed dramatically (only n times k matrices have to be calculated for k steps for n different signals compared to k-times calculating k-1 matrices) but also produced better results. This is why the final algorithm implemented this method and is used for identifying reference curves.

4.1.7 Longest Common Subsequence

The last approach is called longest common subsequence. This method is often used for spell checking where it tries to find the closest resembling word in the dictionary or in biology were resemblances of DNA patterns want to be found. Basically the LCSS is a case of an edit distance problem and can be described as follows: If we have two strings $S1[1..n]$ and $S2[1..m]$ then a subsequence $q(S1, S2)$ is a sequence that occurs in both strings. If it is the longest possible subsequence, the LCSS $Q[1..r]$ has been found. Therefore, in order to transform $S1$ to $S2$, first $m - r$ characters have to be deleted and then $n - r$ characters have to be added to achieve the transformation [8, 19]. This means that the length of the subsequence can be seen as a indication of distance between the sequences. Instead of characters numerical values have to be compareed to each other when using it on signals recorded by prostheses. Again subsequences are calculated to obtain distances from all steps to each other step. After that, the step with the maximum cumulative distance is chosen to be the reference with the limit for inclusion being the average of the distances for all other curves to that chosen reference. For this method no normalisation on signal value has to be done, as only the length of the subsequences is important, which contains no information about the amplitude of the signal. To compute the longest common subsequence a matrix of $(n + 1) \times (m + 1)$ is used. The procedure resembles the operations for DTW but instead of always adding the minimum, the maximum values are added. First one row and one column of zeros is added as the first row and column of the matrix. After that string $S1$ is written on top of the first row in a way that each character is labelling one column. String $S2$ is written down in a way that each character is written in front of each row. If character $s1_i$ and character $s2_j$ are the same, one is added to the value of $m_{j-1,i-1}$ and the result is written in cell $m_{j,i}$. Furthermore an arrow is drawn to that diagonal element $m_{j-1,i-1}$. If the characters do not match, the maximum value of the previous column $m_{j,i-1}$ or row $m_{j-1,i}$ element is written inside the current cell $m_{j,i}$ and an arrow is drawn to that cell. This procedure is done until all cells have been calculated. The length of the subsequence can be found in the last entry of the matrix, while the sequence itself can be found by looking at the diagonal arrows in the matrix (see fig.4.4). As the sequence itself was not relevant for our application only the length was used.

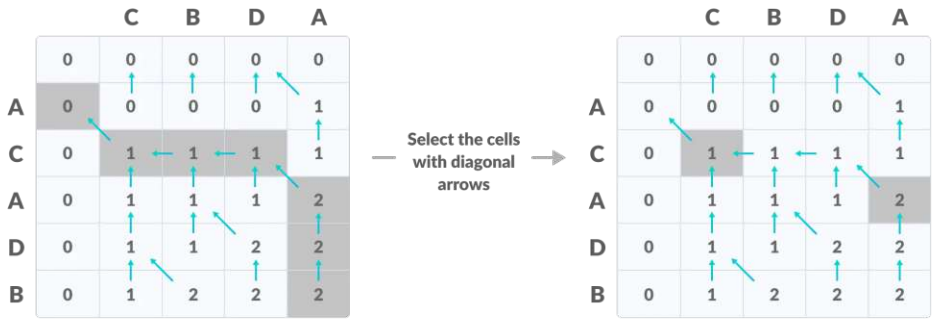

Fig. 4.4: Finished matrix of the LCSS method. The length can be seen in the last entry of the matrix while the subsequence itself is *CA*. This can be seen by following the diagonal arrows. (Source: `https://www.programiz.com/dsa/longest-common-subsequence`, accessed 12.01.2022

4.2 Implemented Process

The process on how the reference curve is calculated can be seen in figure 4.5 and is going to be discussed in this section. Generally it can be said, that more than three steps should be available before calculating a reference and the boundary values. At a value of less than three only one reference curve can be found but no upper or lower boundary measures can be given as the other two available datasets are automatically discarded. Therefore, no array of valid curves can be provided if three or less steps are given.

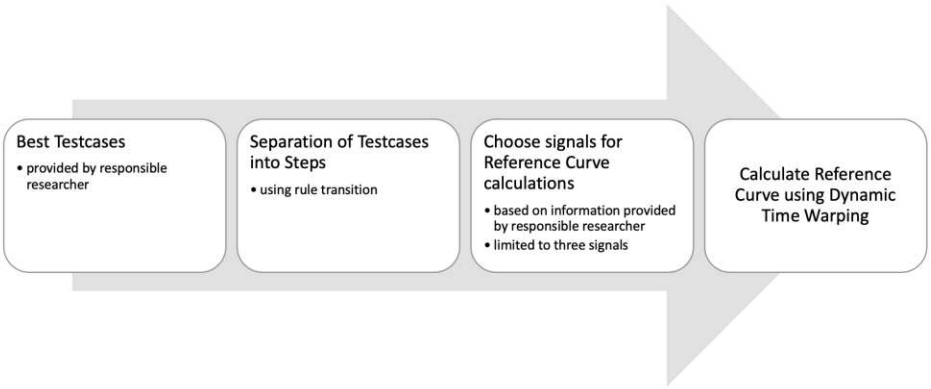

Fig. 4.5: Process for finding Reference Curves

Determine Best Test Cases Before one step representative for a whole trial can be chosen it has to be ensured, that everything in that particular test went as planned and that the results (determined by the researcher working on that particular prosthesis) are the best results that could be achieved for that trail with the particular prosthesis or changed algorithm. If that is the case, the test session is going to be included in the process. If however something went wrong or the subject does not feel comfortable with the prosthesis or the tested settings, the test will not be included as this would produce wrong results.

Separation of Testcases into Steps One recording of a test can last several minutes and thus include multiple steps. In order to analyse the steps they have to be separated and identified. Because the prosthesis is microprocessor controlled, the program that controls the device is already establishing initial contact, where it changes from swing to stance control. On the device this is done by changing the state of the finite state machine. This can be seen in fig. 4.6, where the green signal indicates the knee angle and the red signal shows the currently active state. It can be seen that when the state is changing from four to six, initial contact is occurring. This is also indicated by the pink vertical lines in the chart.

$$t_{step-average} = \sum_{i=1}^{3} \frac{n_i * t_i}{\sum_{j=1}^{3} n_j} \tag{4.3}$$

After successfully detecting all initial contacts only valid steps should be taken into account. If e.g. the subject stumbles or has to rotate around because he/she has reached the end of the laboratory, the initial contact detected should mark the end of a step series and the detected initial contact should not mark the beginning of a new gait cycle. This is indicated by a blue vertical line in fig. 4.6. In order to identify only those valid and equal steps, the time duration between two consecutive initial contacts is taken into consideration. The duration of each step is rounded to tenth of a second and steps that last for the same duration are counted. The three durations that are occurring the most are then used to calculated a weighted average (see equation 4.3, where $t_{step-average}$ is the weighted average step duration and n_i indicates the frequency of steps that last for t_i). Each step exceeding this number by more than 15 percent is considered as the end of a step or series of steps and hence the initial contact is indicated by a blue line in the chart. If different speeds were recorded in one test trail, the vertical lines can easily be toggled by just clicking on them once.

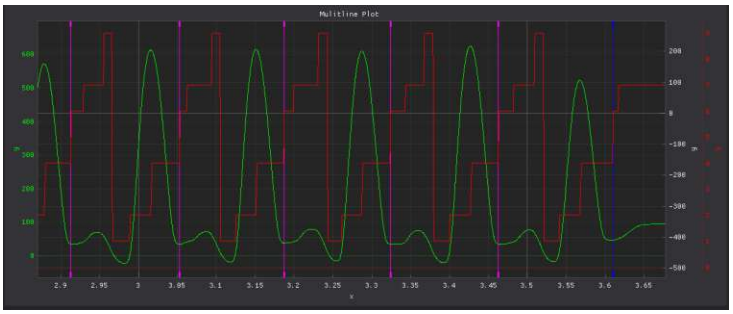

Fig. 4.6: Multiple steps in a recording. Initial contact is indicated by the vertical marker. Pink indicates that the step starting at given point in time might be included. Blue indicates that the step series has ended. The green signal is showing knee angle and the red one shows the rules that are currently active. Initial contact happens in that recording when the rule changes from four to six.

Choose Signals for Reference Calculations After separate steps have been identified the next step is to choose the signals on which the reference calculations should be based. This information is usually provided by the responsible researcher and is only limited by the signals that are available. For active devices the motor current is usually considered as one of the signals which is not available in passive devices. Other signals that were usually taken into account were knee angle and ground reaction force.

Calculate Reference Curve using Dynamic Time Warping The last step is to establish the reference step and steps that are within a certain range of that reference. To achieve that, a combined algorithm of dynamic time warping and median is used (see section 4.1.6). The references and metadata of the trail is stored in a database afterwards that can be accessed by prosthesis developers.

Chapter 5

Gait Analysis

5.1 Method

5.1.1 Investigated Prostheses

The gait parameters of three different prostheses were compared. The C-Leg® and the Genium® are both manufactured by Otto Bock and are already available on the market. Both were compared to a novel active prosthesis that currently only exists as a prototype.

5.1.1.1 C-Leg®

With over 60.000 units sold and remaining in production since 1997 the C-Leg® is the most widely known prosthesis manufactured and developed by Otto Bock. It was continuously revised until now and is still the favourable device for many users. The prosthesis features independently controllable two-way hydraulic cylinders that allow to alter flexion and extension damping. This is achieved via proportional valves that are driven by servo motors. It features hydraulic force and knee angle sensors as well as a six degrees of freedom IMU, to calculate the best damping parameters with a control that operates at 100 Hz. Because the C-Leg® is equipped with an IMU the detection of the swing phase is easier compared to its predecessors, where it was roughly estimated based on ankle torque measurements. These design iterations allowed improvements over previous versions of the prosthesis in small step walking, walking on soft surfaces, walking backwards and walking with a wider range of gait velocities [45, 47].

5.1.1.2 Genium®

The Genium® was introduced in 2011 closely followed by the Genium® X3 which was introduced in 2013. The main difference is, that the X3 features resistance against water and corrosion. The main goal in developing the Genium® was to minimize the difference between prosthesis and sound foot by e.g. making sure that walking with the prosthesis becomes more intuitive. The prosthesis allows more stance phase flexion compared to other knee joints from Otto Bock, thus making gait more symmetrical and protecting the locomotor system. Other improvements are the automatic detection of different scenarios like standing, sitting, walk to run transitions and stepping over obstacles. The prosthesis control works with 100 Hz and features a knee angle and hydraulic force sensor, a six degrees of freedom IMU and a tube equipped with a strain gauge that allow to measurement of the sagittal torque and ground reaction force [46, 48]

5.1.1.3 Novel active Prosthesis

The novel active prosthesis features a net positive power output, hence the name active. This is achieved by a custom built motor that together with a belt drive and a coaxial drive results in a total transmission of approximately 1:70 and is able to output 60 Nm of torque. The motor drives the knee axis of the prosthesis via the transmission. Because it uses the same battery system

(18V) as other Otto Bock products it is not dependent on cables and allows free movement. In parallel to the motor a two way linear hydraulic damper is operating that allows independent control of extension and flexion movements via a proportional valve that is controlled by servo motors. The low level motor control operates at 1 kHz and allows both torque and impedance control. The high level control operates at 100 Hz which is the same as for the C-Leg® and the Genium®. To function properly, it features multiple sensors like

- Hydraulic force sensor
- Knee angle sensor
- IMU mounted to the shank with six degrees of freedom
- Tube fitted with strain gauges which is recording axial forces and sagittal torque

Altogether this results in a novel active prosthesis that is able to assist with stance phase, swing phase flexion and extension of the knee.

5.1.2 Equipment

5.1.2.1 Gait Laboratory

The gait data was recorded in the in-house gait laboratory of Otto Bock in GÃűttingen, Germany. It is equipped with a Vicon® (`https://www.vicon.com/`) system that consists of 12 infrared cameras and features two force plates manufactured by Kistler® (type 9287A, `https://www.kistler.com/en/`) that are aligned consecutively on the 12 meter long walkway (see fig.5.1a). To ensure that only one foot is touching the force plates they are lowered into the ground and the pressure is transferred onto them by using beams that are either supported by the force plate or do not touch the force plate at all (see fig.5.1b). These beams are set up to fit the subjects step length and are altered accordingly. The force plates are recording at 1000 Hz and are featuring piezoelectric force sensors at each corner of the plate. Two light optical barriers are used to start and stop the recording. The markerset was applied by following the Plug-in Gait Reference Guide (`https://docs.vicon.com/display/Nexus212/Plug-in+Gait+Reference+Guide`), but is enhanced to provide better compatibility for trans-femoral amputees. The recording frequency of the system was 200 Hz for all markers and processed values like e.g. angles or torque.

(a) Picture of the gait laboratory of Otto Bock. The walkway with the force plates aligned at the centre and infrared cameras can be seen as well as the marker on the floor before the force plates that indicate the light barrier that start the recording.

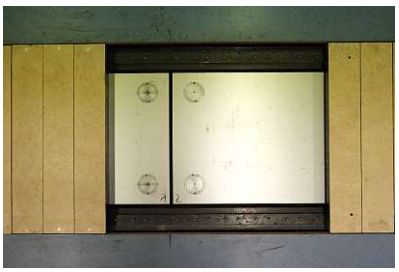

(b) The force plate underneath the beams can be seen in this picture. The beams are adjusted to fit each subjects walk and to ensure that only the heel strike of one foot is recorded by the force plate.

Fig. 5.1: Image of the gait laboratory and the force plate used in the experiments

Marker Set The marker set was applied according to the *Plug-in Gait Reference Guide* (see `https://docs.vicon.com/display/Nexus212/Plug-in+Gait+Reference+Guide`) that has to be used if gait is recorded and analysed with the Vicon Nexus® software. Generally, the markers are placed on anatomical landmarks (see table 5.1) that are described within the procedure. To

Marker label	Position
Pelvis	
SACR	mid way between posterior iliac spines in the pane defined by ASIS and PSIS
LASI	left anterior superior iliac spine
RASI	right anterior superior iliac spine
LPSI	left posterior superior iliac spine
RPSI	right posterior superior iliac spine
Lower Limb	
LTHI/RTHI	on the lower lateral 1/3 surface of the thighs
LKNE/RKNE	on the flexion/extension axis of the knee
LTIB/RTIB	on the lower 1/3 surface of the shank
LANK/RANK	lateral malleolus along an imaginary line through the transmalleolar axis
LHEE/RHEE	calcaneus at the same height above the plantar surface as the toe marker
LTOE/RTOE	second metatarsal head on the mid-foot side of the equines break

Tab. 5.1: Overview of markers used for the lower limb model and how to apply them (source: `https://docs.vicon.com/display/Nexus212/Plug-in+Gait+Reference+Guide` accessed on 22.01.2022)

track motion of TFAs as good as possible and because the positioning of the markers on the prosthesis can not be done in accordance with a sound limb, additional markers were used (see fig.5.2). One additional marker is on the opposite side of the KNE markers to determine the knee joint center of the prosthesis. As both markers are applied on the knee axis of the prosthesis the centre of the knee joint is estimated to be in the middle of those two markers. Two additional markers are applied at the end of the DMS tube and two markers are positioned below those markers right at the beginning of the prosthetic foot. These markers are used to estimate the ankle and its joint centre. Because there are no metatarsal heads on the prosthetic foot four markers are used to estimate the foots movement. One is attached to the front of the shoe in a way that avoids it from touching the ground when the foot rolls of at the transition from stance to swing phase. Two other markers are placed on the metatarsophalangeales joints on the medial and lateral side of the sound foot and mirrored on the prosthetic side. In between these two markers and in axis between the marker at the front of the shoe and the heel marker another marker is applied at the top of the foot.

5.1.3 Subjects

The data of two subjects A and B could be collected in the gait laboratory. Their weight and height as well as which prosthesis used everyday can be seen in table 5.2. Because this was only preliminary testing the number of subjects was limited. It has to be noted, that the subjects weight increases slightly when used with the novel active prosthesis as the device is significantly heavier than their non active counterparts. However, this is already accounted for in the results as they are normalised to bodyweight where it is necessary.

Fig. 5.2: The markerset that was used in the experiments is shown. It differs slightly from the standard marker set as some anatomical landmarks are absent in trans-femoral subjects.

Subject A Subject A is using a Boa socket with sealing lip with both prostheses. For everyday use, the patient is using a C-Leg® 4, manufactured by Otto Bock. Both prostheses did use the same foot, the Triton® 1C60 and the same shoes were worn throughout the tests in the gait laboratory. The prostheses were aligned by using the L.A.S.A.R (Lasar assisted static alignment reference) Posture system developed by Otto Bock. The shoes used were standard training shoes in both trails.

Subject B Subject B is using his everyday socket with both prostheses. The patient is using a Genium® X3 as his everyday prosthesis. For both settings the feet were kept the same which was a Triton® 1C60, which is the same foot subject A used in the tests. Again the prostheses were aligned using the L.A.S.A.R Posture system developed by Otto Bock to align them equally. The shoes were standard training shoes in both settings again.

ID	Sex	everyday Prosthesis	prosthetic Limb	Weight [kg]	Height [cm]
Subject A	m	Otto Bock C-Leg	Left	72.5	190
Subject B	m	Otto Bock Genium	Left	90	182

Tab. 5.2: Overview of subjects weight, height, sex and everyday prosthesis as well as the side on which the prosthesis is worn.

5.1.3.1 Test Procedure

The tests took place on three different days and only level ground walking was recorded. For subject A the first test with the everyday prosthesis took place on 23.06.2021, while the trails

with the novel active prosthesis were recorded on 5.10.2021. After eliminating trails which could not be included e.g. due to false placement of the foot on the force plate, ten trails for slow walking and nine for fast walking with the everyday prosthesis, respectively, as well as eleven trails for slow walking and seven trails for fast walking with the novel prosthesis, respectively, were included in the results (see table 5.3). Both speeds were self selected and were not controlled to match the velocities for the different prosthesis. This did result in differences in walking speeds from up to 0.1 m/s which could potentially affect the results, especially the hip torque and ground reaction forces.
For subject B both tests were done on the 31.01.2022 to limit the variability between the two scenarios and limit differences in anthropometric data. Slow, fast and normal walking was recorded. The speeds were self selected and not controlled for subject A. For subject B first the preferred walking speeds for slow, fast and normal walking while using the everyday prosthesis were determined. The walking speeds with the novel active prosthesis were then controlled by using a metronome to guide the subject to the before determined speeds. This was done in order to limit variabilities caused by different walking speeds that showed within the first subject. The trails were conducted in both directions of the gait laboratory. The force plate on which the subject walked with their prosthetic and sound legs were always the same, to limit variabilities caused by different accuracies of the two force plates. Both subjects used the same socket, foot and shoe that they wore with their everyday prosthesis.

ID	Prosthesis	valid trails slow	valid trails fast	total number of trails
Subject A	C-Leg	10	9	23
Subject A	AKN	11	7	42
Subject B	Genium	16	15	31
Subject B	AKN	16	15	33

Tab. 5.3: Overview of valid trails for each subject and walking speeds.

5.1.4 Analysis

After the tests were recorded the values for angles, torque and power were calculated with the Vicon Nexus® software. To process the different trails and evaluate the trails statistically Python (`https://www.python.org/`) was used. In order to be able to read the c3d files created by the Vicon system it was necessary to use the pyc3dserver plug-in (`https://pypi.org/project/pyc3dserver/`) which requires an installation of C3DServer (`https://www.c3dserver.com/`) to be able to read the specified file format. To test the hypothesis specified in section 1 different signals and parameters were evaluated (see table 5.4). All parameters were tested with a two sided Student's t-test for paired samples with a significance level of 0.05. For intraindividual symmetry evaluation as well as inter individual differences Statistical Parametric Mapping (SPM) was used. To take advantage of SPM the Python package called SPM1d (`https://spm1d.org/`) utilizing SPM was used to evaluate and smooth the signals. Before analysis of the signals each set of signals was analysed by using DTW to eliminate signals that were not usable due to noise or wrong estimates.

Walking Speed, Stance Phase Duration and Double Support Phase In the first step spatio-temporal parameters were analysed including walking speed, stance phase duration, double support phase duration and linear correlation between stance phase duration and walking speeds. The focus thereby was on symmetry between the sound and the prosthetic leg with the hypothesis

Signal/Parameter	Unit
Stance Phase Duration	% of Gait Cycle
Walking Speed	m/s
Foot Clearance	mm
Hip Angles	°
Knee Angles	°
Ankle Angles	°
C7 Movement	mm
SACR Movement	mm
SACR Velocity	m/s
Ground Reaction Force	% BW
Centre of Pressure	mm
Hip Torque	N m/kg
Hip Power	W/kg
Hip Work	J/kg

Tab. 5.4: Overview of parameters and signals that were used to analyse the data of the gait laboratory for both prostheses.

that the novel active prosthesis would increase symmetry in these values. Because the events like heel-strike and toe-off are provided from the Vicon software it was not necessary to manipulate the data in any way, however, the speeds were calculated by differentiating the marker data of the SACR (sacrum) marker trajectory. The mean value is then assumed to be the speed of that step.

C7 and SACR Movement and velocity During the test the attention was drawn to movements of the upper body as subjects said that they feel like they were able to walk smoother with the novel active prosthesis and felt like their body was more upright during walking. Therefore, the markers C7, marking the C7 vertebra in the cervical spine and SACR, identifying the sacrum, were analysed. This allows to analyse side-to-side (sway) and up and down movements. Moreover, sagittal velocity of the SACR marker trajectory was analysed to investigate the differences in walking speeds over the time of one stance phase duration for each limb.

Foot Clearance The novel active prosthesis is actively helping with foot clearance by supporting swing flexion and extension of the knee. The foot clearance is estimated by using the RTOEF or LTOEF marker for right and left foot clearance respectively. This marker is applied on the front of the shoe in such a way that it is not affected by the roll off mechanism happening at late stance phase, hence never touching the ground.

Hip, Knee and Ankle Angles The prototype prosthesis is allowing stance phase flexion and is assisting with flexion and extension in the swing phase. Therefore, it was assumed that knee angles would become more symmetrical. In order to be able to analyse the whole gait cycle hip and ankle angles were investigated as well. The differences were best seen in the sagittal plane, therefore, these angles were investigated for improved symmetry. All angles are relative between segments. The hip angle is defined as the angle between pelvis and thigh, the knee angle is found between the thigh and the shank and the ankle angle is the angle between the shank and the foot (see fig.5.3).

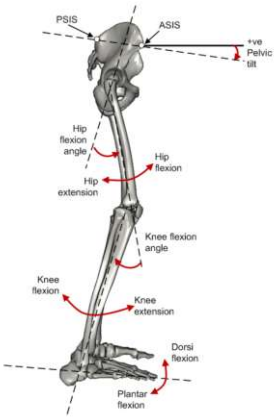

Fig. 5.3: Angles in the sagittal plane as defined by the Plug in Gait Reference Guide. (Source: `https://usermanual.wiki/Document/Plugin20Gait20Reference20Guide.754359891/view`, accessed on 28.01.2022)

Hip Torque, Ground Reaction Force and Centre of Pressure Because the prototype prosthesis is able to output net positive power, the main attention was on the torque, power and work values. As for trans-femoral amputees the hip is the remaining joint of the limb these values were calculated for that joint for both limbs. Because the Vicon Nexus® software is able to calculate these values based on marker and ground reaction force data, it was not necessary to implement a model itself. However, in order to understand and examine the calculated values the torque was calculated manually first. This was only done in stance phase because the development of a model for the dynamic parts of the torque was not the main focus of the analysis. Moreover, the torque caused by movements is estimated to be small compared to the torque resulting from the ground reaction force. While comparing torque values the local coordinate system can be reviewed as well, because the torque calculated by the Vicon software is given in local coordination systems. For the hip joint this system were defined as follows (the order of the axis is the order in which they are calculated):

- Z axis: the axis connecting the hip joint centre with the knee joint centre
- Y axis: the axis that is found by calculating the cross product of the z axis with another axis from the hip joint centre to the knee joint peripheral marker
- X axis: the cross product of y and z axis determines the x axis

This means that the x represents the sagittal torque, y the frontal torque and z the transversal torque of the hip joint. Because force plate do not work properly on the first impact it can lead to artefacts at the beginning of the calculated torque signals. Because this happened in almost all signals it was decided, that the first five percent of the torque signal was excluded of the analysis.
Because the torque is influenced greatly by the ground reaction force and centre of pressure, both values were analysed as well to identify the source of the differences, especially for subject A were velocity differed substantially between the two prosthesis.

Hip Power Hip power was investigated as well, because it was assumed that power would become more symmetrical and less power would be needed in the prosthetic leg hip because the prosthesis is also able to provide power, in contrast to the subjects everyday prosthesis. It has to

be kept in mind that the walking speeds differed greatly for subject A which affected the hip power values.

Hip Work It was assumed that the work done in the hip joint would become more symmetrical or at least decrease slightly because the prototype knee joint is able to assist with power output. Therefore, the power graph was separated in positive and negative sections and these sections were then integrated with the composite trapezoidal rule. The results identify the positive and negative work values in the course of one gait cycle.

5.1.5 Statistical Parametric Mapping (SPM)

Statistical parametric mapping (SPM) is a procedure that was originally developed for analysing neurological images. It was especially designed for analysing continuous data and allows to interpret the findings directly in the original (in our case biomechanical) space. Therefore, no assumptions based on single parameters (e.g. reduction of local minima at 30 % GC) have to be made but rather the whole GC can be analysed for statistical inference [72]. SPM applies the random field theory and general linear model (GLM) to compute the test statistic and correct the significance level for large samples, respectively. The result is a continuos statistical analysis in the original sampling space, that reduces the need for focusing on single events and thus is getting rid of the danger of potentially biasing the data [73].

General Linear Model The description of the General Linear Model (GLM) and its equation to calculate a t-statistic are based on the book Statistical Parametric Mapping. The analysis of functional brain images by Karl Friston [28]. The general linear model is used to calculate the test statistic of a given signal (e.g. the t value for a Student's t test).The GLM calculates a response variable by a linear combination of unknown parameters β_L with explanatory variable x_{jL} and an error term ϵ_j. In this example J observations have been made with each being described with $L(L < J)$ explanatory variables (see eq. 5.1). The error ϵ_j is all independent and identically distributed with a mean of zero and σ^2 as its variance.

$$Y_j = x_{j1}\beta_1 + \ldots + x_{jl}\beta_l + \ldots + x_{jL}\beta_L + \epsilon_j \tag{5.1}$$

For a two sample t-test we can assume that we have two groups of random data Y_{j1} and Y_{j2} with each having a mean of μ_q for $q = 1, 2$ and variance of σ^2. The model can be written as:

$$Y_{qj} = \mu_q + \epsilon_{qj} \tag{5.2}$$

This model can be rewritten to match the structure of GLM by using two dummy variables x_{qj1}, x_{qj2} that indicate group 1 or 2. To achieve that x is defined in equation 5.3. That allows to rewrite equation 5.2 to match equation 5.1 (see eq. 5.4)

$$x_{qj1} = \begin{cases} 1 & , \quad q = 1 \\ 0 & , \quad \text{otherwise} \end{cases} \tag{5.3}$$

$$Y_{qj} = x_{qj1}\mu_1 + x_{qj2}\mu_2 + \epsilon_{qj} \tag{5.4}$$

Now we can use this equation to formulate the problem in matrix formulation to get a set of equations for each observation. In equation 5.5 Y is a vector containing all observations while ϵ is the column vector containing error terms and β the vector of parameters. Therefore, X is the

design matrix consisting of $J \times L$ entries which means one row per observation and one column for each model parameter.

$$Y = X\beta + \epsilon \tag{5.5}$$

Because β is still unknown it is estimated by using the method of ordinary least squares. This means that $\hat{\beta}$ can be calculated if $(X^T X)$ can be inverted. If that is the case the least square estimates for $\hat{\beta}$ are

$$\hat{\beta} = (X^T X)^{-1} X^{-T} Y \tag{5.6}$$

To formulate the test statistic σ^2 is estimated by the residual sum-of-squares divided by the degrees of freedom which is assumed to be $J - p, p = rank(X)$. With that and a contrast vector c that is of shape $J \times 1$ the statistic can be written as

$$T = \frac{c^T \hat{\beta} - d}{\sqrt{\sigma^2 c^T (X^T X)^{-1} c}} \tag{5.7}$$

This means that for a two sample t-test the null hypotheses is written as $H : c^T \beta = 0$ with $\beta = [\mu_1, \mu_2]^T$, $c = [1, -1]^T$. The design matrix consist of two columns. The first column contains n_1 ones and n_2 zeros and the second with n_1 zeros and n_2 ones, indicating the two groups. Therefore, the t value can be rewritten to

$$T = \frac{\hat{\mu_1} - \hat{\mu_2}}{\sqrt{\sigma^2 (\frac{1}{n_1} + \frac{1}{n_2})}} \tag{5.8}$$

which is the standard t value for a Student's t-distribution with $n_1 + n_2 - 2$ degrees of freedom.

Random Field Theory SPM uses the Random Field Theory (RFT) to correct the t value of the Student's t-statistic. This is done because a large sample size can lead to a lot of false positive results that are above the t-statistics threshold. This is usually done with a Bonferroni correction $\alpha = \frac{p}{n}$ that corrects the p value when the number of samples n is very high. However, in many cases the Bonferroni correction is too conservative for functional imaging or biomechanical signals because in biomechanics the signals have spatial correlation to some extent. This means that the observations are not independent and can be related in bigger groups as is the case for functional imaging of activated brain cells. These images are smoothed with a Gaussian filter that replaces each value in an image with a weighted average and thus reducing the number of independent observations. The resulting smoothed image is then consisting of less pixels and these areas are then called resels which is short for resolution elements [13, 29]. To correct the p value based on RFT the Euler characteristic is used. This characteristic is defined as the number of connected areas that are above a certain threshold if all values below are set to e.g. zero and all above are set to 1 (see fig. 5.4). It is obvious that for a high threshold the expected areas are either one or zero. Therefore, it can be said that the expected EC $E(EC)$ corresponds directly to the probability, hence $p \approx E(EC)$ [13]. If the number of resels R in an image are known and the threshold is set to a Z score of Z_t the expected EC for a two dimensional image can be calculated: [44]

$$E(EC) = R(4\lg(2))(2\pi)^{-\frac{2}{3}} Z_t e^{-\frac{1}{2} Z_t^2} \tag{5.9}$$

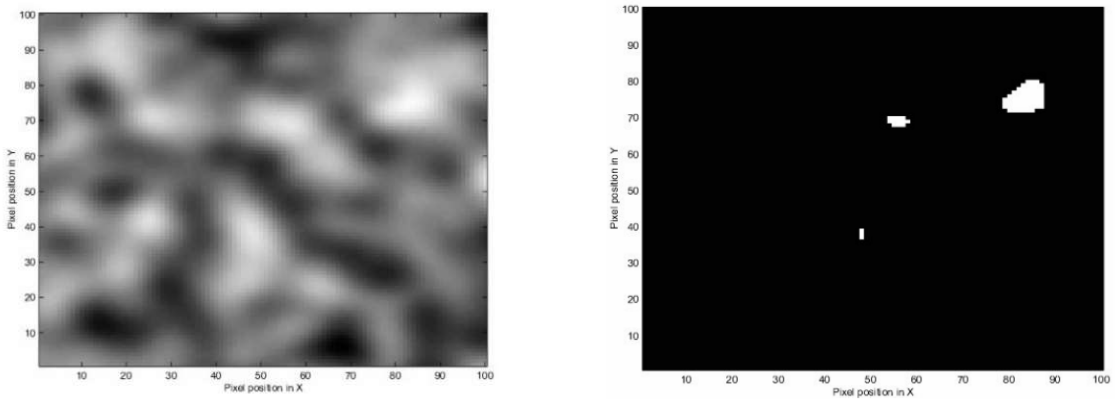

(a) Smoothed image with random numbers. The more white areas are, the more positive their value. (Source: [13, p. 18])

(b) Same smoothed image but now with threshold. All elements that are below the threshold are black while the values above the threshold are white. Three areas can be seen, which corresponds to an EC value of three. (Source: [13, p. 19])

Fig. 5.4: Image with random numbers after smoothing and the same image after a threshold is applied.

5.2 Results

5.2.1 Walking Speed

5.2.1.1 Slow walking

The tests were done for slow and fast walking speed which were both self selected for subject A. Speed was derived from the movement of the SACR marker over one complete GC. It can be seen (see fig.5.5a) that for both the everyday prosthesis and the prototype prosthesis the walking speeds were almost equal for the prosthetic and the sound leg. The averages are $0.88\frac{m}{s}$ for the sound and the prosthetic leg and 0.78 and $0.77\frac{m}{s}$ for the prototype prosthesis. The walking speeds are therefore slower for the prototype compared to the everyday prosthesis for subject A. For subject B the walking speeds were first self selected with the everyday prosthesis. After that the corresponding beat per minute were fixed for the walking trails with the prototype prosthesis. This can be seen in figure 5.5b where the speeds match very well between the two settings. With the everyday prosthesis the average speed was $0.73\frac{m}{s}$, while when using the prototype the average speed was slightly lower at $0.69\frac{m}{s}$.

5.2.1.2 Fast walking

For the fast walking condition the average walking speed for subject A (see fig.5.6a) with the everyday prosthesis was just below $1.55\frac{m}{s}$ while for the prototype prosthesis subject A averaged higher speeds of $1.625\frac{m}{s}$. Furthermore, the distribution of walking speeds is greater when using the prototype prosthesis. For subject B the walking speeds can be seen in figure 5.6b. It can be seen that both the everyday and prototype prosthesis are averaging similar speeds of $1.38\frac{m}{s}$ and $1.425\frac{m}{s}$, respectively.

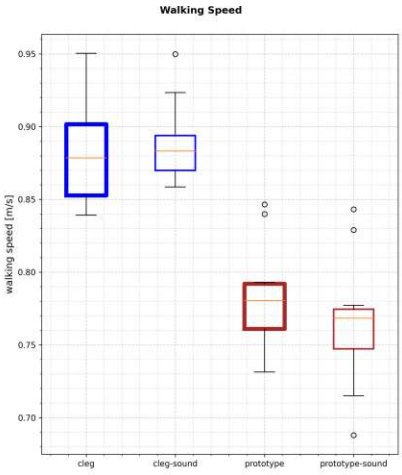

(a) The walking speeds of the left (prosthetic) and right leg of Subject A with the prototype (brown) and everyday prosthesis (blue) can be seen.

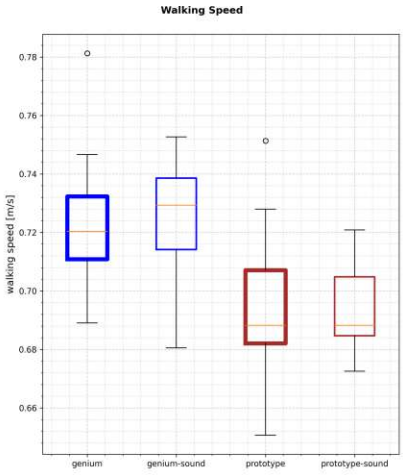

(b) The walking speeds of the left (prosthetic) and right leg of Subject B with the prototype (brown) and everyday prosthesis (blue) can be seen.

Fig. 5.5: Walking speeds for slow walking for both subjects A and B. Walking speed was calculated by differentiating the movement of the SACR marker and taking the mean value over the course of one GC.

5.2.2 Stance Phase Duration

5.2.2.1 Slow walking

The stance phase duration for slow walking in percent of GC is shown in figure 5.7 for subject A and subject B. It can be seen that for subject A (see fig.5.7a) stance phase is substantially longer for the sound (=right) leg averaging around 0.637% of the GC than it is for the prosthetic leg where the average is calculated to be 0.6%. This leads to asymmetry that can also be seen in the t-test for which the null hypothesis of having equal means is rejected with a p-value of 0.00023. For the prototype the average stance phase duration is almost equal for the prosthetic and sound leg averaging 0.625 on the prosthetic leg and slightly above for the sound leg. This results in not rejecting the null hypothesis that both averages are equal with a p-value of 0.59837. For subject B (see fig.5.7b) the stance phase durations between the left and right leg can not be seen as statistically similar. For the stance phase of the left (prosthetic) limb the average duration is 0.63% regardless of the prosthesis. On the right (sound) side the stance phase duration is slightly longer while using the prototype prosthesis at 0.685% compared to 0.675% when wearing the everyday prosthesis.

5.2.2.2 Fast walking

The fast walking trail for subject A can be seen in figure 5.8. For both the everyday prosthesis and the prototype the null hypothesis of having equal average stance phase duration has to be rejected with p-values of 1.236e-6 and 0.00474, respectively (see fig.5.8a). For subject A it can be seen that stance phase duration when using the prototype prosthesis is slightly increasing on the prosthetic side (=left) while the stance phase duration for the sound leg is almost equal for both prostheses. For the everyday prosthesis the average stance phase durations are approximately 0.62% and 0.575% for the sound and prosthetic limb, respectively, while for the prototype prosthesis these values change to 0.62% and 0.59% for subject A. Looking at the stance phase

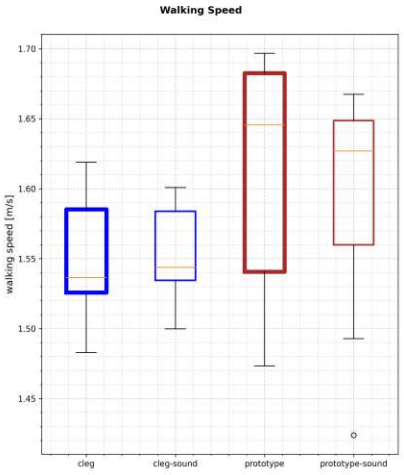

(a) The walking speeds of the left (prosthetic) and right leg of Subject A with the prototype (brown) and everyday prosthesis (blue) can be seen.

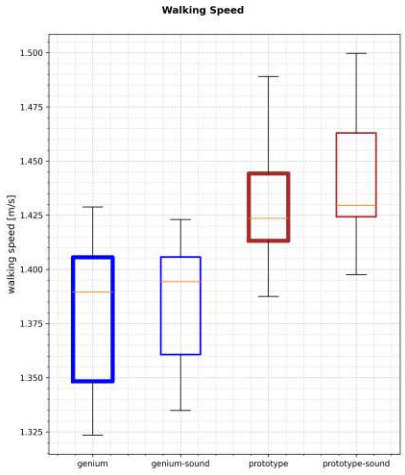

(b) The walking speeds of the left (prosthetic) and right leg of Subject B with the prototype (brown) and everyday prosthesis (blue) can be seen.

Fig. 5.6: Walking speeds for fast walking for both subjects A and B. Walking speed was calculated by differentiating the movement of the SACR marker and taking the mean value over the course of one GC.

durations of subject B (see fig.5.8b) it can be seen that the null hypothesis of having equal mean values has to be rejected for the prototype prosthesis with a p value of 1e-8. This can also be seen when looking directly at the average values of 0.645% and 0.62% for the sound and prosthetic limb when wearing the prototype prosthesis. When using the everyday prosthesis it can be seen that the symmetry can be found with a p value of 0.646. This translates to stance phase durations of 0.64% for both limbs.

5.2.3 Foot Clearance

5.2.3.1 Slow walking

Subject A Figure 5.9 shows the signals of the foot clearance for slow walking for subject A. The null hypothesis for the statistical evaluation is that both signals from the sound and prosthetic foot are equal. It can be seen that for the prototype (see fig.5.9a) three areas exist for which this hypothesis has to be rejected. Looking at the everyday prosthesis (see fig.5.9b) three areas for which the null hypotheses has to be rejected can be established as well. Furthermore, it can be seen that the temporal correlation of the minimum (at 59% GC and 64% GC) and maximum value (90% GC vs 95% GC) is shifted in time for the prosthetic and sound limb in figure 5.9b. When using the prototype prosthesis it can be observed, that the sound foot has a wider distribution than the same foot in the everyday prosthesis (see fig.5.9a and fig.5.9b pink graphs). The foot clearance in mid swing is the crucial value for establishing foot clearance. For the everyday prosthesis vales of 55mm at 78% and 50mm at 82% GC for the prosthetic and sound leg can be established. Looking at the same values while wearing the prototype prosthesis 50mm at 80% GC and on average 60mm at 80% GC can be seen in the diagram.

Subject B In figure 5.10 the foot clearance of subject B while walking slowly can be seen. The SPM{t} analysis is showing seven areas of statistical differences while using the everyday

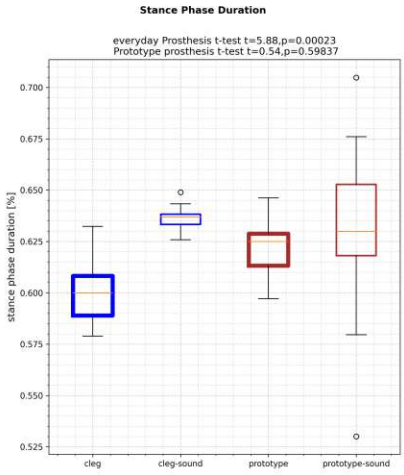

(a) The stance phase duration of the left (prosthetic) and right leg of Subject A with the prototype (brown) and everyday prosthesis (blue) can be seen.

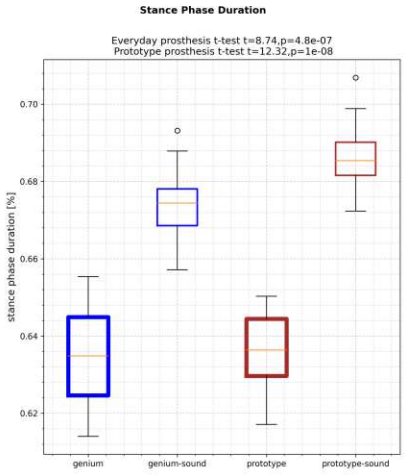

(b) The stance phase duration of the left (prosthetic) and right leg of Subject A with the prototype (brown) and everyday prosthesis (blue) can be seen.

Fig. 5.7: Stance phase duration for subject A and B for both prostheses and slow walking.

prosthesis compared to six areas while using the prototype prosthesis. When looking at the crucial foot clearance in the middle of the swing phase it can be seen that while using the everyday prosthesis the minimal foot clearance happens at 78% GC and 82% GC averaging 50mm and 55mm for the prosthetic and sound foot, respectively (see fig.5.10b). In the end the maxima are at slightly different points in time as well at 90% GC for the artificial foot compared to 95% GC for the sound foot. The values at this point are the same at 200mm. Looking at foot clearance for the prototype prosthesis temporal differences can be seen as well. The minimal foot clearance in the swing phase is occurring at 78% GC averaging 55mm on the prosthetic foot while on the sound side the minimum is happening later at 85% averaging roughly 50mm. Looking at the end of the gait cylce the maximum foot clearance is happening at 90% GC for the prosthetic side compared to 97% GC for the sound foot.

5.2.3.2 Fast walking

Subject A In figure 5.11 the foot clearance for subject A is plotted. For the prototype prothesis (fig.5.11a) it can be seen that the signals for the sound and prosthetic foot (pink and brown graphs, respectively) match very well in a temporal manner which is also indicated by just two small thresholds in the SMP{T} statistics. The foot clearance at around 80% GC is approximately 75mm for the prosthetic side compared to 50mm on the sound foot. The maxima at the end are for both feet happening at 95% GC but have different magnitudes of 180mm on the sound foot and 150mm on the prosthetic foot. For the everyday prosthesis an offset in temporal space can be observed (see fig.5.11b) between the prosthetic and sound leg. The foot clearance at approximately 80% GC is about 50mm for the everyday prosthesis compared to the foot clearance of the sound leg which is happening at 85% GC averaging 35mm. At the end of the GC the foot clearance for the prosthesis is higher than for the sound leg at approximately 190mm compared to 175mm and is happening earlier on the prosthetic limb at 90% compared to 95% GC.

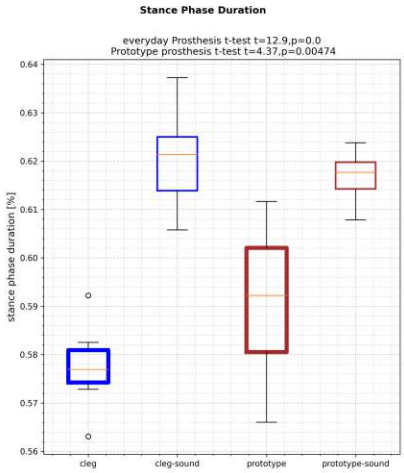

(a) The stance phase duration of the left (prosthetic) and right leg of Subject A with the prototype (brown) and everyday prosthesis (blue) can be seen.

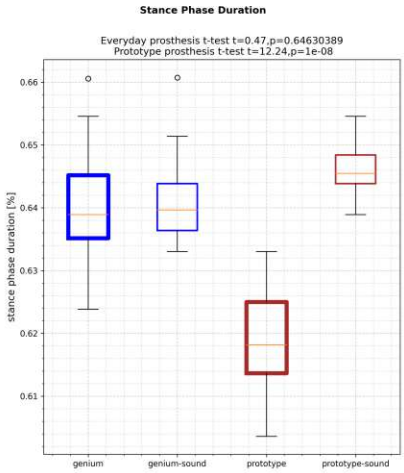

(b) The stance phase duration of the left (prosthetic) and right leg of Subject A with the prototype (brown) and everyday prosthesis (blue) can be seen.

Fig. 5.8: Stance phase duration for subject A and B for both prostheses and fast walking.

Subject B In figure 5.12 the foot clearance for the everyday and prototype prosthesis when walking fast can be seen. Looking at the SPM{t} analysis for the everyday prosthesis (see fig.5.12b) three areas of statistical differences can be seen, however, for the most part the signals fit well, especially in a temporal perspective. Looking at the crucial foot clearance in mid swing it can be noted that both minima are occurring at the same time at approximately 80% GC and are averaging 50mm for both limbs. At the end the maximum foot clearance is happening simultaneously at roughly 95% GC of 175mm and 225mm for the prosthetic and sound limb, respectively. The SPM{t} analysis when wearing the prototype shows five areas for which the signals are statistically different. The biggest deviations are occurring from 65% GC to 90% GC, hence in the swing phase. This can also be seen when looking at the values for the minimum foot clearance in mid swing, which is happening at 83% for both sides, but with approximately 40mm on the sound side and 80mm on the prosthetic side they are very different in magnitude. The maxima at the end of the swing phase are aligning well in a temporal perspective but have different values of 200mm for the prosthetic limb and 220mm for the sound limb.

5.2.4 Ankle Angles

5.2.4.1 Slow walking

Subject A Looking at the sagittal ankle angles in figure 5.13 it can be seen that the difference between the sound limb and the prosthetic limb is almost apparent everywhere except for two small regions at 55% to 60% and 65% to 70% GC for the everyday prosthesis (see fig.5.13b). When compared to the prototype prosthesis, the regions of statistically relevant difference become smaller, however, the signal for the sound limb shows big deviations, which influences the results (see fig.5.13a). For the everyday prosthesis the plantar-flexion angle reaches its maximum at approximately 10% and 5% for the prosthetic limb and sound limb, respectively, with maximum values of -27 and -37 degrees. After the maximum both feet are almost linearly moving into dorsal extension with the sound foot reaching a plateau at 30% GC while the prosthetic limb

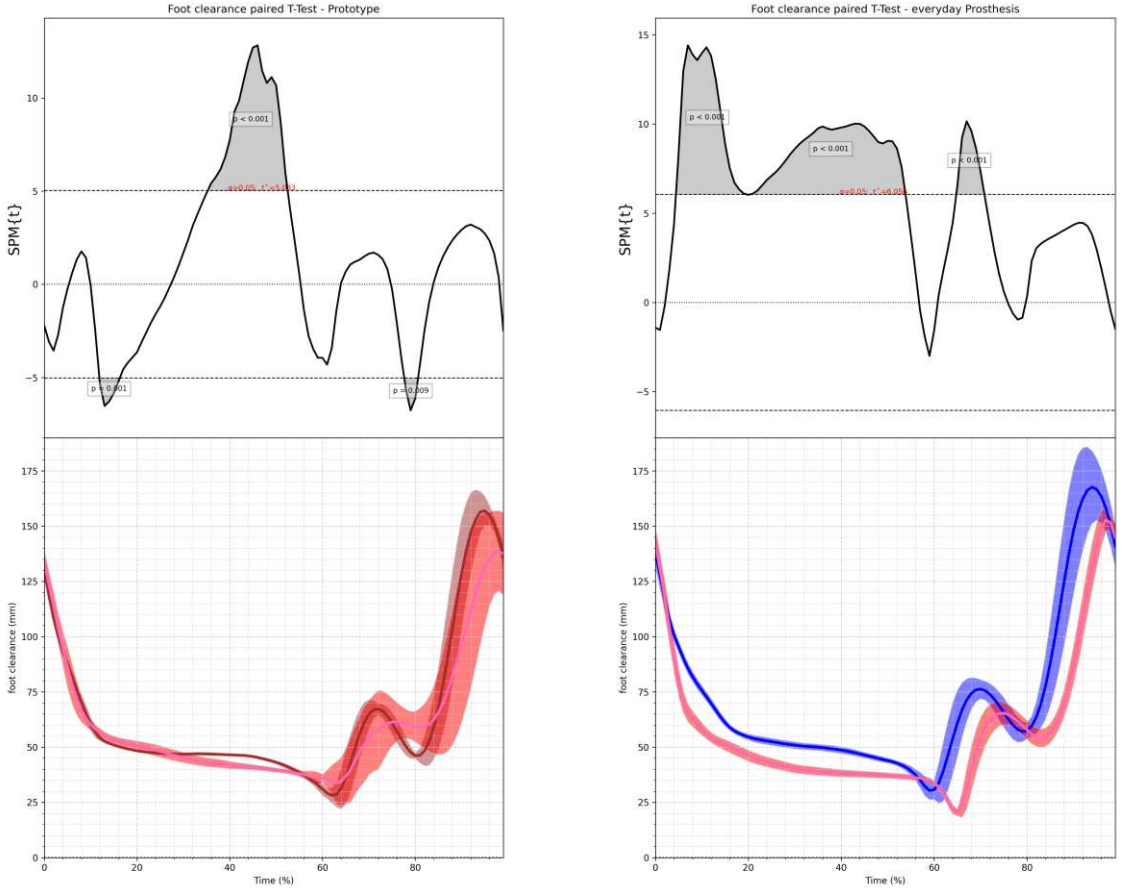

(a) At the top the SPM analysis of the foot clearance with the null hypothesis that both signals are equal can be seen. At the bottom the mean foot clearance with standard deviation is shown for the prototype prosthesis. The pink graph is showing the sound leg while the brown one is showing the prosthetic foot.

(b) At the top the SPM analysis of the foot clearance with the null hypothesis that both signals are equal can be seen. At the bottom the mean foot clearance with standard deviation is shown for the everyday prosthesis. The pink graph is showing the sound leg while the blue one is showing the prosthetic foot.

Fig. 5.9: Foot clearance for subject A, slow walking for both everyday and prototype prosthesis. The null hypothesis is that the clearance of the left and right foot are equal.

is still advancing into dorsal extension until 45% GC. After the plateau of the sound leg the dorsal extension continues until its maximum is reached at 45% GC which aligns well with the prosthetic limb. After the maximum both feet rapidly change direction and move into plantar flexion with the sound foot reaching a maximum angle of -37 degrees compared to the maximum of -30 degrees of the artificial foot. In the swing phase the movement in direction of dorsal extension can be observed for the sound ankle while the artificial ankle is showing almost no movement. The novel active prosthesis (see fig.5.13a) reaches its maximum plantar flexion angle of approximately -25 degrees at 10% GC which is almost the same for the sound foot, which has a maximum angle of -25 degrees at 8% GC. After that, both signals increase until a plateau in the prosthesis signal at around 30% GC is reached, after which the maximum dorsal flexion of -7 and -10 is achieved for the artificial ankle and the sound ankle, respectively, at 45 and 50% GC. The rapid change into plantar flexion can be observed in the prosthesis as well but does not reach such high values as the sound limb of -20 and and -32 degrees at 60% and 65%

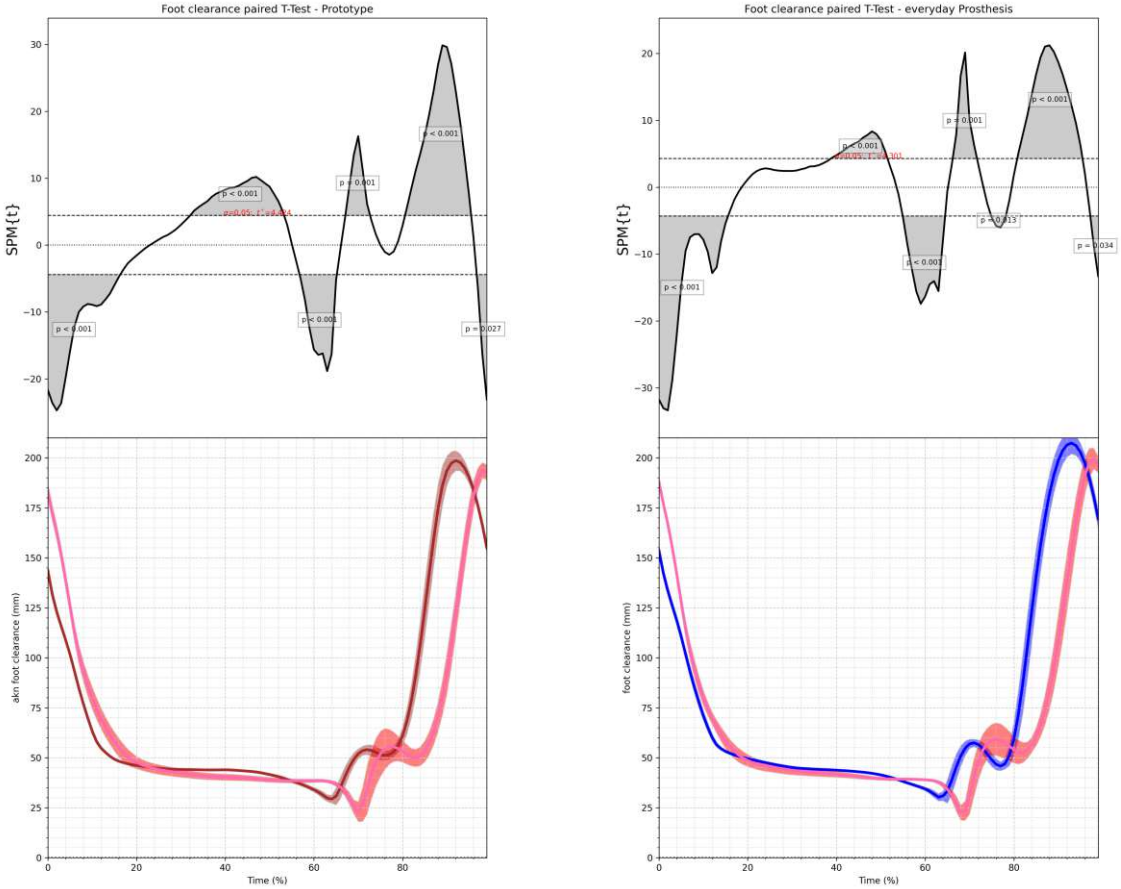

(a) At the top the SPM analysis of the foot clearance with the null hypothesis that both signals are equal can be seen. At the bottom the mean foot clearance with standard deviation is shown for the prototype prosthesis. The pink graph is showing the sound leg while the brown one is showing the prosthetic foot.

(b) At the top the SPM analysis of the foot clearance with the null hypothesis that both signals are equal can be seen. At the bottom the mean foot clearance with standard deviation is shown for the everyday prosthesis. The pink graph is showing the sound leg while the blue one is showing the prosthetic foot.

Fig. 5.10: Foot clearance for subject B, slow walking for both everyday and prototype prosthesis. The null hypothesis is that the clearance of the left and right foot are equal.

GC, respectively. After that, the artificial foot remains flat throughout the rest of the swing phase, while the sound foot is reversing its movement again. It can also be seen that although the prosthetic ankle is showing limited variation over the course of one GC the variations within the sound leg are significant, which is of course influencing the statistical evaluation as well. It is obvious that the signals are having an offset in the direction of plantar flexion as the ankle on the prosthetic side should ly remain neutral in the swing phase.

Subject B Figure 5.14 shows the sagittal ankle angle of subject B when walking slowly. It can be seen that when wearing either of the two prostheses the SPM{t} analysis shows only small regions of significant similarities. Looking at the angles when wearing the everyday prosthesis (see fig.5.14b) it can be observed that at the beginning the sound foot is slightly in dorsal flexion of 3 degrees compared to the prosthetic ankle, which shows no angle at all in the beginning and moves straight into plantar flexion angles. At approximately 18% GC both ankles reach

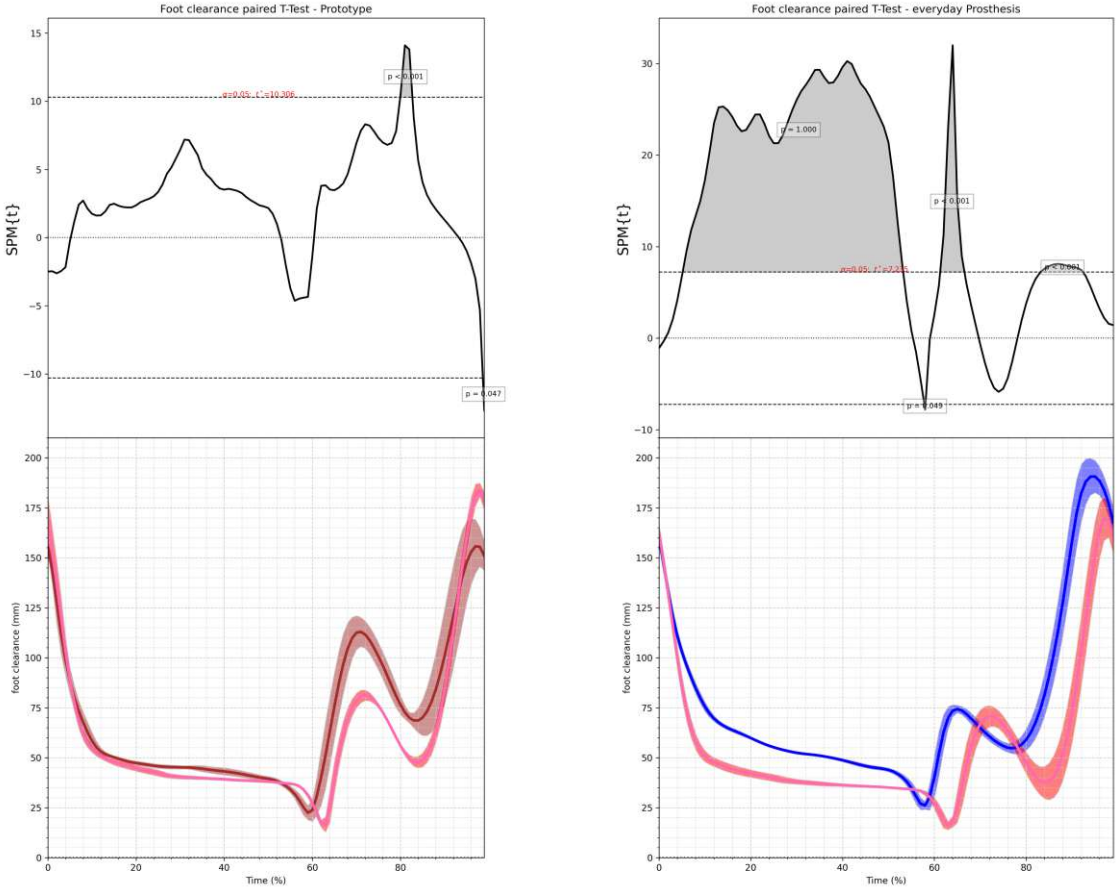

(a) At the top the SPM analysis of the foot clearance with the null hypothesis that both signals are equal can be seen. At the bottom the mean foot clearance with standard deviation is shown for the prototype prosthesis. The pink graph is showing the sound leg while the brown one is showing the prosthetic foot.

(b) At the top the SPM analysis of the foot clearance with the null hypothesis that both signals are equal can be seen. At the bottom the mean foot clearance with standard deviation is shown for the everyday prosthesis. The pink graph is showing the sound leg while the blue one is showing the prosthetic foot.

Fig. 5.11: Foot clearance for subject A, fast walking for both everyday and prototype prosthesis. The null hypothesis is that the clearance of the left and right foot are equal.

their stance phase maximum plantar flexion angle of -8 degrees on the prosthetic side and -5 degrees on the sound side. After that, both feet are moving into dorsal flexion until reaching their maximum angles of 15 degrees and 5 degrees for the prosthetic and sound ankle, respectively. Interestingly a slight decrease in the rate of angular changes can be seen on the prosthetic side at 30% GC. After the maximum in late stance the sound foot shows plantar flexion movement, but the prosthetic foot, being a passive device, stays flat throughout the swing phase. When wearing the prototype prosthesis (see fig.5.14a) it can be seen that at the beginning the sound ankle starts with 3 degrees of dorsal flexion compared to the prosthetic ankle, which starts in a neutral position and is moving straight into plantar flexion. Both reach their maximum plantar flexion angles at 10% GC of -8 degrees and -4 degrees for the prosthetic ankle and sound ankle, respectively. While the sound ankle is almost linearly moving into dorsal flexion until the maximum angle of 8 degrees at 58% GC, the prosthetic ankle shows a concave trajectory until 40% GC where it shortly remains at 10 degrees. After that, it moves linearly again until reaching

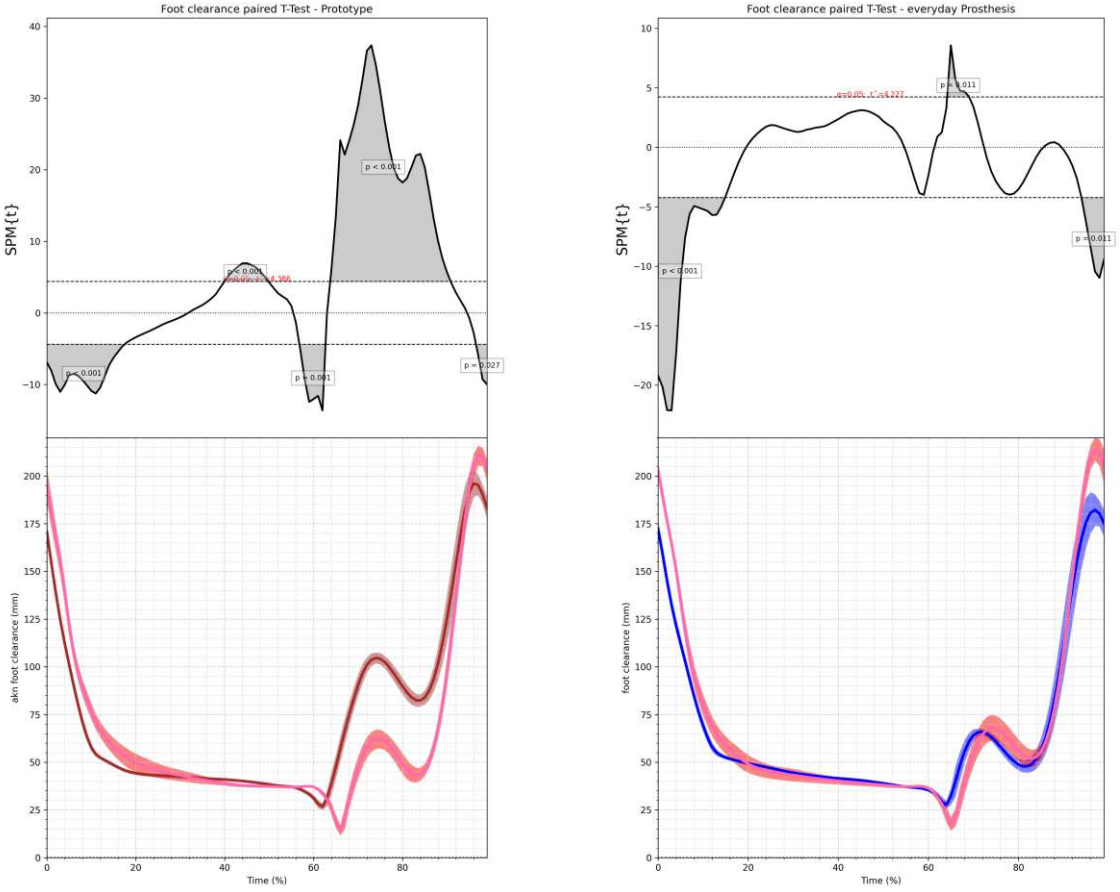

(a) At the top the SPM analysis of the foot clearance with the null hypothesis that both signals are equal can be seen. At the bottom the mean foot clearance with standard deviation is shown for the prototype prosthesis. The pink graph is showing the sound leg while the brown one is showing the prosthetic foot.

(b) At the top the SPM analysis of the foot clearance with the null hypothesis that both signals are equal can be seen. At the bottom the mean foot clearance with standard deviation is shown for the everyday prosthesis. The pink graph is showing the sound leg while the blue one is showing the prosthetic foot.

Fig. 5.12: Foot clearance for subject B, fast walking for both everyday and prototype prosthesis. The null hypothesis is that the clearance of the left and right foot are equal.

its maximum dorsal flexion angles of 15 degrees at 50% GC. In late stance the sound ankle is moving rapidly into maximum plantar flexion, which decreases until the end of the GC where the ankle becomes slightly dorsally flexed again to prepare for heelstrike. The prosthetic ankle on the other hand is a passive device and stays in a neutral position throughout the swing phase.

5.2.4.2 Fast walking

Subject A For fast walking the sagittal ankle angle for both prostheses for subject A can be seen in figure 5.15. Looking at the ankle when wearing the everyday prosthesis (see fig.5.15b) it can be seen that the both signals do not have big standard deviations and look very clean. The maximum plantar flexion at the beginning of the stance phase is at -40 degrees at 10% GC while it is -22.5 degrees at 8% for the sound ankle. After that, both angles are moving into dorsal extension almost linearly, however, the sound leg is soon reaching a plateau and decreases

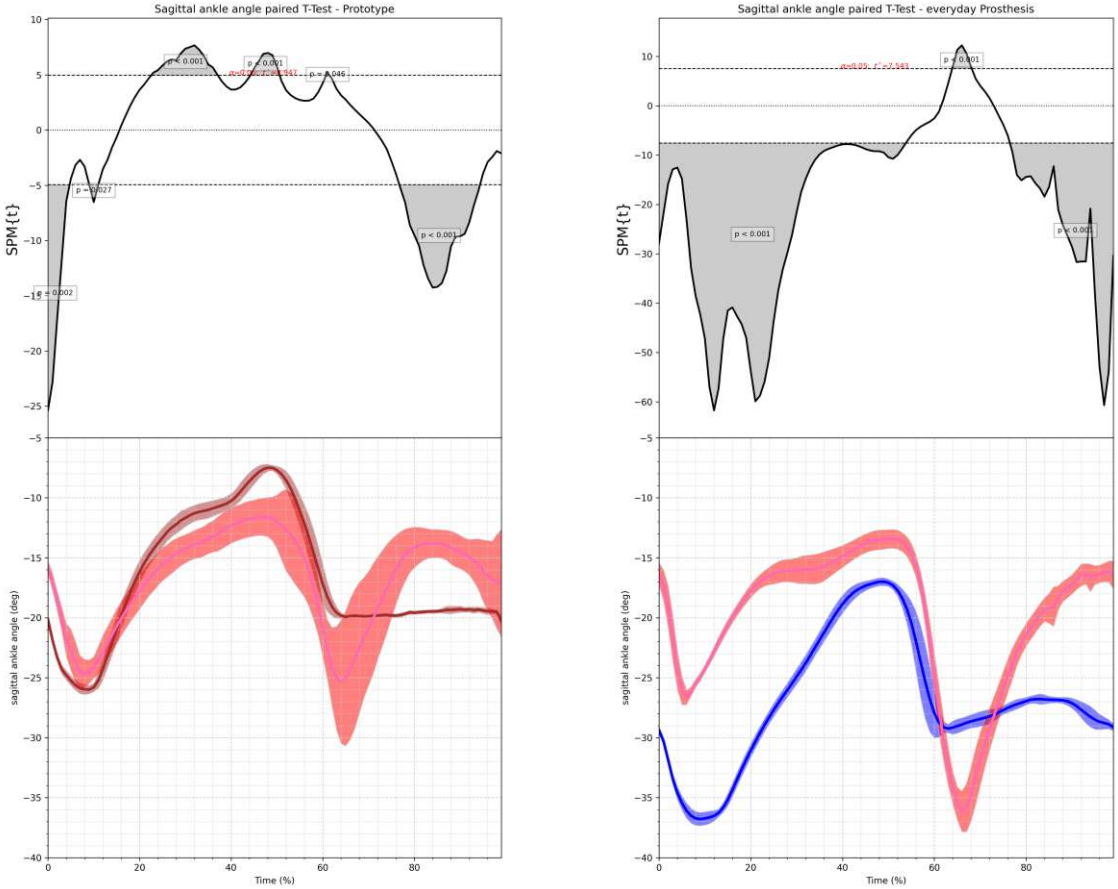

(a) At the top the SPM analysis of the ankle angle with the null hypothesis that both signals are equal can be seen. At the bottom the mean sagittal ankle angle with standard deviation is shown for the prototype prosthesis. The pink graph is showing the sound leg while the brown one is showing the prosthetic limb.

(b) At the top the SPM analysis of the ankle angle with the null hypothesis that both signals are equal can be seen. At the bottom the mean sagittal ankle angle with standard deviation is shown for the everyday prosthesis. The pink graph is showing the sound leg while the blue one is showing the prosthetic limb.

Fig. 5.13: Ankle angle for subject A, slow walking for both everyday and prototype prosthesis. The null hypothesis is that the angle of the left and right ankle are equal. Positive values correspond to dorsal flexion while negative values are plantar flexion angles.

again at 25% while the prosthesis is still moving into dorsal extension. After a short change of movement of the sound ankle the maximum dorsal extension of -10 degrees and -18 degrees is reached at 50% GC. The transition from stance to swing phase is then marked by a fast plantar flexion movement. The prosthetic leg stops at approximately -30 degrees while the sound leg continues to -43 degrees of plantar flexion angle at 60 and 65% GC, respectively. After that, the ankle is slowly returning to its initial position. For the prototype prosthesis (see fig.5.15a) the movement of the sound leg does not differ substantially from the movement of the sound leg when combined with the everyday prosthesis apart from the fact that the deviations are ever so slightly bigger. However, changes can be seen in the prosthetic limb starting off at reaching the maximum plantar flexion angle of -30 degrees at 8% GC, which aligns well with the sound leg. After that the slow change into dorsal flexion can be observed as well, but a decrease of the rate of change can be seen at approximately 30% GC in alignment with the inversion of the

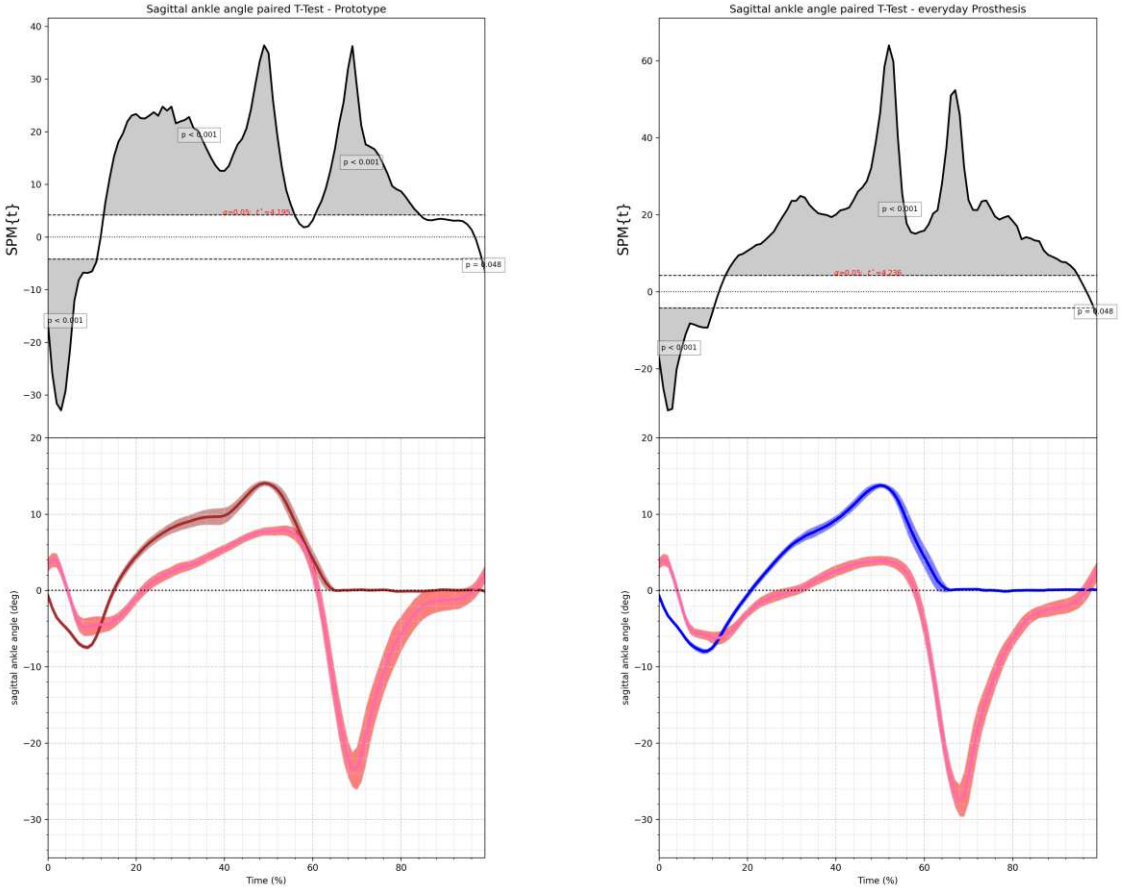

(a) At the top the SPM analysis of the ankle angle with the null hypothesis that both signals are equal can be seen. At the bottom the mean sagittal ankle angle with standard deviation is shown for the prototype prosthesis. The pink graph is showing the sound leg while the brown one is showing the prosthetic limb.

(b) At the top the SPM analysis of the ankle angle with the null hypothesis that both signals are equal can be seen. At the bottom the mean sagittal ankle angle with standard deviation is shown for the everyday prosthesis. The pink graph is showing the sound leg while the blue one is showing the prosthetic limb.

Fig. 5.14: Ankle angle for subject B, slow walking for both everyday and prototype prosthesis. The null hypothesis is that the angle of the left and right ankle are equal. Positive values correspond to dorsal flexion while negative values are plantar flexion angles.

movement of the sound foot which starts at 20% and continues until 37% GC. After that the maximum dorsal flexion is reached with -7 and -12 degrees at 50% GC. Until the end of the GC the sound ankle movement is almost equal to the everyday prosthesis reaching the maximum plantar flexion angle at 60% GC of -43 degrees. The prosthetic ankle is moving into plantar flexion as well but reaching a maximum of -20 degrees at 58% GC and does not change its angle in the swing phase afterwards. The SPM{t} results are revealing the differences between the prosthetic and sound limb of both settings. However, the everyday prosthesis shows significant differences almost all the time except for two small regions at the end of stance and mid swing phase. For the prototype, regions of significant differences are still large but the range where the signals fit become larger. However, the bigger standard deviation of the sound limb has to be kept in mind and is influencing the results. It is obvious that the signals are having an offset

in the direction of plantar flexion as the ankle on the prosthetic side should normally remain neutral in the swing phase.

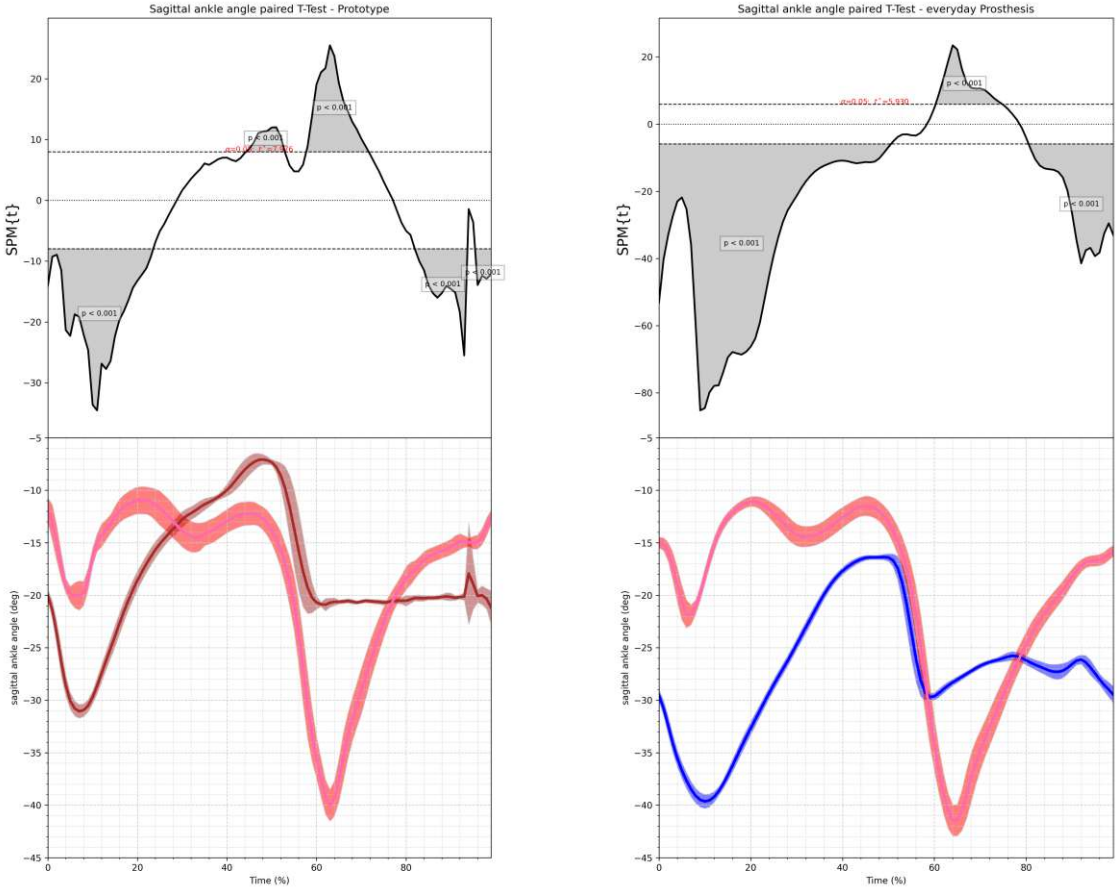

(a) At the top the SPM analysis of the ankle angle with the null hypothesis that both signals are equal can be seen. At the bottom the mean sagittal ankle angle with standard deviation is shown for the prototype prosthesis. The pink graph is showing the sound leg while the brown one is showing the prosthetic limb.

(b) At the top the SPM analysis of the ankle angle with the null hypothesis that both signals are equal can be seen. At the bottom the mean sagittal ankle angle with standard deviation is shown for the everyday prosthesis. The pink graph is showing the sound leg while the blue one is showing the prosthetic limb.

Fig. 5.15: ankle angle for subject A, fast walking for both everyday and prototype prosthesis. The null hypothesis is, that the angle of the left and right ankle are equal. Positive values correspond to dorsal flexion while negative values are plantar flexion angles.

Subject B The angle of the ankle in the sagittal plane of subject B when walking fast can be seen in figure 5.16. Similarly to the slow walking setting the SPM{t} results show only two small regions of significant agreement between the right and left ankle for both prostheses. Since the sound ankle is moving similarly when wearing either prostheses, both can be describes as one. At the beginning of the GC the sound ankle starts with 4 degrees of dorsal flexion and continues to move in the direction of dorsal flexion shortly afterwards until 3% GC. After that, the sound ankle changes its direction until the maximum plantar flexion angle of -4 degrees at 8% GC is reached. The movement into dorsal flexion starts after reaching the maximum and is decreased in speed at approximately 20% GC. Both stay almost at a constant angle of 3 degrees when

wearing the everyday prosthesis and 5 degrees when wearing the prototype prosthesis. At 55% GC both sound ankles move rapidly into plantar flexion reaching angles of -35 degrees which are reduced in a concave trajectory until final dorsal flexion of the ankle is preparing the foot for heel strike. The signals of the prosthetic ankles are slightly different. Both start in a neutral position and move into plantar flexion immediately after heel strike. When wearing the everyday prosthesis (see fig.5.16b) the maximum stance phase plantar flexion angle is reached at 12% GC of -10 degrees. After that, the ankle is moving almost linearly to the maximum dorsal flexion angle of 14 degrees at 50% GC. Looking at the ankle when wearing the prototype prosthesis (see 5.16a)it can be noted that the maximum plantar flexion angle occurs at 10% GC of -12 degrees. The movement is immediately reversed and the artificial ankle is moving fast into dorsal flexion. However, the fast movement is slowed down significantly at 20% GC and is only increasing again shortly before reaching the maximum dorsal flexion angle of 15 degrees at 50% GC. Both prosthetic ankles are passive devices which can be seen after their maximum angles in late stance where both decrease to a neutral position and remain there until the end of the gait cycle.

5.2.5 Knee Angles

5.2.5.1 Slow walking

Subject A In figure 5.17 the sagittal knee angle for subject A for the slow walking trails can be seen. Looking at the figures for the prototype prosthesis (5.17a) it is obvious that the null hypotheses of both angles being equal can not be confirmed. Statistically relevant difference occur until 50% of the GC and can only be neglected in early and late swing phase for both prostheses. Moreover, figure 5.17a shows that the prototype prosthetic knee joint is allowing stance phase flexion of approximately 15 degrees at 20% GC. For the sound limb it is apparent that stance phase flexion is non existent and around -8 degrees, which indicates a hyperextension of the sound knee joint. This could also be seen during the test session. Furthermore, the large distribution of the sound leg in contrast to the more controlled knee angle of the prosthetic leg in the swing phase of around 55% to 100% GC can be seen. An offset between the prosthesis and the sound knee angles is evident in both the prototype and the everyday prosthesis signals. Looking at the everyday prosthesis signals in figure 5.17b it becomes immediately apparent that this prosthesis is not able to allow as much stance phase flexion as the prototype averaging only 8 degrees at around 20% GC. On the other hand, both knee angle signals have only small divergences in contrast to the sound limb when using the prototype. The timing of the maximum knee flexion angle in swing phase is slightly later in the sound compare to the prosthetic leg at 75% GC and 70%, respectively. Both devices are already fully extended at 90% GC compared to the sound knee angles that are still in an extending movement.

Subject B Looking at the sagittal knee angles of subject B when walking slowly (see fig.5.18) it can be noted that for the most part the SPM{t} analysis is recordings statistically relevant differences. Looking directly at the angles when using the everyday prosthesis (see fig.5.18a) it can be seen, that the prosthetic knee joint is in a flexed position of 5 degrees in the beginning and is almost immediately increasing flexion until reaching a plateau of 10 degrees of flexion from 15% to 30% GC. The sound knee joint starts the gait cycle in extension of -4 degrees and is progressing into flexion at 10% reaching its peak stance phase flexion of 10 degrees at 25% GC. After both knee joints reached their maximum flexion angles both decrease their angles with the sound leg staying slightly flexed at 55% GC while the prosthetic knee becomes extended moderately. Because the artificial knee joint is progressing faster into maximum swing phase flexion, it reaches its maximum earlier at 70% GC of 65 degrees compared to at 78% of 55 degrees.

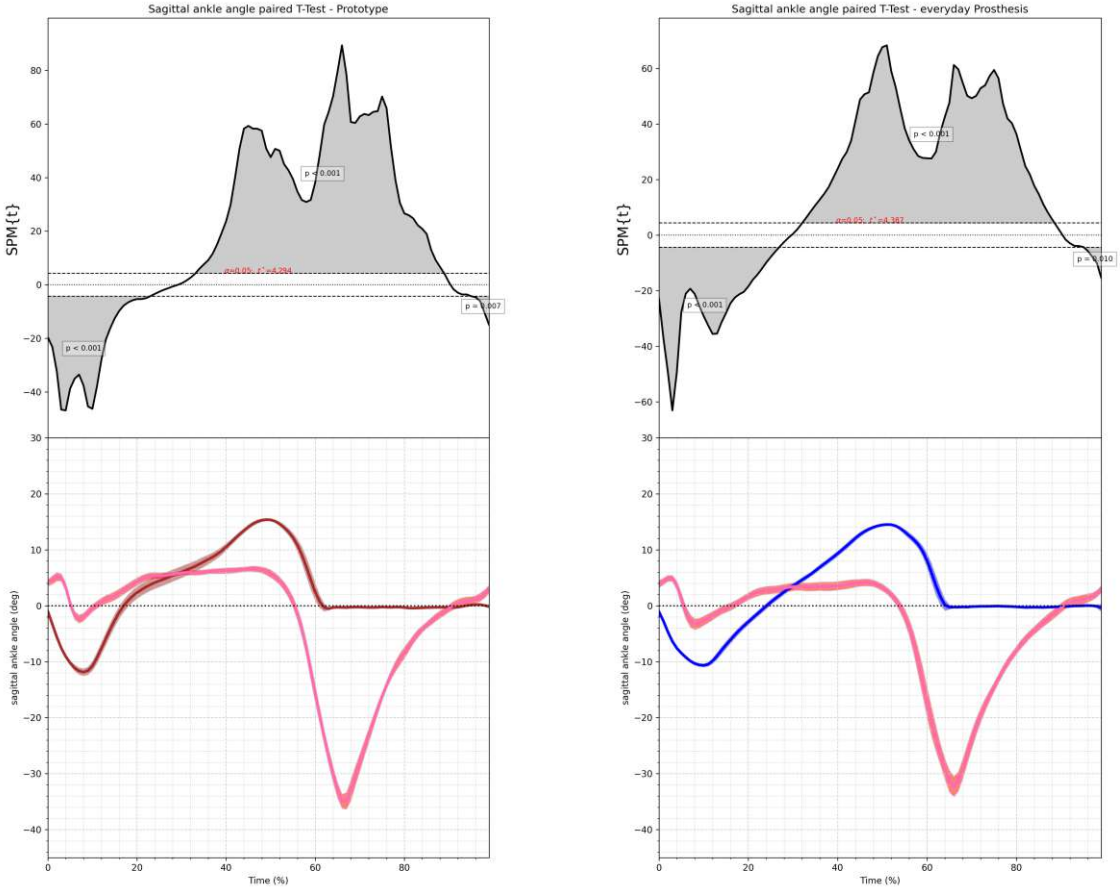

(a) At the top the SPM analysis of the ankle angle with the null hypothesis that both signals are equal can be seen. At the bottom the mean sagittal ankle angle with standard deviation is shown for the prototype prosthesis. The pink graph is showing the sound leg while the brown one is showing the prosthetic limb.

(b) At the top the SPM analysis of the ankle angle with the null hypothesis that both signals are equal can be seen. At the bottom the mean sagittal ankle angle with standard deviation is shown for the everyday prosthesis. The pink graph is showing the sound leg while the blue one is showing the prosthetic limb.

Fig. 5.16: ankle angle for subject B, fast walking for both everyday and prototype prosthesis. The null hypothesis is that the angle of the left and right ankle are equal. Positive values correspond to dorsal flexion while negative values are plantar flexion angles.

When both knees have reached their maxima, their flexion angles are decreasing, which ends with a flexion angle of 5 degrees at 85% GC on the prosthetic side and with an extension angle of -10 degrees at 95% GC on the sound side. When wearing the prototype prosthesis (see fig.5.18a) a flexion angle of the artificial knee of 8 degrees compared to a extension angle of -5 degrees of the sound knee can be observed. Shortly after initial contact the prosthetic knee is increasing its flexion following a convex path until the maximum stance phase flexion angle of 18 degrees at 17% GC is reached. The sound knee on the other hand moves in an almost linear fashion with two different inclinations into its peak stance phase flexion of 10 degrees at 20% GC. After both reaching their maxima the angles are decreasing again until the prosthetic knee joint is in a neutral position at 40% GC and the sound side is reaching a flexion angle of 3 degrees at 50% GC. After that, both are increasing their flexion angle rapidely, however, the artificial knee has a steeper inclination, resulting in a maximum swing phase flexion angle of 65 degrees at 72%

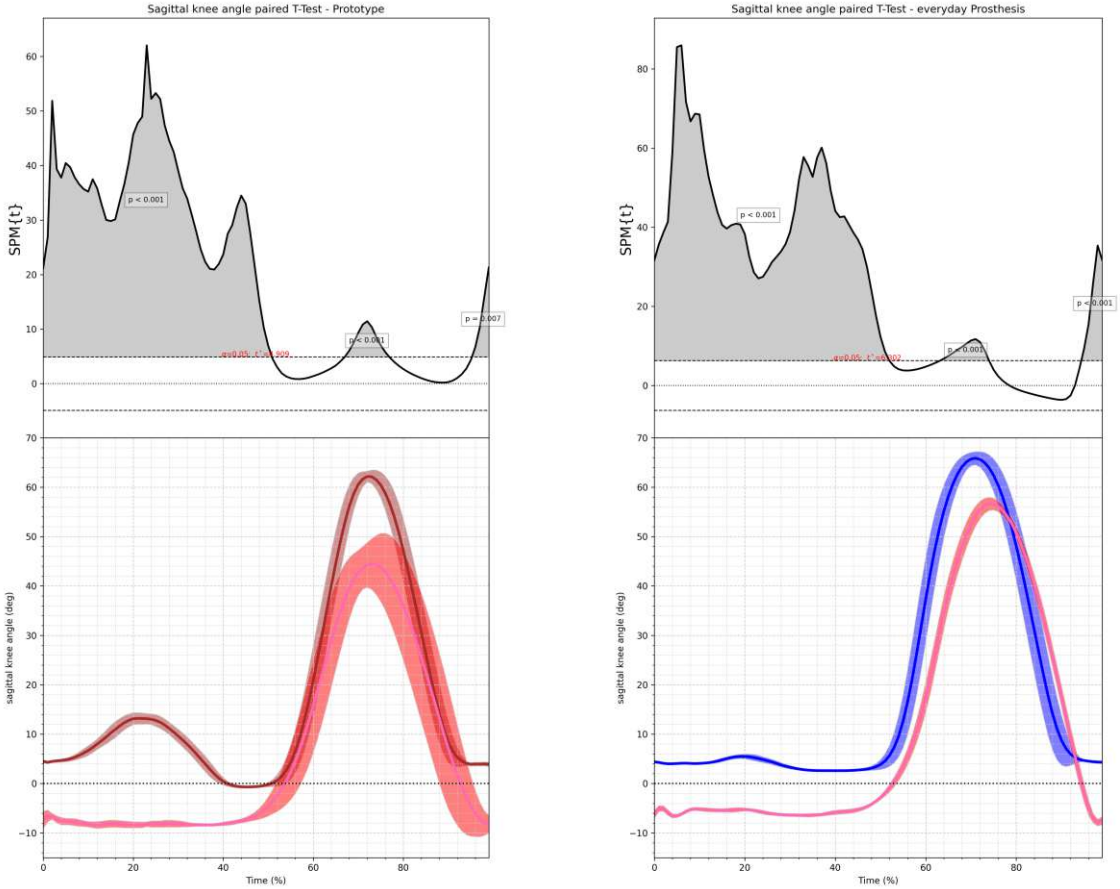

(a) At the top the SPM analysis of the knee angle with the null hypothesis that both signals are equal can be seen. At the bottom the mean sagittal knee angle with standard deviation is shown for the prototype prosthesis. The pink graph is showing the sound leg while the brown one is showing the prosthetic limb.

(b) At the top the SPM analysis of the knee angle with the null hypothesis that both signals are equal can be seen. At the bottom the mean sagittal knee angle with standard deviation is shown for the everyday prosthesis. The pink graph is showing the sound leg while the blue one is showing the prosthetic limb.

Fig. 5.17: Knee angle for subject A, slow walking for both everyday and prototype prosthesis. The null hypothesis is that the angle of the left and right knee are equal. Positive values correspond to flexion of the knee while negative values are extension angles.

GC compared to the sound knee, which reaches its maximum of 65 degrees at 78% GC. After that, both angles are decreasing at a similar rate, but the artificial knee is coming to a stop at a flexion angle of 8 degrees at 90% GC in contrast to the sound knee which is reaching a extension angle of -10 degrees at 95% GC.

5.2.5.2 Fast walking

Subject A In contrast to the sound limb sagittal knee angles in slow walking (see fig.5.17), in fast walking (see fig. 5.19) a stance phase flexion with a maximum flexion angle at approximately 15% GC of 20 degrees for the sound limb can be seen. Looking at the stance phase flexion it becomes immediately apparent that the everyday prosthesis is not able to allow more than a few degrees of flexion while the prototype prosthesis is able to produce approximately 18

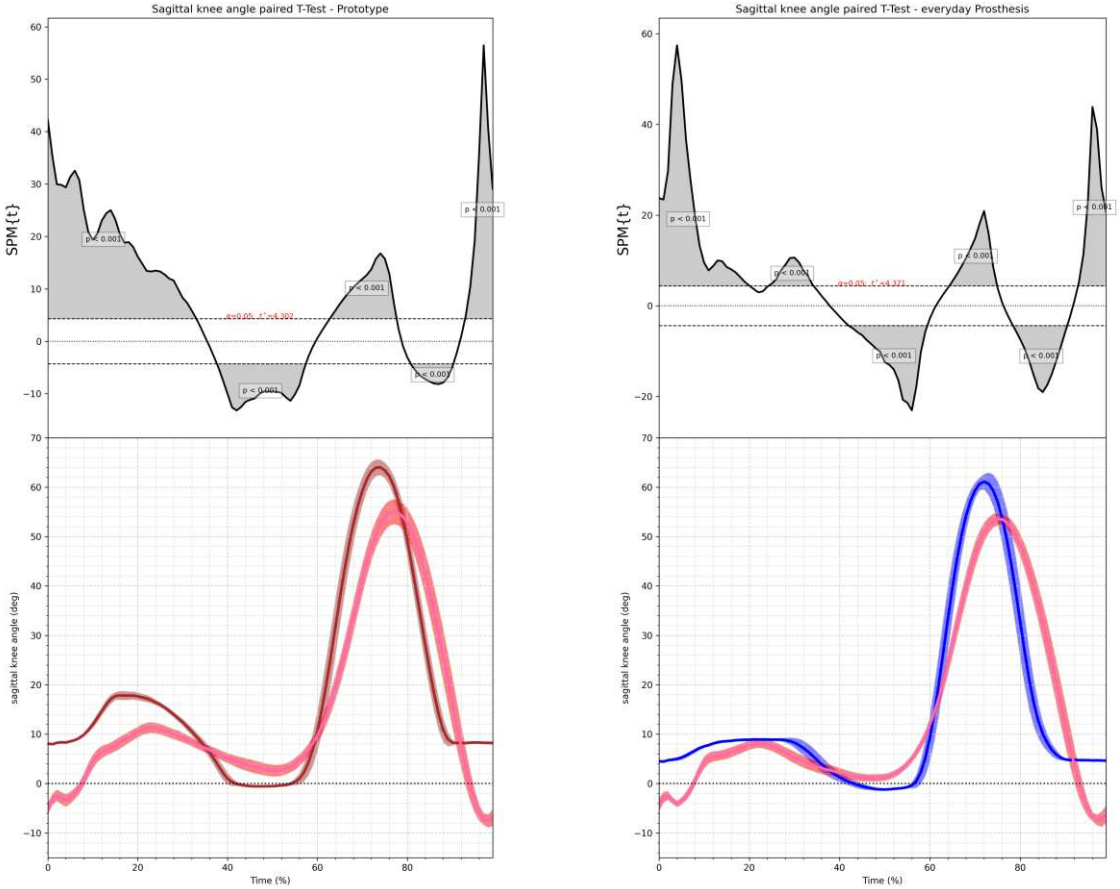

(a) At the top the SPM analysis of the knee angle with the null hypothesis that both signals are equal can be seen. At the bottom the mean sagittal knee angle with standard deviation is shown for the prototype prosthesis. The pink graph is showing the sound leg while the brown one is showing the prosthetic limb.

(b) At the top the SPM analysis of the knee angle with the null hypothesis that both signals are equal can be seen. At the bottom the mean sagittal knee angle with standard deviation is shown for the everyday prosthesis. The pink graph is showing the sound leg while the blue one is showing the prosthetic limb.

Fig. 5.18: Knee angle for subject B, slow walking for both everyday and prototype prosthesis. The null hypothesis is that the angle of the left and right knee are equal. Positive values correspond to flexion of the knee while negative values are extension angles.

degrees of flexion at 20%. Additionally it can be seen that the sound leg is in hyperextension at the beginning, late stance and at the end of the GC for both setups. Both prostheses have a maximum swing flexion angle of around 70 degrees but at different points in time. While the everyday prosthesis is already achieving its maximum at roughly 65% GC, which does not align well with the sound limbs maximum occuring at 75% GC, the novel active prosthesis reaches its maximum at approximately 70%, which aligns well with the sound limb. At the end of the GC of the prototype prosthesis the knee angle of the artificial knee is still in an extending movement, while the every day prosthesis already finished the extending movement at 90% GC and prepared for heel strike. The knee angles of both prostheses have an offset in the flexion direction of the angle of approximately five degrees. Both SPM{t} statistical results show substantial differences. For the everyday prosthesis significant differences between the two signals affect almost the whole GC with only short periods at the beginning of stance phase, mid stance and mid swing, where

the signals can be seen as statistically equal. The signals for the prototype prosthesis do align better as can be seen in the SPM{t} results, however, statistical differences can still be seen during the majority of the GC, especially at mid to late stance, mid swing and at the end of the swing phase.

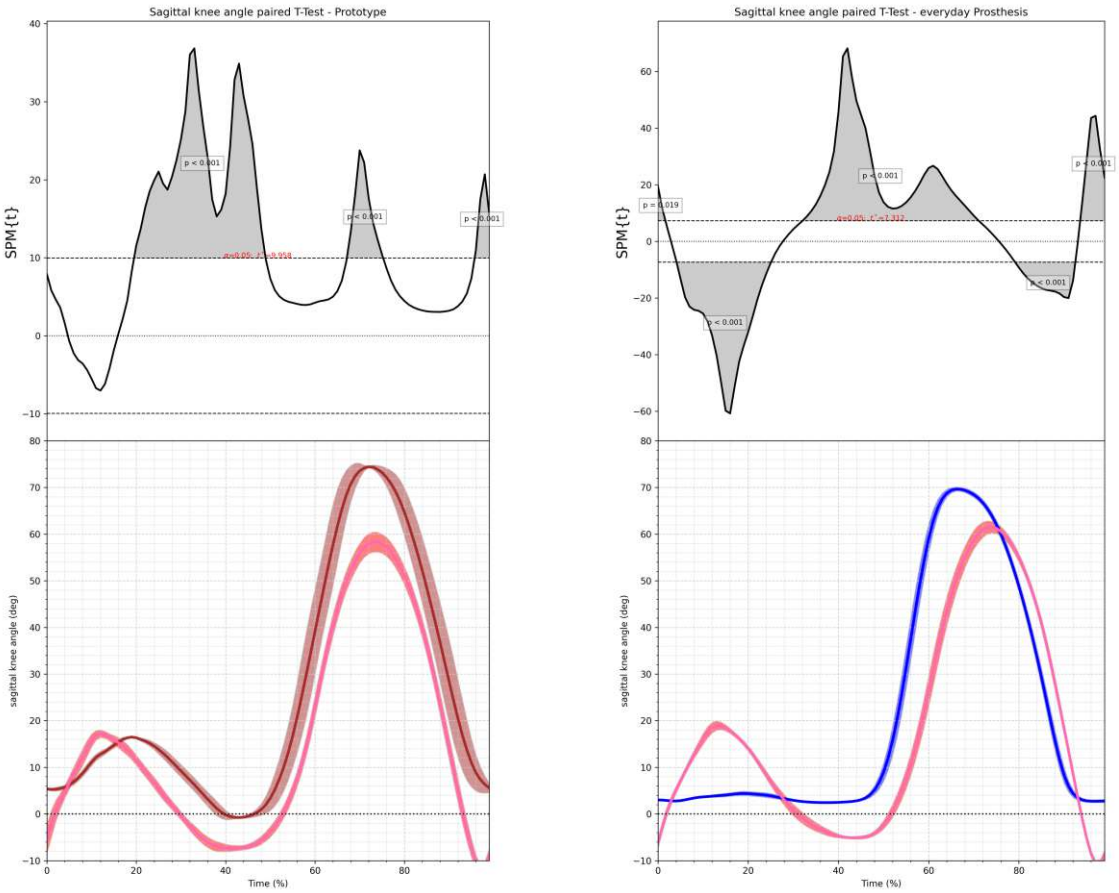

(a) At the top the SPM analysis of the knee angle with the null hypothesis that both signals are equal can be seen. At the bottom the mean sagittal knee angle with standard deviation is shown for the prototype prosthesis. The pink graph is showing the sound leg while the brown one is showing the prosthetic limb.

(b) At the top the SPM analysis of the knee angle with the null hypothesis that both signals are equal can be seen. At the bottom the mean sagittal knee angle with standard deviation is shown for the everyday prosthesis. The pink graph is showing the sound leg while the blue one is showing the prosthetic limb.

Fig. 5.19: Knee angle for subject A, fast walking for both everyday and prototype prosthesis. The null hypothesis is that the angle of the left and right knee are equal. Positive values correspond to flexion of the knee while negative values are extension angles.

Subject B In figure 5.20 the sagittal knee angles of the artificial and sound knee while walking fast can be seen. Looking at the angles when wearing the prototype prosthesis (5.20a) it can be observed, that at the beginning of the gait cycle the artificial knee is flexed with an angle of approximately 5 degrees while the sound knee begins the gait cycle extended at an angle of -5 degrees. After that, both knees are moving towards their maximum stance phase flexion of 18 degrees at 20% GC for the prosthetic leg and 23 degrees from 15% GC to 25% GC. After that, both are decreasing their flexion angle simultaneously until they both reach a neutral position

at 55% GC. In swing phase, the artificial knee joint is moving fast, which results in a higher maximum flexion angle of 80 degrees compared to 60 degrees of the sound knee. When both knees have reached their maxima the knees are reducing their angles again until reaching 5 degrees of flexion at 95% GC and -10 degrees of extension at 95% GC for the prosthetic and sound knee, respectively. The movement on the sound side (see fig.5.20b) when using the everyday prosthesis closely resembles the movement of the sound knee when wearing the prototype. However, the artificial knee joint shows differences. At the beginning the flexion angle is 5 degrees and is increasing, beginning at 10% GC, until reaching a plateau at 15% GC of 10 degrees. At 30% GC the flexion angle of the prosthetic knee is decreasing again until reaching a neutral position at 45% GC, which is remained until 55% GC. The maximum swing phase flexion angle is approximately 70 degrees at 78% GC. After reaching the maximum flexion angle the knee is moving into its starting position, which is reached at 95% GC.

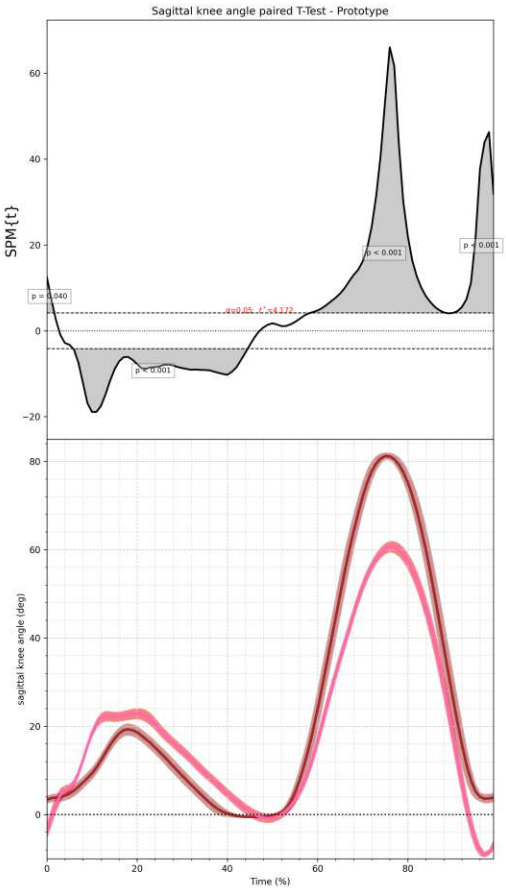

(a) At the top the SPM analysis of the knee angle with the null hypothesis that both signals are equal can be seen. At the bottom the mean sagittal knee angle with standard deviation is shown for the prototype prosthesis. The pink graph is showing the sound leg while the brown one is showing the prosthetic limb.

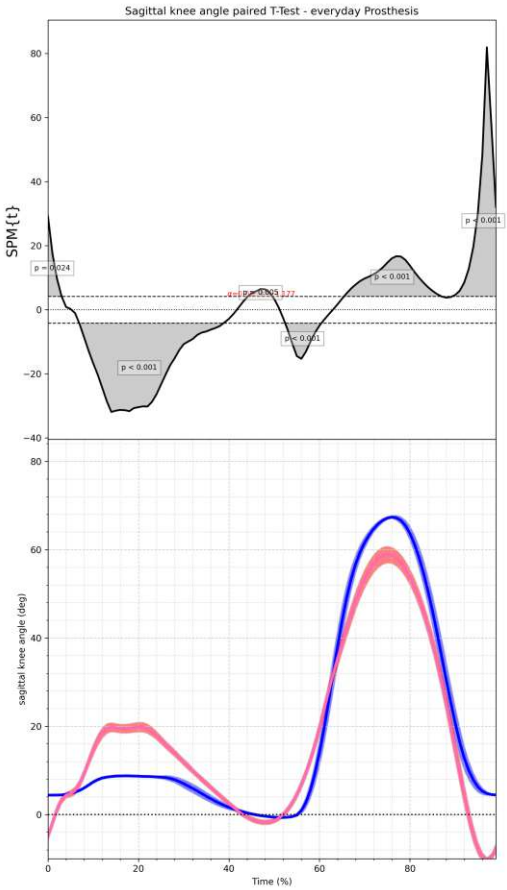

(b) At the top the SPM analysis of the knee angle with the null hypothesis that both signals are equal can be seen. At the bottom the mean sagittal knee angle with standard deviation is shown for the everyday prosthesis. The pink graph is showing the sound leg while the blue one is showing the prosthetic limb.

Fig. 5.20: Knee angle for subject B, fast walking for both everyday and prototype prosthesis. The null hypothesis is that the angle of the left and right knee are equal. Positive values correspond to flexion of the knee while negative values are extension angles.

5.2.6 Hip Angles

5.2.6.1 Slow walking

Subject A Figure 5.21 shows the sagittal hip angle of the sound and prosthetic leg for both settings using the everyday and the prototype prosthesis. At the beginning of the stance phase (see fig.5.21b) both angles are similar for the everyday prosthesis, reaching 19 and 17 degrees at zero percent GC. After that, both decrease steadily up to a maximum extension angle of -18 degrees at 50% GC for both limbs. The movement into flexion can be seen as equal between both limbs, differing only at the last 25% of the GC where the sound limb is still moving into flexion to a maximum of 21 degrees at 85% GC while the maximum of the prosthetic leg was reached at 75% GC and is decreasing until 85% GC only to increase again in late swing phase. At the beginning of the prototype prosthesis (see fig.5.21a) angles it is obvious that compared to the everyday prosthesis the prototype is starting the GC with a higher flexion angle of 20 degrees compared to the sound limb of 15 degrees. After that, the movement into extension is almost linear on the prosthetic side while for the sound leg it slows down around 30% GC until it reaches it maximum of -15 degrees at 57% GC. On the side of the prosthetic limb a maximum extension angle of -20 degrees is reached also at 57% GC. After that, the movement is changing into flexion and it becomes apparent that the change into flexion is more rapid on the prosthetic side, compared to the sound leg. While the prosthetic leg reaches its maximum swing flexion angle at 80% GC the sound leg reaches its maximum angle later at 95% GC. These differences can also be seen when looking at the SPM{t} curves at the top of each signal pairing. For the prototype prosthesis the signals are rarely comparable and only for brief sections at mid to late stance and early swing can be seen as equal. Although the signals are quite different for the everyday prosthesis as well, the SPM{t} values that are above the significance level appear to be slightly smaller and similarity can be found at early stance, late stance to early swing, mid and late swing phase.

Subject B The sagittal hip angle of the prosthetic and sound limb can be seen in figure 5.22. It can be seen that when wearing the everyday prosthesis (see fig.5.22) the SPM{t} analysis shows only three areas where the signals can be seen as statistically equal. Starting with approximately 30 degrees of hip flexion on the prosthetic side, the angle is steadily decreasing afterwards until it reaches its maximum extension angle of -8 degrees at 60% GC. While the hip on the sound side is starting with 30 degrees of flexion as well, it is not decreasing steadily. Instead a short plateau can be seen from 5 to 10% GC where the angle is kept constant at 28 degrees. After that, it continues to decrease in a linear fashion until an extension angle of -10 degrees is reached at 60% GC. After that, both sides are changing into flexion again. The hip on the sound side is reaching its maximum flexion angle of the swing phase at 85% GC while the hip of the prosthetic limb is increasing its flexion angle faster, reaching 30 degrees at 75% GC. Afterwards the angle shortly decreases only to increase again and averaging 35 degrees at 90% GC. When wearing the prototype prosthesis (see fig5.22a) both hips start with an angle of 28 degrees of flexion. The hip of the prosthetic limb is linearly decreasing afterwards, until the maximum extension angle of -10 degrees at 57% GC is reached. The movement of the hip on the sound side is almost similar, except that from 5% to 10% GC the flexion angle is kept constant at 27 degrees. The maximum extension angle of the hip on the sound side is -10 degrees at 60% GC. After both hips have reached their maximum extension angle, they rapidly change into flexion reaching their maximum swing phase flexion angle of 27 degrees at 85% GC on the sound side and 35 degrees at 80% GC on the prosthetic side. In contrast to the hip on the sound side which stays at an almost constant flexion angle until the end of the gait cycle, the other hip is decreasing its

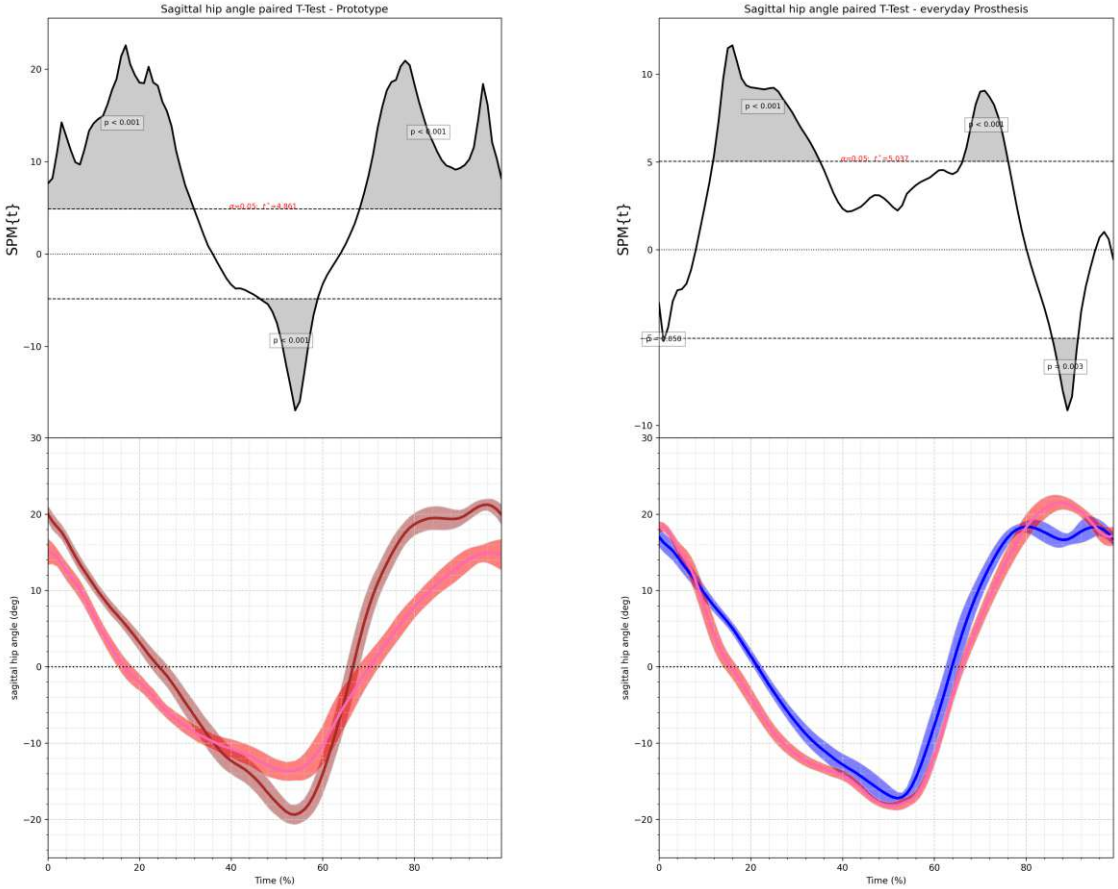

(a) At the top the SPM analysis of the hip angle with the null hypothesis that both signals are equal can be seen. At the bottom the sagittal hip angle with standard deviation is shown for the prototype prosthesis. The pink graph is showing the sound leg while the brown one is showing the prosthetic limb.

(b) At the top the SPM analysis of the hip angle with the null hypothesis that both signals are equal can be seen. At the bottom the mean sagittal hip angle with standard deviation is shown for the everyday prosthesis. The pink graph is showing the sound leg while the blue one is showing the prosthetic limb.

Fig. 5.21: Hip angle for subject A, slow walking for both everyday and prototype prosthesis. The null hypothesis is that the angle of the left and right hip are equal. Positive values are representing flexion angles while negative values correspond to extension angles.

flexion angle shortly reaching a second maximum of 35 degrees at 90% GC. After that, the angle is decreasing again until the end of the gait cycle.

5.2.6.2 Fast walking

Subject A The sagittal hip angle of the fast walking condition can be seen in figure 5.23. Looking at the SPM{t} values it can be observed that the two hip angles of the prototype setting (see fig.5.23a) are aligning good in early stance (1% to 5% GC), mid stance (10% to 20% GC) and late stance to mid swing (30% to 80% GC), compared to the everyday prosthesis (see fig.5.23b) for which the alignment between both limbs is good from 20%-30%, 65%-80% and 90%-100% GC. This becomes also apparent when looking at the actual hip angle signals. Beginning with

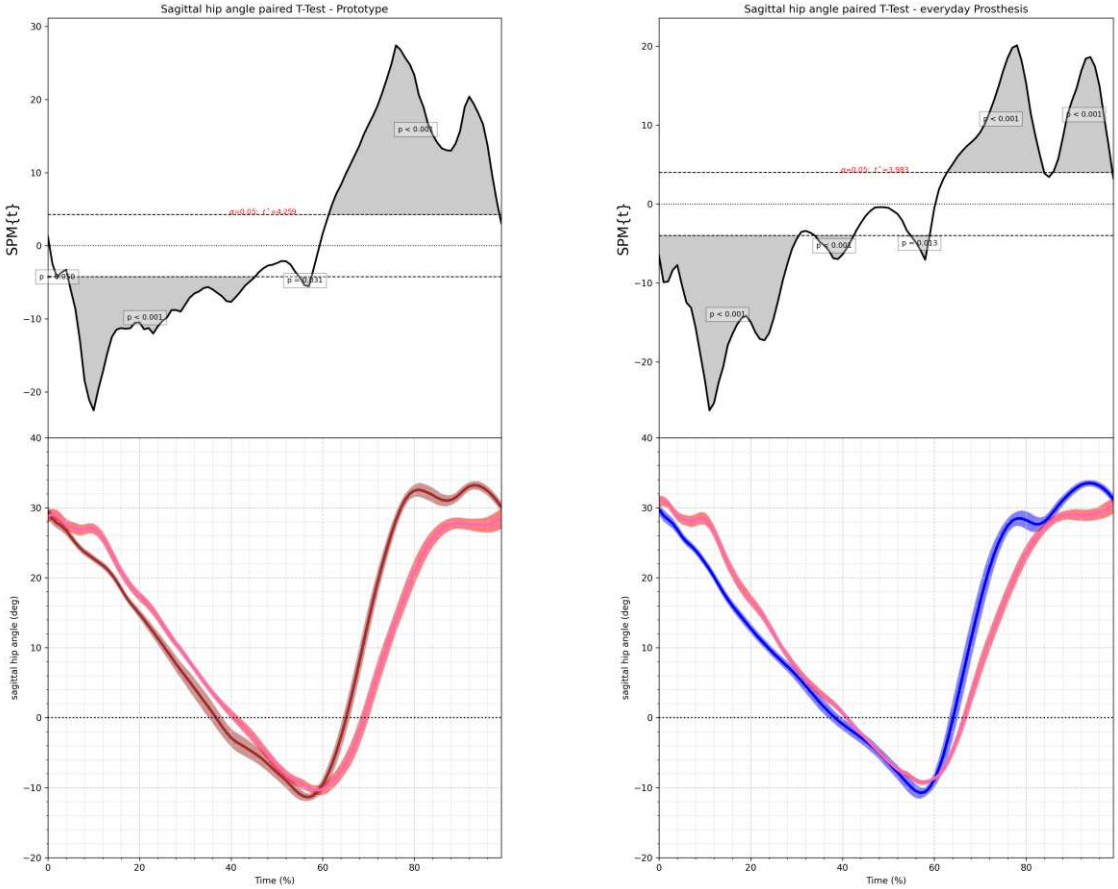

(a) At the top the SPM analysis of the hip angle with the null hypothesis that both signals are equal can be seen. At the bottom the sagittal hip angle with standard deviation is shown for the prototype prosthesis. The pink graph is showing the sound leg while the brown one is showing the prosthetic limb.

(b) At the top the SPM analysis of the hip angle with the null hypothesis that both signals are equal can be seen. At the bottom the mean sagittal hip angle with standard deviation is shown for the everyday prosthesis. The pink graph is showing the sound leg while the blue one is showing the prosthetic limb.

Fig. 5.22: Hip angle for subject B, slow walking for both everyday and prototype prosthesis. The null hypothesis is that the angle of the left and right hip are equal. Positive values are representing flexion angles while negative values correspond to extension angles.

the heel strike of the prototype setting where the prosthetic limb is reaching 28 degrees of flexion and is decreasing instantly compared to the sound limb whose hip angle is increasing until 10% GC reaching a maximum of 25 degrees of flexion. After that, both hips are equally decreasing until 55% GC with a maximum extension angle of -25 degrees. In contrast to the rate of change in stance phase, the changing rate in the swing phase is different for both limbs. The prosthetic limb is changing faster into swing flexion, which is peaking at a value of 28 degrees at 90% GC, while the sound leg is reaching a maximum flexion angle of 20 degrees at 90% GC. After that, both angles are steadily decreasing with a small change of direction at the last percent of the GC at the sound leg. Looking at the setting with the everyday prosthesis it can be seen that the maximum flexion angle of the prosthetic leg is smaller at 20 degrees compared to 23 degrees of the sound leg at initial contact. While the angle is still increasing on the sound limb, reaching its

maximum at 5% GC of 27 degrees after initial contact, it is immediately moving into extension at the prosthetic leg. Both limbs are moving into extension almost linearly but the sound limb is changing its direction faster which results in a bigger maximum extension angle of -25 degrees at 50% GC compared to the prosthetic limb's angle of -20 degrees at 53% GC. After that, both limbs are moving into flexion in an almost linear fashion, with the sound leg displaying a faster rate of change. The maximum swing flexion angle is therefore 27 degrees at 85% GC compared to 20 degrees at 80% GC of the prosthetic limb. At late swing it can be observed that the flexion angle is slightly decreasing and increasing again which can also be seen on the sound leg but shifted in time. The two peaks at the end are both happening in late swing on the prosthetic side, while for the sound leg the two peaks are at late swing and early stance.

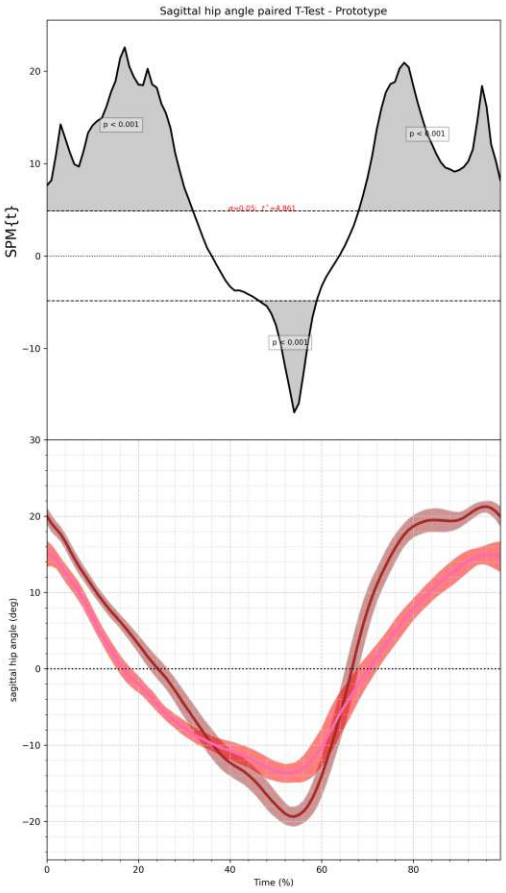

(a) At the top the SPM analysis of the hip angle with the null hypothesis that both signals are equal can be seen. At the bottom the sagittal hip angle with standard deviation is shown for the prototype prosthesis. The pink graph is showing the sound leg while the brown one is showing the prosthetic limb.

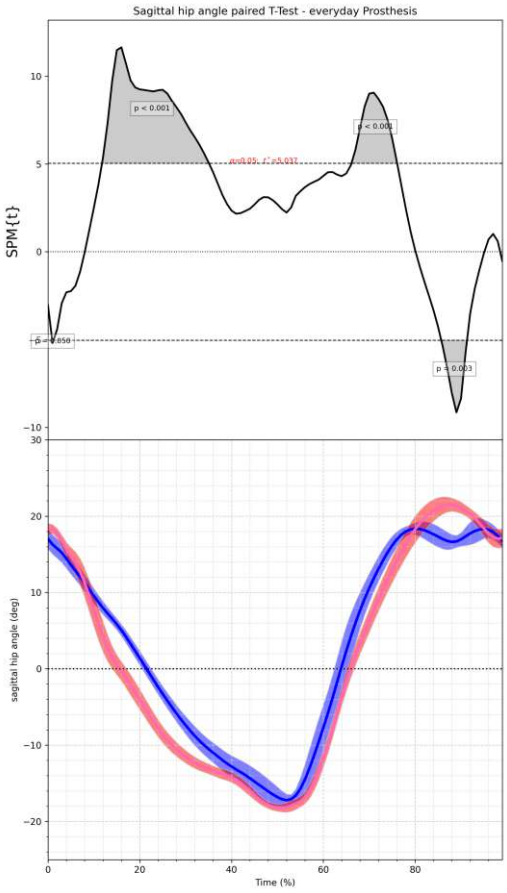

(b) At the top the SPM analysis of the hip angle with the null hypothesis that both signals are equal can be seen. At the bottom the mean sagittal hip angle with standard deviation is shown for the everyday prosthesis. The pink graph is showing the sound leg while the blue one is showing the prosthetic limb.

Fig. 5.23: Hip angle for subject A, fast walking for both everyday and prototype prosthesis. The null hypothesis is that the angle of the left and right hip are equal. Positive values are representing flexion angles while negative values correspond to extension angles.

Subject B In figure 5.24 the sagittal hip angle for fast walking can be seen. Looking at the angles when the everyday prosthesis is worn, it can be observed (see fig.5.24b) that there are four areas where the signals can not be seen as statistically equal. The first section is easily recognisable, because although the hip on the prosthetic side is starting with a flexion angle of 35 degrees equal to the hip on the opposite side, it is steadily decreasing until reaching its maximum extension angle of -12 degrees at 55% GC. On the other hand, the hip on the sound side is increasing its flexion slightly to 38 degrees after the initial flexion, subsequently decreases to 35 degrees at 5% GC and increases again to 38 degrees at 10% GC, before it starts to decrease until the maximum flexion angle is matching the angle of the other side at 55% GC. In the swing phase the angles are revised and both hips do so in a similar way, reaching maximum swing phase flexion angles of 35 degrees at 85% GC. After a short decrease of both angles the flexion angles increase to 38 degrees again at the end of the gait cycle. When wearing the prototype prosthesis, the hip angles on the sound side are similar to the angles on the sound side when using the everyday prosthesis. The angles of the prosthetic limb show a difference from 10% to 15% GC where the decrease of the flexion angle comes to a stop and the angle is kept constant at 20 degrees. The second difference that can be seen compared to wearing the everyday prosthesis is occurring at the end of the swing phase. By using the prototype prosthesis the maximum hip flexion angle in swing phase on the prosthetic side is averaging 40 degrees at 85% GC. After that, the angle is decreasing until reaching its final value of 35 degrees at 95% GC.

5.2.7 SACR lateral movement

5.2.7.1 Slow walking

Subject A The lateral movement of the SACR marker identifying the mid point between the left and right anterior superior iliac spine can be seen for the everyday (see fig.5.25b) and the prototype prosthesis (see fig.5.25a). Looking at the SMP{t} values of the prototype prosthesis there is only one area between 20% and 50% GC where the two signals are significantly different. However, the signals have bigger standard deviations compared to the everyday prosthesis, which does affect the results. The maximum lateral movement is in the middle of the stance phase at 35% GC where it reaches -100mm and -40mm at the sound and the prosthetic leg, respectively. Another difference that comes to mind is that at the beginning of the stance phase of the sound leg the lower back is moving towards the centre line and only at 5% GC the direction is reversed into the direction of the sound leg. Because the prosthetic movement in the prosthetic limb stance phase has no change of direction in early stance and the maximum is more than half of that of the sound leg, the movement seems smoother overall. Looking at the everyday prosthesis lateral movement (see fig.5.25b) the same characteristics as for the prototype prosthesis can be observed. The change in direction at 5% GC is apparent, as is the bigger lateral movement of the sound limb compared to the prosthetic limb at -75mm and -30mm for the sound and prosthetic side. When looking at the SPM{t} results it becomes obvious that the lateral movement is not symmetrical, because they can only be considered statistically equal from 2% to 8% GC.

Subject B The lateral movement of the SACR marker for both prostheses for subject B can be seen in figure 5.26. Looking at their SPM{t} values it can be seen that when using the everyday prosthesis (see fig.5.26b) the signals can be regarded as statistically different from 0% to 10% and from 50% to 60% GC. When looking at the actual movement the trajectories of the marker when either of the two limbs is in stance phase are almost the same. Apart from the two areas highlighted by the SPM{t} analysis another difference can be observed regarding the maximum lateral movement, which not only is happening earlier, when the sound limb is in

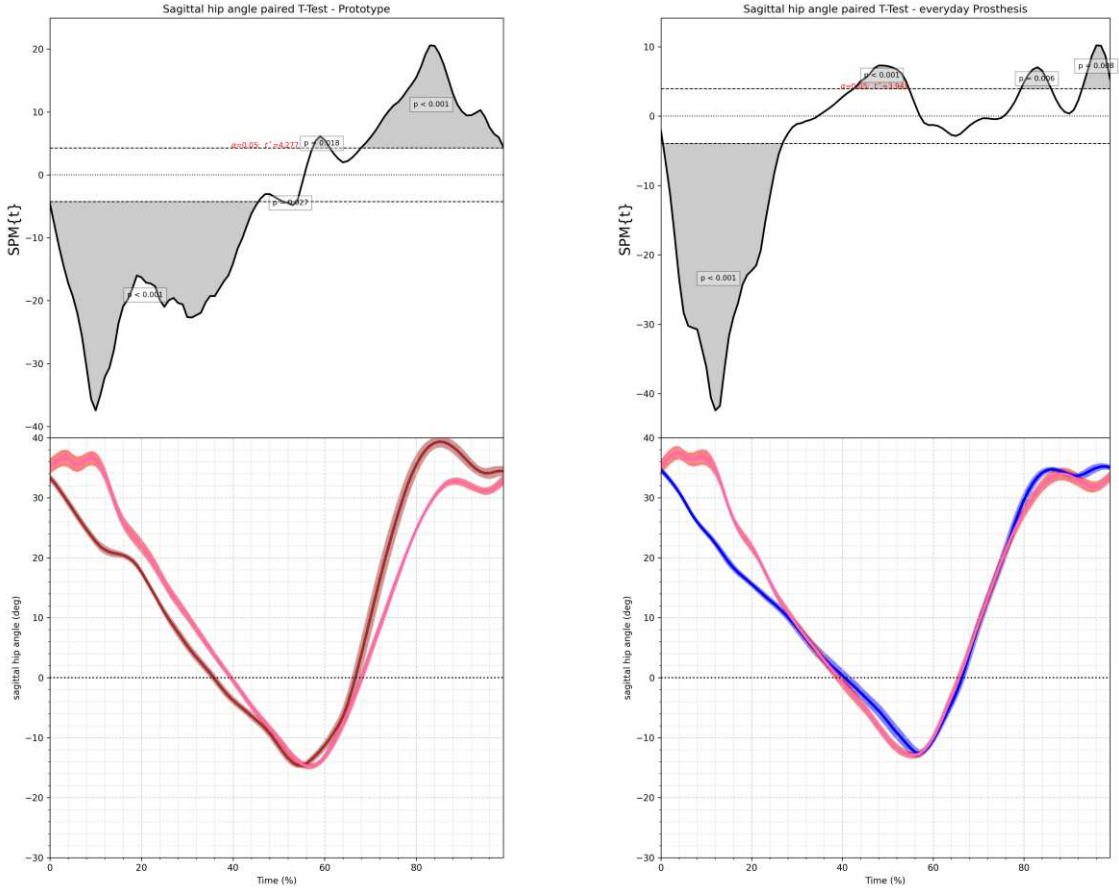

(a) At the top the SPM analysis of the hip angle with the null hypothesis that both signals are equal can be seen. At the bottom the sagittal hip angle with standard deviation is shown for the prototype prosthesis. The pink graph is showing the sound leg while the brown one is showing the prosthetic limb.

(b) At the top the SPM analysis of the hip angle with the null hypothesis that both signals are equal can be seen. At the bottom the mean sagittal hip angle with standard deviation is shown for the everyday prosthesis. The pink graph is showing the sound leg while the blue one is showing the prosthetic limb.

Fig. 5.24: Hip angle for subject B, fast walking for both everyday and prototype prosthesis. The null hypothesis is that the angle of the left and right hip are equal. Positive values are representing flexion angles while negative values correspond to extension angles.

stance phase at 30% GC compared to 35%, but is bigger as well: -85mm compared to -75mm when the prosthetic leg is in stance phase. It has to be noted, that the deviations are rather big for both sides which does influence the statistical analysis. Big deviations can also be seen when wearing the prototype prosthesis (see fig.5.26a) which is influencing the SPM{t} values. This results in only one area of significant differences from 20% GC to 30% GC. This is also the only region where differences can be seen for both lateral movements. While both movements start with equal speeds at the beginning, when the prosthetic side is in stance phase the movement is slowed down at 15% GC and finally peaking at 35% GC at -60mm, compared to the steadily increasing movement when the sound leg is in stance phase, which peaks at 30% GC at -90mm.

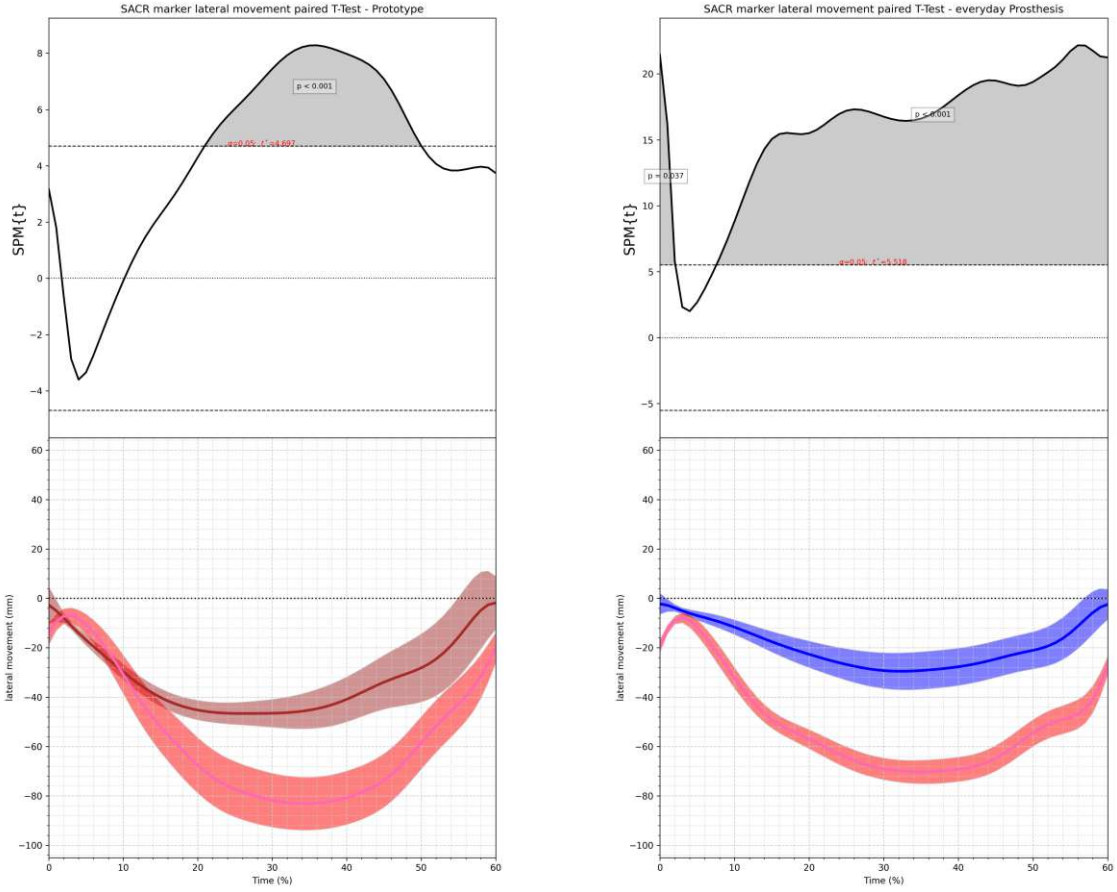

(a) At the top the SPM analysis of the lateral movement of the SACR marker with the null hypothesis that both signals are equal can be seen. At the bottom the lateral movement of the SACR marker with standard deviation is shown for the prototype prosthesis. The pink graph is showing the sound leg while the brown one is showing the prosthetic limb.

(b) At the top the SPM analysis of the lateral movement of the SACR marker with the null hypothesis that both signals are equal can be seen. At the bottom the lateral movement of the SACR marker with standard deviation is shown for the everyday prosthesis. The pink graph is showing the sound leg while the blue one is showing the prosthetic limb.

Fig. 5.25: Lateral movement of the SACR marker for subject A, slow walking for both everyday and prototype prosthesis. The null hypothesis is that the movement of the left and right hip are equal. The movements were transferred to one side to allow direct comparison of the values regardless of the walking direction.

5.2.7.2 Fast walking

Subject A The lateral movement of the SACR marker for the fast walking trail can be seen in figure 5.27. When looking at the SPM{t} values for the everyday (see fig.5.27b) and the prototype prosthesis (see fig.5.27a) it becomes apparent that for the prototype prosthesis the null hypothesis can be confirmed almost everywhere except for a small region at the beginning of the stance phase. When looking at the statistical results for the everyday prosthesis the opposite can be seen, with the null hypothesis being declined almost everywhere except from 0% to 10% GC and from 50% to 60% GC. Interestingly, the standard deviation of both test settings are almost equal, except at the end of the stance phase where the standard deviation is getting

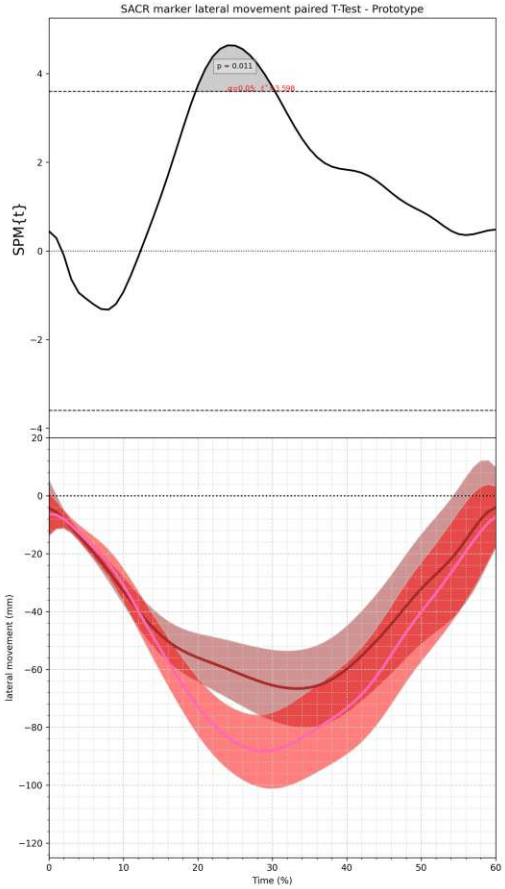

(a) At the top the SPM analysis of the lateral movement of the SACR marker with the null hypothesis that both signals are equal can be seen. At the bottom the lateral movement of the SACR marker with standard deviation is shown for the prototype prosthesis. The pink graph is showing the sound leg while the brown one is showing the prosthetic limb.

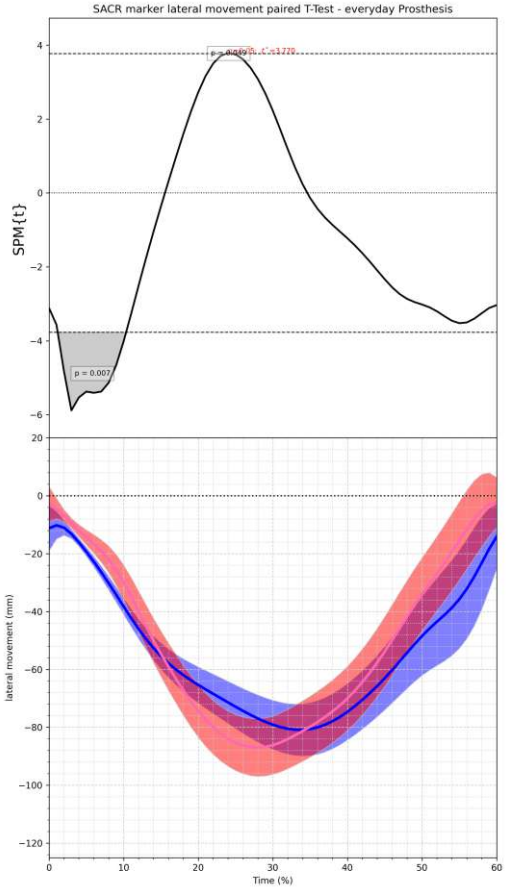

(b) At the top the SPM analysis of the lateral movement of the SACR marker with the null hypothesis that both signals are equal can be seen. At the bottom the lateral movement of the SACR marker with standard deviation is shown for the everyday prosthesis. The pink graph is showing the sound leg while the blue one is showing the prosthetic limb.

Fig. 5.26: Lateral movement of the SACR marker for subject B, slow walking for both everyday and prototype prosthesis. The null hypothesis is that the movement of the left and right hip are equal. The movements were transferred to one side to allow direct comparison of the values regardless of the walking direction.

bigger when using the prototype, in contrast to the everyday prosthesis where it gets smaller at the end of stance phase. It is also true, that for both settings the movement is smaller when the prosthetic limb is supporting the body, compared to the lateral movement when the sound leg is in stance phase. Another difference that can be seen is that the movement is crossing the centre line (equally to leaning towards the leg in swing phase) at the beginning and at the end of stance phase of the sound leg for the prototype prosthesis, while when using the everyday prosthesis it stays on the same side in regards to the centre.

Subject B Figure 5.28 shows the lateral movement of the SACR marker when wearing both prostheses. Both statistical evaluations show two areas of significant differences at the beginning

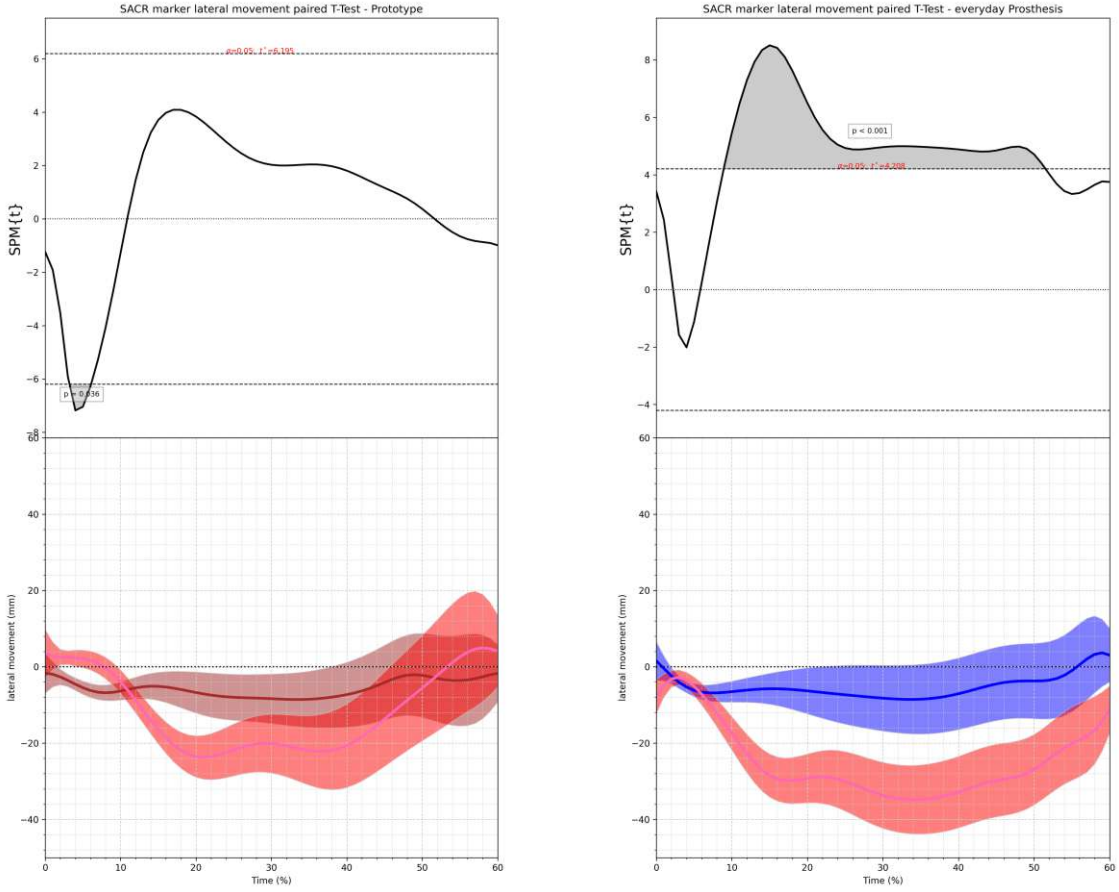

(a) At the top the SPM analysis of the lateral movement of the SACR marker with the null hypothesis that both signals are equal can be seen. At the bottom the lateral movement of the SACR marker with standard deviation is shown for the prototype prosthesis. The pink graph is showing the sound leg while the brown one is showing the prosthetic limb.

(b) At the top the SPM analysis of the lateral movement of the SACR marker with the null hypothesis that both signals are equal can be seen. At the bottom the lateral movement of the SACR marker with standard deviation is shown for the everyday prosthesis. The pink graph is showing the sound leg while the blue one is showing the prosthetic limb.

Fig. 5.27: Lateral movement of the SACR marker for subject A, fast walking for both everyday and prototype prosthesis. The null hypothesis is that the movement of the left and right hip are equal. The movements were transferred to one side to allow direct comparison of the values regardless of the walking direction.

from 0% to 15% GC and from 20% to 30% GC. Looking at the actual movement when walking with the everyday prosthesis (see fig.5.28b) it can be seen, that both signals have big deviations. While the movement starts at the centre when the sound foot is in stance phase and stays there until 10% GC, the marker has already moved to -5mm at the beginning and is immediately moving further away from the centre when the prosthetic leg is in stance phase. However, because the movement from the centre is rapidly increasing when the sound limb is supporting the body the maximum excursion of the marker is at 30% averaging -35mm compared to the maximum of -20mm at 35% GC when the prosthetic limb is in stance phase. After that, both markers are decreasing their excursions, moving back to 0mm and -5mm at the end of the gait cycle when the sound leg and the prosthetic leg are in stance phase, respectively. The movement

when wearing the prototype prosthesis and the sound leg is in stance phase (see fig.5.28a) is looking similar to that when using the everyday prosthesis. However, at the beginning instead of keeping at the centre line until 10% GC the marker is leaning towards the prosthetic limb which is currently in swing phase peaking at 8% GC at 8mm. After that, the signals are almost the same. Nevertheless, this cannot be said for the lateral movement of the marker when the prosthetic limb is in stance phase. Looking at the signal it can be noted, that the movement is almost constant, averaging -10mm with small movements up and down.

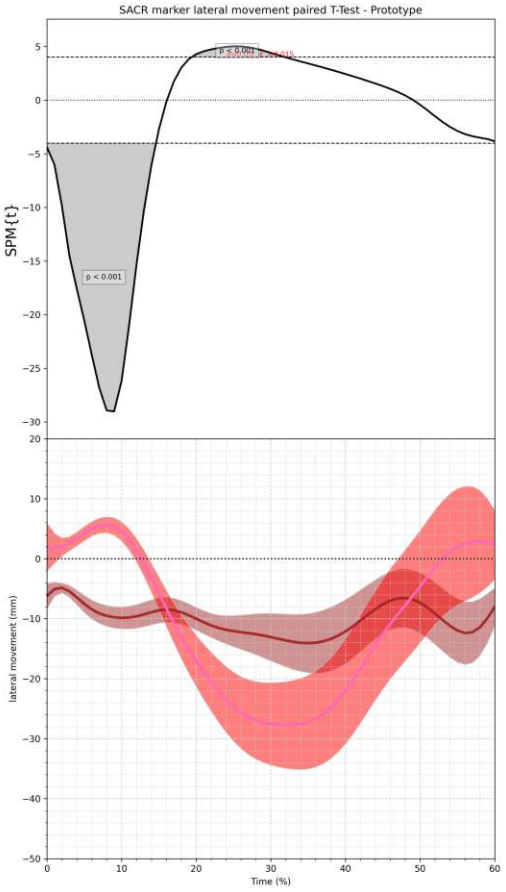

(a) At the top the SPM analysis of the lateral movement of the SACR marker with the null hypothesis that both signals are equal can be seen. At the bottom the lateral movement of the SACR marker with standard deviation is shown for the prototype prosthesis. The pink graph is showing the sound leg while the brown one is showing the prosthetic limb.

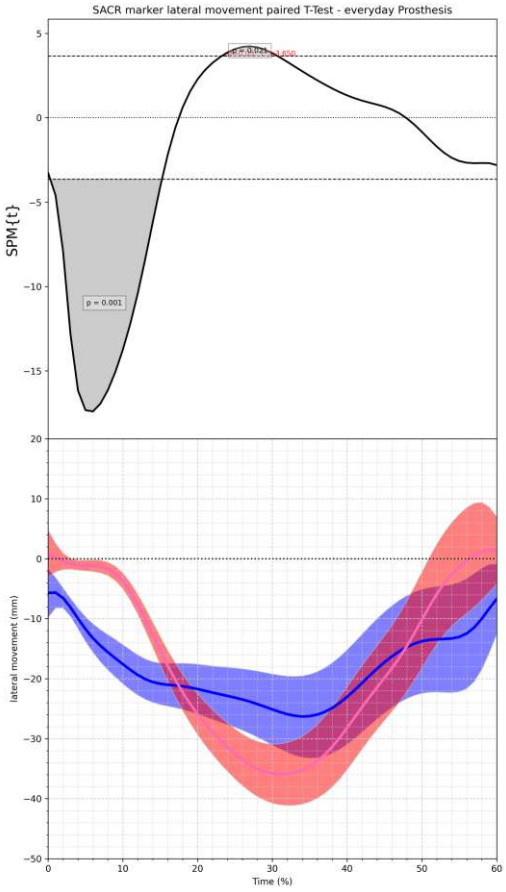

(b) At the top the SPM analysis of the lateral movement of the SACR marker with the null hypothesis that both signals are equal can be seen. At the bottom the lateral movement of the SACR marker with standard deviation is shown for the everyday prosthesis. The pink graph is showing the sound leg while the blue one is showing the prosthetic limb.

Fig. 5.28: Lateral movement of the SACR marker for subject B, fast walking for both everyday and prototype prosthesis. The null hypothesis is that the movement of the left and right hip are equal. The movements were transferred to one side to allow direct comparison of the values regardless of the walking direction.

5.2.8 SACR cranial movement

5.2.8.1 Slow walking

Subject A As part of the movement analysis of the upper body, the up and down movement at the SACR marker during stance phase was investigated and can be seen in figure 5.29. It can be seen that the SPM{t} analysis for the prototype setting can not confirm the null hypothesis for most of the stance phase (see fig.5.29a). The difference can also be seen when looking directly at the movements. The movement is substantially smaller when the prosthetic side is in stance phase and is changing direction at mid stance and late stance at 35% and 50% where it becomes negative while the sound leg stays positive during the whole stance phase. The maximum up movements align well between the sound and prosthetic leg in stance phase but the sound leg is substantially higher, peaking at 25mm compared to 8mm. The minimum values are at different positions. When the sound leg is in stance phase the minimum movement is at 5% GC at approximately -2mm, while the minimum for the prosthetic leg in stance phase is occuring at 50% GC at -12mm. The everyday prosthesis signals have much more similarity as shown in the SPM{t} analysis at the top of figure 5.29b where only three small areas at the beginning, at 10-20% GC and at the end of the stance phase, have significant differences. However, the maximum values are not aligning properly between the two limbs with the prosthetic side reaching its maximum cranial movement at 30% GC at 18mm and the sound limb reaching the maximum movement at 40% GC at 20mm. For the minima the movement location can be compared to the prototype prosthetic setting because the minimum at the sound leg can be found right at the beginning of stance phase at 5%, being approximately -2mm while for the prosthetic side the minimum is at 53% at roughly -10mm.

Subject B The cranial movement of the SACR marker while using both prostheses can be seen in figure 5.30. The SPM{t} analysis shows only one region of statistical equality from 8% to 15% GC, regardless of the prosthesis. When looking at the signals when wearing the everyday prosthesis (see fig.5.30b) it can be seen that when the prosthetic leg is in stance phase the maximum cranial displacement is happening at 35% averaging 15mm, compared to 28% GC of approximately 10mm. Another difference can be seen at 50% GC where the movement has a minimum of -5mm when the prosthetic limb is in stance phase, compared to -12mm when the sound leg is supporting the body. The same difference can be seen when wearing the prototype prosthesis (see fig5.30a). The maximum cranial displacement with the prosthetic leg in stance phase is 20mm at 35% GC compared to 10mm at 30% GC when the sound leg is in stance phase. At the end of the gait cycle it can be observed, that the cranial movement has its minimum of 0mm at 50% GC while when the sound limb is in stance phase the minimum is averaging -15mm at 50% GC.

5.2.8.2 Fast walking

Subject A The cranial movement of the SACR marker in the fast walking setting can be seen in figure 5.31. Looking at the SPM{t} values it can be seen that the signals align very well when the prototype prosthesis is worn (see fig.5.31a). There are no regions in which the signals are significantly different from each other. This can also be seen in the good alignment between the maximum upwards movement, which occurs for both limbs in stance phase at 30% GC and approximately 40 and 42mm for the prosthetic and sound limb. Although no statistical relevant differences where detected, at the end of the stance phase the signals do differ substantially. While the movement is not changing direction and is not becoming negative, when the sound leg is in stance phase the movement is becoming negative and is changing direction at 55% GC.

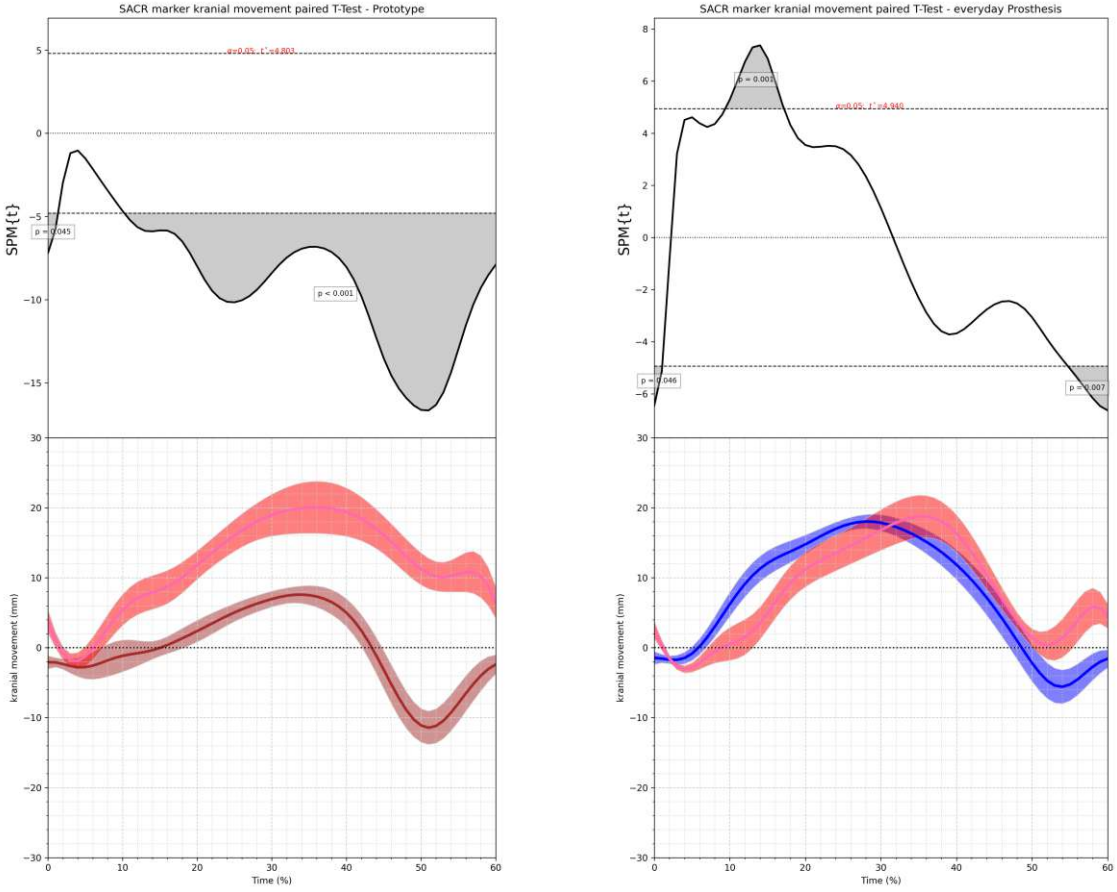

(a) At the top the SPM analysis of the cranial movement of the SACR marker with the null hypothesis that both signals are equal can be seen. At the bottom the cranial movement of the SACR marker with standard deviation is shown for the prototype prosthesis. The pink graph is showing the sound leg while the brown one is showing the prosthetic limb.

(b) At the top the SPM analysis of the cranial movement of the SACR marker with the null hypothesis that both signals are equal can be seen. At the bottom the cranial movement of the SACR marker with standard deviation is shown for the everyday prosthesis. The pink graph is showing the sound leg while the blue one is showing the prosthetic limb.

Fig. 5.29: Cranial movement of the SACR marker for subject A, slow walking for both everyday and prototype prosthesis. The null hypothesis is that the movement of the left and right hip are equal.

Looking at the signals when the everyday prosthesis is worn, it becomes immediately apparent, that the signals do not align well, which can also be seen in the SPM{t} analysis. Only at the beginning and at the end of the stance phase the signals are aligning well. When the sound leg is in stance phase the SACR marker is steadily moving downwards, until it reaches its minimum at 10% GC of approximately 30mm. After that, the marker is rising again until its maximum at 35% GC of 20mm where it is decreasing again until 55% after which it is increasing yet again. If the prosthetic limb is in stance phase the movement looks different and is beginning with an increase until it reaches its maximum of 50mm at 30% GC. After that, the position of the marker is decreasing until it reaches its minimum at 58% GC of 10mm where it begins to incline again until the end of stance phase.

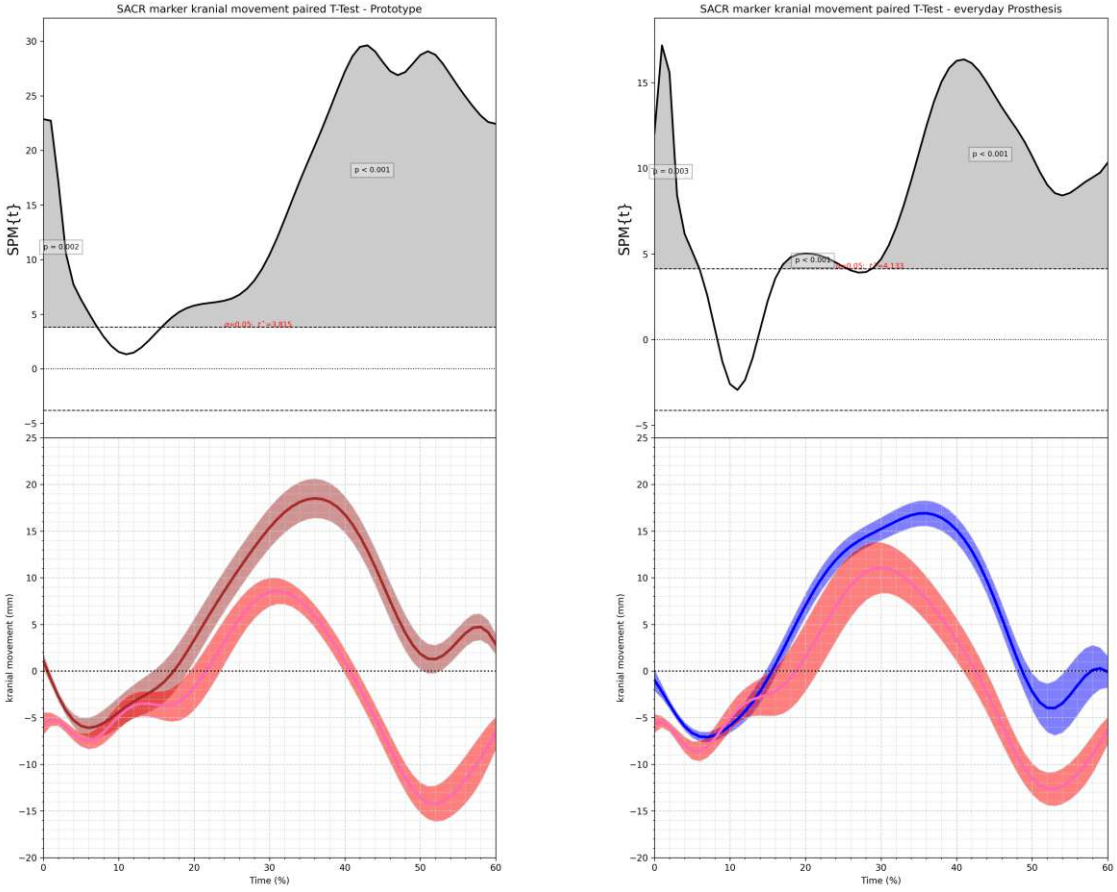

(a) At the top the SPM analysis of the cranial movement of the SACR marker with the null hypothesis that both signals are equal can be seen. At the bottom the cranial movement of the SACR marker with standard deviation is shown for the prototype prosthesis. The pink graph is showing the sound leg while the brown one is showing the prosthetic limb.

(b) At the top the SPM analysis of the cranial movement of the SACR marker with the null hypothesis that both signals are equal can be seen. At the bottom the cranial movement of the SACR marker with standard deviation is shown for the everyday prosthesis. The pink graph is showing the sound leg while the blue one is showing the prosthetic limb.

Fig. 5.30: Cranial movement of the SACR marker for subject B, slow walking for both everyday and prototype prosthesis. The null hypothesis is that the movement of the left and right hip are equal.

Subject B Figure 5.31 is showing the cranial movement of the SACR marker while using either of the two prostheses. The SPM{t} analysis shows only two small areas of significant equality for both prostheses, however, the analysis shows bigger regions of equality when using the prototype prosthesis. Looking at the movement when using the everyday prosthesis (see fig.5.32b) it can be seen that both start at roughly -8mm but move in opposite directions from there. While a minimum is reached at 18% GC of -25mm when the sound limb is in stance phase, the marker is steadily increasing from the initial -8mm until reaching a maximum displacement of 35mm at 30% GC when the prosthetic leg is supporting the body. The corresponding maximum when the opposite limb is supporting the body is 20mm at 35% GC. After reaching their maximum displacements, both marker trajectories are decreasing again until reaching a second minimum of -15mm at 50% GC and -10mm at 55% GC when the sound leg and the prosthetic leg are in stance

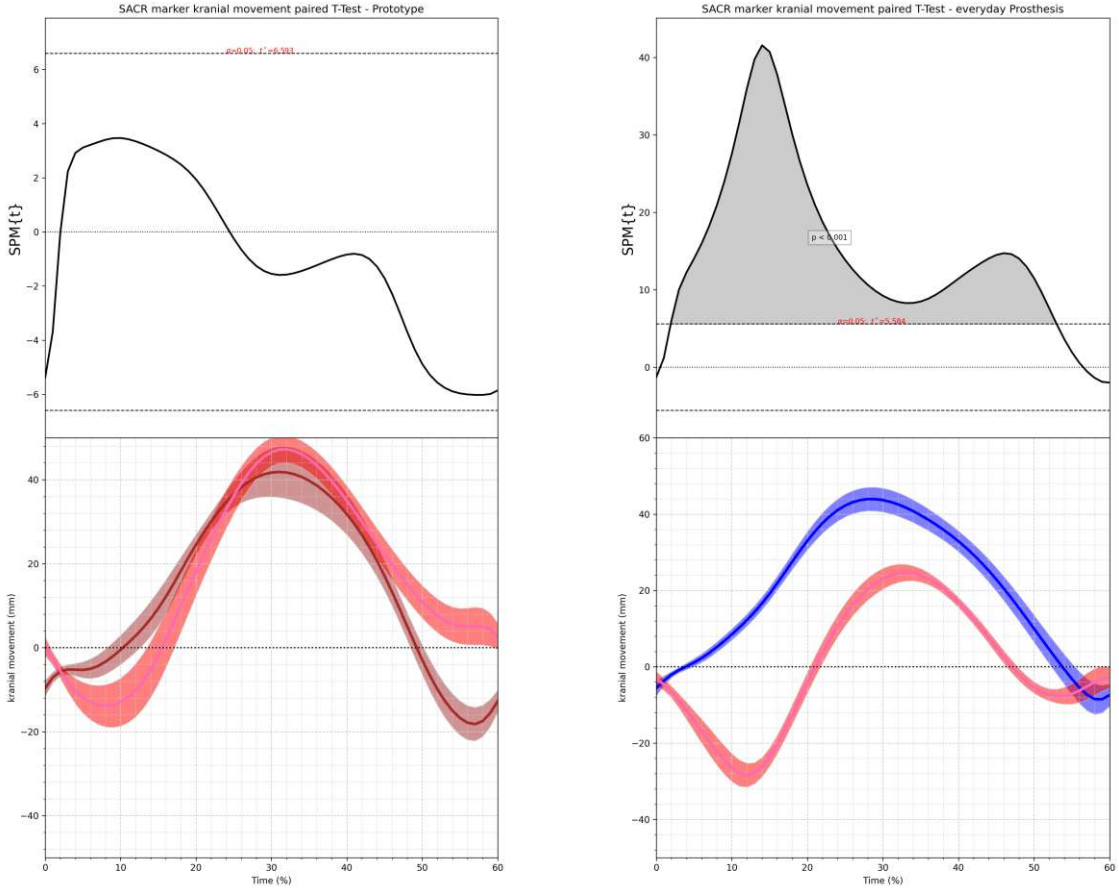

(a) At the top the SPM analysis of the cranial movement of the SACR marker with the null hypothesis that both signals are equal can be seen. At the bottom the cranial movement of the SACR marker with standard deviation is shown for the prototype prosthesis. The pink graph is showing the sound leg while the brown one is showing the prosthetic limb.

(b) At the top the SPM analysis of the cranial movement of the SACR marker with the null hypothesis that both signals are equal can be seen. At the bottom the cranial movement of the SACR marker with standard deviation is shown for the everyday prosthesis. The pink graph is showing the sound leg while the blue one is showing the prosthetic limb.

Fig. 5.31: Cranial movement of the SACR marker for subject A, fast walking for both everyday and prototype prosthesis. The null hypothesis is that the movement of the left and right hip are equal.

phase, respectively. When describing the cranial movements when the prototype prosthesis was used, the movements are similar to the movements recorded when the everyday prosthesis was worn. Starting at -12mm and -8mm the cranial displacement is increasing when the prosthetic leg is in stance phase while it is decreasing when the sound leg is in stance phase. After reaching a minimum of -25mm at 15% GC the movement is reversing and reaching a maximum of 30mm at 35% GC when the sound leg is in stance phase. After that, the height of the marker is decreasing again until reaching another minimum of -8mm at 53% GC. When the prosthetic leg is supporting the body, the height is increasing almost immediately to its maximum height of 30mm at 32% GC, followed by a decrease to a minimum height of -25mm at 55% GC. After both signals reached their minimum values at 53% GC and 55% GC, the height is slowly increasing again.

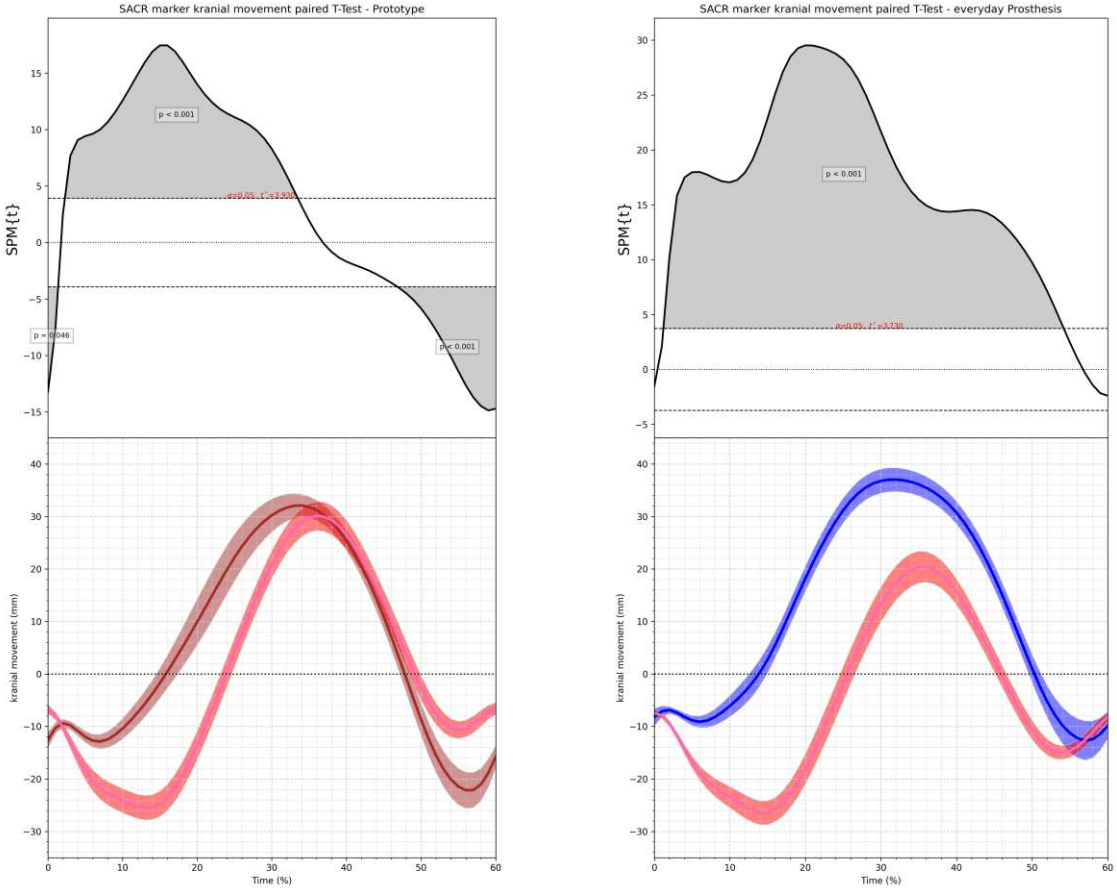

(a) At the top the SPM analysis of the cranial movement of the SACR marker with the null hypothesis that both signals are equal can be seen. At the bottom the cranial movement of the SACR marker with standard deviation is shown for the prototype prosthesis. The pink graph is showing the sound leg while the brown one is showing the prosthetic limb.

(b) At the top the SPM analysis of the cranial movement of the SACR marker with the null hypothesis that both signals are equal can be seen. At the bottom the cranial movement of the SACR marker with standard deviation is shown for the everyday prosthesis. The pink graph is showing the sound leg while the blue one is showing the prosthetic limb.

Fig. 5.32: Cranial movement of the SACR marker for subject B, fast walking for both everyday and prototype prosthesis. The null hypothesis is that the movement of the left and right hip are equal.

5.2.9 SACR velocity anterior

5.2.9.1 Slow walking

Subject A In figure 5.33 the velocity of the SACR marker in direction of the general movement is shown. When looking at the prototype setting the velocity of the SACR marker does fit well between the sound leg and the prosthetic leg in stance phase. Only two areas are statistically different from 10% to 30% GC and from 55% GC until the end of stance phase, as can be seen when looking at the SPM{t} values at the top of figure 5.33a. This can also be seen at the bottom of figure 5.33a, where it shows that the two signals fit very well and follow the same directions throughout the stance phase. However, there are minor differences concerning the timing of the minima (30% GC and 20% GC for prosthetic and sound leg, respectively) and

the maxima at the end of the stance phase (50% GC for the prosthetic and 55% GC for the sound limb in stance phase). Furthermore, it can be seen that the decrease in velocity for the prosthetic side is bigger than on the sound side at the end of the stance phase. Looking at the recordings, when using the everyday prosthesis (see fig. 5.33b) it can be noted, that both signals match very well except for one region between 30% and 45% GC. When looking at both signals themselves it becomes apparent that at the beginning and at the end of the stance phase the velocity of the SACR marker can be seen as almost equal. However, at 10% GC of the sound limb in stance phase, the signal shows a slower decrease of the velocity until 18% where it begins to decrease with the same rate as before again. This can not be seen for the other limb. The peak to peak values are also different for both sides with -400 mm/s for the sound limb in stance phase and approximately -250 mm/s for the prosthetic leg in stance phase.

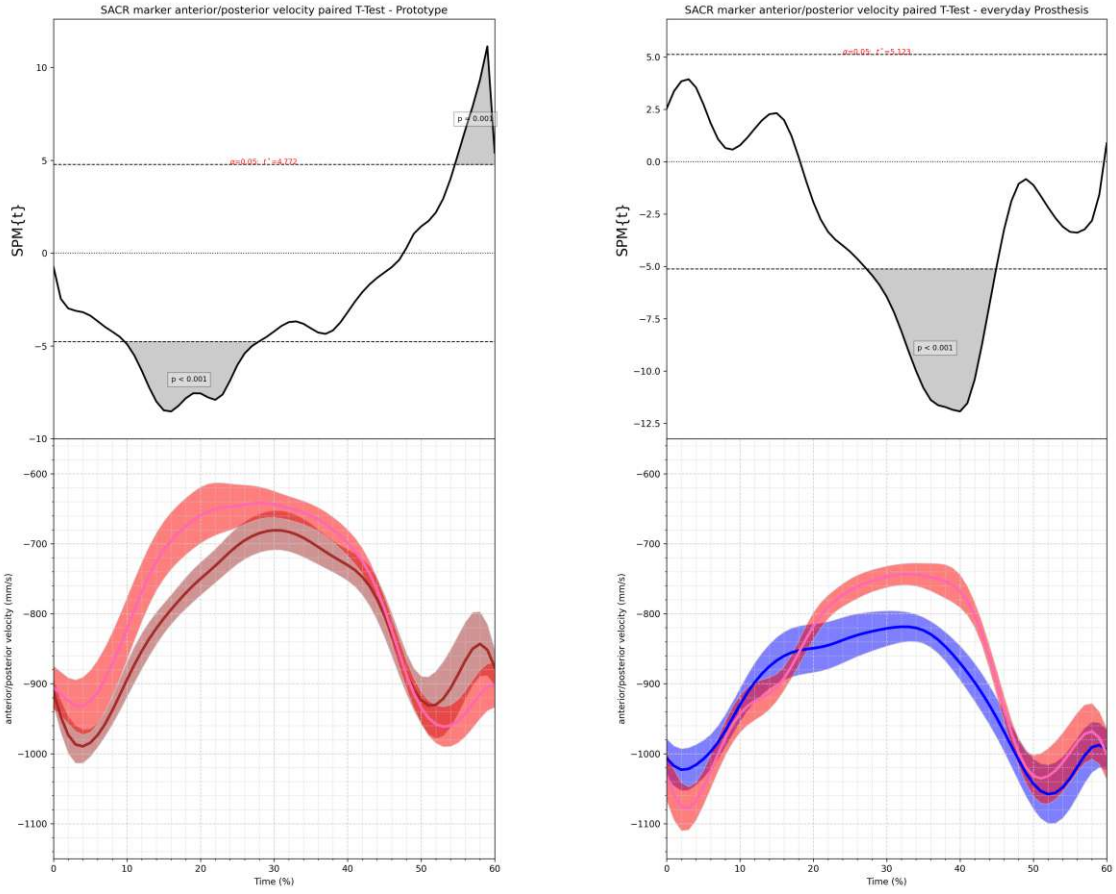

(a) At the top the SPM analysis of the anterior velocity of the SACR marker with the null hypothesis that both signals are equal can be seen. At the bottom the anterior velocity of the SACR marker with standard deviation is shown for the prototype prosthesis. The pink graph is showing the sound leg while the brown one is showing the prosthetic limb.

(b) At the top the SPM analysis of the anterior velocity of the SACR marker with the null hypothesis that both signals are equal can be seen. At the bottom the anterior velocity of the SACR marker with standard deviation is shown for the everyday prosthesis. The pink graph is showing the sound leg while the blue one is showing the prosthetic limb.

Fig. 5.33: Anterior velocity of the SACR marker for subject A, slow walking for both everyday and prototype prosthesis. The null hypothesis is that the movement of the left and right hip are equal.

Subject B Looking at the statistical analysis when wearing either of the two prostheses it can be seen that the velocity of the SACR marker is different from 0-30% GC and 45-65% when wearing the prototype and from 5-40% GC and from 45-65% GC when using the everyday prosthesis in stance phase (see fig.5.34). However, when studying the velocities directly it can be seen that while using the everyday prosthesis (see fig.5.34b) the trajectories are matching quite well and the main differences are concerning the magnitude of the velocities for the most part. At the beginning both velocities are increasing from -850 mm/s to -900 mm/s at 5% GC when the sound leg is in stance phase, compared to starting at -850 mm/s and reaching a maximum of -950 mm/s at 8% GC when the prosthetic leg is supporting the body. After that, both velocities are decreasing steadily until reaching a minimum at -650 mm/s and -600 mm/s for the prosthetic and the sound leg in stance phase, respectively. After that, the velocity is increasing faster on the sound side and is peaking at 50% GC at -950 mm/s, compared to the prosthetic which peaks at -850 mm/s at 50% GC. Compared to the velocities recorded while using the everyday prosthesis, the velocities when the prototype prosthesis is used are showing different trajectories and different values (see fig.5.34a). While the signals are starting both at roughly -800 mm/s the velocity when the prosthetic leg is in stance phase is increasing rapidly to almost -950 mm/s at 10% GC, compared to -830 mm/s when the opposite leg is in stance phase. After that, both signals are decreasing until they reach their minimum of -550 mm/s and -600 mm/s at 25% GC when the sound leg is supporting the body and at 30% GC when the prosthetic leg is in stance phase. The maximum velocity is also very different at the end of the stance phase, which is averaging -800 mm/s at 50% GC when the prosthetic leg is in stance phase and -950 mm/s when the sound leg is in stance phase.

5.2.9.2 Fast walking

Subject A In figure 5.35 the velocity of the SACR marker in stance phase of the sound and prosthetic leg in the fast walking setting can be seen. For the everyday prosthesis there are three areas where the signals are significantly different,which is from 10% to 20% GC, at 45% GC and from 50% to 55% GC (see fig.5.35b). This can also be seen when looking directly at the signals. While the velocity decreases steadily when the prosthetic leg is in stance phase, the decrease of the velocity comes to a stop at 10% to 20% GC when the sound leg is in stance phase. After the minimum at 25% GC of -1450 mm/s and -1350 mm/s for the prosthetic and the sound leg the velocity is increasing again in both settings. However, from 45% GC until 53% GC the rate of the velocity increase is bigger at the sound side, which peaks at -1900 mm/s at 53% GC, whereas the prosthetic side is peaking at 50% GC at approximately -1700 mm/s. Compared to the sound leg the peak at the end of the stance phase at 50% is not the global but rather a local maximum as the global maximum is located at the beginning at 5% GC with -1850 mm/s. The two velocities of the SACR marker match very well in the prototype prosthetic setting (see fig.5.35a). This can be seen in the SPM{t} scores as well, where only one area, which ranges from 25% to 35% GC is statistically different. Furthermore, the two signals look very similar at the beginning of the stance phase. The global maxima are in different locations at 5% GC with -2000 mm/s for the prosthetic side and at 52% with -2000 mm/s on the sound side. However, the minima do align well and can both be located at 30% GC with -1600 mm/s and -1500 mm/s when the prosthetic and the sound limb are in stance phase, respectively. Another difference can be seen at the end of the stance phase from 40% GC to 50% GC where the increase in velocity is slowing down when the prosthetic side is in stance phase in, comparison to when the sound limb is supporting the body, for which there is a steady increase in velocity from 35% to 55% GC.

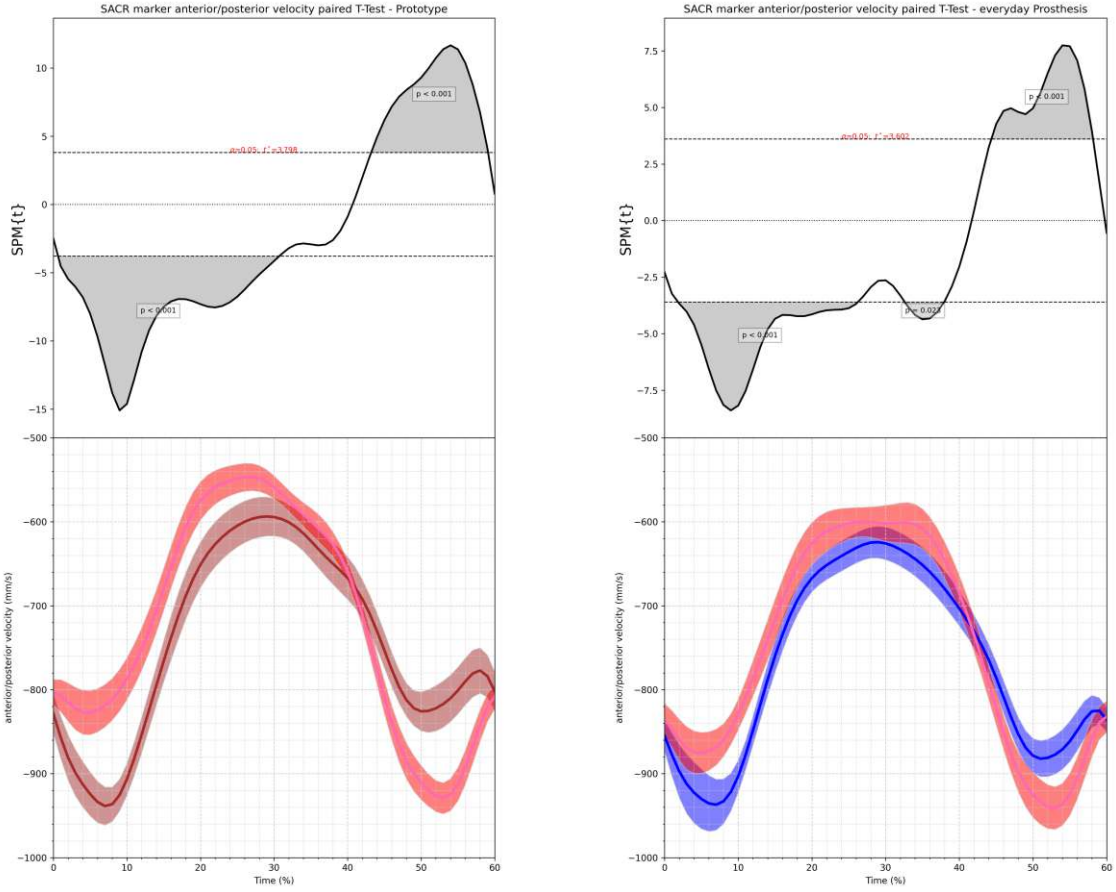

(a) At the top the SPM analysis of the anterior velocity of the SACR marker with the null hypothesis that both signals are equal can be seen. At the bottom the anterior velocity of the SACR marker with standard deviation is shown for the prototype prosthesis. The pink graph is showing the sound leg while the brown one is showing the prosthetic limb.

(b) At the top the SPM analysis of the anterior velocity of the SACR marker with the null hypothesis that both signals are equal can be seen. At the bottom the anterior velocity of the SACR marker with standard deviation is shown for the everyday prosthesis. The pink graph is showing the sound leg while the blue one is showing the prosthetic limb.

Fig. 5.34: Anterior velocity of the SACR marker for subject B, slow walking for both everyday and prototype prosthesis. The null hypothesis is that the movement of the left and right hip are equal.

Subject B In figure 5.36 the change of velocity of the SACR marker in direction of the general movement can be seen. Looking at the signals while using the everyday prosthesis (see fig.5.36b) it can be seen, that the statistical analysis is identifying only two regions of equality from 10-20% GC and from 55-60% GC. Yet again, the trajectories are looking quite similar and the signals do align well temporally. However, the maximum and minimum values show differences. While the first maxima are both at 5% GC, they are averaging -1650 mm/s when the prosthetic leg is in stance phase, compared to -1550 mm/s when the sound leg is supporting the body. The same can be seen at the minimum velocity at 25% GC, which accounts for -1250 mm/s when the prosthetic limb is supporting the body and -1300 mm/s otherwise. In the end the maxima are averaging -1550 mm/s and -1700 mm/s for the prosthetic and sound side, respectively. While the SPM{t} results show three regions of statistical equality, when using the prototype prosthesis

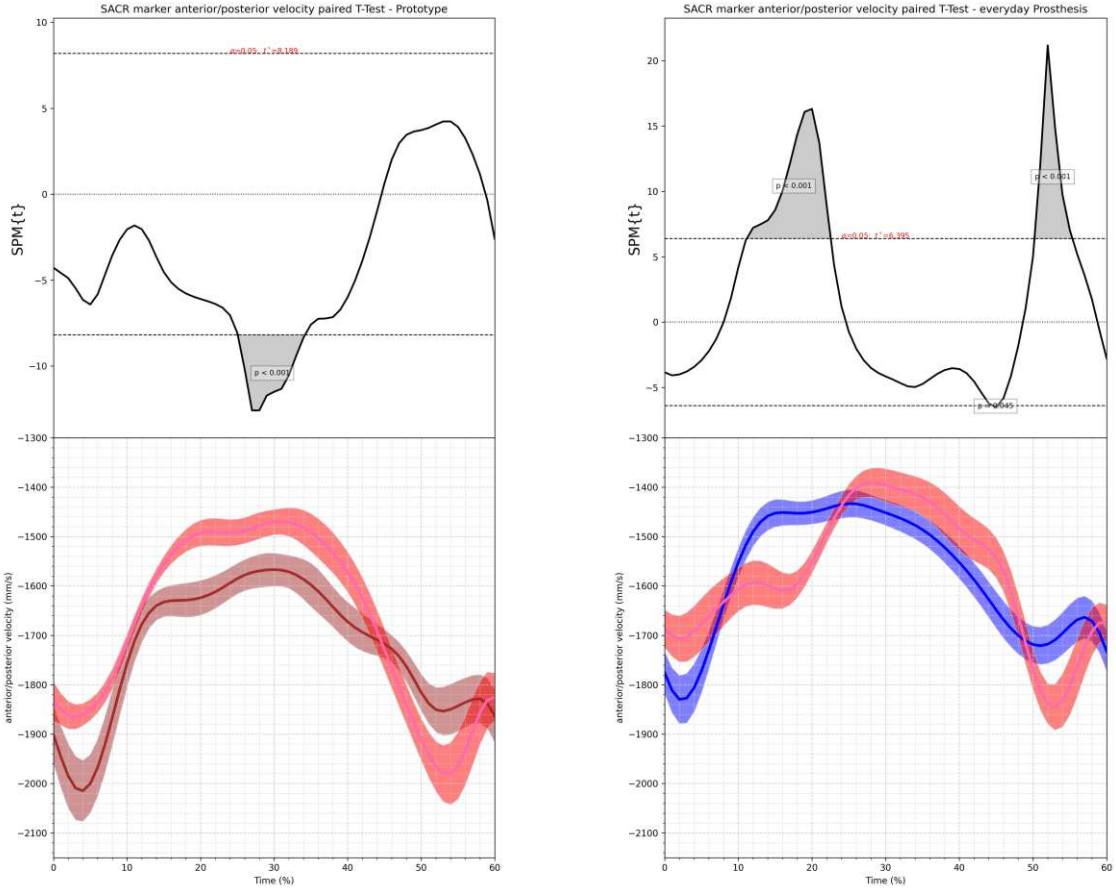

(a) At the top the SPM analysis of the anterior velocity of the SACR marker with the null hypothesis that both signals are equal can be seen. At the bottom the anterior velocity of the SACR marker with standard deviation is shown for the prototype prosthesis. The pink graph is showing the sound leg while the brown one is showing the prosthetic limb.

(b) At the top the SPM analysis of the anterior velocity of the SACR marker with the null hypothesis that both signals are equal can be seen. At the bottom the anterior velocity of the SACR marker with standard deviation is shown for the everyday prosthesis. The pink graph is showing the sound leg while the blue one is showing the prosthetic limb.

Fig. 5.35: Anterior velocity of the SACR marker for subject A, fast walking for both everyday and prototype prosthesis. The null hypothesis is that the movement of the left and right hip are equal.

(see fig.5.36a) the trajectories are looking different between both sides. The first maximum is occurring at 5% GC averaging -1750 mm/s when the prosthetic leg is in stance phase and -1650 mm/s otherwise. The minima are not aligning as well and can be found at 20% GC when the sound leg is in stance phase with approximately -1250 mm/s, compared to 28% GC with -1300 mm/s otherwise. The maxima at the end of the stance phase are aligning well. Both can be seen at 52% GC and are averaging -1750 mm/s and -1600 mm/s when the sound limb and the prosthetic limb are in stance phase, respectively.

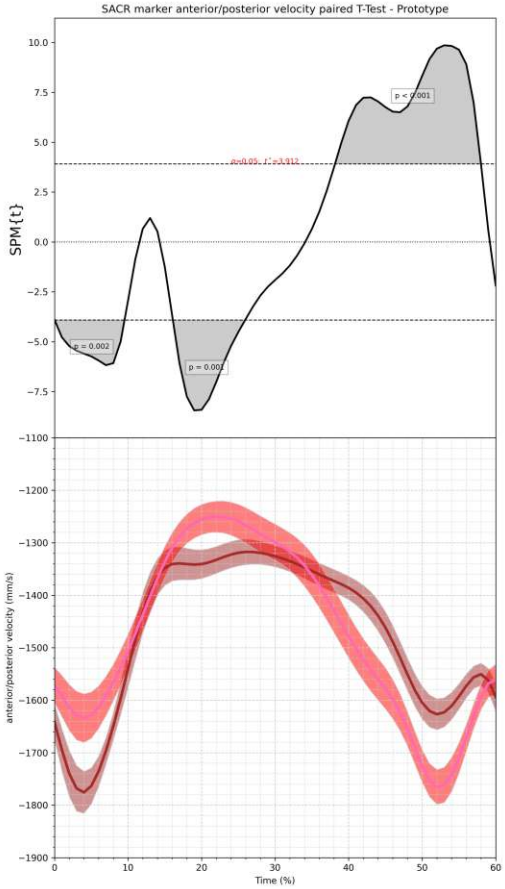

(a) At the top the SPM analysis of the anterior velocity of the SACR marker with the null hypothesis that both signals are equal can be seen. At the bottom the anterior velocity of the SACR marker with standard deviation is shown for the prototype prosthesis. The pink graph is showing the sound leg while the brown one is showing the prosthetic limb.

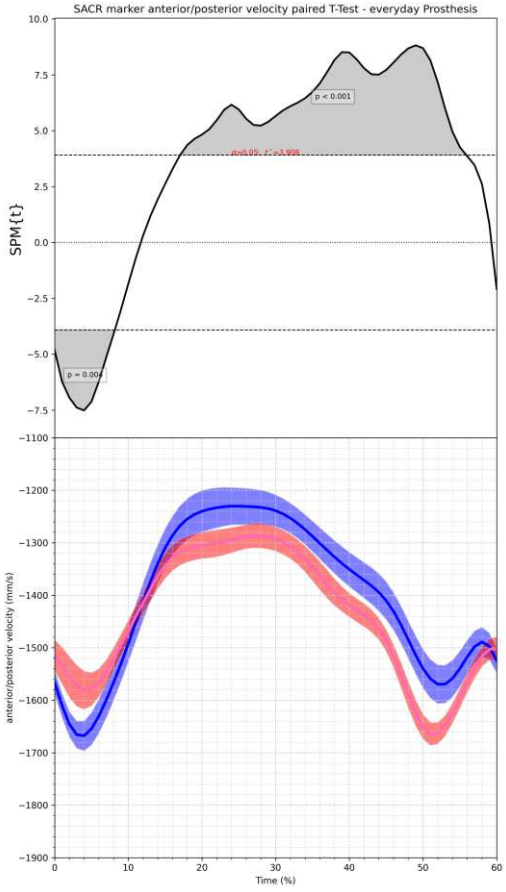

(b) At the top the SPM analysis of the anterior velocity of the SACR marker with the null hypothesis that both signals are equal can be seen. At the bottom the anterior velocity of the SACR marker with standard deviation is shown for the everyday prosthesis. The pink graph is showing the sound leg while the blue one is showing the prosthetic limb.

Fig. 5.36: Anterior velocity of the SACR marker for subject B, fast walking for both everyday and prototype prosthesis. The null hypothesis is that the movement of the left and right hip are equal.

5.2.10 Hip Moment sagittal

5.2.10.1 Slow walking

Subject A The sagittal hip moment for the prototype and everyday prosthesis for slow walking can be seen in figure 5.37. When looking at the everyday prosthesis figure in more detail (see fig.5.37b), it immediately can be noticed that the torque at the sound hip has big deviations in the stance phase, compared to the hip moment of the prosthetic limb. The maximum flexion torque is occurring at the same time at 45% GC with -0.75 Nm/kg on the sound side, compared to -1.25 Nm/kg on the other limb. Right at the beginning the extending moment is bigger on the sound side with 0.3 Nm/kg, compared to 0.125 Nm/kg on the opposite hip. At the far end of the hip moment signals a peak in the hip torque of the prosthetic limb can be seen, compared to

the sound leg, where the moment at the end is steadily increasing. The SPM{t} analysis of the signals are only showing three areas where there are significant differences, however, because of the big deviations on the sound side this has to be interpreted with caution. When looking at the prototype signals in figure 5.37a it can be seen that although the signals are statistically different almost all of the time, the shape of the two signals are fairly identical. At the beginning there is an extension moment on the sound side of approximately 0.35 Nm/kg while on the opposite side there is a small flexion moment of -0.05 Nm/kg already. The shape of the two signals are very similar afterwards. This can also be seen due to the fact that the maximum flexion torques happen both at 45% GC with -1.125 Nm/kg on the prosthetic side and -0.5 Nm/kg on the sound limb. After that, both increase sharply to a small extension torque but continue to evolve in different directions at the end of the GC, where after the peak flexion torque of -0.125 Nm/kg at 90% GC the value decreases again on the prosthetic side, while it is still increasing until reaching 0.3 Nm/kg at the end of GC on the sound side.

Subject B In figure 5.38 the sagittal hip moments of subject B when walking slowly can be seen. Looking at the hip moments when wearing the everyday prosthesis (see fig.5.38b) it can be seen that only three areas exist where the signals can be seen as statistically equal. This becomes immediately apparent when looking at the beginning of the gait cycle, where the hip moment on the sound limb is starting with 0.35 Nm/kg and increasing until reaching a maximum at 5% GC of 0.5 Nm/kg, compared to the hip on the prosthetic side which starts with -0.1 Nm/kg and is decreasing more or less steadily until reaching a minimum at 50% GC of -0.7 Nm/kg. The sound side hip is also showing its minimum at 50% GC averaging -0.25 Nm/kg. After both hips recorded their minimum torque, or their maximum flexion moment, the flexion torque is decreasing again until both reach a small peak of an extending moment, averaging 0.05 Nm/kg at 63% GC on the sound side and 0.1 Nm/kg at 72% GC on the prosthetic side. At 80% GC both hips show similar flexion moments of -0.05 Nm/kg. The hip on the sound side is ending the gait cycle with an extension moment of 0.3 Nm/kg while the hip on the opposite side is ending with a flexion moment of -0.1 Nm/kg. When using the prototype prosthesis three areas of statistical equality between moment of the hip on the sound side and the prosthetic side can be seen (see fig.5.38a). Similar to the moments when using the everyday prosthesis, the hip on the sound side is starting with an extension moment of 0.4 Nm/kg and is increasing until 0.5 Nm/kg at 5% GC, where it begins to decrease until reaching its maximum flexion moment of -0.2 Nm/kg at 55% GC. The hip of the prosthetic leg on the other hand is starting with a small flexion moment of -0.075 Nm/kg, which is decreasing a little bit until 5% GC where it starts to increase flexion torque until reaching a maximum at 45% GC of -0.6 Nm/kg. After both hips reached their maximum flexion torques, both start to decrease again until a small peak of an extending moment of 0.05 Nm/kg is reached at 62% GC on the sound side and at 72% GC on the prosthetic side. In the end the hip on the sound side is averaging 0.3 Nm/kg while the hip on the opposite side ends with -0.1 Nm/kg.

5.2.10.2 Fast walking

Subject A Figure 5.39 shows the sagittal hip moment of the sound and prosthetic limb for the everyday and prototype prosthesis of the fast walking trail. It can be seen that for both prostheses the SPM{t} values have multiple areas where the signals are different. For the everyday prosthesis (see fig.5.39b) there two areas exist from 30% GC to 45% GC and from 60% GC to 85% GC where a statistically relevant difference can be seen. However, the deviation of the hip moment on the sound side is very big at the beginning, which influences the statistical values. Looking at the signals themselves, the trajectories of both signals can be seen as similar. At

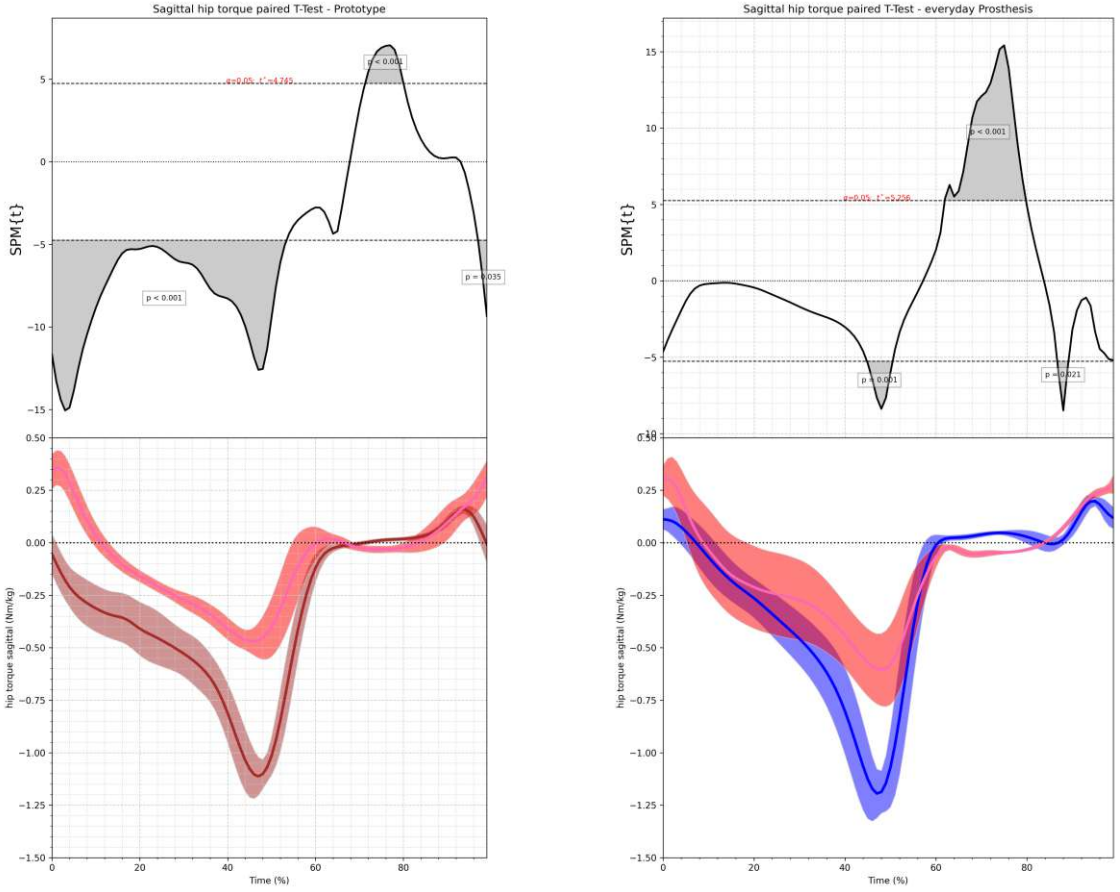

(a) At the top the SPM analysis of the sagittal hip moment the null hypothesis that both signals are equal can be seen. At the bottom the sagittal hip moment with standard deviation is shown for the prototype prosthesis. The pink graph is showing the sound leg while the brown one is showing the prosthetic limb.

(b) At the top the SPM analysis of the sagittal hip moment with the null hypothesis that both signals are equal can be seen. At the bottom the sagittal hip moment with standard deviation is shown for the everyday prosthesis. The pink graph is showing the sound leg while the blue one is showing the prosthetic limb.

Fig. 5.37: Sagittal hip moment for subject A, slow walking for both everyday and prototype prosthesis. The null hypothesis is that the movement of the left and right hip are equal. Positive values correspond to an extending moment, hence, negative values are flexion moments.

the beginning the sound leg shows a higher extension moment of 0.6 Nm/kg, compared to 0.25 Nm/kg on the prosthetic limb. After that, both are moving into flexion torques which peak at 45% GC and account for approximately 1 Nm/kg and 1.75 Nm/kg for the sound and prosthetic limb, respectively. After that, the moments are beginning to reverse until being almost zero on the prosthetic side and increasing into an extending moment, which peaks at 0.25 Nm/kg on the prosthetic side, where it begins to decrease again afterwards. Although the mean torque on the sound side is showing the same movement, there are a few samples whose extension moment is still increasing until the end of the GC. The SPM{t} values of the prototype setting show multiple areas of differences, however, the trajectories are similar. It can be noticed that, at the beginning the extension moments differ largely with 0.8 Nm/kg and 0.25 Nm/kg for the sound and prosthetic side, respectively. After that, both begin to change direction in a similar

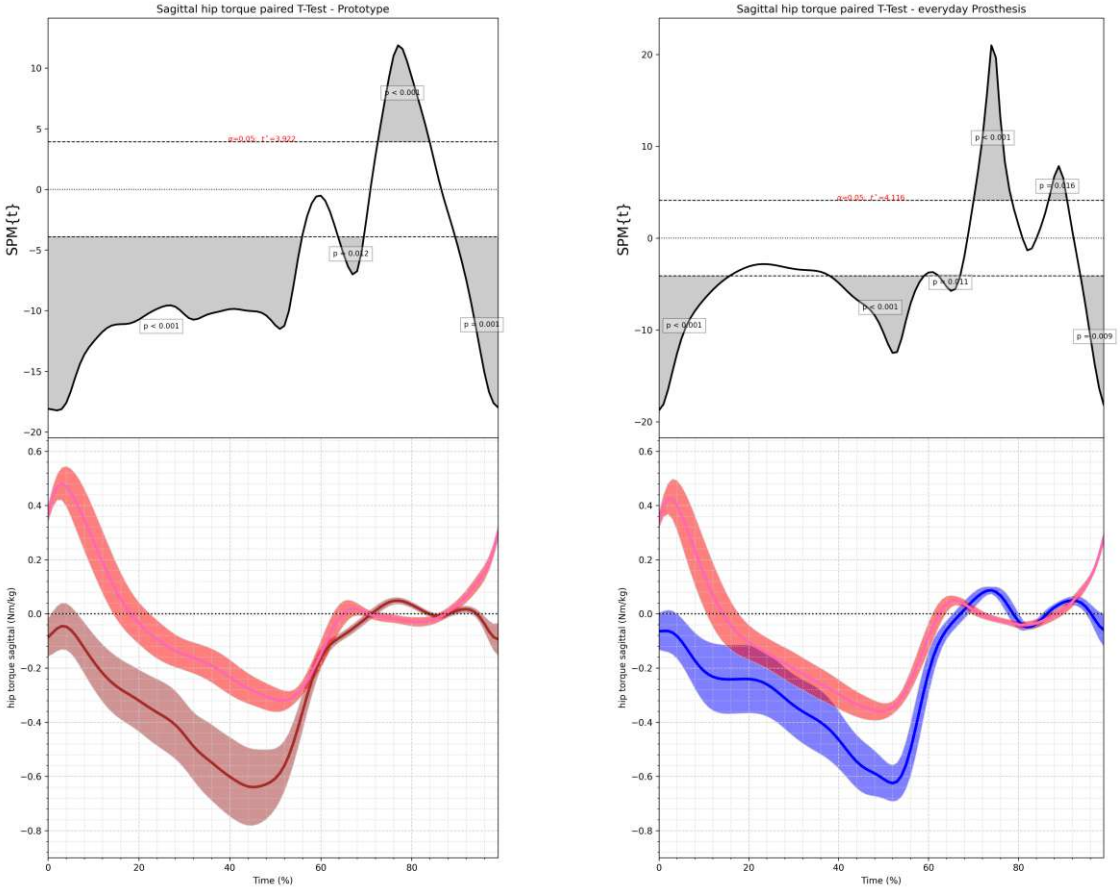

(a) At the top the SPM analysis of the sagittal hip moment the null hypothesis that both signals are equal can be seen. At the bottom the sagittal hip moment with standard deviation is shown for the prototype prosthesis. The pink graph is showing the sound leg while the brown one is showing the prosthetic limb.

(b) At the top the SPM analysis of the sagittal hip moment with the null hypothesis that both signals are equal can be seen. At the bottom the sagittal hip moment with standard deviation is shown for the everyday prosthesis. The pink graph is showing the sound leg while the blue one is showing the prosthetic limb.

Fig. 5.38: Sagittal hip moment for subject B, slow walking for both everyday and prototype prosthesis. The null hypothesis is that the movement of the left and right hip are equal. Positive values correspond to an extending moment, hence, negative values are flexion moments.

fashion until they reach their maximum flexion torque of 1.8 Nm/kg on the prosthetic side and 0.8 Nm/kg on the opposite limb at 45% GC. After the maximum flexion moment the moment is decreasing until it becomes extending again at 65% on the prosthetic side and increasing afterwards, peaking at 0.25 Nm/kg at the end of the gait cycle. The sound side is changing from a flexing to an extending moment at 80% GC but is increasing its value faster afterwards, which leads to a maximum flexion torque of 0.75 Nm/kg at the end.

Subject B Looking at the sagittal hip moment when walking fast it can be recognised that the statistical analysis is producing similar results, when using either of the two prostheses (see fig.5.40). The areas of statistical equality are almost the same with one area in stance phase, another one at the beginning of the swing phase and the last one at mid swing. When using

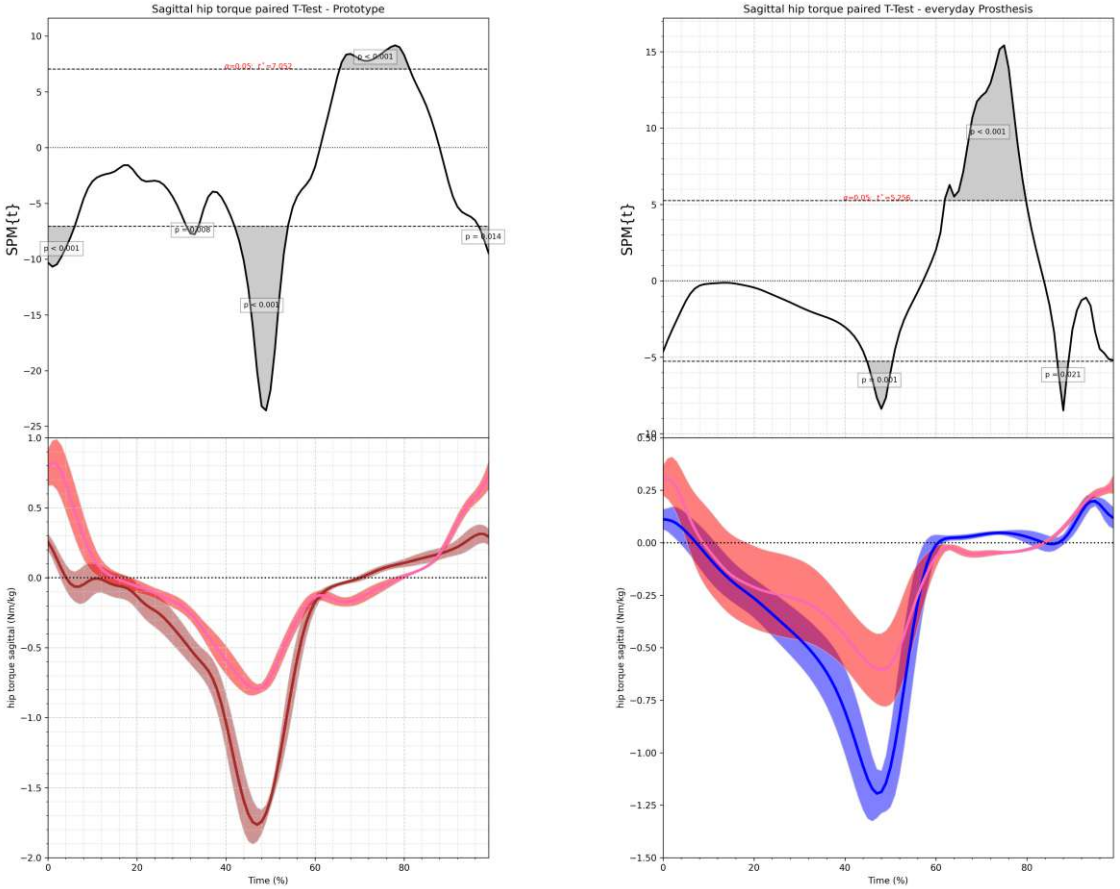

(a) At the top the SPM analysis of the sagittal hip moment the null hypothesis that both signals are equal can be seen. At the bottom the sagittal hip moment with standard deviation is shown for the prototype prosthesis. The pink graph is showing the sound leg while the brown one is showing the prosthetic limb.

(b) At the top the SPM analysis of the sagittal hip moment with the null hypothesis that both signals are equal can be seen. At the bottom the sagittal hip moment with standard deviation is shown for the everyday prosthesis. The pink graph is showing the sound leg while the blue one is showing the prosthetic limb.

Fig. 5.39: Sagittal hip moment for subject A, fast walking for both everyday and prototype prosthesis. The null hypothesis is, that the movement of the left and right hip are equal. Positive values correspond to an extending moment, hence, negative values are flexion moments.

the everyday prosthesis the hip on the sound side (see fig.5.40b) starts the gait cycle with an extension moment of 0.6 Nm/kg and is increasing until 0.75 Nm/kg at 5% GC. The hip on the prosthetic limb on the other hand is starting with a smaller extending moment of 0.1 Nm/kg and is immediately decreasing afterwards. At 20% GC both moments have changed into a flexing direction until reaching -0.1 Nm/kg. Afterwards both are decreasing until their maximum flexion torque of -0.5 Nm/kg is reached on the sound side, compared to 55% GC with -1.3 Nm/kg on the opposite side. In the swing phase the hip moment of the sound side changes from a flexing to an extending orientation at 80% GC and is increasing until reaching 0.5 Nm/kg at the end. The hip moment on the prosthetic side is changing its orientation from flexion to extension earlier at 70% GC and has two equally high peaks at 80% GC and 95% GC with 0.25 Nm/kg afterwards. The prosthetic limb hip ends the gait cycle with 0.1 Nm/kg. When the prototype prosthesis is

used (see fig.5.40a) the sagittal hip moment on the prosthetic and sound sides are 0.75 Nm/kg and almost zero at the beginning, respectively. Both hips have small peaks at 5% GC, although mirror-inverted with 0.9 Nm/kg on the sound side and -0.1 Nm/kg on the opposite side. After these peaks both moments are decreasing until reaching their maximum flexion torque of -1.25 Nm/kg and -0.4 Nm/kg at 50% GC for the prosthetic and sound side, respectively. While the hip torque on the sound side is changing its orientation from flexion to extension at 80% GC, the opposite hip is changing orientation already at 65% GC. In the end the sagittal hip moment is averaging 0.6 Nm/kg on the sound side and 0.1 Nm/kg on the prosthetic side.

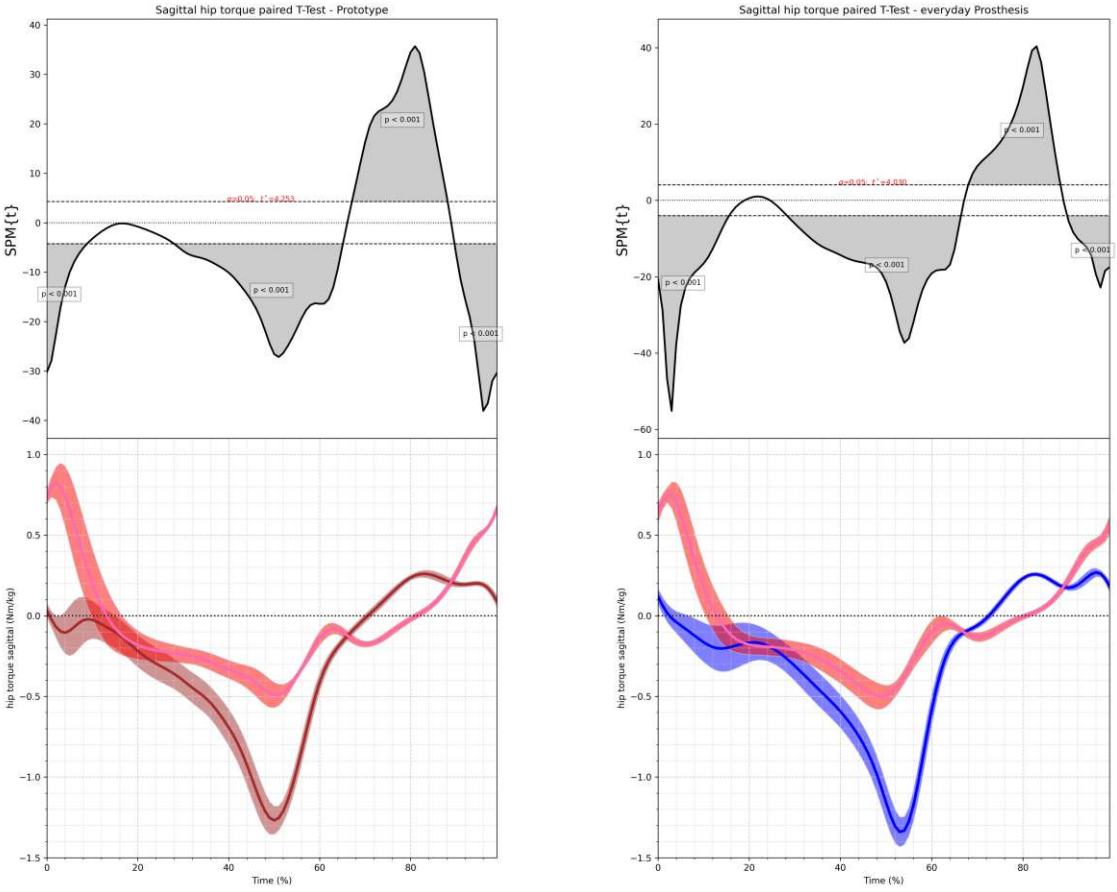

(a) At the top the SPM analysis of the sagittal hip moment the null hypothesis that both signals are equal can be seen. At the bottom the sagittal hip moment with standard deviation is shown for the prototype prosthesis. The pink graph is showing the sound leg while the brown one is showing the prosthetic limb.

(b) At the top the SPM analysis of the sagittal hip moment with the null hypothesis that both signals are equal can be seen. At the bottom the sagittal hip moment with standard deviation is shown for the everyday prosthesis. The pink graph is showing the sound leg while the blue one is showing the prosthetic limb.

Fig. 5.40: Sagittal hip moment for subject B, fast walking for both everyday and prototype prosthesis. The null hypothesis is that the movement of the left and right hip are equal. Positive values correspond to an extending moment, hence, negative values are flexion moments.

5.2.11 Hip Moment frontal

5.2.11.1 Slow walking

Subject A In figure 5.41 the frontal moments of the prototype and everyday prosthesis for slow walking can be seen. When looking at the details for the everyday prosthesis (see fig.5.41b) it can be seen that there are only three areas where the SPM{t} analysis indicates similarity (between 30% and 55%, 70% until 85% and 90% until the end). This is also seen when looking at the signals themselves. While the frontal torque on the sound side is peaking at an abduction moment of 0.9 Nm/kg at 5% GC, the corresponding value is reached later on the prosthetic side at 15% GC averaging 0.6 Nm/kg. Afterwards the torque remains fairly constant until 50% GC, whereas on the opposite limb the moment is decreasing rapidly to 0.7 Nm/kg at 20% GC and is still decreasing afterwards. At 50% GC both start to decrease rapidly. The decrease stops on the prosthetic side at 60% GC where a small abduction moment of 0.1 Nm/kg is still remaining, compared to the sound limb, which is decreasing until it changes direction and becomes an adduction moment of 0.15 Nm/kg at 60% GC. After that, the adduction moment on the sound side is decreasing again, while on the prosthetic side, after the plateau of 0.1 Nm/kg of abduction torque, the moment is reversed and becomes an adduction torque shortly from 80% to 90% GC, where it changes direction once again. After the decrease in adduction moment on the sound side it stays almost zero until the end where it rapidly changes into abduction moment of 0.2 Nm/kg. This rapid change is almost followed identically by the prosthetic side. For the prototype setting seen in figure 5.41a the SPM{t} values show three areas where the values are different. However, the deviations on the sound side are bigger as well, compared to the everyday prosthesis. Looking at the actual values it can be noted that the maximum abduction torque is happening at 10% GC on the sound side, followed by a sharp decrease until 20% GC, after which it increases again to 0.8 Nm/kg at 30% GC. On the opposite hip the frontal moment is increasing sharply until 10% GC where the increase is becoming smaller until it reaches the maximum abduction torque of 0.6 Nm/kg at 23% GC. After that, the moment is decreasing simultaneously with the sound side until the prosthetic side reaches an abduction torque of 0.1 Nm/kg at 60% GC, while the opposite side is decreasing until the moment changes its direction and becomes an adduction moment of 0.1 Nm/kg at 60% GC. After that, both torques are almost similar and at the end both signals increase rapidly to 0.2 Nm/kg into an abduction moment.

Subject B The frontal hip torque when walking slowly can be seen in figure 5.42. The SPM{t} analysis is producing similar results when wearing either of the two prostheses with three areas of statistical equality. However, for the most part the two torque signals are significantly different. This can also be seen when looking at the values while using the everyday prosthesis (see fig.5.42b). While two peaks of abduction torque of 0.8 Nm/kg at 15% and 0.75 Nm/kg at 35% can be seen on the sound side, the hip on the prosthetic side has only one peak at 25% GC of 0.55 Nm/kg. After that, both moments are decreasing until coming to a stop at an adduction torque of -0.15 Nm/kg at 60% GC on the sound side and zero at 65% GC on the opposite side. The torque of the hip on the prosthetic side is steadily increasing afterwards until reaching 0.1 Nm/kg at the end of the GC, compared to the opposite side, which has a peak of 0.1 Nm/kg at 80% GC and is ending at 0.2 Nm/kg. The trajectories, when using the prototype prosthesis, are looking similar to those of the everyday prosthesis (see fig.5.42a). The hip moment on the prosthetic side shows two peaks at 15% and 40% GC of 0.85 Nm/kg and 0.8 Nm/kg, respectively. The peak adduction torque is reached at 60% GC with -0.2 Nm/kg. Torque is increasing afterwards until reaching another peak of 0.1 Nm/kg in the swing phase at 80% GC and ending at 0.2 Nm/kg. The hip on the prosthetic side on the other hand shows only one peak in stance phase at 25% GC of 0.5 Nm/kg and is decreasing afterwards until reaching almost zero at 65% GC. The frontal hip

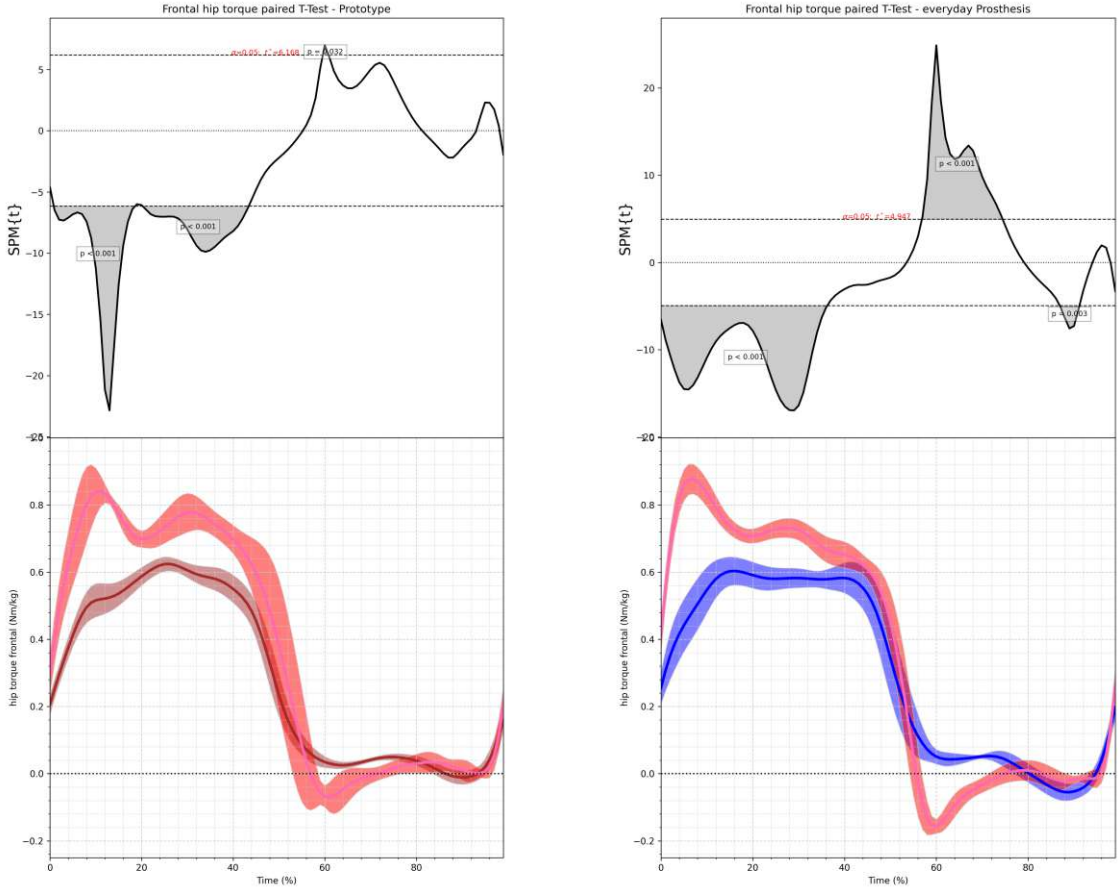

(a) At the top the SPM analysis of the frontal hip moment the null hypothesis that both signals are equal can be seen. At the bottom the frontal hip moment with standard deviation is shown for the prototype prosthesis. The pink graph is showing the sound leg while the brown one is showing the prosthetic limb.

(b) At the top the SPM analysis of the frontal hip moment with the null hypothesis that both signals are equal can be seen. At the bottom the frontal hip moment with standard deviation is shown for the everyday prosthesis. The pink graph is showing the sound leg while the blue one is showing the prosthetic limb.

Fig. 5.41: Frontal hip moment for subject A, slow walking for both everyday and prototype prosthesis. The null hypothesis is that the movement of the left and right hip are equal. Positive values correspond to an abduction moment, hence, negative values are adduction moments.

torque of the prosthetic limb is steadily increasing in swing phase until reaching 0.1 Nm/kg at the end of the gait cylce.

5.2.11.2 Fast walking

Subject A In figure 5.43 the frontal moments for the fast walking trail can be seen. Looking at the everyday prosthesis figure (see fig.5.43b) it can be noticed that the SPM{t} analysis shows three areas where the signals are significantly different. Looking at the actual signals it becomes obvious that the trajectories of both signals match closely, however, their values differ greatly. While the maximum abduction torque on the sound leg is at 8% GC and is approximately 1.3 Nm/kg, the maximum on the prosthetic side is averaging 0.7 Nm/kg. After that, both values are

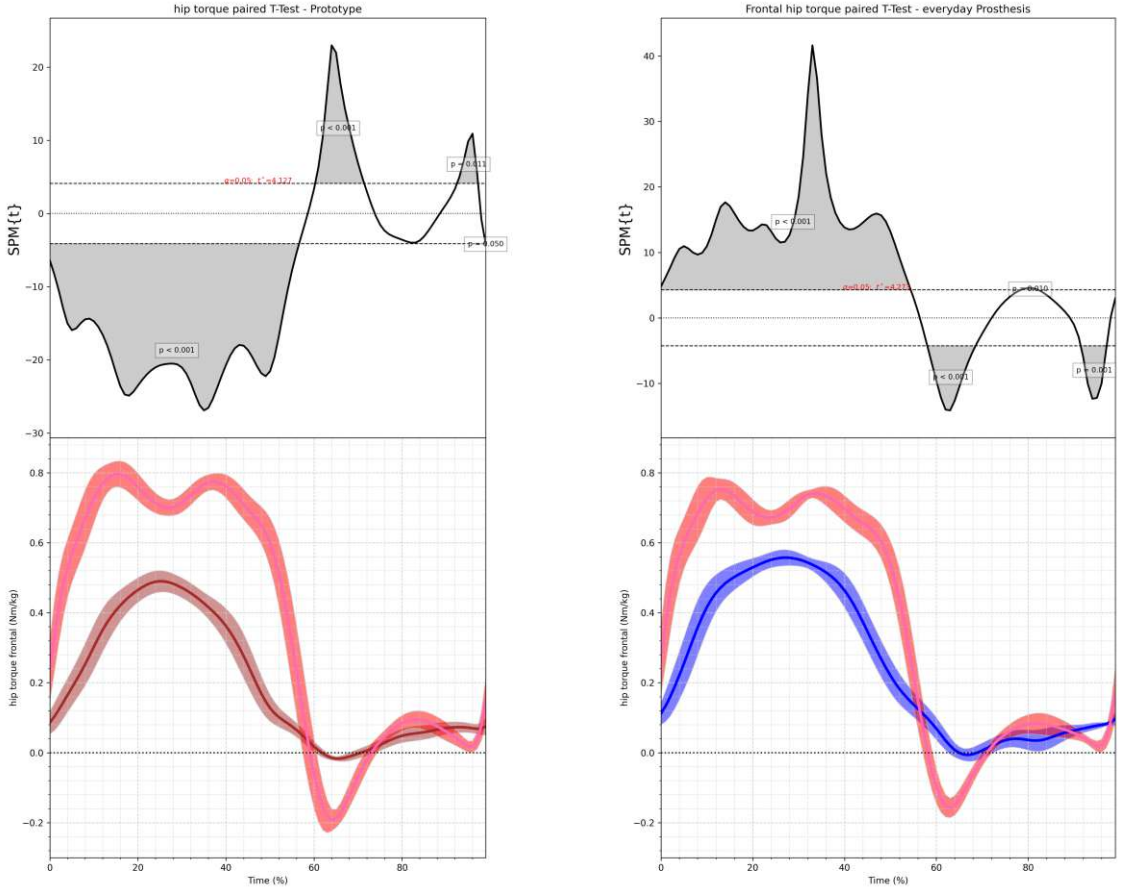

(a) At the top the SPM analysis of the frontal hip moment the null hypothesis that both signals are equal can be seen. At the bottom the frontal hip moment with standard deviation is shown for the prototype prosthesis. The pink graph is showing the sound leg while the brown one is showing the prosthetic limb.

(b) At the top the SPM analysis of the frontal hip moment with the null hypothesis that both signals are equal can be seen. At the bottom the frontal hip moment with standard deviation is shown for the everyday prosthesis. The pink graph is showing the sound leg while the blue one is showing the prosthetic limb.

Fig. 5.42: Frontal hip moment for subject B, slow walking for both everyday and prototype prosthesis. The null hypothesis is that the movement of the left and right hip are equal. Positive values correspond to an abduction moment, hence, negative values are adduction moments.

decreasing until they reach a turning point at 25% GC on the prosthetic side and at 30% GC on the opposite side. After that, abduction torque is increasing again until it reaches a second peak at 45% GC for both sides, averaging 0.6 Nm/kg and 0.8 Nm/kg for the prosthetic and the sound side, respectively. Both are decreasing after that until the moment changes direction and becomes an adduction moment briefly. Both sides increase simultaneously at the end and reach 0.2 Nm/kg of abduction moment right at the end of the gait cycle. When comparing the prototype prosthesis frontal hip torque it can be seen that the SPM{t} analysis shows only one area of significant differences from 5% to 10% GC. When looking at the signals it can be seen that there are two peaks at 8% GC and 43% GC with 1.2 Nm/kg and 1 Nm/kg on the sound side. This can also be seen on the prosthetic side, however, not as distinct as on the sound side, averaging 0.6 Nm/kg at 8% GC and 0.5 Nm/kg at 40% GC. Both hip torques are decreasing to

0.5 Nm/kg in between the two peaks. After the second peak both signals are decreasing again, but the sound side is changing from abduction into an adduction moment, whereas the opposite side becomes zero and afterwards stays in abduction until 80% GC. The sound side adduction torque peak is at 60% GC, averaging approximately 0.3 Nm/kg. After that, it is changing into a small abduction moment again. At the end the sound leg is changing into abduction yet again, while the prosthetic limb finishes with a small adduction moment.

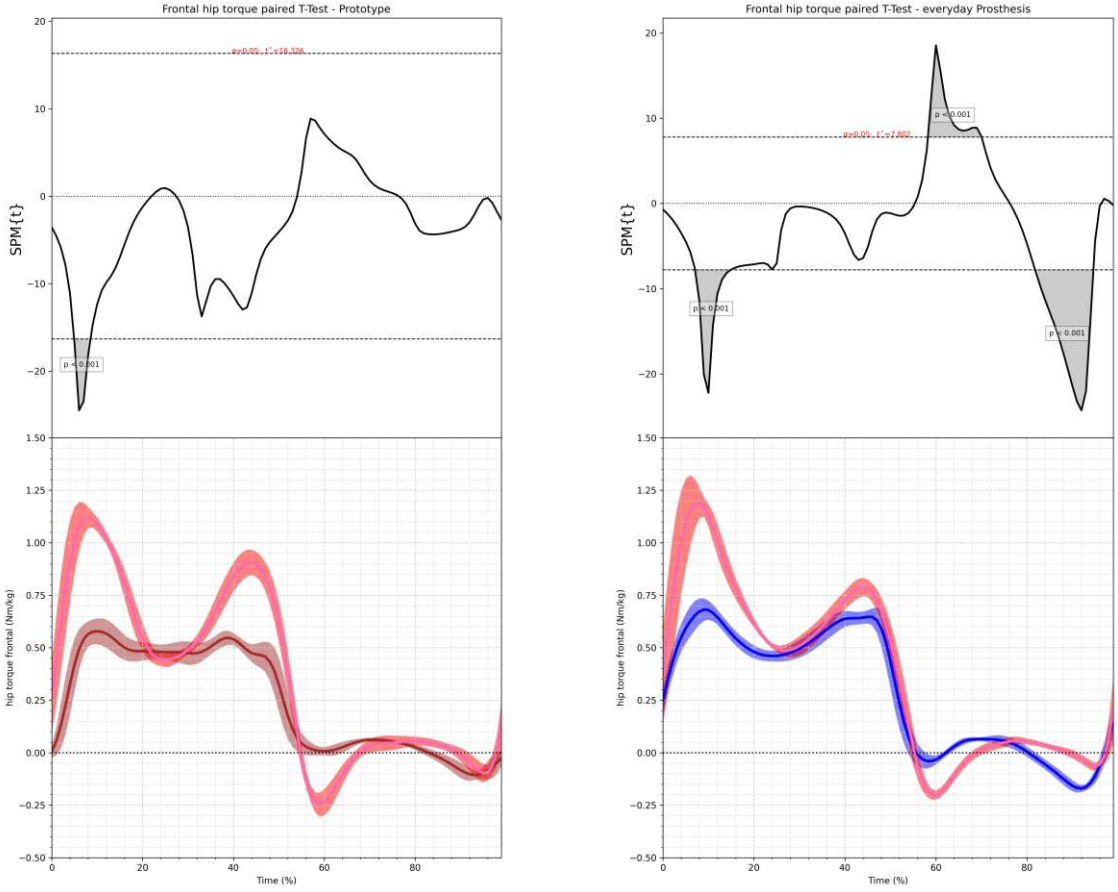

(a) At the top the SPM analysis of the frontal hip moment the null hypothesis that both signals are equal can be seen. At the bottom the frontal hip moment with standard deviation is shown for the prototype prosthesis. The pink graph is showing the sound leg while the brown one is showing the prosthetic limb.

(b) At the top the SPM analysis of the frontal hip moment with the null hypothesis that both signals are equal can be seen. At the bottom the frontal hip moment with standard deviation is shown for the everyday prosthesis. The pink graph is showing the sound leg while the blue one is showing the prosthetic limb.

Fig. 5.43: Frontal hip moment for subject A, fast walking for both everyday and prototype prosthesis. The null hypothesis is that the movement of the left and right hip are equal. Positive values correspond to an abduction moment, hence, negative values are adduction moments.

Subject B The frontal torque of the hip joint when walking fast can be seen in figure 5.44. The SPM{t} analysis when using either of the two prostheses are looking similar with only three small regions where statistical equality can be seen. When wearing the everyday prosthesis (see fig.5.44b) both hips are starting with an abduction torque of approximately 0.1 Nm/kg with

both moments increasing afterwards. However, the torque on the sound side is increasing faster and thus is peaking at 0.9 Nm/kg at 10% GC compared to the prosthetic side which peaks at 0.5 Nm/kg at 10% GC. While the torque is steadily decreasing on the prosthetic side until changing orientation and reaching a peak adduction torque of -0.1 Nm/kg at 65% GC afterwards, the hip on the opposite side is reaching a second peak of abduction torque at 45% GC of 0.7 Nm/kg until also changing its direction and reaching its peak adduction torque of -0.3 Nm/kg at 60% GC. In the subsequent swing phase the torque on the prosthetic side is almost linearly increasing until changing orientation and reaching 0.1 Nm/kg at the end. The hip on the sound side on the other hand has a peak of 0.2 Nm/kg at 75% GC followed by another peak of -0.1 Nm/kg until ending with a small abduction moment. The trajectories of the sound and prosthetic side hip torque while using the everyday prosthesis are matching closely to those when using the prototype (see fig.5.44a). The hip torque on the sound side shows two peaks of abduction moment in stance phase at 10% GC and 45% GC of 0.9 Nm/kg and 0.7 Nm/kg, respectively. After that, the torque deceases rapidly until reaching a peak adduction torque at 60% GC of -0.3 Nm/kg. In swing phase another peak of abduction torque with 0.15 Nm/kg at 80% GC followed by a small peak of -0.1 Nm/kg in an adducting orientation can be seen. The hip on the prosthetic side on the other hand has its first peak abduction moment at 10% GC with 0.4 Nm/kg. After a small plateau the moment is decreasing until changing its orientation to adduction and peaking at -0.1 Nm/kg. In the swing phase the moment is steadily increasing until reaching 0.15 Nm/kg at the end of the GC.

5.2.12 Hip Power

5.2.12.1 Slow walking

Subject A Figure 5.45 shows the hip power for the everyday and prototype prosthesis. When looking closer at the everyday prosthesis trails it can be seen that there are five areas where the SPM{t} analysis showed significant differences (see fig.5.45b). However, the sound side shows big deviations which influence the statistical results. When studying the power curves a short period of power generation can be observed at the beginning of the gait cycle which peaks at 3% GC with values of 0.2 W/kg and 0.6 W/kg for the prosthetic and sound side, respectively. After that, the prosthetic side starts to absorb power at 10% GC which peaks in 0.5 W/kg power absorption at 40% GC. The sound side hip power changes into power absorption later at 20% GC and its peak can be found at 40% GC as well, averaging 0.2 W/kg. After that, both sides show a rapid change into power generation with peaks of 1 W/kg at 50% GC on the prosthetic side and 0.5 W/kg at 55% GC on the sound side. After the peak power generation both sides quickly decrease to small power generation on the sound side and small power absorption on the other limb. At the end of the gait cycle both hips start to generate power again, but the sound limb is starting earlier at 85%, compared to the prosthetic side which starts at 90%. When wearing the prototype the SPM{t} result is indicating five areas of significant differences as well (see fig.5.45a). Looking closer at the two power curves of the hips, it becomes immediately apparent that the hip on the prosthetic side is already absorbing power at the beginning of the gait cycle, while the hip on the sound side is generating power, peaking at 0.5 W/kg at 3%. After that, the power generation is decreasing until 20%, where it changes to power absorption. On the prosthetic limb the power absorption is steadily increasing until it reaches its maximum at 40% of 0.75 W/kg. After that, it changes rapidly to its peak power generation at 55% of 0.5 W/kg. The corresponding peak power generation of the hip on the sound side is happening slightly earlier at 52% and is smaller with only 0.25 W/kg. After that, both power curves are decreasing

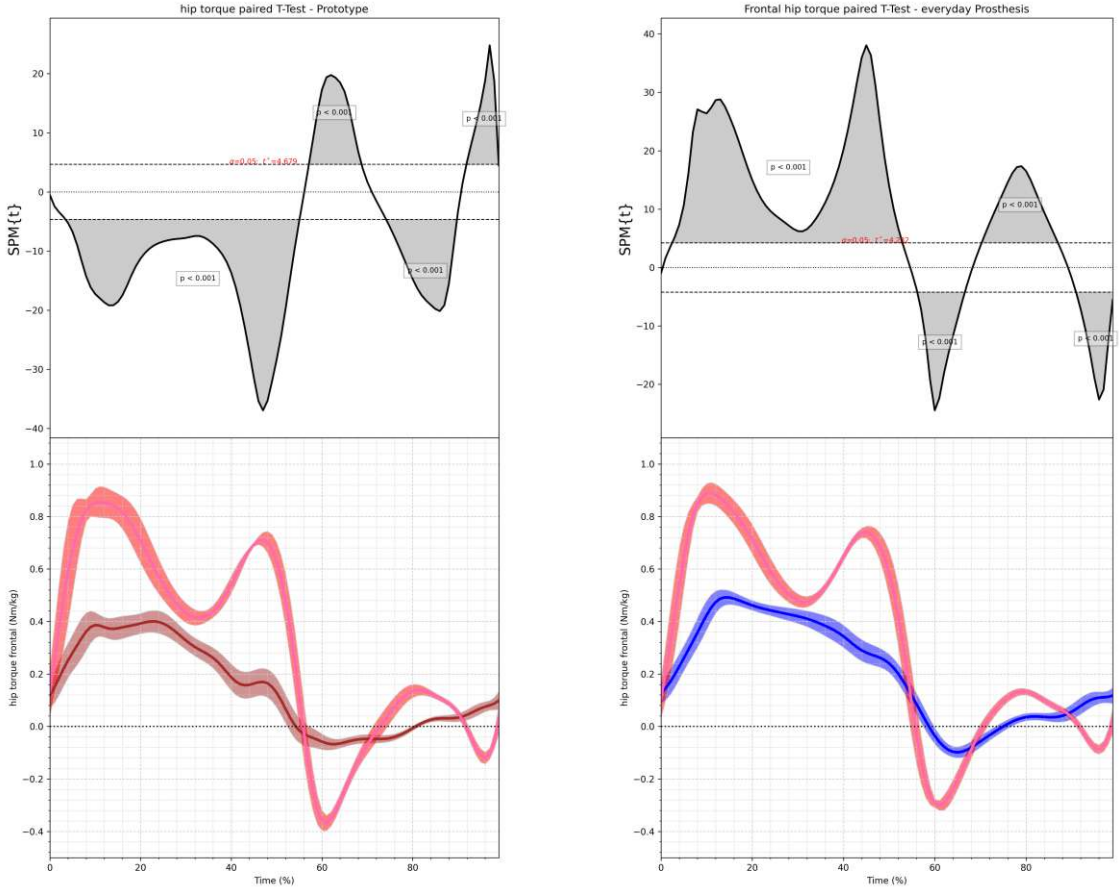

(a) At the top the SPM analysis of the frontal hip moment the null hypothesis that both signals are equal can be seen. At the bottom the frontal hip moment with standard deviation is shown for the prototype prosthesis. The pink graph is showing the sound leg while the brown one is showing the prosthetic limb.

(b) At the top the SPM analysis of the frontal hip moment with the null hypothesis that both signals are equal can be seen. At the bottom the frontal hip moment with standard deviation is shown for the everyday prosthesis. The pink graph is showing the sound leg while the blue one is showing the prosthetic limb.

Fig. 5.44: Frontal hip moment for subject B, fast walking for both everyday and prototype prosthesis. The null hypothesis is that the movement of the left and right hip are equal. Positive values correspond to an abduction moment, hence, negative values are adduction moments.

to almost zero until the end of the gait cycle, except for the hip on the sound side, which shows a small burst of power generation right at the end of the gait cycle.

Subject B The power generation of absorption while walking slowly can be seen in figure 5.45. Looking at the recordings while using the everyday prosthesis (see fig.5.46b) it can be seenn that the hip on the sound side is producing power until 25% GC with at peak at 5% GC of 0.6 W/kg. On the contrary, the hip on the prosthetic leg is absorbing power throughout the stance phase until 55% GC with a peak at 45% GC of -0.4 W/kg. The peak power generation on the prosthetic side is found at almost 60% GC of 0.5 W/kg. The corresponding peak of the hip on the sound side is noticeably smaller with 0.2 W/kg at 5% GC. After that, two small peaks of power generation at 65% GC and 70% GC of -0.1 W/kg can be seen for the sound and prosthetic

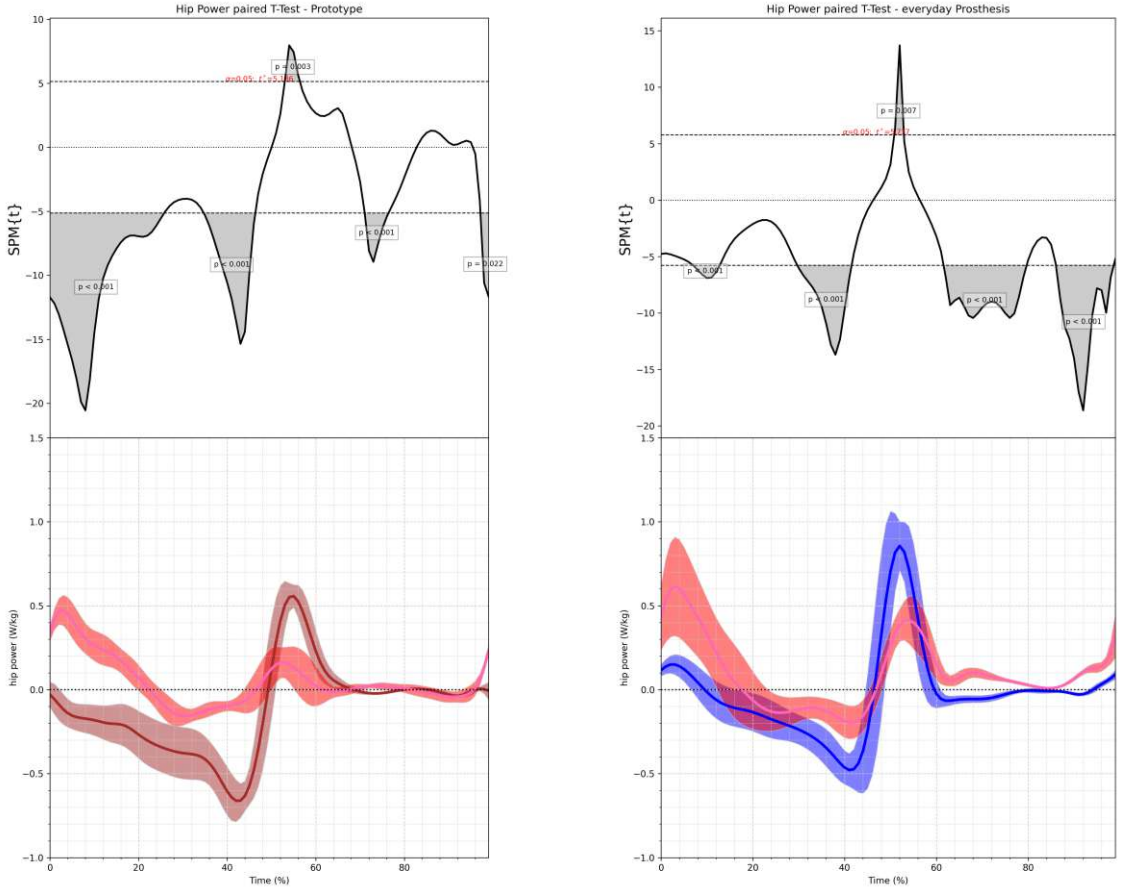

(a) At the top the SPM analysis of the hip power the null hypothesis that both signals are equal can be seen. At the bottom the hip power with standard deviation is shown for the prototype prosthesis. The pink graph is showing the sound leg while the brown one is showing the prosthetic limb.

(b) At the top the SPM analysis of the hip power with the null hypothesis that both signals are equal can be seen. At the bottom the hip power with standard deviation is shown for the everyday prosthesis. The pink graph is showing the sound leg while the blue one is showing the prosthetic limb.

Fig. 5.45: Hip power for subject A, slow walking for both everyday and prototype prosthesis. The null hypothesis is that the movement of the left and right hip are equal. Negative values correspond to power absorption, while positive values mean power generation.

side, respectively. At the end of the GC the hip of the sound side is recording 0.1 W/kg, while the opposite hip is almost zero. When the prototype prosthesis is worn (see fig.5.46a) almost the same features can be seen when describing the trajectories, compared to when wearing the everyday prosthesis. The hip on the sound side is producing power until approximately 30% GC with a peak of 0.6 W/kg at 5% GC. A very brief power generation of the hip on the prosthetic side can be sen at 5% GC with a peak value of 0.05 W/kg. After that, the hip is absorbing power with a steady increase in magnitude until reraching a peak value of -0.3 W/kg at 45% GC. The peak power absorption is earlier when looking at the values of the hip on the sound side at 30% GC, averaging -0.1 W/kg. A short burst of power generation can be seen at the end of the stance phase which is peaking at 0.2 W/kg at 55% GC on the sound side compared to 0.3 W/kg at almost 60% GC on the prosthetic side. After that, the power generation drops steadily

until reaching zero on both sides. In the end the hip on the sound side is averaging 0.1 W/kg compared to -0.05 W/kg for the hip on the prosthetic side.

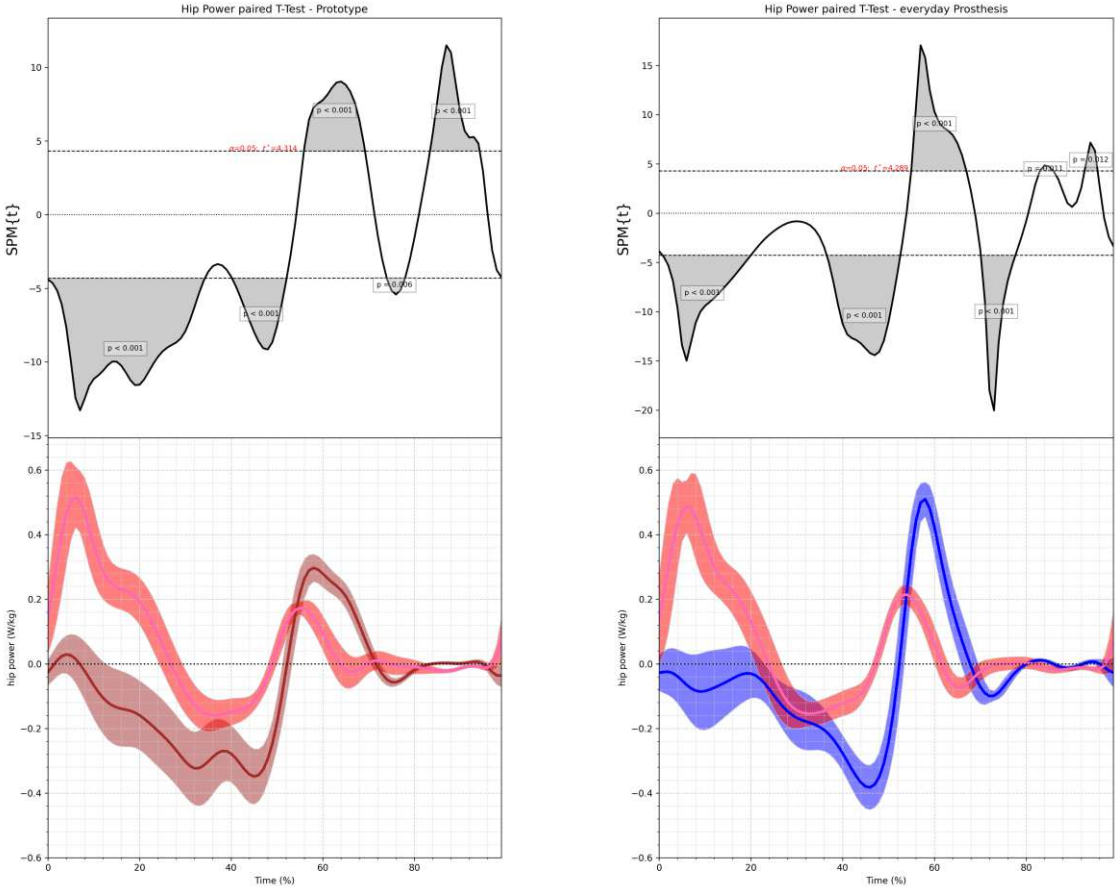

(a) At the top the SPM analysis of the hip power the null hypothesis that both signals are equal can be seen. At the bottom the hip power with standard deviation is shown for the prototype prosthesis. The pink graph is showing the sound leg while the brown one is showing the prosthetic limb.

(b) At the top the SPM analysis of the hip power with the null hypothesis that both signals are equal can be seen. At the bottom the hip power with standard deviation is shown for the everyday prosthesis. The pink graph is showing the sound leg while the blue one is showing the prosthetic limb.

Fig. 5.46: Hip power for subject B, slow walking for both everyday and prototype prosthesis. The null hypothesis is that the movement of the left and right hip are equal. Negative values correspond to power absorption, while positive values mean power generation.

5.2.12.2 Fast walking

Subject A The hip power for the fast walking trail can be seen in figure 5.47. Looking closer at the everyday prosthesis figure (see fig.5.47b) it can be seen that, at the beginning, the power has large deviations on the sound side which are decreasing until 20%. Therefore, the SPM{t} results have to be interpreted with care until then. Afterwards, four areas of significant differences can be seen. Both signals start with small power generation at the beginning. The hip power on the prosthetic side is decreasing afterwards until it becomes zero at 10% followed by a short burst of power generation at 18% with 0.25 W/kg. After that, both hips begin to absorb until they peak

at 40% at 1 W/kg and 0.25 W/kg for the prosthetic side and the sound side, respectively. This peak absorption is followed by a rapid change and big power generation at 50% with 1.5 W/kg on the prosthetic side and 1.0 W/kg on the sound side. While the hip on the sound side continues to generate power until 78%, the hip power changes to absorption immediately after the peak power generation. At 90% a short peak of power generation on the sound side is visible, while the peak can only be seen at the very end on the other side. When looking at the prototype setting (see fig.5.47a) three areas of statistical differences, when looking at the SPM{t} score, can be seen. Right at the beginning the signals look different with the prosthetic side changing from power generation to power absorption at 0% and 7%, then to power generation at 15%, after which it decreases steadily into absorption until it reaches its peak value of 1.75 W/kg power absorption. Looking at the hip power of the sound side the peak generation power is at 7% averaging 0.75 W/kg followed by a steady decrease until the power changes to absorption at 20%. After that, the peak power absorption is reached at 38% at approximately 0.5 W/kg. Both hip powers are generating power shortly after the peak absorption at 55% with values of 1.25 W/kg on the prosthetic side and 0.5 W/kg on the sound side. In contrast to the sound side, the hip on the prosthetic side is constantly decreasing after the peak power generation. The hip on the sound side shows another short burst of power at 68% of 0.5 W/kg and is decreasing afterwards until it reaches zero. A small peak of power generation marks the end of the gait cycle, compared to the prosthetic side that is still increasing until it reaches approximately 0.5 W/kg at the end of the gait cycle.

Subject B The power absorption or generation of both hips can be seen in figure 5.48. The statistical analysis while using the everyday prosthesis shows six areas of significant differences, which indicates that the signals are quite different overall (see fig.5.48b). Looking at the recorded power values for both hips it can be seen that, right at the beginning, the hip on the sound side is generating power with a peak at 5% GC of 0.8 W/kg, compared to the opposite hip which is absorbing power with a peak at 10% GC of -0.2 W/kg. While the peak power absorption for the hip on the sound side is at 40% GC, averaging -0.4 W/kg, the corresponding peak of the hip on the prosthetic side can be found at 45% GC of approximately -1.1 W/kg. After that, both hips start to generate power again which peaks at almost 1.5 W/kg at 60% GC on the prosthetic side and 0.5 W/kg at 50% GC on the prosthetic side. The sound hip remains in power generation afterwards with a second peak of 0.5 W/kg at 65% GC. The hip on the prosthetic side on the other hand is quickly absorbing power again until a peak at 80% GC of -0.3 W/kg. Both powers are returning to zero at the end of the GC. When switching to the prototype prosthesis six areas of significant differences can be seen as well, when studying the SPM{t} analysis (see fig.5.48a). The hip on the sound side is starting with a sharp increase of power generation reaching 1.2 W/kg at 5% GC, compared to the opposite hip which has a peak of power absorption at that point of 0.2 W/kg. The hip on the sound side is producing power until roughly 20% GC, where it starts to absorb power until a peak of -0.4 W/kg at 40% GC. The hip on the prosthetic side on the other hand is reaching its peak power absorption at 45% GC of -1.3 W/kg. At the end of the stance phase both sides start to produce power again which can be seen in a peak of 1.0 W/kg at 55% GC on the prosthetic side, compared to 0.2 W/kg at 50% GC on the prosthetic side. In contrast to the hip on the prosthetic side, a second peak of 0.75 W/kg can be seen at 65% GC on the sound side. After a short period of power absorption on both sides the power is reaching zero at the end of the gait cycle.

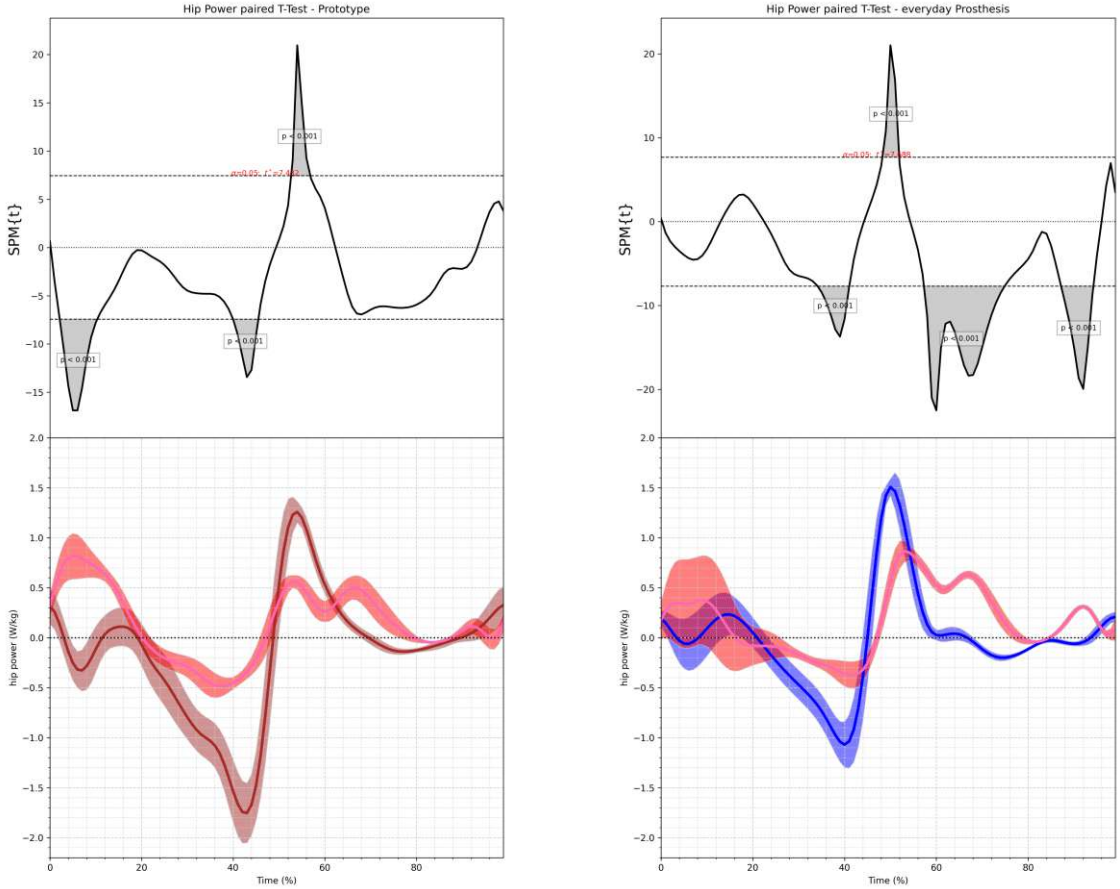

(a) At the top the SPM analysis of the hip power the null hypothesis that both signals are equal can be seen. At the bottom the hip power with standard deviation is shown for the prototype prosthesis. The pink graph is showing the sound leg while the brown one is showing the prosthetic limb.

(b) At the top the SPM analysis of the hip power with the null hypothesis that both signals are equal can be seen. At the bottom the hip power with standard deviation is shown for the everyday prosthesis. The pink graph is showing the sound leg while the blue one is showing the prosthetic limb.

Fig. 5.47: Hip power for subject A, fast walking for both everyday and prototype prosthesis. The null hypothesis is that the movement of the left and right hip are equal. Negative values correspond to power absorption, while positive values mean power generation.

5.2.13 Hip Work

5.2.13.1 Slow walking

Subject A In figure 5.49 the hip work split into positive and negative values can be seen for slow walking. The positive work values are averaging slightly above 0.125 J/kg for the everyday prosthesis and slightly below 0.125 J/kg for the prototype on the sound side. On the prosthetic side the average value is 0.125 J/kg when using the everyday prosthesis and 0.08 J/kg when wearing the prototype prosthesis. Looking at the negative work it can be observed that the hips on the prosthetic side are averaging -0.15 J/kg and -0.275 J/kg when using the everyday and prototype prosthesis, respectively. For the sound side both mean values are the same at approximately -0.06 J/kg.

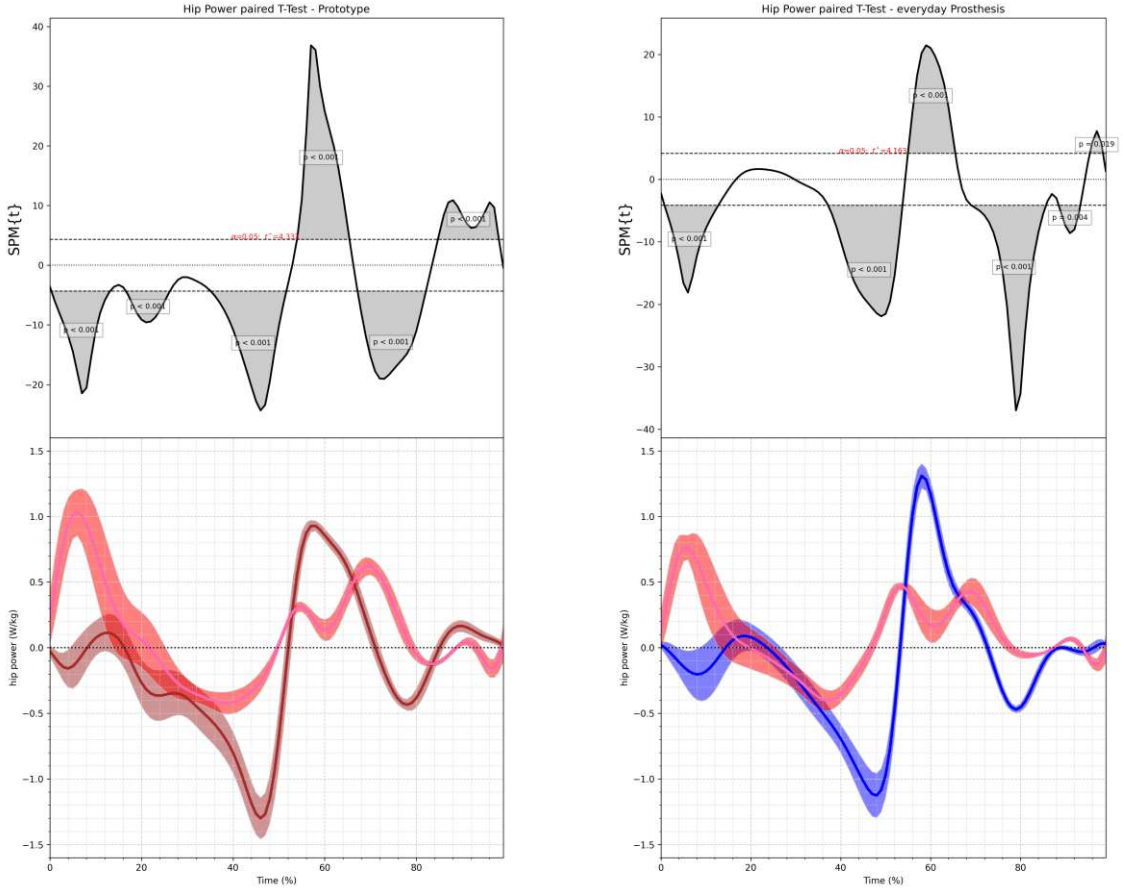

(a) At the top the SPM analysis of the hip power the null hypothesis that both signals are equal can be seen. At the bottom the hip power with standard deviation is shown for the prototype prosthesis. The pink graph is showing the sound leg while the brown one is showing the prosthetic limb.

(b) At the top the SPM analysis of the hip power with the null hypothesis that both signals are equal can be seen. At the bottom the hip power with standard deviation is shown for the everyday prosthesis. The pink graph is showing the sound leg while the blue one is showing the prosthetic limb.

Fig. 5.48: Hip power for subject B, fast walking for both everyday and prototype prosthesis. The null hypothesis is that the movement of the left and right hip are equal. Negative values correspond to power absorption, while positive values mean power generation.

Subject B When looking at the work done at the hip for subject B (see 5.50) it can be seen that the positive work of the residual hip is averaging 0.09 J/kg and 0.08 J/kg when using the everyday and prototype prosthesis, respectively. The values of the hip of the sound side are almost similar as well, with 0.15 J/kg when using the everyday prosthesis and 0.16 J/kg when the prototype prosthesis is used.

5.2.13.2 Fast walking

Subject A When looking at the values for the positive and negative work done at the hip (see fig.5.51) it can be seen that the mean values are very similar for the positive work. Both hips on the prosthetic leg are averaging approximately 0.155 J/kg with similar percentile ranges. On the sound side the averages are approximately 0.213 J/kg when using the everyday prosthesis and

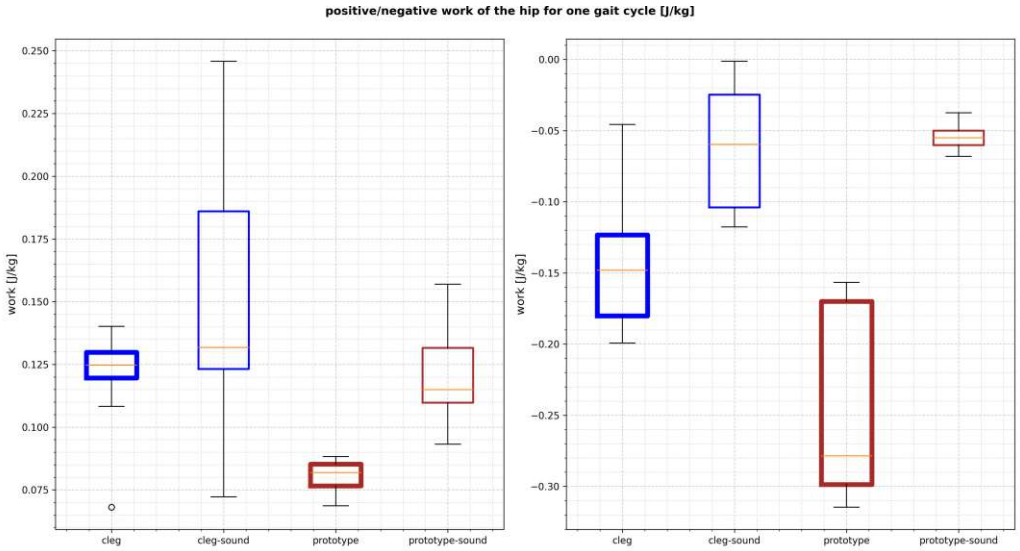

Fig. 5.49: On the left side the values for the positive work (corresponding to power generation) can be seen and on the right side the values for the negative work (corresponding to power absorption) is displayed. The blue colour indicates the everyday prosthesis, while the brown shows the values for the novel active prosthesis for subject A and slow walking.

0.225 J/kg when using the prototype prosthesis. However, when using the everyday prosthesis the deviations are much higher, compared to the deviations when wearing the prototype. Looking at the values for the negative work, it can be observed that there are differences when wearing the prototype, compared to the everyday prosthesis. While the hip on the prosthetic side is averaging -0.22 J/kg, the mean on the same side while using the prototype is -0.35 J/kg. For the sound limb the negative hip work is averaging the same value of roughly -0.09 J/kg.

Subject B The hip work separated in positive and negative values can be seen in figure 5.52. The hips on the prosthetic side are averaging positive work input of 0.155 J/kg and 0.137 J/kg for the everyday and prototype prosthesis, respectively. Looking at the sound side these values differ largely with 0.19 J/kg for the everyday prosthesis and 0.23 J/kg for the prototype prosthesis. Looking at the negative values, it can be observed that the prosthetic side is averaging -0.30 J/kg for both prostheses and on the sound side mean values are -0.09 J/kg and -0.1 J/kg for the everyday prosthesis and prototype, respectively.

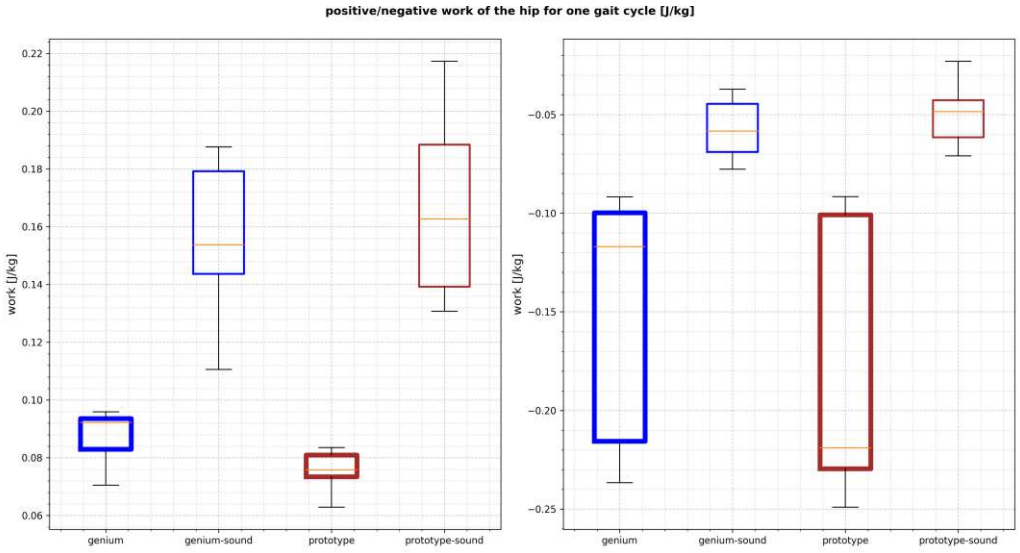

Fig. 5.50: On the left side the values for the positive work (corresponding to power generation) can be seen and on the right side the values for the negative work (corresponding to power absorption) is displayed. The blue colour indicates the everyday prosthesis, while the brown shows the values for the novel active prosthesis for subject B and slow walking.

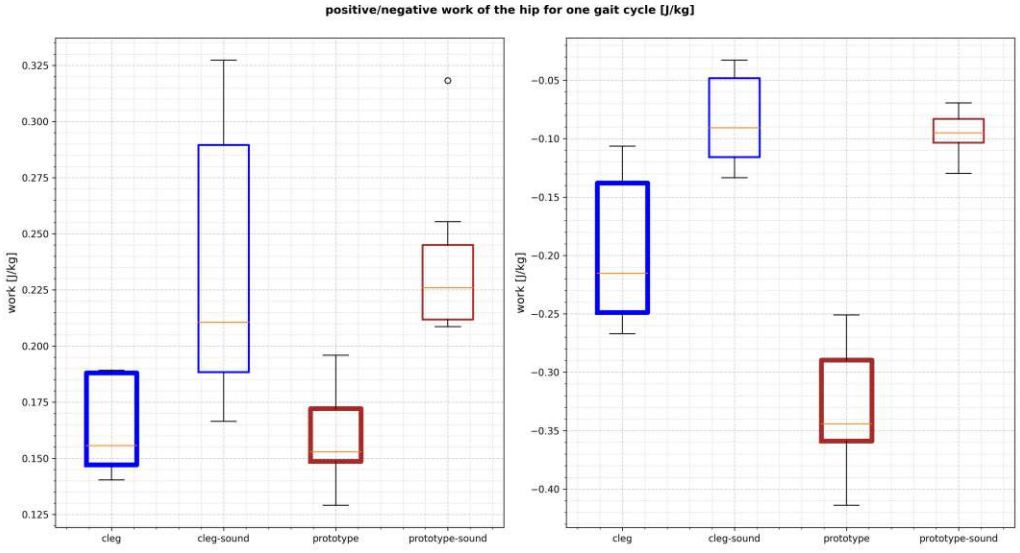

Fig. 5.51: On the left side the values for the positive work (corresponding to power generation) can be seen and on the right side the values for the negative work (corresponding to power absorption) are displayed. The blue colour indicates the everyday prosthesis, while the brown shows the values for the novel active prosthesis for subject A and fast walking.

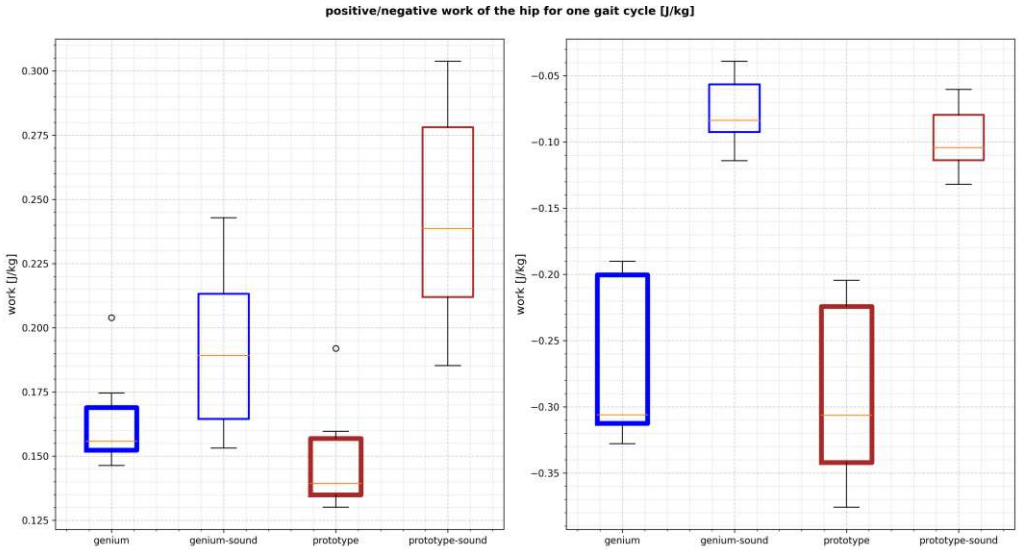

Fig. 5.52: On the left side the values for the positive work (corresponding to power generation) can be seen and on the right side the values for the negative work (corresponding to power absorption) can be seen. The blue colour indicates the everyday prosthesis, while the brown shows the values for the novel active prosthesis for subject B and fast walking.

5.3 Discussion

The aim of this thesis was to record two velocities while using the prototype prosthesis in the gait laboratory equipped with a Vicon™ system and test seven developed hypotheses with regards to the subjects everyday non-active prostheses. The hypotheses were either developed by trying to interpret subjective user feedback into objective criteria or by exploiting the known differences of the prototype prostheses and the subjects everyday prostheses to find parameter for which differences were most likely to be seen. Because no standardized data for prosthetic gait exists and prosthetic gait is quite different compared to healthy gait, comparing the symmetry between the sound and the prosthetic limb was chosen to be the most objective method to identify differences. However, hip power, work and torque were also investigated for different peak values as the hip is the remaining joint of a trans-femoral amputee and therefore the only way to actively manipulate gait.

5.3.1 Stance Phase more symmetrical

The stance phase of trans-femoral amputees is more asymmetrical compared to that of non-amputees where almost perfect agreement between the left and right stance phase can be found [42]. The stance phase is usually longer on the sound side compared to the prosthetic side which is in agreement with the results of this thesis [18, 42, 76, 87, 90]. An improvement in symmetry could be found in two trails: slow and fast walking with subject A, with the slow walking trail also being statistically significant. In contrast, the symmetry became worse for all walking trails regardless of walking speed, when subject B was using the prototype prosthesis. This could have to do with the fact that, before testing the prosthesis on subject A, a whole day of testing and modifying the settings was done in order to get the best results possible. Subject B did already have some experience with the prototype and the latest good settings that were recorded with him where used. Another possible influence might be that, when recording with subject B, the speeds were controlled to match the self selected speeds when walking with the everyday prosthesis. Because controlling the walking speed with a metronome is changing the relationship between step frequency and stance time durations [98], this could have an effect on the results recorded with subject B.

5.3.2 Symmetry and Control of the Foot Clearance improves

The motor of the prototype prosthesis allows to control not only stance phase flexion but also swing phase flexion and extension of the knee. This allows to control and alter the minimum foot clearance, because it is not only dependent on the ability to plantar-flex the angle but also dependent on the knee flexion angle and the timing of the flexion movement of the hip [52, 61]. Increasing foot clearance can not only help to reduce the probability to stumble but also reduce compensating mechanisms like vaulting or hip hiking [22]. Furthermore, it could potentially get rid of the need to shorten the prosthetic limb, compared to the sound limb, which is usually done to compensate for the elongation of the prosthetic limb in swing phase due to vertical displacements of the socket in relation to the stump and is thought to be the source of lower back pain [61]. The relevant value represents the minimum, at the transition from initial to mid swing, occurring at 75% to 85% GC. It has to be said that the timing of the hip flexion is influencing the foot clearance as well, but the differences in the hip angles, while using either of the two prostheses, did not show any statistical relevant changes of the movement into flexion after maximum extension intra-subjectively. Because the prosthetic setup was the same for each subjects everyday prosthesis and prototype prosthesis, changes occurring because of different components used can be seen as very unlikely. The marker of the trochanter was also analysed

to make sure that no hip hiking was present to gain more foot clearance. An effect could only be seen for subject A while walking fast. However, after studying the ankle angles it could be established that the movement was due to vaulting and not due to hip hiking (see figures 7.1 to 7.4).

Slow Walking When looking at the foot clearance when walking slowly (see section 5.2.3) it can be seen that, regardless of the subject, the timing of the minimum foot clearance does not improve when using the prototype prosthesis. In all trails the minimum foot clearance is occurring earlier in the swing phase, compared to the subjects sound limb. This can also be seen when looking at the maximum flexion angles of the knee in swing phase (see section 5.2.5) which occur earlier as well, compared to their sound counterparts, which indicates,that greater symmetry in the knee flexion could produce greater symmetry in the foot clearance timing as well. Another strong indication of increased symmetry in the knee flexion angles, resulting in greater symmetry of the foot clearance as well, can be seen when studying the foot clearance in the fast walking setting. Concentrating on the values of the minimum toe clearance it can be seen that the maximum knee flexion is also influencing the clearance directly. The maximum flexion angle of subject A, when using the prototype prosthesis is smaller compared to when using the everyday prosthesis, which is resulting in a decreased foot clearance when using the prototype. For subject B the maximum knee flexion angle is slightly larger when using the prototype prosthesis which corresponds to slightly bigger values of the minimum foot clearance when using the prototype. Furthermore, when looking at the ankle angle (see section 5.2.4) no vaulting can be observed, which can be seen in a second peak happening at 15% to 25% GC [22]. This can be confirmed when studying ankle moments as well (see fig.7.11), where no additional ankle moment from 15% to 25% GC on the contralateral limb can be noticed.

Fast Walking When walking fast and wearing the prototype prosthesis it can be seen that the foot clearance does align better to the sound limb in a temporal perspective, compared to using the everyday prosthesis is being used. This behaviour can also be seen when looking at the knee angles (see section 5.2.5), where the peak swing flexion is aligning perfectly to that of the sound knee when using the prototype prosthesis. The minimum foot clearance is also higher when using the prototype prosthesis for both subjects. When looking at the knee angles it can be seen that the higher foot clearance might be caused by higher knee flexion angles in the swing phase, which in return means that symmetry in the knee angles is reduced. When looking at the ankle angle (see section 5.2.4) it can be observed that for subject A a vaulting mechanism is existing. Vaulting can be recognised by two peaks in single stance on the contralateral limb [22] as well as by a second peak in ankle torque (see fig.7.12). This is the case when reviewing the result of subject A. However, because the mechanism can be seen while using both prostheses, it can still be assumed that the increased foot clearance is a result achieved by the prototype prosthesis.

5.3.3 Symmetry in Hip, Knee and Ankle Angles improves

The gait of unilateral trans-femoral amputees is not only asymmetric in spatio-temporal variables but also in kinematic considerations [42, 50]. Because asymmetric gait is widely believed to be the reason for secondary physical conditions after amputations, like pain and joint degeneration [15, 89] or greater incidences of osteoarthritis of the intact limb [56], it is valuable to see if symmetry is increasing not only in spatio-temporal or kinetic parameters but also in kinematic parameters of the hip, knee and ankle joints. The SPM{t} analysis is allowing to analyse the recordings directly without having to summarize or focus on one specific area of interest. Asymmetry can appear temporally (e.g. the peak flexions of the knees are not aligning properly) or in absolute

values (e.g. the peak flexion angles of both knees are different). With the SPM analysis symmetry is only found when both characteristics are fulfilled. However, an increased knee flexion angle in the swing phase of the prosthetic knee might be the reason for increased foot clearance and thus can also be beneficial in preventing stumbling.

Ankle Angle Improved symmetry in the ankle angle can only be found in the stance phase, because passive prosthetic feet were used when testing with either of the two subjects, hence, no movement in the swing phase was recorded on the prosthetic feet. However, no improvement of the symmetry of the ankle angle when using either of the two prostheses for both subjects could be found.

Ankle Angle - Slow Walking When looking at the ankle angles while walking slow it becomes immediately apparent, that in this case no improvement of the symmetry can be found for either of the two subjects (see section 5.2.4). Big deviations in the signal of subject A when using the prototype prosthesis can be seen which are assumed to be caused by the lack of training with the prototype prosthesis. Another variance can be seen in the different prosthetic limb ankle angles of subject A occurred due to the fact that in the first test markers on the foot were no applied onto the foot and later virtually generated, which caused varying angles in the swing phase of the passive ankle joint. The only difference when looking at the ankle angles of subject B can be seen on the prosthetic side. The ankle angle is following a convex path until reaching a plateau at 40% GC which could not be seen when using the everyday prosthesis. This behaviour was assumed to be caused by the activation of the motor of the prosthesis.

Ankle Angle - Fast Walking No improvement of the symmetry in the ankle angle can be seen for either subject in the stance phase (see section 5.2.4). For subject A vaulting could be seen which did increase asymmetry at the beginning of the stance phase for both prostheses. When looking closer at the results of subject B almost no differences can be seen when wearing the everyday or the prototype prosthesis. The only difference was a decrease of the rate of angular change at 20% GC which was assumed to be caused by the activation of the motor of the active prosthesis.

Knee Angle The prototype is not only able to assist with swing flexion and extension of the knee but also allows more degrees of stance phase flexion, as the motor is able to decrease flexion angles of the knee in stance phase that would not be possible with a passive knee device, due to the direction of the ground reaction force vector. Therefore, it was assumed that symmetry is increasing not only in swing or stance phase but throughout the gait cycle.

Knee Angle - Slow Walking An increase in symmetry of the knee angles in stance phase flexion could not be seen when walking slowly (see section 5.2.5). This is mainly due to the fact that on the one hand, subject A was walking slowly with a hyperextended sound knee in stance phase and therefore symmetry did decrease because of the bigger stance phase flexion of the prototype knee joint. On the other hand, the control mechanisms of the prototype knee did not work well when subject B was recording its trails as the knee ended and began with almost 10 degrees of flexion, which could not be seen in the fast walking trails. This meant that the knee angles, at the beginning of the stance phase, were different and because stance phase flexion of the sound knee was smaller when walking slowly the possibility of greater flexion of the prototype knee in stance phase did not improve symmetry overall for subject B. The reason could quite possibly be that subject B has adjusted the walking patterns of the sound knee to match the patterns of

the everyday prosthesis, which are matching very well at peak stance phase flexion. Comparing the maximum swing phase flexion almost no change of the maximum angles can be seen when wearing either of the two prostheses for both subjects. The timing of the peaks in swing phase did not improve either. Overall no improvement of the symmetry of the knee angles could be seen.

Knee Angle - Fast Walking When looking at the knee angles, improved symmetry can be seen in stance phase where bigger flexion angles of the prototype knee is resulting in greater symmetry (see section 5.2.5). However, the timing is a little bit late when subject A is wearing the prototype. The timing of the peak stance phase flexion is very good, when subject B is wearing the prototype, however, the concave trajectory of the knee going into stance phase flexion results in a sharp edge when the maximum flexion angle is reached, which could feel uncomfortable, but no feedback of subject B was received, therefore this assumption could not be proven. In swing phase improvements in symmetry can be seen temporally but not regarding the total value of the peak swing phase flexion. The time for which peak swing phase flexion occurs fits almost perfectly for both subjects. For subject A this can be seen as an improvement as the peak flexion of the C-Leg occurs significantly earlier, compared to the prototype knee. When compared to the Genium knee joint of subject B only small improvements in the symmetry of the timing of peak swing phase flexion can be seen. Regarding the second possible source of asymmetry, the total values, in peak swing phase flexion the asymmetry is increasing when wearing the prototype, because bigger angles are achieved. This is mainly due to a rapidly increasing angle, because the starting points of the movements into swing phase flexion are almost identical in both settings. However, it has to be kept in mind that a bigger knee flexion angle in the swing phase is also resulting in a bigger foot clearance which can reduce the risk of stumbling.

Hip Angle The hip joint is the only joint that is sound on both limbs. The fact that the swing phase flexion of the everyday prosthesis has to be triggered by using momentum generated at the hip, led to the assumption that symmetry would increase when using the prototype prosthesis.

Hip Angle - Slow Walking The overall symmetry of the hip angles when walking slowly did not increase when using the prototype prosthesis (see section 5.2.6). Although both subjects show good agreement between the angles of the sound and prosthetic limb, with either of the prostheses significant differences exist in swing phase. For subject B the maximum extension angle of the hip is greater, compared to the angles of the contralateral hip which increases asymmetry in that area, compared to when using the everyday prosthesis, where the angles are almost identical. This behaviour can not be seen in subject B. However, in swing phase the hips on the prosthetic side are moving much faster into flexion which increases asymmetry in the swing phase. Furthermore, the maximum flexion angles are bigger at the end of the swing phase, compared to the sound hips angles. However, the bigger flexion angles in the end did not result in a bigger step length on the prosthetic side (see fig.7.5). At the end of the hip angles on the prosthetic side a second peak flexion angle can be seen. Looking at the almost equal step lengths of the prosthetic and contralateral limb it can be assumed that this mechanism is causing the step length to be increased to match that of the sound limb. This mechanism did decrease in both subjects when using the prototype prosthesis.

Hip Angle - Fast Walking For subject A it can be seen (see section 5.2.6) that the symmetry overall is increasing. This is partly due to the fact that the movement from flexion into extension is almost equal between the hips on the sound and prosthetic sides. When subject B was using

the prototype prosthesis, the movement of the hip in stance phase did almost stay the same. In swing phase a much faster change from extension to flexion can be seen, similarly to the movement when walking slowly. This has different effects on the symmetry for both subjects. While the symmetry is increasing for subject A, because the angular change was slower, compared to the change of the hip on the sound limb, when using the everyday prosthesis, the symmetry is decreasing for subject B, because the movement of the hip did already match that of the sound limb very well. In both instances the faster change from extension into flexion meant a bigger total flexion angle, compared to the hip flexion of the sound limb at terminal swing when using the prototype prosthesis. However, the bigger flexion angle did get rid of the need of a second peak flexion angle to lengthen the step. Although the step lengthening mechanism can not be seen when using the prototype prosthesis, the step length of the prosthetic and sound limbs were equal overall (see fig.7.6).

5.3.4 Trunk can be held more upright / Smoother Gait

Another focus of the test was to try to find objective reasons for the subjective feedback of the subjects. Subject A told the researches at the gait laboratory that walking felt smoother when walking with the prototype prosthesis and subject B had the feeling as if his trunk could be kept more upright and steady during gait. To test the feedback objectively two markers on the back were investigated. The C7 marker, marking the seventh vertebrae of the cervical spine and the SACR marker, marking the midpoint between the left and right superior iliac spine. Movements in lateral and cranial direction were investigated ,as well as velocities in anterior/posterior directions. However, for both walking speeds only the lateral movement of the SACR marker for subject A showed significant differences (see section 5.2.7). The other investigated signals showed no proof of the subjects feedback and did not show improvements either. Because of the lack of repeatability it can be seen as very unlikely that the found differences for subject A are representative for future subjects and are therefore not discussed in greater detail.

5.3.5 Symmetry of Hip Joint Moments increases / Magnitude decreases

The hip is the solely remaining joint of a trans-femoral amputee. Therefore, it is the only way the subject can interact with the prosthesis and as the only remaining joint it has to do make prosthetic gait possible. Because the prototype is able to produce knee torque, the assumption was made that this would reduce the hip torque. Furthermore, an increased symmetry in kinetic variables could be found when non-microprocessor controlled prostheses were tested against their computer controlled counterparts, which also led to the assumption that torque is decreasing [50].

It can be seen that differences in walking speed are existing in the trail recorded with subject A. Subject A was walking faster in the fast walking trail and on the contrary walking slower in the slow walking trail when using the prototype prosthesis, compared to the everyday prosthesis. Therefore, the results have to be treated carefully, because the ground reaction force is strongly dependent on gait velocity, especially in trans-femoral gait [55]. This could also be seen when looking at the GRF values in the vertical and anterior-posterior directions for subject A (see figures 7.7 to 7.10). It can be seen that in the beginning the anterior-posterior GRF as well as the vertical GRF are larger when using the everyday prosthesis (see fig.7.9 and fig.7.10). This correlates with the different walking speeds that can be seen in the trails of subject A. When walking slowly the GRF in the vertical direction (see fig.7.8) was the same for both prostheses, although the speed was significantly lower when using the prototype prosthesis. However, the

anterior-posterior component of the vector showed bigger forces at the beginning of the gait cycle (see fig.7.7), which contrasts the findings of [55]. In order to exclude influences of different walking speeds on the kinetic parameters, the cadence was controlled when the trails of subject B were recorded. It can be seen that this resulted in almost no difference in either component of the GRF (see figures 7.7 to 7.10).

Another characteristic that can be seen when looking at the recordings of the hip moments is that there are big deviations for some of the signals (see section 5.2.10). After closer inspection it could be seen that the big deviations occur because the calculation of the sagittal hip moment is resulting in two groups (see figures 7.13 to 7.16). These groups are dependent on the directions in which the subject was walking in the laboratory. Because it could not be established which of the groups is the one closer to reality, the big deviations are remaining and are part of this analysis. Furthermore, peaks of the sagittal hip moment could be seen at the beginning of the gait cycle. These peaks were not present in all recordings. Therefore, after consulting with the gait laboratory it was decided to exclude the first five percent of the gait cycle to get a smoother signal. These peaks occur because of the sudden impact on the force plate at heel strike and are not a result of the gait itself but rather due to the limitations of the recording equipment.

Slow Walking Looking at the results of the statistical analysis no improvement in symmetry could be found when walking slowly in either subjects sagittal hip moments (see section 5.2.10). When the hip moments are compared sidewise, it can be seen that hardly any differences can be found (see figures 7.17 and 7.18). When looking at subject A it has to be kept in mind that the walking speed was slower while using the prototype prosthesis. It can be seen that in stance phase the hip extension moment of the sound side is bigger, however, when the moment reverses its direction the flexion torque is smaller in the remaining stance phase. Looking at the swing phase of the sound limb no differences in the sagittal hip moment was found. Looking at the hip on the prosthetic side it can be seen that the peak flexion moment was reduced for both subjects. Differences can be seen in the swing phase as well, where smaller extension torques can be found on the prosthetic limb.

Fast Walking When walking fast statistical improvements of the symmetry of the contralateral and ipsilateral sagittal hip moment can not be seen. This is mostly due to the fact that the hip moments are very different for both sides, especially at the beginning of the gait cycle and the end of stance phase. When comparing the hip moments on the sound side when using either of the two prostheses almost no difference can be seen in both subjects (see figures 7.19 and 7.20). The differences that can be seen at the beginning of the the gait cycle of the hip on the sound side of subject A (see fig.7.19) can not be seen as significant, as the calculated hip torques show a grouping effect (see fig.7.15). When looking at the sagittal hip moments of subject B differences can be seen in the peak flexion moment at pre swing, where when using the prototype prosthesis the moment is smaller compared to when using the everyday prosthesis. However, for the most part the moments are almost equal.

5.3.6 Symmetry of Hip Power increases / Magnitude decreases

When analysing the hip power curves, four regions of interest exist. The first phase (H1 see 5.53) is defined by a small peak of concentric hip extensor work, followed by a power absorption period from early to late stance (H2), where the hip flexors are used eccentrically and hip extension is continuing. The third phase (H3) is defined by activating the hip flexors and the hip moving into

flexion, resulting in power generation. The last point of interest can be found at the end of the gait cycle (H4), where a short period of concentric hip extensor activity can be seen [88, 96, 97]. However, in some cases the last phase (H4) can be neglected as the hip can be seen as almost static at the end of the gait cycle and thus very little power generation occurs [94]. Looking at the results in section 5.2.12 it can be seen that the H1 phase can only be found on the hip of the sound limb with varying results depending on walking speed and subject. While subject A shows a reduction of the sound hip power when walking slowly and an increase when walking fast (see figures 7.25 and 7.26), subject B shows an increased peak H1 value for all walking speed (see figures 7.27 and 7.28). However, the first peak has to be read with care, because the effect of grouped ground reaction forces and hip moments at the beginning of the gait cycle, depending on the walking direction in the gait laboratory, is at its highest at the beginning of the gait cycle. Another point to keep in mind is that the results for the hip moment and hip power are displayed five percent after initial contact, because vibrations and the harsh impact on the force plate resulted in peaks that could not be explained by biomechanical coherencies. Furthermore, it has to be kept in mind that walking speeds were not controlled when testing with subject A, compared to controlling the cadence when recording with subject B. In that aspect the results of subject B can be seen as more suitable for interpretation. An increased hip power generation at H1 can be seen, which indicates increased hip extensor work in early stance. Looking at the hip moments in sagittal, frontal and transversal orientations the differences between wearing the everyday and the prototype prosthesis are very small. The biggest differences can be seen in the transversal hip moment, which might be an indication that the increased weight of the prototype prosthesis increases the need for stabilization on the hip of the sound side (see fig. 7.24). For subject A no such indication can be seen (see fig.7.23). Looking at the hip power of the prosthetic side no peak corresponding to H1 can be found (see figures 7.25-7.28). Moreover, there is hardly any power generation until 50 % GC but only increasing power absorption. This might be due to the subjects walking style and is in agreement with the literature [24]. After power generation a power absorption follows, which is indicated by the H2 peak (see fig.5.53). Looking at the hip on the sound side no differences can be seen regardless of the used prosthesis (see figures 7.25 - 7.28). Because the hip is absorbing power almost immediately on the amputated side, the peak power absorption is higher compared to the sound side. When comparing the hip power of the prosthetic limb while using either of the two prostheses, it can be seen that absorption is bigger when the prototype prosthesis is used. However, there is not much difference looking at the peak values of subject B, whose cadence was controlled during the recording. Furthermore, it has to be noted that both subjects feedback on walking with the prototype prosthesis was that they felt like they had almost no work to do when walking. This can be seen as an indication that the slightly increased eccentric work at the hip, necessary when walking with the prototype prosthesis, is not experienced as negative, which could also be due to the fact that eccentric muscle contraction is capable of greater muscle force [41], compared to concentric or isometric contraction. This is also in agreement with the fact that eccentric muscle contraction is consuming less energy overall, compared to other contractions [1]. The next peak of the hip power (H3) is peak power generation due to the hip pull off with active hip flexors and the hip moving into flexion. Looking at the sound limb different results can be observed. On the one hand two consecutive peaks can be seen (see figures 7.26, 7.28), whereas only one peak can be seen when both subjects are walking slowly (see fig.7.25 and fig.7.27). This could be due to the fact that calculating the hip power is very sensitive to the centre of pressure, magnitude of the ground reaction force and estimation of the hip joint centre when calculated with inverse dynamics [30]. Overall the results are not consistent, neither for walking speed nor subject and therefore are not discussed in further detail. Looking at the hip power of the prosthetic limb it can be seen that regardless of walking speed and subject, peak power generation is reduced when walking with the prototype

prosthesis. A reduction between 0.2 W/kg and 0.4 W/kg, compared to when using the everyday prosthesis can be seen. This magnitude is similar to a mass and moment of inertia reduction of 75 percent when compared to the everyday prosthesis, which is remarkable given the fact that the prototype prosthesis has more than twice the weight [66]. This is also in agreement with the subjects reporting that walking with the prototype prosthesis felt almost effortlessly and could also be seen in early stages of testing with other active knee/ankle prostheses [91]. At the end of the gait cycle a small peak of power generation can be seen (H4) as the hip extensors are stabilizing the hip [88, 96, 97], however, other sources suggest little to no power generation at the end of the stance phase [94] or claiming small power absorption at the end of the gait cycle [30]. Looking at the peak hip power at the end of the gait cycle of the sound limb different characteristics can be seen, from small power generation (see figures 7.26, 7.28) to almost no power generation when walking slowly (see figures 7.25 and 7.27). The same can be said for the hip of the amputated side where no differences can be seen for slow and fast walking of subject A (see figures 7.25 and 7.26). Only for the fast walking trail of subject B differences at the end of the gait cycle can be seen with an increased power generation, compared to when wearing the everyday prosthesis (see fig. 7.28). This might have to do with the fact that the hip angle is greater when using the prototype prosthesis, especially for fast walking of subject B (see fig. 5.24a) and the subsequent isometric muscle force to stabilize the hip. For the slow walking trail of subject B no differences in hip power can be seen (see fig.7.27). For these reasons and additional different indications in the literature no further discussion is presented.

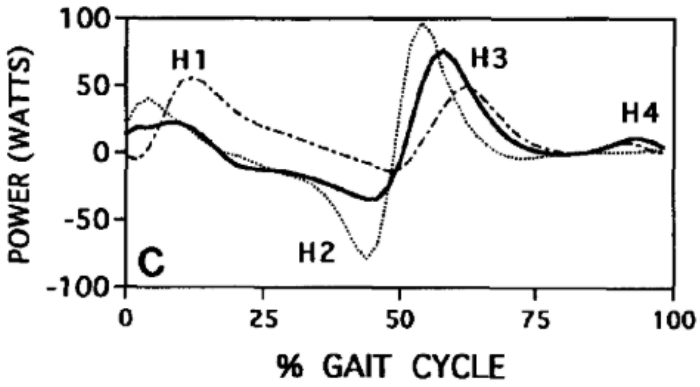

Fig. 5.53: The power phases of the hip of sound versus trans-femoral amputees can be seen. The intact limb hip power (.-.-.) and the hip power on the prosthetic side (—) can be observed. (source: [88, p. 1212])

5.3.7 Work done in the hip joint gets more symmetrical

When looking at the values of the hip work for both subjects while walking slowly (see fig.5.49 and fig.5.50) it can be seen that increased symmetry cannot be found which is mainly caused by two things. The positive work is decreasing, but the negative work is increasing on the prosthetic side when using the prototype prosthesis. This is also in agreement with the findings of the hip power recordings when walking slowly (see section 5.3.6). However, large deviations can be seen as well, which has to do with the fact that two groups can be seen when looking at the power values, which are caused by the inconsistent calculations of the ground reaction force and centre of pressure. Almost no difference of the positive and negative work performed throughout the gait cycle can be observed. This can can also be recognised when looking at the power curves which are showing only minor differences for the hip of the sound limb. When looking

at the values for the fast walking trails of both subjects (see figures 5.51 and 5.52) the results are looking quite similar to those of the slow walking trails. A reduction of positive work on the prosthetic side can be seen for subject B, while for subject A the average values are the same. However, walking speed was not controlled when recording the trails for subject A, which has an influence on the total work values at the hip [11]. In contrast to the slow walking trails, hip work is increasing at the sound side for subject B. Looking at the sagittal and frontal hip moments (see fig.7.20 and fig.7.22) no increase can be seen, which means that the hip angular velocity has to be greater. This could have to do with the fact that subjects had little time to get used to the new prosthesis, which showed in an increased stance phase duration as well (see fig.5.8b). Because a longer stance phase results in a shorter swing phase, the time in which the hip is changing from extension to flexion is shorter and therefore higher angular velocities are necessary at the hip. This can also be seen in a second short burst of power generation at the transition from stance to swing phase for subject B (see fig.7.28).

5.3.8 Limitations

The limitations of the results have been mentioned where they needed to be considered, however, they should be discussed for more clarity. The thesis is trying to find preliminary results of improvements in 3D gait recordings and provide possible hints on where these improvements can be seen best. Because the testing included a prototype, it has to be kept in mind that both subjects were not able to get used to the different prosthesis. That said, subject A was provided with one day of testing before the recording, in contrast to subject B which had no time prior to the recording but did already know the prosthesis from former tests. In other aspects the two subjects had different preconditions as well. While multiple months passed between the recordings of subject A, due to difficulties of prototype, gait laboratory and subject availability, the recordings of subject B were done on the same day. Other differences were only found when the data of subject A was investigated and it turned out that walking speed was substantially different between both prostheses. This lead to the conclusion that cadence was controlled when recording the trails with subject B. Another critical and potentially limiting factor is addressing the prototype prosthesis as being a prototype. It is much heavier than a non active prosthesis and much heavier than it will ever be when potentially coming to market. The limited space of knee prostheses made it necessary to attach the motor and gearbox to the lateral side, which results in imbalance of the weight distribution of the artificial limb. These two limiting factors are resulting in bigger moments of inertia, further resulting in bigger swing phase knee flexion angles. However, because a marketable product cannot weigh as much and keep the motor and gearbox mounted laterally, no efforts where made to limit the high swing phase flexion angles of the knee. Lastly, it has to be said that two subjects can not be seen as a representative group of trans-femoral amputees. It should also be added that the two subjects are experienced prostheses users and are often asked to try new prototypes or newly developed control algorithms with Ottobock.

Chapter 6

Conclusion

The present Master thesis had two main objectives. The first was to find and evaluate a method to detect representative steps within a cohort of recorded steps in order to be stored in a database. This data was collected regardless of subject, prosthesis or walking scenario and can then be used for further development of already existing or new prototype prosthesis. Furthermore, it is also used to estimate design restrictions such as needed motor torque for best support throughout the gait phases. With seven different methods implemented and the results evaluated by staff members of Ottobock, Dynamic Time Warping (DTW) to the median of the group of steps proved to provide not only the best results but also reasonable calculation time.
The second objective was to find improvements of a novel active prosthesis, compared to the subjects everyday prostheses in level walking gait. For one subject slow and fast walking was recorded, while for the second subject recordings of slow, normal and fast walking trails were made. While analysing the gait data of the first subject it was found that the walking speeds differed largely between the everyday prosthesis and the prototype prosthesis. Therefore, the cadence of the prototype prosthesis was controlled when the recordings of the second subject were made. In the course of deciding which variables to investigate the feedback of the subjects on how they felt during walking with the prototype prosthesis was consulted. This lead to investigating the movements and velocities of two markers at the spine, the C7 marker, which marks the seventh cervical spine and the SACR marker, which indicates the mid point between the left and right anterior superior iliac spine. However, no indications of the ability to keep the trunk more upright or less movement of the trunk could be found when investigating these data. Other variables were chosen based on literature, like stance phase duration, and others were chosen based on the design of the prototype and its capability of assisting with stance and swing phase flexion of the knee.
Overall, it has to be said that finding improvements of a system that subjects could not get used to is not easy and prone to produce lot of results that have to be dismissed when looking into further detail. Nevertheless, it could be seen that improvements can be detected in some parameters like hip power, where the peak power generation was reduced when using the prototype prosthesis. In other parameters, like hip work or hip torque, the great potential of the prototype could be seen, but needs further investigation due to the limited time at the gait laboratory.
For statistical evaluation of improved symmetry Statistical Parametric Mapping was used. However, while some variables showed great potential of improved symmetry it was difficult to prove in others, because trans-femoral amputee's gait is very asymmetric due to removal of most of the limb and its muscles. Nevertheless, investigating differences by using SPM is reducing the need of focussing on single parameters of the gait cycle and differences could easily be seen in the statistical analysis.
To conclude this thesis, it can be stated that the novel active prosthesis is a good starting point and proved to be potentially capable of assisting trans-femoral amputees better, compared to its passive contesters. Variables that can be assessed and give valuable results in early stages of prototype development could be found and it could also be seen that users are responding

well to the newly designed prosthesis. Furthermore, it could be demonstrated that Dynamic Time Warping is suitable for detecting differences between steps and using this method to find a representative step out of a cohort of steps of one walking trail.

Chapter 7

Appendix

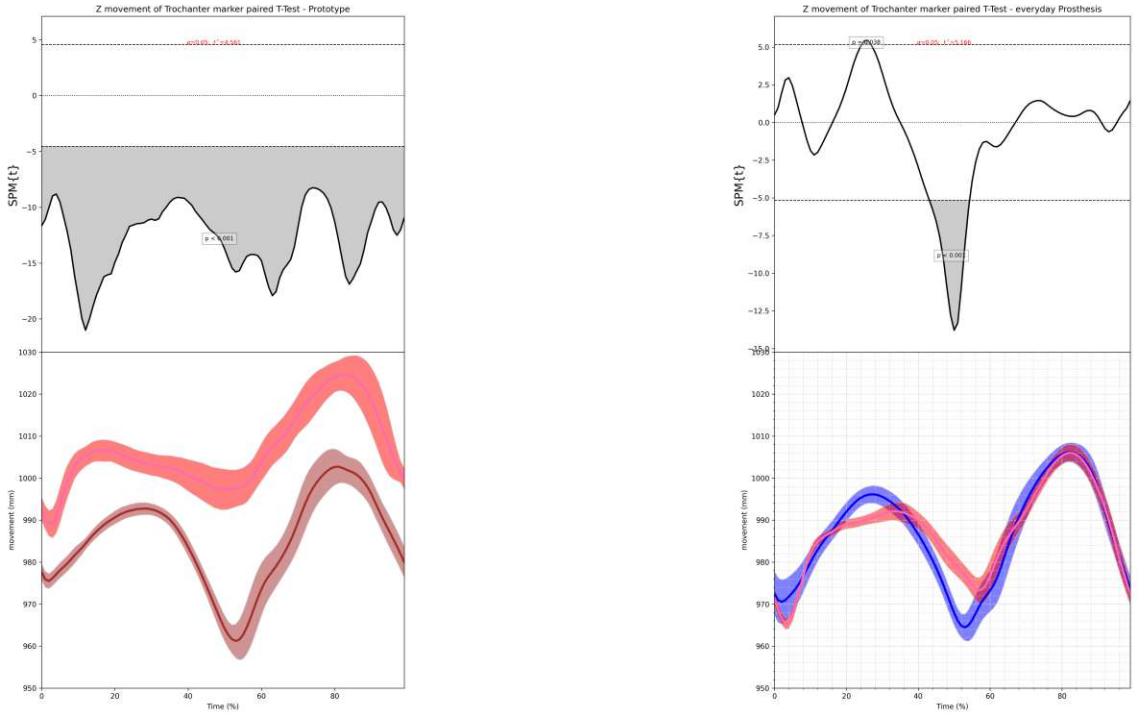

Fig. 7.1: The movement in global Z-direction of the trochanter marker analysis can be seen for subject A while using the everyday (left) and prototype (right) prosthesis. Slow walking.

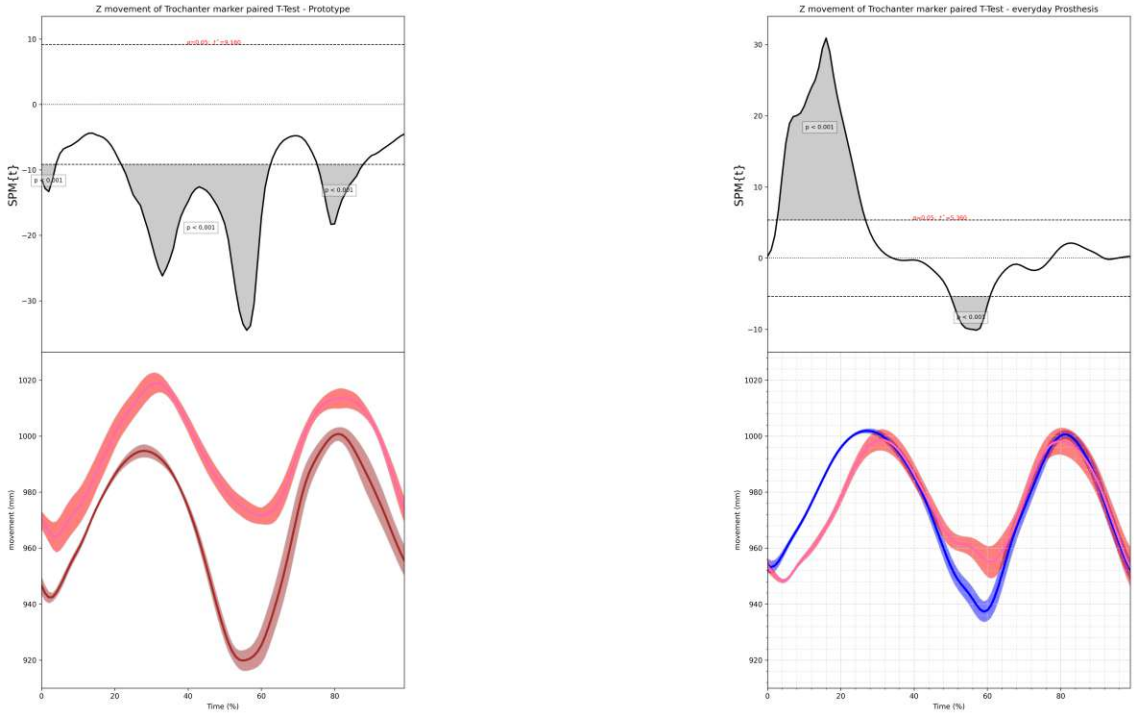

Fig. 7.2: The movement in global Z-direction of the trochanter marker analysis can be seen for subject A while using the everyday (left) and prototype (right) prosthesis. Fast walking.

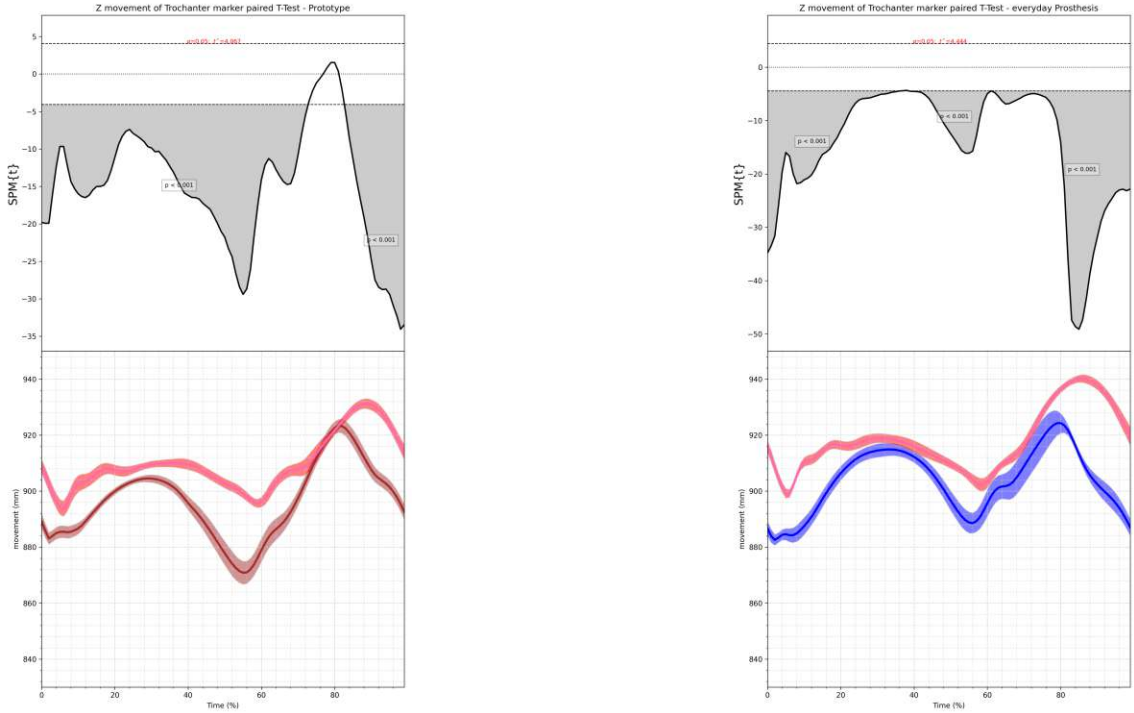

Fig. 7.3: The movement in global Z-direction of the trochanter marker analysis can be seen for subject B while using the everyday (left) and prototype (right) prosthesis. Slow walking.

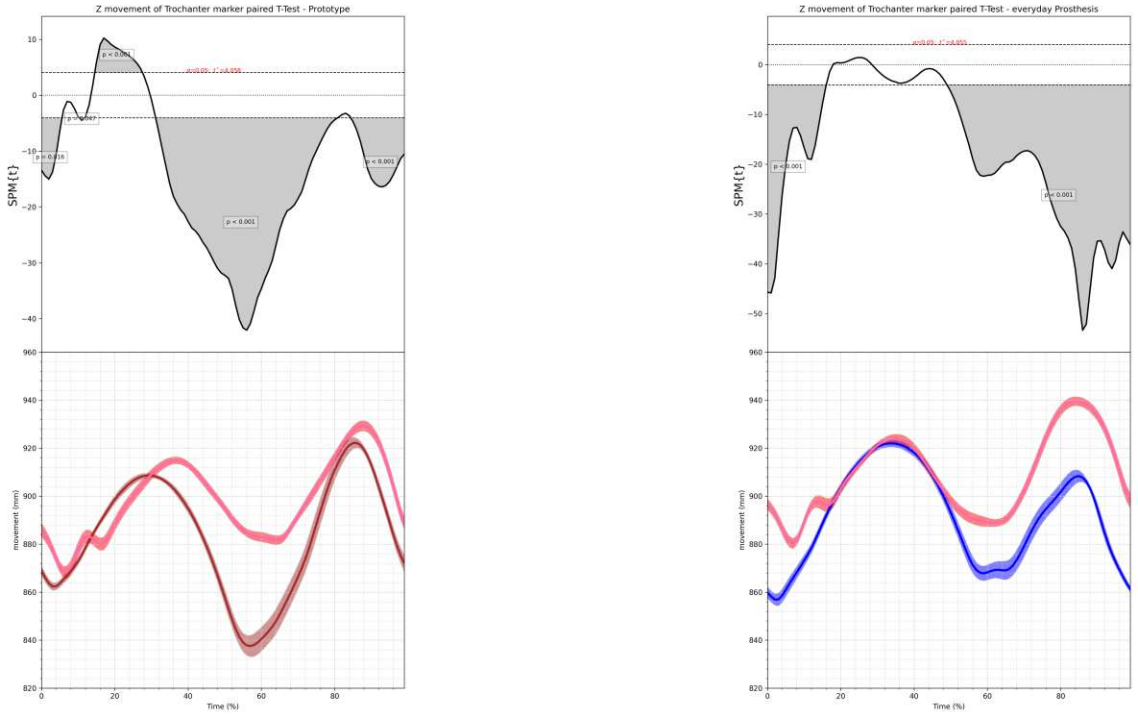

Fig. 7.4: The movement in global Z-direction of the trochanter marker analysis can be seen for subject B while using the everyday (left) and prototype (right) prosthesis. Fast walking.

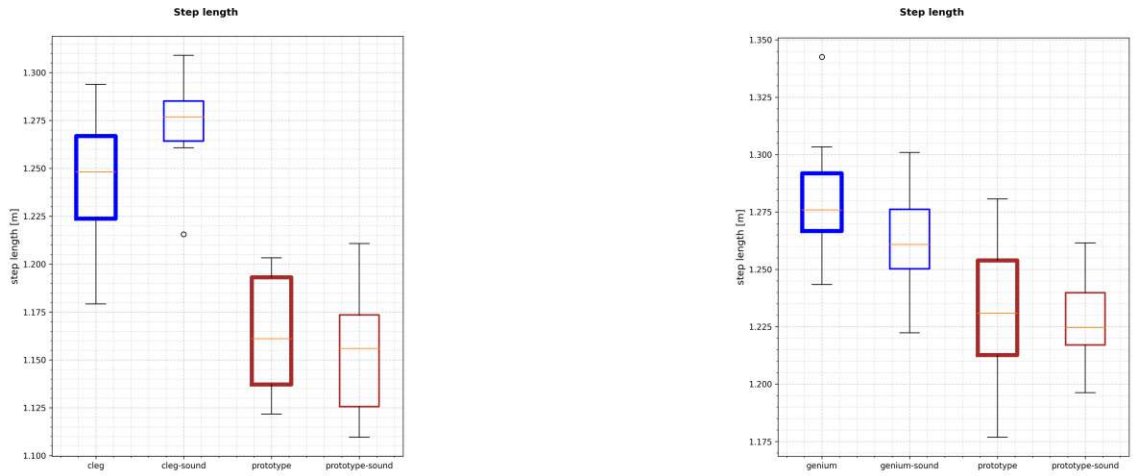

Fig. 7.5: The step length for both limbs for subject A(left) and subject B(right) while using the everyday (blue) and prototype (brown) prosthesis can be seen. The thick lines indicate the prosthetic side. Slow walking.

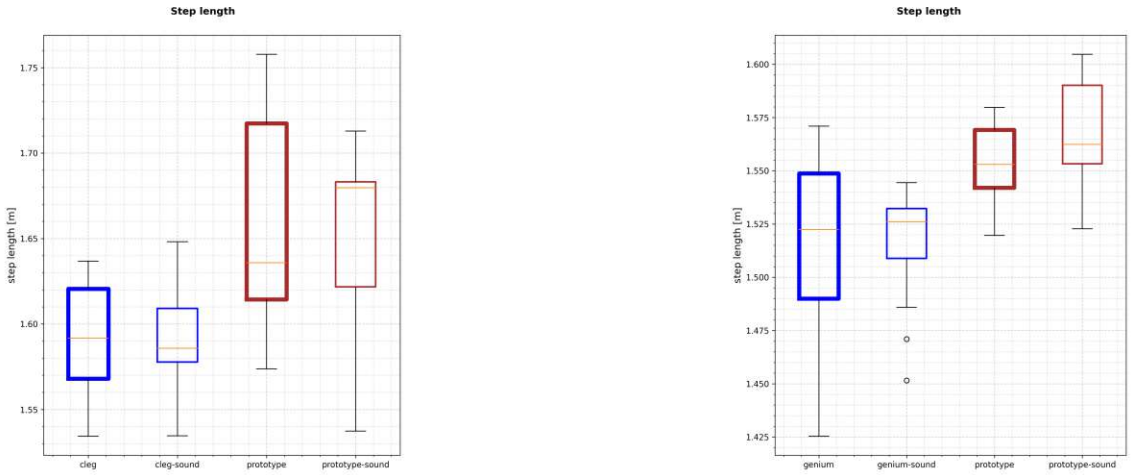

Fig. 7.6: The step length for both limbs for subject A(left) and subject B(right) while using the everyday (blue) and prototype (brown) prosthesis can be seen. The thick lines indicate the prosthetic side. Fast walking.

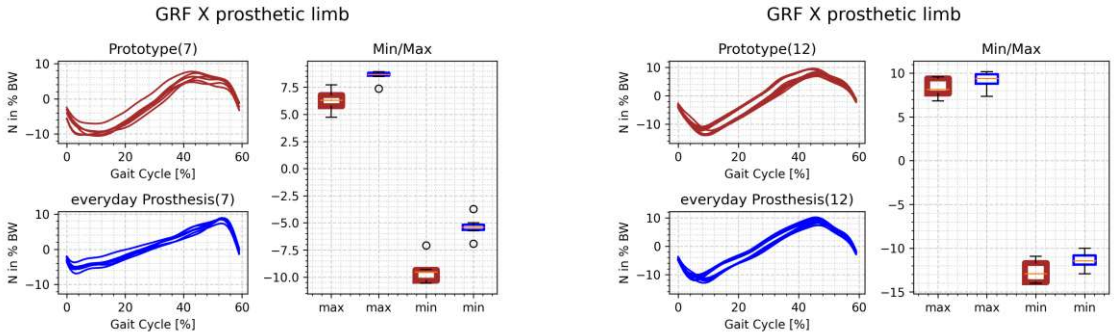

Fig. 7.7: The ground reaction force in anterior-posterior direction can be seen for subject A(left) and subject B(right) for the prosthetic limb. The everyday prosthesis can be seen in blue and the prototype in brown. Slow walking.

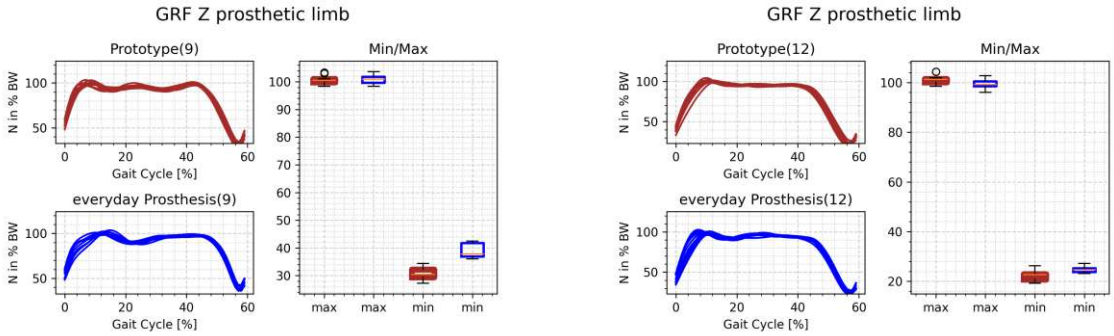

Fig. 7.8: The ground reaction force in vertical direction can be seen for subject A(left) and subject B(right) for the prosthetic limb. The everyday prosthesis can be seen in blue and the prototype in brown. Slow walking.

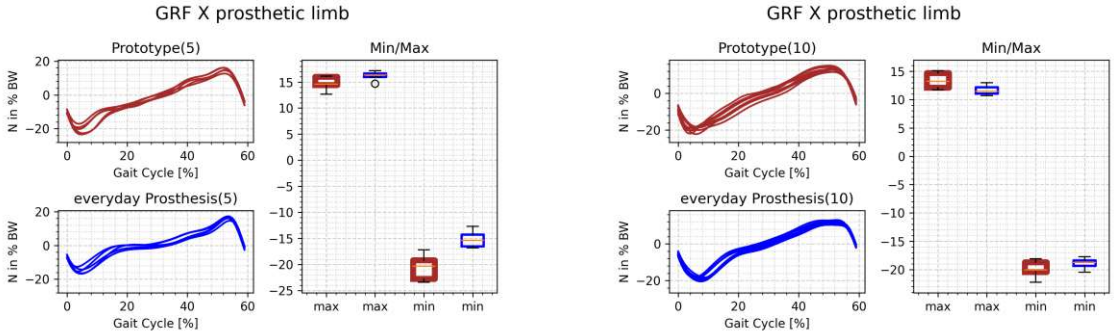

Fig. 7.9: The ground reaction force in anterior-posterior direction can be seen for subject A(left) and subject B(right) for the prosthetic limb. The everyday prosthesis can be seen in blue and the prototype in brown. Fast walking.

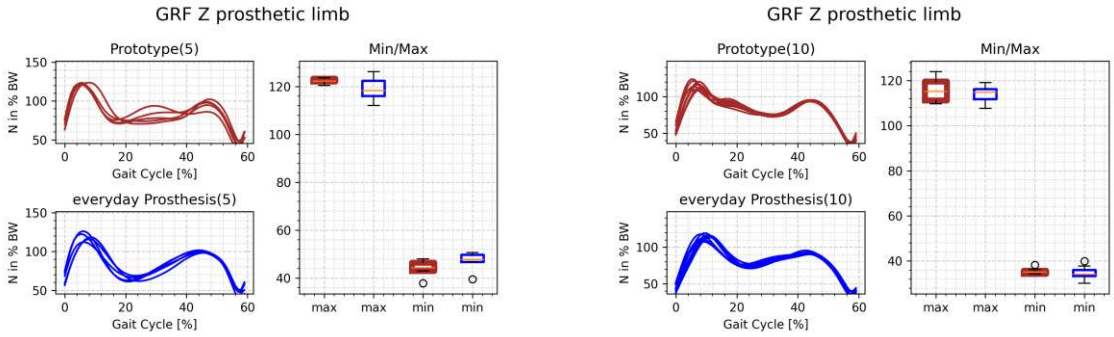

Fig. 7.10: The ground reaction force in vertical direction can be seen for subject A(left) and subject B(right) for the prosthetic limb. The everyday prosthesis can be seen in blue and the prototype in brown. Fast walking.

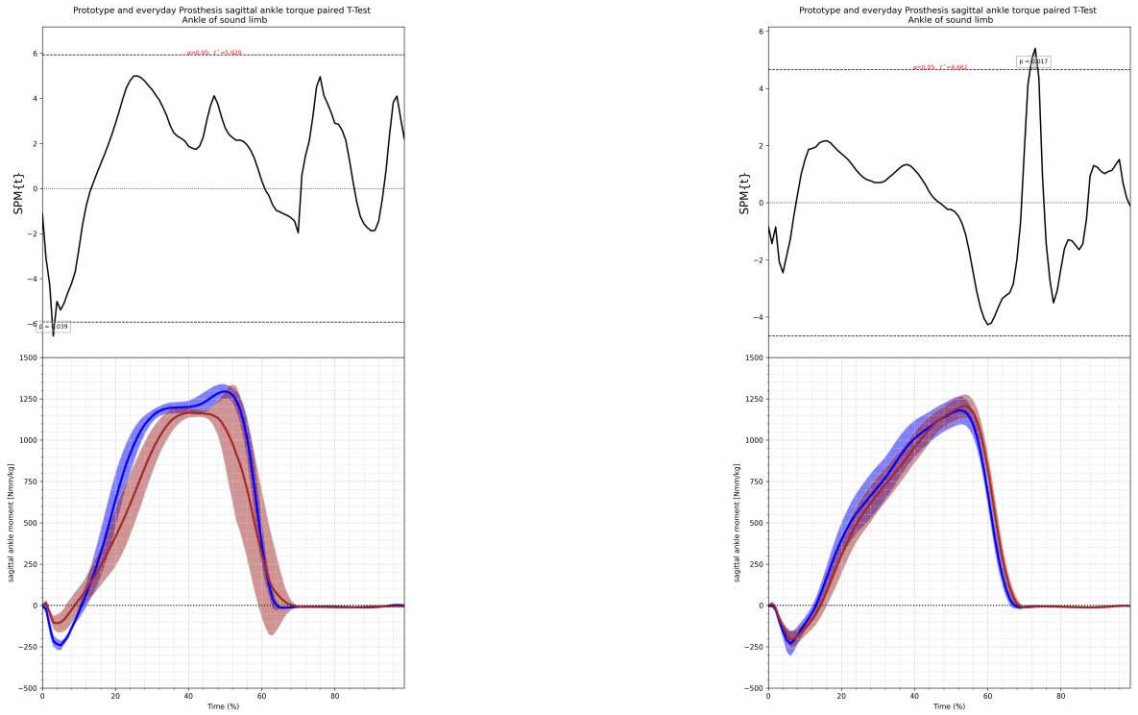

Fig. 7.11: Sagittal ankle moment and SPM{t} analysis can be seen for subject A (left) and subject B (right) for their contralateral (=sound) ankle. Positive values correspond to dorsal flexion moments and negative values indicate plantar flexion moments.

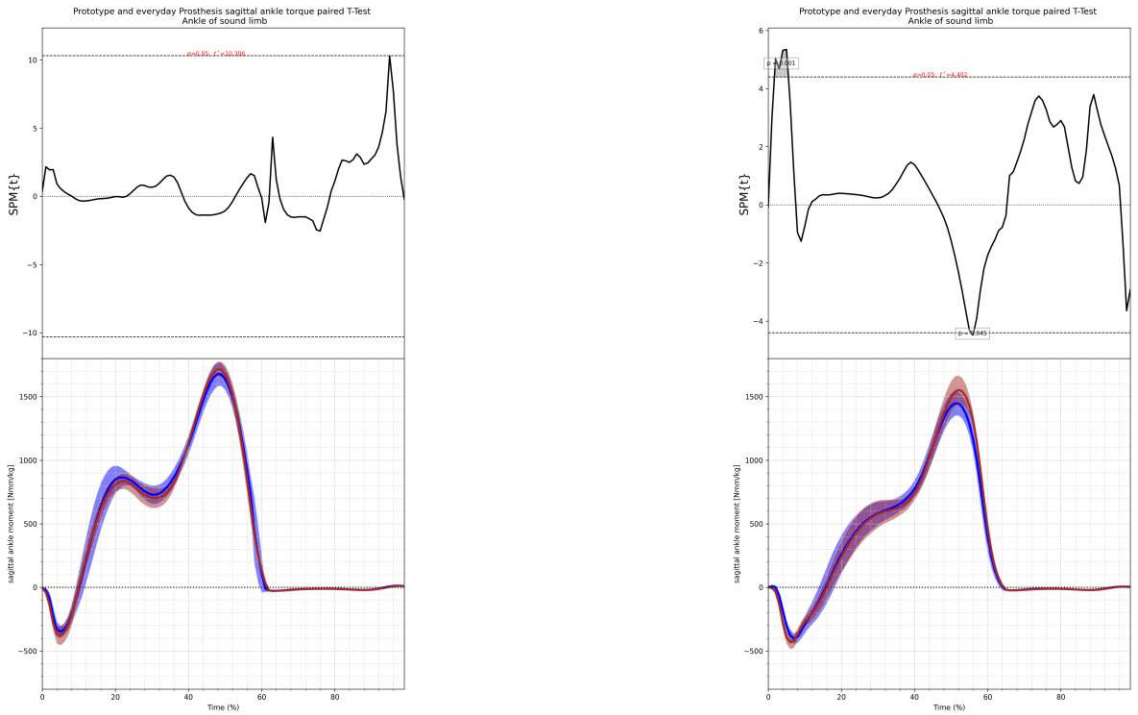

Fig. 7.12: Sagittal ankle moment and SPM{t} analysis can be seen for subject A (left) and subject B (right) for their contralateral (=sound) ankle. Vaulting can be seen on the right, were a peak in at 20% GC can be seen. Positive values correspond to dorsal flexion moments and negative values indicate plantar flexion moments.

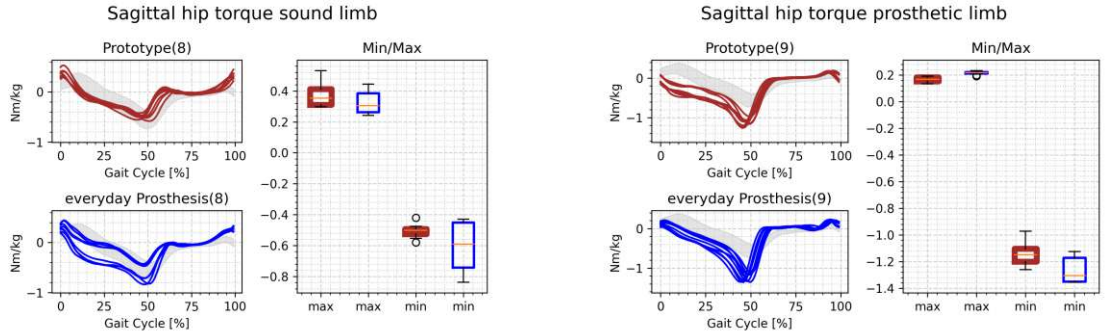

Fig. 7.13: The sagittal hip moment can be seen for the sound (left) and prosthetic (right) limb of subject A. The everyday prosthesis can be seen in blue and the prototype in brown. Slow walking.

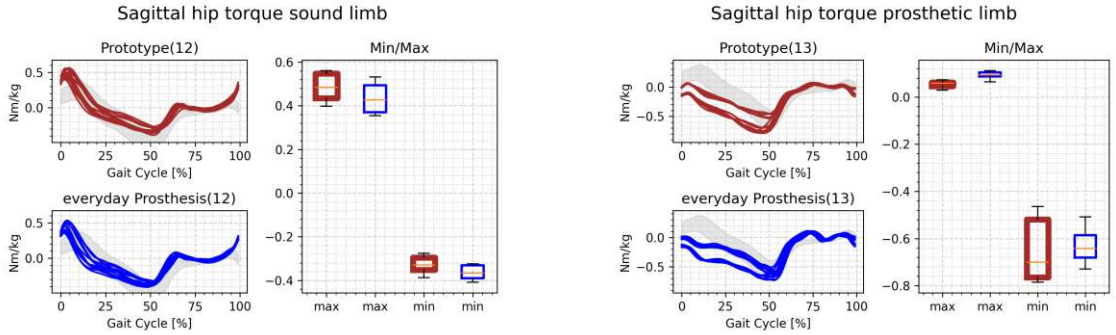

Fig. 7.14: The sagittal hip moment can be seen for the sound (left) and prosthetic (right) limb of subject B. The everyday prosthesis can be seen in blue and the prototype in brown. Slow walking.

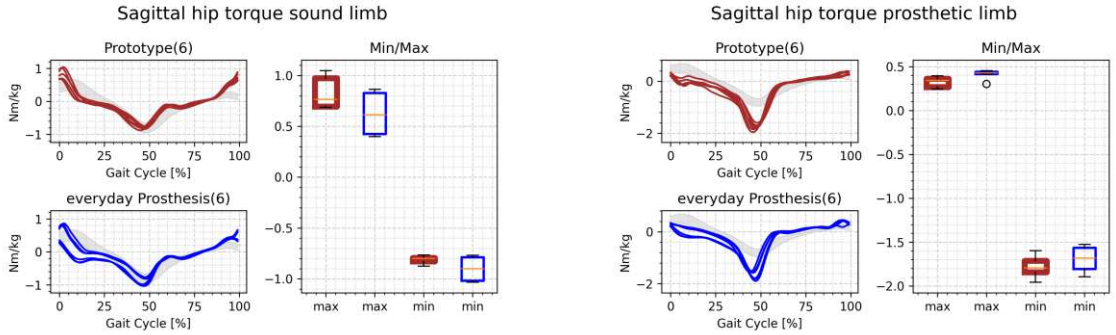

Fig. 7.15: The sagittal hip moment can be seen for the sound (left) and prosthetic (right) limb of subject A. The everyday prosthesis can be seen in blue and the prototype in brown. Fast walking.

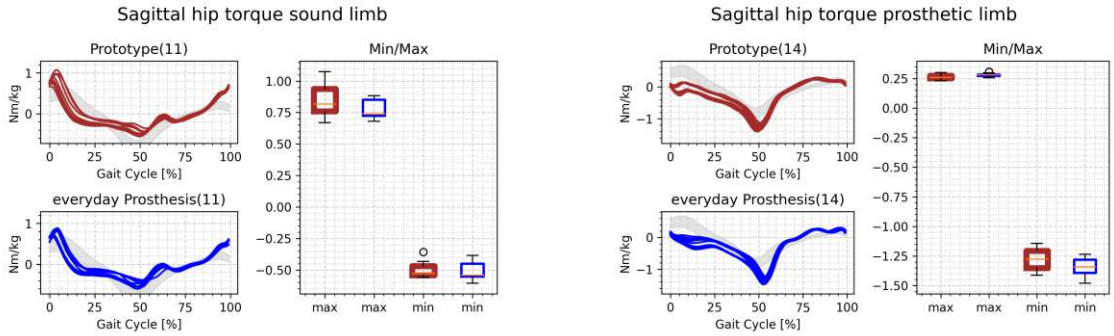

Fig. 7.16: The sagittal hip moment can be seen for the sound (left) and prosthetic (right) limb of subject B. The everyday prosthesis can be seen in blue and the prototype in brown. Fast walking.

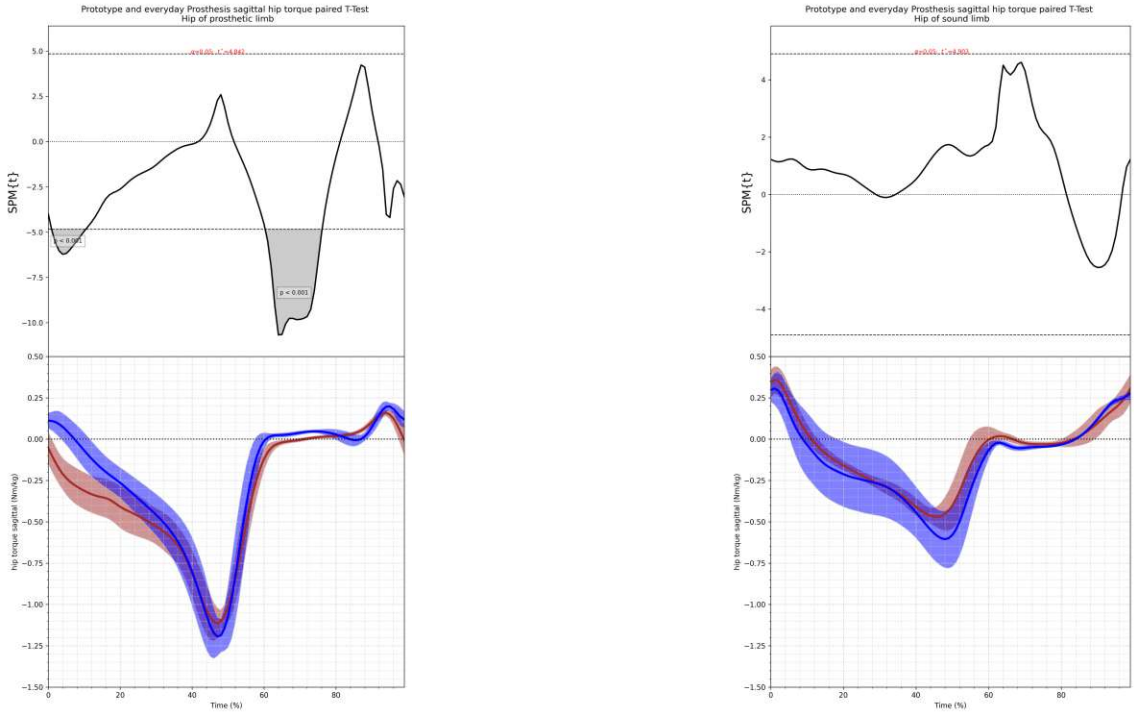

Fig. 7.17: Sagittal hip moment and SPM{t} analysis can be seen for the prosthetic (left) and contralateral (right) sides for subject A. Trails where the prototype prosthesis was used are depicted in brown. The records while using the everyday prosthesis are depicted in blue. Positive values correspond to extension moments.

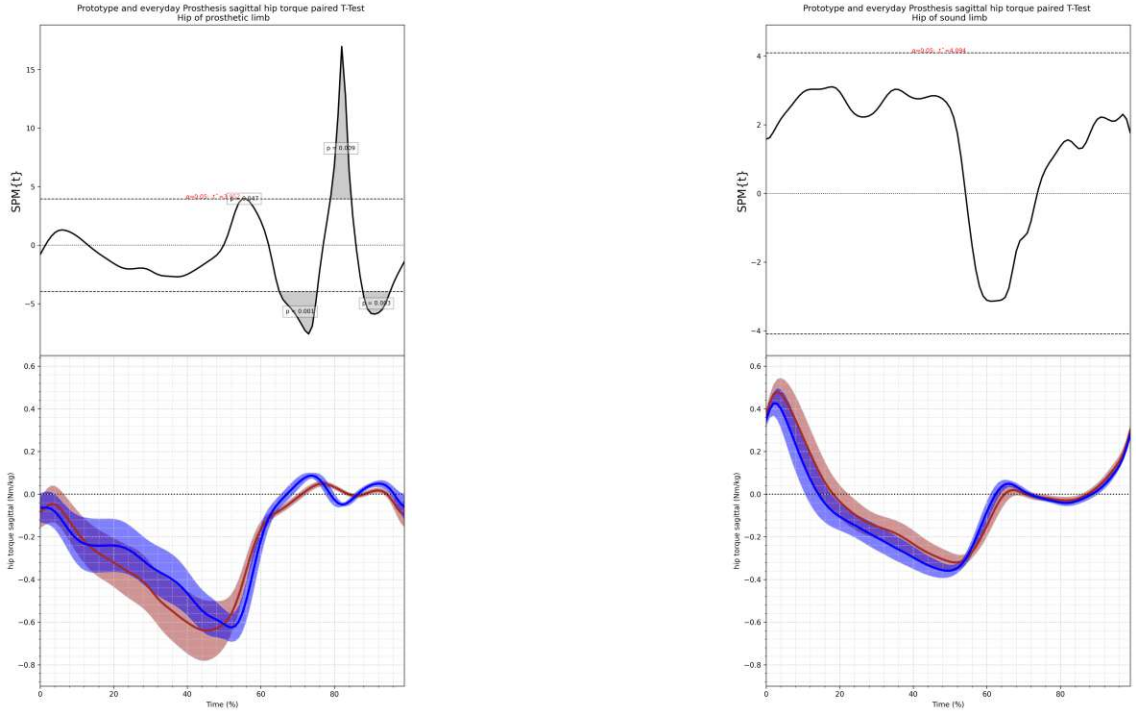

Fig. 7.18: Sagittal hip moment and SPM{t} analysis can be seen for the prosthetic (left) and contralateral (right) sides for subject B. Trails where the prototype prosthesis was used are depicted in brown. The records of using the everyday prosthesis are depicted in blue. Positive values correspond to extension moments.

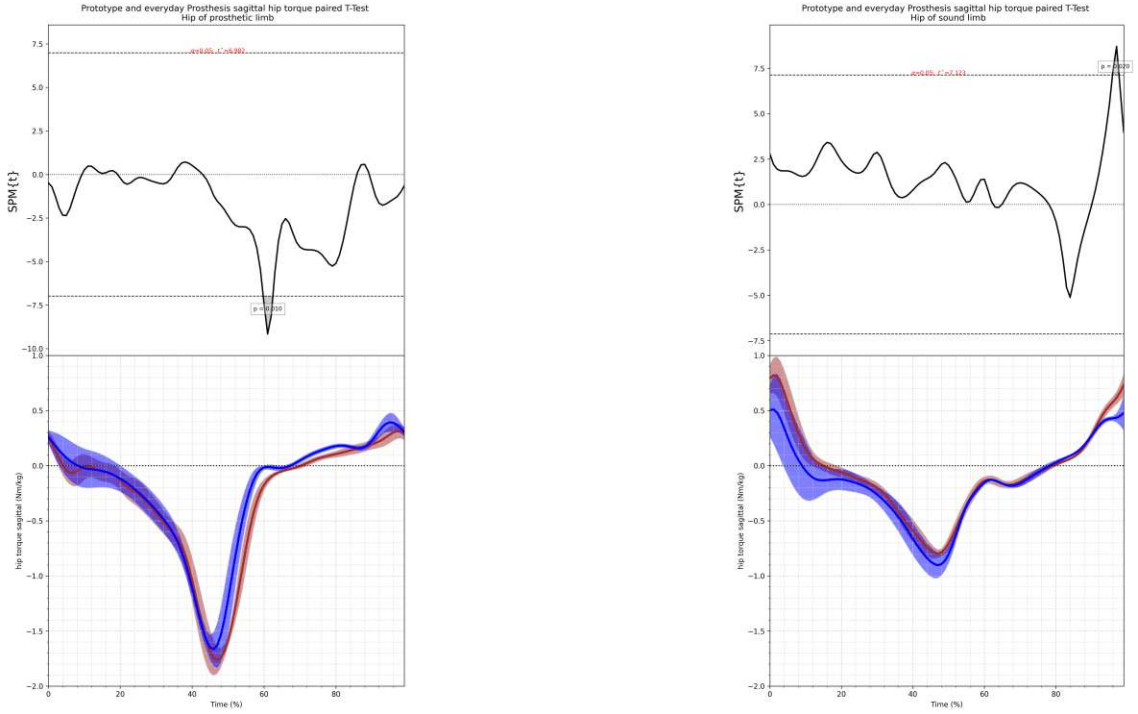

Fig. 7.19: Sagittal hip moment and SPM{t} analysis can be seen for the prosthetic (left) and contralateral (right) sides for subject A. Trails where the prototype prosthesis was used are depicted in brown. The records while using the everyday prosthesis are depicted in blue. Positive values correspond to extension moments.

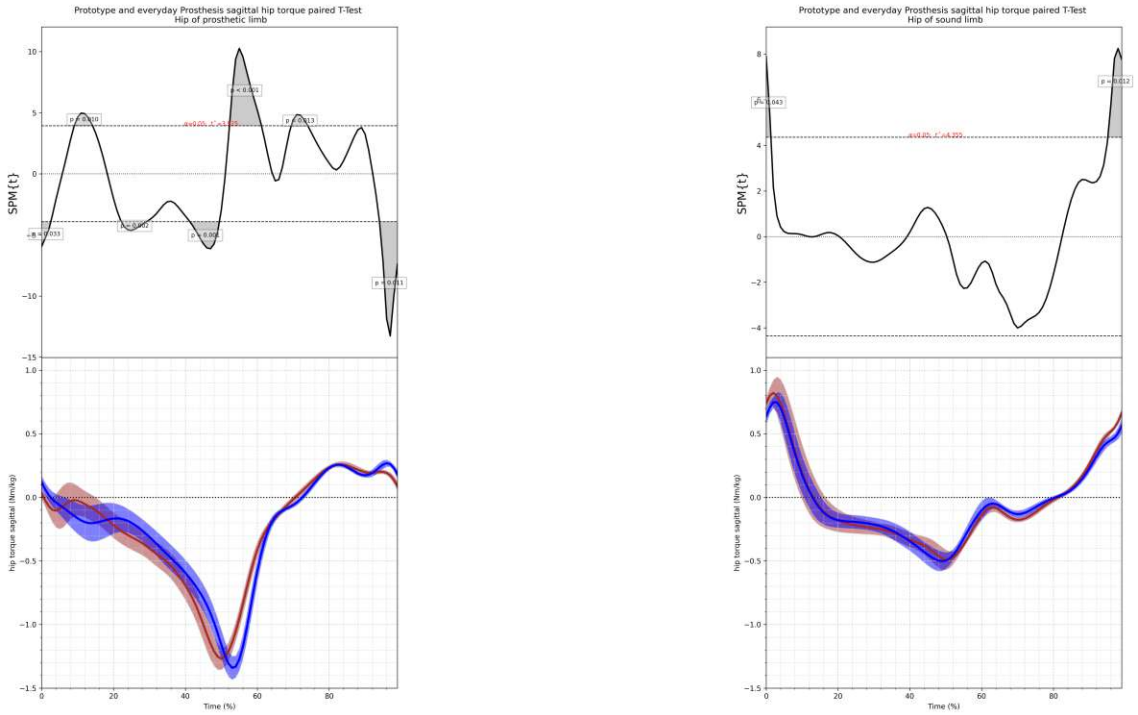

Fig. 7.20: Sagittal hip moment and SPM{t} analysis can be seen for the prosthetic (left) and contralateral (right) sides for subject B. Trails where the prototype prosthesis was used are depicted in brown. The records while using the everyday prosthesis are depicted in blue. Positive values correspond to extension moments.

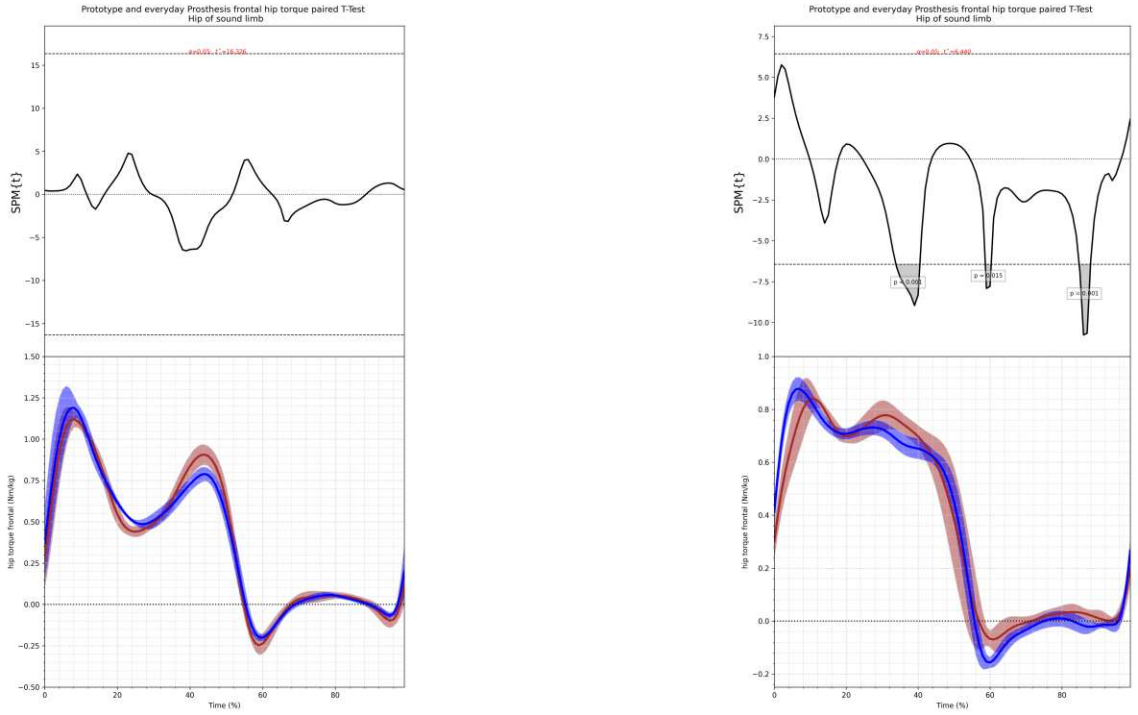

Fig. 7.21: The frotnal hip torque of the hip of the sound limb when using the prototype (brown) and everyday prosthesis of subject A can be seen. The left shows fast walking, while the right is displaying the results of the slow walking trail.

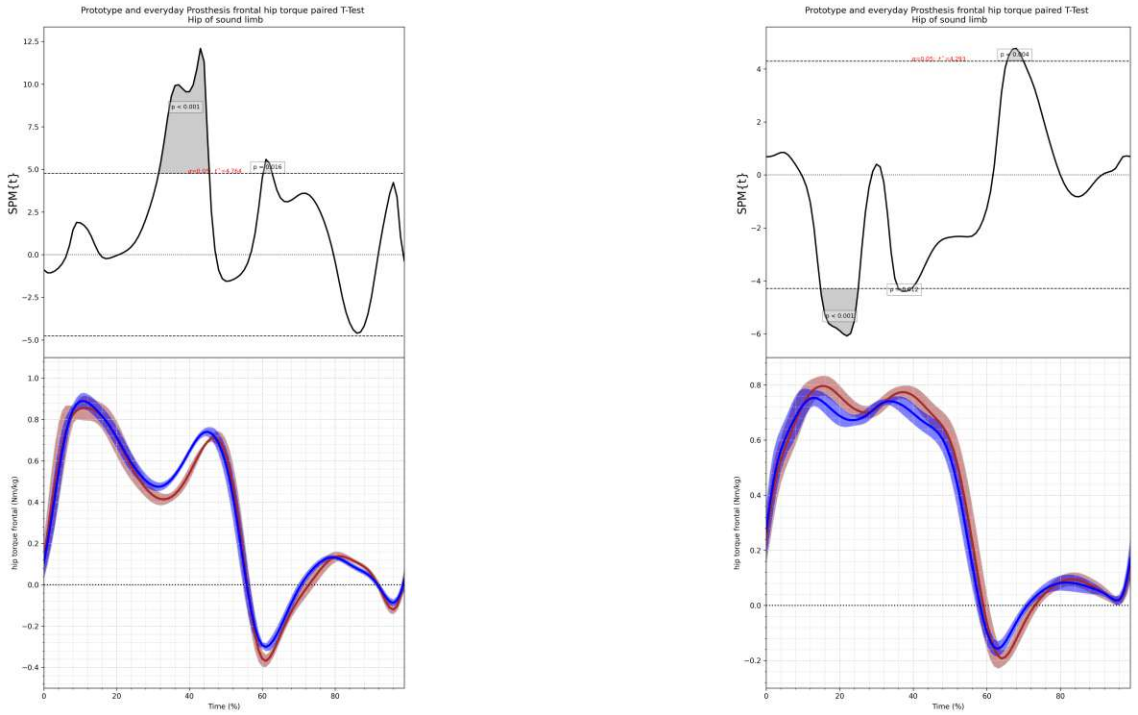

Fig. 7.22: The frontal hip torque of the hip of the sound limb when using the prototype (brown) and everyday prosthesis of subject B can be seen. The left shows fast and the right shows the results of the slow walking trail.

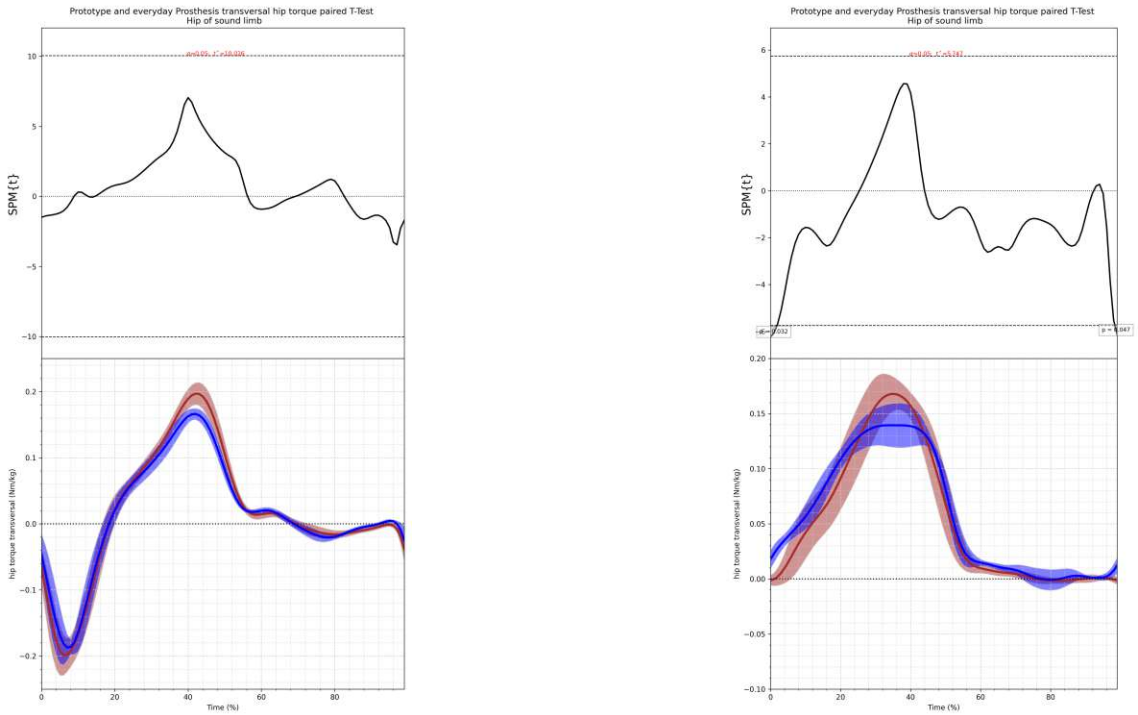

Fig. 7.23: The transversal hip torque of the hip of the sound limb when using the prototype (brown) and everyday prosthesis of subject A can be seen. The left shows fast walking, while the right is displaying the results of the slow walking trail.

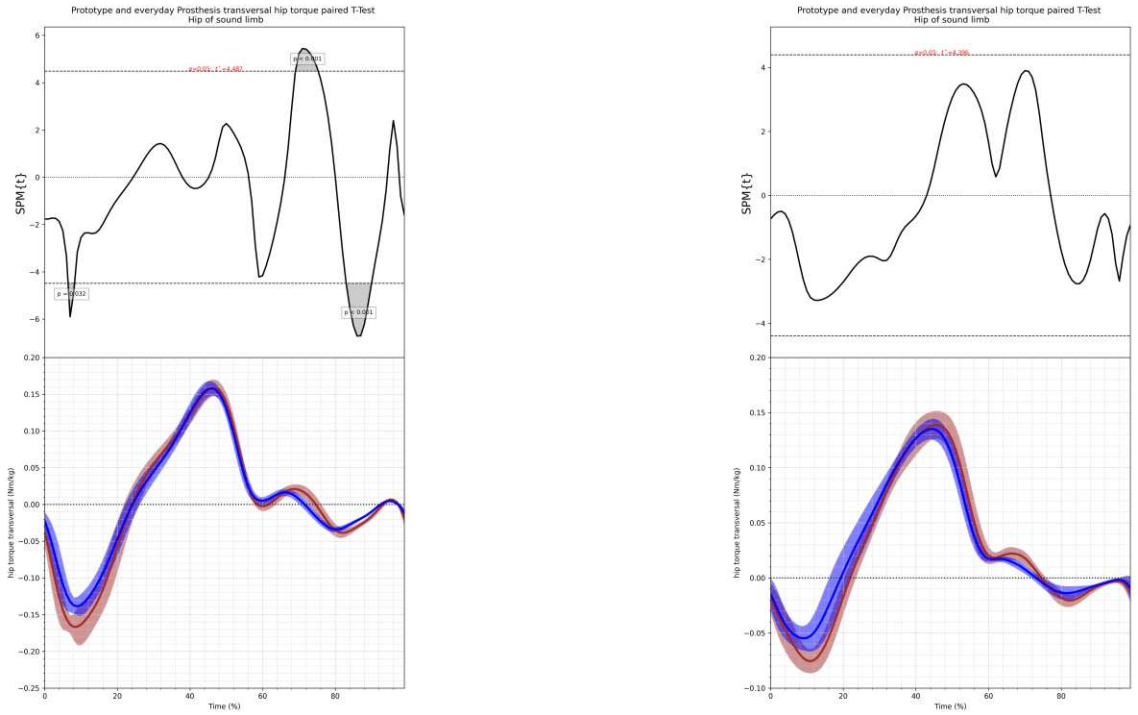

Fig. 7.24: The transversal hip torque of the hip of the sound limb when using the prototype (brown) and everyday prosthesis of subject B can be seen. The left shows fast and the right shows the results of the slow walking trail.

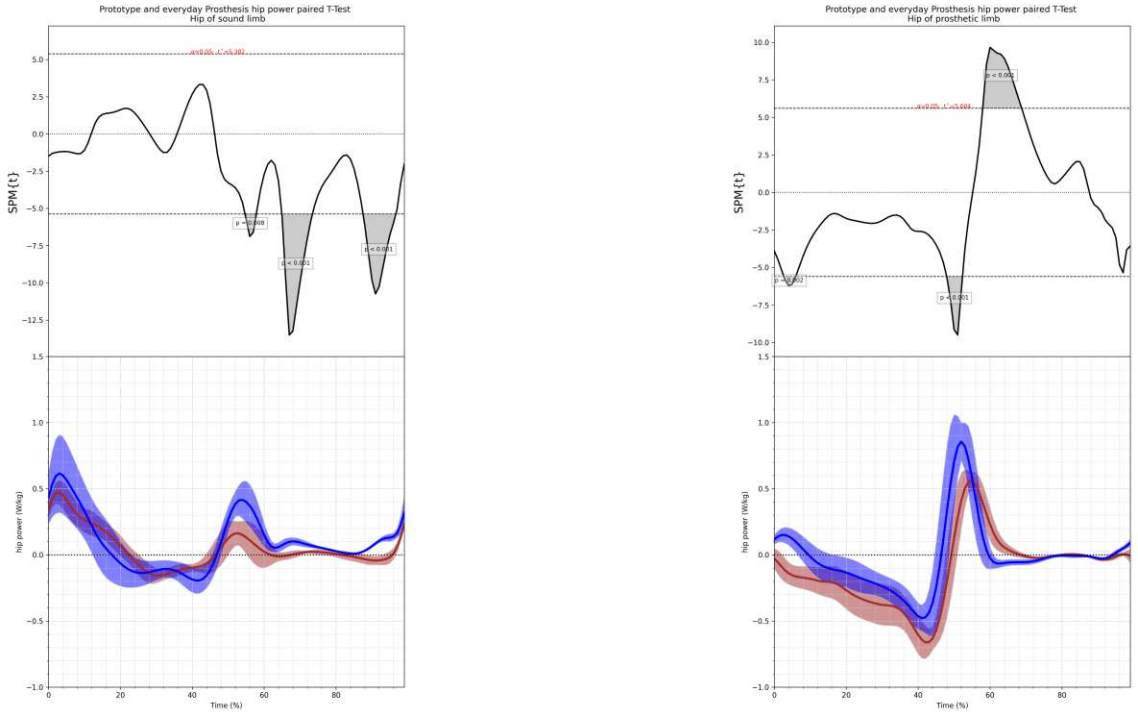

Fig. 7.25: The hip power when using the prototype (brown) and everyday prosthesis while walking with a slow self selected speed of subject A can be seen. The hip power of the sound limb can be seen on the left while the hip power of the amputated limb can be seen on the right.

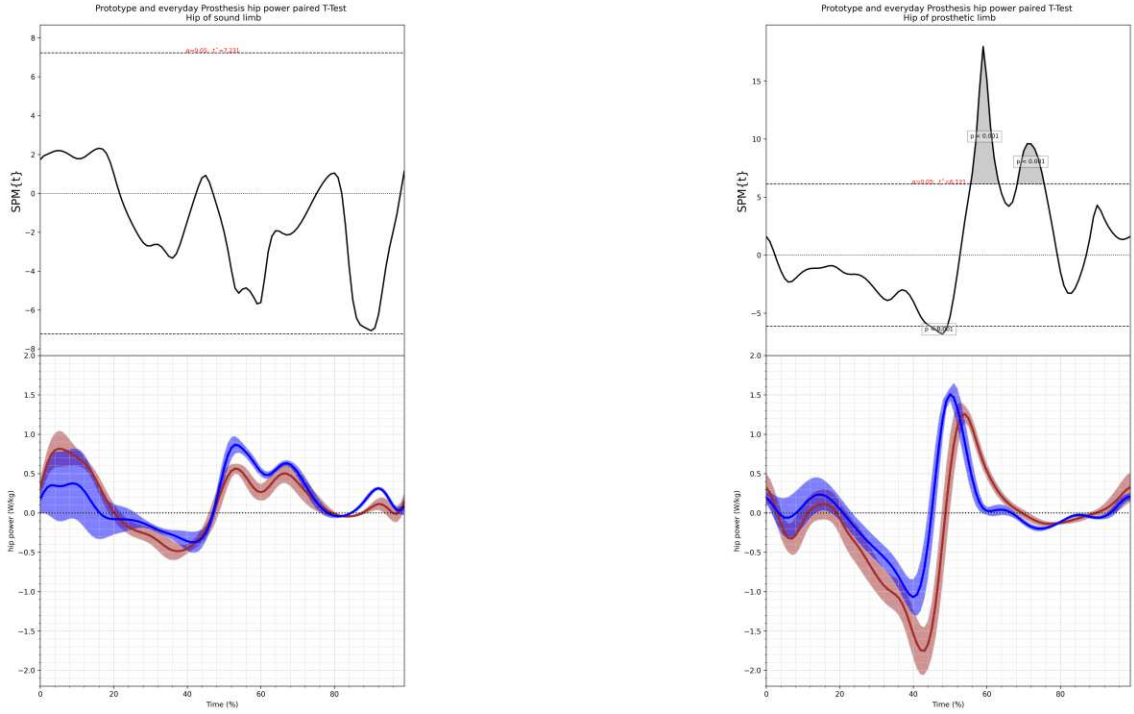

Fig. 7.26: The hip power when using the prototype (brown) and everyday prosthesis while walking with a fast self selected speed of subject A can be seen. The hip power of the sound limb can be seen on the left while the hip power of the amputated limb can be seen on the right.

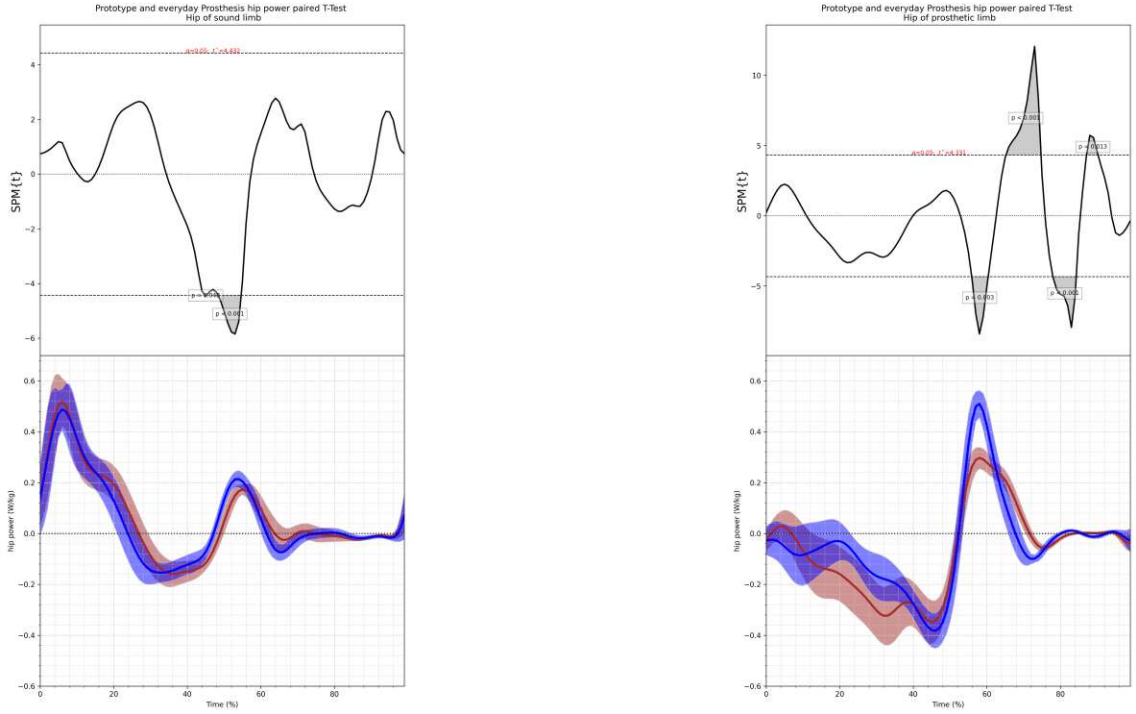

Fig. 7.27: The hip power when using the prototype (brown) and everyday prosthesis while walking with a slow self selected speed of subject B can be seen. The hip power of the sound limb can be seen on the left while the hip power of the amputated limb can be seen on the right.

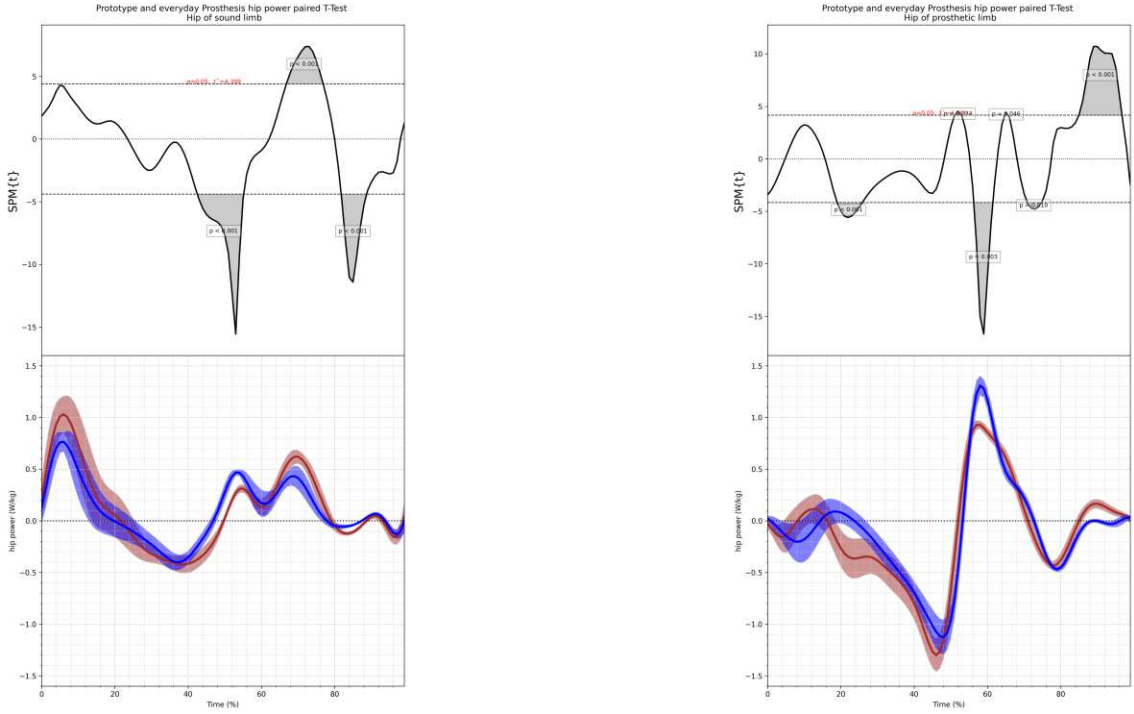

Fig. 7.28: The hip power when using the prototype (brown) and everyday prosthesis while walking with a fast self selected speed of subject B can be seen. The hip power of the sound limb can be seen on the left while the hip power of the amputated limb can be seen on the right.

Bibliography

[1] B. C. ABBOTT, B. BIGLAND, and J. M. RITCHIE. "The physiological cost of negative work". eng. In: *The Journal of physiology* 117.3 (1952). Journal Article, pp. 380–390. ISSN: 0022-3751. DOI: 10.1113/jphysiol.1952.sp004755. eprint: 14946742.

[2] F. Amirabdollahian, E. Burdet, and L. Masia, eds. *2017 International Conference on Rehabilitation Robotics (ICORR). QEII Centre, London, UK, July 17-20, 2017*. eng. Amirabdollahian, Farshid (HerausgeberIn) Burdet, Etienne (HerausgeberIn) Masia, Lorenzo (HerausgeberIn). Piscataway, NJ: IEEE, 2017. 8 pp. ISBN: 9781538622964. URL: http://ieeexplore.ieee.org/servlet/opac?punumber=8001594.

[3] J. Andrysek, S. Klejman, R. Torres-Moreno, W. Heim, B. Steinnagel, and S. Glasford. "Mobility function of a prosthetic knee joint with an automatic stance phase lock". In: *Prosthetics & Orthotics International* 35.2 (2011), pp. 163–170. ISSN: 0309-3646. DOI: 10.1177/0309364611408495.

[4] T. S. Bae, K. Choi, D. Hong, and M. Mun. "Dynamic analysis of above-knee amputee gait". eng. In: *Clinical biomechanics (Bristol, Avon)* 22.5 (2007). Journal Article, pp. 557–566. DOI: 10.1016/j.clinbiomech.2006.12.009. eprint: 17321021.

[5] R. Baker. "The history of gait analysis before the advent of modern computers". eng. In: *Gait & Posture* 26.3 (2007). Historical Article Journal Article, pp. 331–342. ISSN: 0966-6362. DOI: 10.1016/j.gaitpost.2006.10.014. eprint: 17306979.

[6] R. Baumgartner and P. Botta. *Amputation und Prothesenversorgung der unteren Extremitaet. Indikationsstellung, operative Technik, Nachbehandlung, Prothesenversorgung, Gangschulung, Rehabilitation ; 21 Tabellen*. ger. 2., neu bearb. und erw. Aufl. Stuttgart: Enke, 1995. 415 pp. ISBN: 3-432-97502-3.

[7] C.-A. Behrendt, B. Sigvant, Z. Szeberin, B. Beiles, N. Eldrup, I. A. Thomson, M. Venermo, M. Altreuther, G. Menyhei, J. Nordanstig, M. Clarke, H. C. Riess, M. Bjoerck, and E. S. Debus. "International Variations in Amputation Practice: A VASCUNET Report". eng. In: *European journal of vascular and endovascular surgery : the official journal of the European Society for Vascular Surgery* 56.3 (2018). Journal Article Multicenter Study, pp. 391–399. DOI: 10.1016/j.ejvs.2018.04.017. eprint: 29859821.

[8] L. Bergroth, H. Hakonen, and T. Raita. "A survey of longest common subsequence algorithms". In: *Proceedings Seventh International Symposium on String Processing and Information Retrieval. SPIRE 2000*. SPIRE'2000 - String Processing and Information Retrieval. (A Curuna, Spain, Sept. 27–29, 2000). IEEE Comput. Soc, 2000, pp. 39–48. ISBN: 0-7695-0746-8. DOI: 10.1109/SPIRE.2000.878178.

[9] D. Berndth and J. Clifford. *Using dynamic time warping to find patterns in time series*. 1994. URL: https://www.aaai.org/library/workshops/1994/ws94-03-031.php.

[10] S. Blumentritt, H. W. Scherer, U. Wellershaus, and J. W. Michael. "Design Principles, Biomechanical Data and Clinical Experience with a Polycentric Knee Offering Controlled Stance Phase Knee Flexion: A Preliminary Report". In: *Journal of Prosthetics and Orthotics* 1997.9 ().

[11] X. Bonnet, C. Villa, P. Fodé, F. Lavaste, and H. Pillet. "Mechanical work performed by individual limbs of transfemoral amputees during step-to-step transitions: Effect of walking velocity". eng. In: *Proceedings of the Institution of Mechanical Engineers. Part H, Journal of engineering in medicine* 228.1 (2014), pp. 60–66. DOI: 10.1177/0954411913514036. eprint: 24288379.

[12] R. Borjian, J. Lim, M. B. Khamesee, and W. Melek. "The design of an intelligent mechanical Active Prosthetic Knee". In: *2008 34th Annual Conference of IEEE Industrial Electronics*. IECON 2008 - 34th Annual Conference of IEEE Industrial Electronics Society. (Orlando, FL, Nov. 10, 2008). IEEE, 112008, pp. 3016–3021. ISBN: 978-1-4244-1767-4. DOI: 10.1109/IECON.2008.4758441.

[13] M. Brett, W. Penny, and S. Kiebel. "Introduction to Random Field Theory". In: *Human brain function*. Ed. by R. S. J. Frackowiak. 2. ed., [2. Dr.] Amsterdam: Elsevier Acad. Press, 2007, pp. 867–879. ISBN: 9780122648410. DOI: 10.1016/B978-012264841-0/50046-9.

[14] B. Budaker. *Proceedings for the joint conference of ISR 2014, 45th International Symposium on Robotics, Robotik 2014, 8th German Conference on Robotics. 2 - 3 June 2014 parallel to Automatica, Munich, Germany*. eng. Berlin and Offenbach: VDE-Verl., 2014. 1 CD-ROM. ISBN: 9783800736010.

[15] M. J. Burke, V. Roman, and V. Wright. "Bone and joint changes in lower limb amputees". eng. In: *Annals of the rheumatic diseases* 37.3 (1978). Journal Article, pp. 252–254. ISSN: 0003-4967. DOI: 10.1136/ard.37.3.252. eprint: 150823.

[16] A. Cappozzo, F. Figura, F. Gazzani, T. Leo, and M. Marchetti. "Angular displacements in the upper body of AK amputees during level walking". eng. In: *Prosthetics and Orthotics International* 6.3 (1982). Comparative Study Journal Article Comparative Study Journal Article, pp. 131–138. DOI: 10.3109/03093648209166573. eprint: 7155809.

[17] K. K. Chui, M. Jorge, S.-C. Yen, and M. M. Lusardi, eds. *Orthotics and prosthetics in rehabilitation*. Fourth edition. Chui, Kevin K, (editor.) Jorge, Milagros, (editor.) Yen, Sheng-Che, (editor.) Lusardi, Michelle M, (editor.) St. Louis Missouri: Elsevier, 2020. xiv, 817 pages. ISBN: 9780323609135.

[18] V. Creylman, I. Knippels, P. Janssen, E. Biesbrouck, K. Lechler, and L. Peeraer. "Assessment of transfemoral amputees using a passive microprocessor-controlled knee versus an active powered microprocessor-controlled knee for level walking". eng. In: *Biomedical engineering online* 15.Suppl 3 (2016). Journal Article, p. 142. DOI: 10.1186/s12938-016-0287-6. eprint: 28105945.

[19] M. Crochemore and R. Wojciech. *Text Algorithms*. Oxford University Press, 1994. 397 pp. ISBN: 0-19-508609-0.

[20] Y. Dabiri, S. Najarian, M. R. Eslami, S. Zahedi, and D. Moser. "A powered prosthetic knee joint inspired from musculoskeletal system". In: *Biocybernetics and Biomedical Engineering* 33.2 (2013). PII: S0208521613000053, pp. 118–124. ISSN: 02085216. DOI: 10.1016/j.bbe.2013.03.004.

[21] G. Das, D. Gunopulos, and H. Mannila. "Finding similar time series". In: *Principles of data mining and knowledge discovery. First European symposium, PKDD '97, Trondheim, Norway, June 24 - 27, 1997; proceedings*. Ed. by J. Komorowski. Vol. 1263. Lecture notes in computer science Lecture notes in artificial intelligence 1263. Berlin and Heidelberg: Springer, 1997, pp. 88–100. ISBN: 978-3-540-63223-8. DOI: 10.1007/3-540-63223-9_109.

[22] X. Drevelle, C. Villa, X. Bonnet, I. Loiret, P. Fode, and H. Pillet. “Vaulting quantification during level walking of transfemoral amputees”. eng. In: *Clinical biomechanics (Bristol, Avon)* 29.6 (2014). Journal Article Research Support, Non-U.S. Gov’t, pp. 679–683. DOI: 10.1016/j.clinbiomech.2014.04.006. eprint: 24835798.

[23] D. M. Ehde, D. G. Smith, J. M. Czerniecki, K. M. Campbell, D. M. Malchow, and L. R. Robinson. “Back pain as a secondary disability in persons with lower limb amputations”. eng. In: *Archives of physical medicine and rehabilitation* 82.6 (2001). Journal Article Multicenter Study Research Support, U.S. Gov’t, P.H.S., pp. 731–734. DOI: 10.1053/apmr.2001.21962. eprint: 11387575.

[24] T. Elery, S. Rezazadeh, E. Reznick, L. Gray, and R. D. Gregg. “Effects of a Powered Knee-Ankle Prosthesis on Amputee Hip Compensations: A Case Series”. eng. In: *IEEE transactions on neural systems and rehabilitation engineering : a publication of the IEEE Engineering in Medicine and Biology Society* 28.12 (2020), pp. 2944–2954. DOI: 10.1109/TNSRE.2020.3040260. eprint: 33232241.

[25] A. Ferrari, M. G. Benedetti, E. Pavan, C. Frigo, D. Bettinelli, M. Rabuffetti, P. Crenna, and A. Leardini. “Quantitative comparison of five current protocols in gait analysis”. eng. In: *Gait & Posture* 28.2 (2008). Comparative Study Journal Article Comparative Study Journal Article, pp. 207–216. ISSN: 0966-6362. DOI: 10.1016/j.gaitpost.2007.11.009. eprint: 18206374.

[26] F. R. FINLEY and P. V. KARPOVICH. “ELECTROGONIOMETRIC ANALYSIS OF NORMAL AND PATHOLOGICAL GAITS”. eng. In: *Research quarterly* 35 (1964). Journal Article, SUPPL:379–84. ISSN: 0034-5377. DOI: 10.1080/10671188.1964.10613327. eprint: 14276376.

[27] K. Friel, E. Domholdt, and D. G. Smith. “Physical and functional measures related to low back pain in individuals with lower-limb amputation: an exploratory pilot study”. eng. In: *Journal of rehabilitation research and development* 42.2 (2005). Comparative Study Journal Article, pp. 155–166. DOI: 10.1682/jrrd.2004.08.0090. eprint: 15944880.

[28] K. J. Friston. *Statistical parametric mapping. The analysis of funtional brain images*. 1st ed. Amsterdam and Boston: Elsevier/Academic Press, 2007. vii, 647. ISBN: 9780123725608.

[29] K. J. Friston. *Statistical parametric mapping. The analysis of funtional brain images*. 1st ed. Amsterdam and Boston: Elsevier/Academic Press, 2007. vii, 647. ISBN: 9780123725608.

[30] L. Frossard, L. Cheze, and R. Dumas. “Dynamic input to determine hip joint moments, power and work on the prosthetic limb of transfemoral amputees: ground reaction vs knee reaction”. eng. In: *Prosthetics and Orthotics International* 35.2 (2011), pp. 140–149. DOI: 10.1177/0309364611409002. eprint: 21697197.

[31] S. A. Fuenzalida Squella, A. Kannenberg, and A. Brandao Benetti. “Enhancement of a prosthetic knee with a microprocessor-controlled gait phase switch reduces falls and improves balance confidence and gait speed in community ambulators with unilateral transfemoral amputation”. eng. In: *Prosthetics and Orthotics International* 42.2 (2018). Comparative Study Journal Article, pp. 228–235. DOI: 10.1177/0309364617716207. eprint: 28691574.

[32] R. Gailey, K. Allen, J. Castles, J. Kucharik, and M. Roeder. “Review of secondary physical conditions associated with lower-limb amputation and long-term prosthesis use”. eng. In: *Journal of rehabilitation research and development* 45.1 (2008). Journal Article Review, pp. 15–29. DOI: 10.1682/jrrd.2006.11.0147. eprint: 18566923.

[33] Y. Geng, P. Yang, X. Xu, and L. Chen. "Design and simulation of Active Transfemoral Prosthesis". In: *2012 24th Chinese Control and Decision Conference (CCDC)*. 2012 24th Chinese Control and Decision Conference (CCDC). (Taiyuan, China, May 23–25, 2012). IEEE, 52012, pp. 3724–3728. ISBN: 978-1-4577-2074-1. DOI: 10.1109/CCDC.2012.6243095.

[34] S. Gerzeli, A. Torbica, and G. Fattore. "Cost utility analysis of knee prosthesis with complete microprocessor control (C-leg) compared with mechanical technology in transfemoral amputees". eng. In: *The European journal of health economics : HEPAC : health economics in prevention and care* 10.1 (2009). Comparative Study Journal Article Research Support, Non-U.S. Gov't, pp. 47–55. ISSN: 1618-7598. DOI: 10.1007/s10198-008-0102-9. eprint: 18379831.

[35] F. Gottschalk. "Transfemoral Amputation: Biomechanics and Surgery". In: *Clinical Orthopaedics and Related Research®* 361.April 1999 (1999), p. 15. ISSN: 0009-921X. URL: https://journals.lww.com/clinorthop/fulltext/1999/04000/transfemoral_amputation__biomechanics_and_surgery.3.aspx.

[36] B. J. Hafner and R. L. Askew. "Physical performance and self-report outcomes associated with use of passive, adaptive, and active prosthetic knees in persons with unilateral, transfemoral amputation: Randomized crossover trial". eng. In: *Journal of rehabilitation research and development* 52.6 (2015). Journal Article Randomized Controlled Trial Research Support, Non-U.S. Gov't, pp. 677–700. DOI: 10.1682/JRRD.2014.09.0210. eprint: 26560243.

[37] B. J. Hafner, L. L. Willingham, N. C. Buell, K. J. Allyn, and D. G. Smith. "Evaluation of function, performance, and preference as transfemoral amputees transition from mechanical to microprocessor control of the prosthetic knee". eng. In: *Archives of physical medicine and rehabilitation* 88.2 (2007). Controlled Clinical Trial Journal Article Research Support, Non-U.S. Gov't, pp. 207–217. DOI: 10.1016/j.apmr.2006.10.030. eprint: 17270519.

[38] S. Handke, G. Matthes, C. Hartz, and A. Ekkernkamp. "Oberschenkelamputation und prothetische Versorgung". In: *Trauma und Berufskrankheit* 4.2 (2002). PII: 603, pp. 266–273. ISSN: 1436-6274. DOI: 10.1007/s10039-002-0603-1.

[39] M. Hekmatfard, F. Farahmand, and I. Ebrahimi. "Effects of prosthetic mass distribution on the spatiotemporal characteristics and knee kinematics of transfemoral amputee locomotion". eng. In: *Gait & Posture* 37.1 (2013). Journal Article, pp. 78–81. ISSN: 0966-6362. DOI: 10.1016/j.gaitpost.2012.06.010. eprint: 22832472.

[40] J. P. Holden, J. A. Orsini, K. L. Siegel, T. M. Kepple, L. H. Gerber, and S. J. Stanhope. "Surface movement errors in shank kinematics and knee kinetics during gait". In: *Gait & Posture* 5.3 (1997). PII: S0966636296010880, pp. 217–227. ISSN: 0966-6362. DOI: 10.1016/S0966-6362(96)01088-0.

[41] T. Hortobágyi, N. J. Lambert, and J. P. Hill. "Greater cross education following training with muscle lengthening than shortening". eng. In: *Medicine and science in sports and exercise* 29.1 (1997). Journal Article Research Support, Non-U.S. Gov't Research Support, U.S. Gov't, P.H.S., pp. 107–112. ISSN: 0195-9131. DOI: 10.1097/00005768-199701000-00015. eprint: 9000162.

[42] S. M. Jaegers, J. H. Arendzen, and H. J. de Jongh. "Prosthetic gait of unilateral transfemoral amputees: A kinematic study". In: *Archives of physical medicine and rehabilitation* 76.8 (1995). PII: S0003999395805281, pp. 736–743. DOI: 10.1016/S0003-9993(95)80528-1.

[43] D. Jarchi, J. Pope, T. K. M. Lee, L. Tamjidi, A. Mirzaei, and S. Sanei. “A Review on Accelerometry-Based Gait Analysis and Emerging Clinical Applications”. eng. In: *IEEE reviews in biomedical engineering* 11 (2018). Journal Article Review, pp. 177–194. DOI: 10.1109/RBME.2018.2807182. eprint: 29994786.

[44] K. J. Worsley, A. C. Evans, S. Marrett, and and P. Neelin. “A Three-Dimensional Statistical Analysis for CBF Activation Studies in Human Brain”. In: *Journal of Cerebral Blood Flow and Metabolism* 1992 ().

[45] P. Kampas, M. Bellmann, and A. Weigl-Pollack. “Das neue C-Leg und seine erweiterten Funktionen”. In: (2011).

[46] P. Kampas, T. Hofmann, M. Mileusnic, E. Gonzalez, and G. Scheider. “Die neuen "Genium"-Kniegelenke - Funktionserweiterung zur Erhoehung des Anwendernutzens”. In: *Orthopaedie Technik* 2018.11 (2018). URL: https://www.wortmann-beyle-sanitaetshaus.de/wp-content/uploads/2020/09/Klinische-Studie-1.pdf (visited on 01/17/2022).

[47] P. Kampas and D. Seifert. “Das neue C-Leg: neue Funktionen und neue Technologie”. In: *Orthopaedie Technik* 2015.10 (2015). URL: https://www.ottobock.de/media/lokale-medien-de_de/prothetik/beinprothetik/files/646d1079-de.pdf (visited on 01/17/2022).

[48] P. Kampas and M. Seyr. “Technologie und Funktionsweise des Genium-Prothesenkniegelenks”. In: *Orthopaedie Technik* (2011).

[49] A. O. Kapti and M. S. Yucenur. “Design and control of an active artificial knee joint”. In: *Mechanism and Machine Theory* 41.12 (2006). PII: S0094114X06000243, pp. 1477–1485. ISSN: 0094114X. DOI: 10.1016/j.mechmachtheory.2006.01.017.

[50] K. R. Kaufman, S. Frittoli, and C. A. Frigo. “Gait asymmetry of transfemoral amputees using mechanical and microprocessor-controlled prosthetic knees”. eng. In: *Clinical biomechanics (Bristol, Avon)* 27.5 (2012). Clinical Trial Journal Article Research Support, N.I.H., Extramural, pp. 460–465. DOI: 10.1016/j.clinbiomech.2011.11.011. eprint: 22221344.

[51] S. Keeratihattayakorn, C. Virulsri, C. Ophaswongse, and P. Tangpornprasert. “Design and evaluation of a hydraulic mechanism with available components for passive knee prostheses”. In: *Disability and Rehabilitation: Assistive Technology* 16.2 (2021), pp. 144–151. ISSN: 1748-3107. DOI: 10.1080/17483107.2019.1642396.

[52] J. A. Kent, V. N. M. Arelekatti, N. T. Petelina, W. B. Johnson, J. T. Brinkmann, A. G. Winter, and M. J. Major. “Knee Swing Phase Flexion Resistance Affects Several Key Features of Leg Swing Important to Safe Transfemoral Prosthetic Gait”. eng. In: *IEEE transactions on neural systems and rehabilitation engineering : a publication of the IEEE Engineering in Medicine and Biology Society* 29 (2021). Journal Article Research Support, N.I.H., Extramural Research Support, U.S. Gov’t, Non-P.H.S., pp. 965–973. DOI: 10.1109/TNSRE.2021.3082459. eprint: 34018934.

[53] E. Keogh and C. A. Ratanamahatana. “Exact indexing of dynamic time warping”. In: *Knowledge and Information Systems* 7.3 (2005). PII: 154, pp. 358–386. ISSN: 0219-1377. DOI: 10.1007/s10115-004-0154-9.

[54] C. Kirtley. *Clinical gait analysis*. eng. Edinburgh and New York: Elsevier, 2006. 316 pp. ISBN: 9780702036712.

[55] T. Kobayashi, M. Hu, R. Amma, G. Hisano, H. Murata, D. Ichimura, and H. Hobara. “Effects of walking speed on magnitude and symmetry of ground reaction forces in individuals with transfemoral prosthesis”. eng. In: *Journal of Biomechanics* 130 (2022). Journal Article, p. 110845. ISSN: 00219290. DOI: 10.1016/j.jbiomech.2021.110845. eprint: 34749160.

[56] J. Kulkarni, J. Adams, E. Thomas, and A. Silman. "Association between amputation, arthritis and osteopenia in British male war veterans with major lower limb amputations". eng. In: *Clinical rehabilitation* 12.4 (1998). Journal Article Research Support, Non-U.S. Gov't Journal Article Research Support, Non-U.S. Gov't, pp. 348–353. ISSN: 0269-2155. DOI: 10.1191/026921598672393611. eprint: 9744670.

[57] P. K. Kumar, M. Charan, and S. Kanagaraj. "Trends and Challenges in Lower Limb Prosthesis". In: *IEEE Potentials* 36.1 (2017), pp. 19–23. ISSN: 0278-6648. DOI: 10.1109/MPOT.2016.2614756.

[58] B. E. Lawson, J. Mitchell, D. Truex, A. Shultz, E. Ledoux, and M. Goldfarb. "A Robotic Leg Prosthesis: Design, Control, and Implementation". In: *IEEE Robotics & Automation Magazine* 21.4 (2014), pp. 70–81. ISSN: 1070-9932. DOI: 10.1109/MRA.2014.2360303.

[59] B. E. Lawson, B. Ruhe, A. Shultz, and M. Goldfarb. "A powered prosthetic intervention for bilateral transfemoral amputees". eng. In: *IEEE transactions on bio-medical engineering* 62.4 (2015). Journal Article Research Support, N.I.H., Extramural, pp. 1042–1050. DOI: 10.1109/TBME.2014.2334616. eprint: 25014950.

[60] T. Liu, Y. Inoue, and K. Shibata. "Development of a wearable sensor system for quantitative gait analysis". In: *Measurement* 42.7 (2009). PII: S0263224109000372, pp. 978–988. ISSN: 02632241. DOI: 10.1016/j.measurement.2009.02.002.

[61] M. Lilja, T. Johansson, and T. Oeberg. "Movement of the tibial end in a PTB prosthesis socket: A sagittal X-ray study of the PTB prosthesis". In: ().

[62] E. C. Martinez-Villalpando and H. Herr. "Agonist-antagonist active knee prosthesis: A preliminary study in level-ground walking". In: *The Journal of Rehabilitation Research and Development* 46.3 (2009), p. 361. ISSN: 0748-7711. DOI: 10.1682/JRRD.2008.09.0131.

[63] J. W. Michael. "Modern_Prosthetic_Knee_Mechanisms.6". In: *Clinical orthopaedics and related research* 1999 (). ISSN: 0009-921X.

[64] A. Muro-de-la-Herran, B. Garcia-Zapirain, and A. Mendez-Zorrilla. "Gait analysis methods: an overview of wearable and non-wearable systems, highlighting clinical applications". eng. In: *Sensors (Basel, Switzerland)* 14.2 (2014). Journal Article Research Support, Non-U.S. Gov't, pp. 3362–3394. DOI: 10.3390/s140203362. eprint: 24556672.

[65] M. P. Murray, S. B. Sepic, G. M. Gardner, and L. A. Mollinger. "Gait patterns of above-knee amputees using constant-friction knee components". eng. In: *Bulletin of prosthetics research* 10-34 (1980). Journal Article Research Support, U.S. Gov't, Non-P.H.S. Research Support, U.S. Gov't, P.H.S., pp. 35–45. ISSN: 0007-506X. eprint: 7260459. URL: https://pubmed.ncbi.nlm.nih.gov/7260459/.

[66] Y. S. Narang and A. G. Winter. "Effects of Prosthesis Mass on Hip Energetics, Prosthetic Knee Torque, and Prosthetic Knee Stiffness and Damping Parameters Required for Trans-femoral Amputees to Walk With Normative Kinematics". In: *Volume 5A: 38th Mechanisms*. DOI: 10.1115/DETC2014-35065.

[67] L. Nolan and A. Lees. "The functional demands on the intact limb during walking for active trans-femoral and trans-tibial amputees". eng. In: *Prosthetics and Orthotics International* 24.2 (2000). Clinical Trial Comparative Study Controlled Clinical Trial Journal Article, pp. 117–125. DOI: 10.1080/03093640008726534. eprint: 11061198.

[68] L. Nolan, A. Wit, K. Dudzinski, A. Lees, M. Lake, and M. Wychowanski. "Adjustments in gait symmetry with walking speed in trans-femoral and trans-tibial amputees". In: *Gait & Posture* 17.2 (2003). PII: S0966636202000668, pp. 142–151. ISSN: 0966-6362. DOI: 10.1016/S0966-6362(02)00066-8.

[69] V. Oesterreich. *Fuesse sind das am haeufigsten genutzte Verkehrsmittel*. 2021. URL: https://www.vcoe.at/files/vcoe/uploads/Infografiken/Mobilitaet%20Allgemein/F%C3%BC%C3%9Fe%20sind%20das%20am%20h%C3%A4ufigsten%20genutzte%20Verkehrsmittel.jpg (visited on 11/12/2021).

[70] V. Oesterreich. *Oesterreichs Bevoelkerung ist vielfaeltig mobil*. 2020. URL: https://www.vcoe.at/files/vcoe/uploads/Infografiken/Mobilitaet%20Allgemein/%C3%96sterreichs%20Bev%C3%B6lkerung%20ist%20vielseitig%20mobil.png (visited on 11/12/2021).

[71] "Outcomes_Associated_with_the_Use_of.2". In: ().

[72] T. C. Pataky. "Generalized n-dimensional biomechanical field analysis using statistical parametric mapping". eng. In: *Journal of Biomechanics* 43.10 (2010). Journal Article Research Support, Non-U.S. Gov't, pp. 1976–1982. ISSN: 00219290. DOI: 10.1016/j.jbiomech.2010.03.008. eprint: 20434726.

[73] T. C. Pataky. "One-dimensional statistical parametric mapping in Python". eng. In: *Computer methods in biomechanics and biomedical engineering* 15.3 (2012). Journal Article Research Support, Non-U.S. Gov't, pp. 295–301. DOI: 10.1080/10255842.2010.527837. eprint: 21756121.

[74] L. Paterno, M. Ibrahimi, E. Gruppioni, A. Menciassi, and L. Ricotti. "Sockets for Limb Prostheses: A Review of Existing Technologies and Open Challenges". eng. In: *IEEE transactions on bio-medical engineering* 65.9 (2018). Journal Article Research Support, Non-U.S. Gov't, pp. 1996–2010. DOI: 10.1109/TBME.2017.2775100. eprint: 29993506.

[75] J. Perry. *Gait analysis. Normal and pathological function*. eng. Thorofare, NJ: Slack, 1992. 524 pp. ISBN: 1556421923.

[76] A. O. Petersen, J. Comins, and T. Alkjaer. "Assessment of Gait Symmetry in Transfemoral Amputees Using C-Leg Compared With 3R60 Prosthetic Knees". In: *JPO Journal of Prosthetics and Orthotics* 22.2 (2010), pp. 106–112. ISSN: 1040-8800. DOI: 10.1097/JPO.0b013e3181ccc986.

[77] M. Rabuffetti, M. Recalcati, and M. Ferrarin. "Trans-femoral amputee gait: socket-pelvis constraints and compensation strategies". eng. In: *Prosthetics and Orthotics International* 29.2 (2005). Journal Article, pp. 183–192. DOI: 10.1080/03093640500217182. eprint: 16281727.

[78] C. W. Radcliffe. "Above-knee prosthetics". In: ().

[79] A. A. Rodriguez, P. O. Black, K. Kile, J. Sherman, B. Stellberg, J. McCormick, J. Roszkoswki, and Swiggum Eileen. "Gait Training Effiacacy Using a Home-Based Practice Model in Chronic Hemiplegia". In: *Archives of physical medicine and rehabilitation* 1996 ().

[80] P. Roland. *Vorlesung Beinprothesen - Grundlagen und Stand der Technik Vortrag - Vorlesung Mechanische Konzepte der Prothetik und Rehabilitation*. Technische Universitat Wien, 2020.

[81] G. K. Rose. "Clinical gait assessment: a personal view". eng. In: *Journal of medical engineering & technology* 7.6 (1983). Journal Article, pp. 273–279. ISSN: 0309-1902. DOI: 10.3109/03091908309018174. eprint: 6668589.

[82] E. Russell Esposito, J. M. Aldridge Whitehead, and J. M. Wilken. "Sound limb loading in individuals with unilateral transfemoral amputation across a range of walking velocities". eng. In: *Clinical biomechanics (Bristol, Avon)* 30.10 (2015). Journal Article Research Support, U.S. Gov't, Non-P.H.S., pp. 1049–1055. DOI: 10.1016/j.clinbiomech.2015.09.008. eprint: 26412015.

[83] E. Russell Esposito and J. M. Wilken. "The relationship between pelvis-trunk coordination and low back pain in individuals with transfemoral amputations". eng. In: *Gait & Posture* 40.4 (2014). Journal Article Research Support, Non-U.S. Gov't, pp. 640–646. ISSN: 0966-6362. DOI: 10.1016/j.gaitpost.2014.07.019. eprint: 25155692.

[84] A. A. Salah and T. Gevers. *Computer Analysis of Human Behavior*. London: Springer London, 2011. 412 pp. ISBN: 978-0-85729-993-2. DOI: 10.1007/978-0-85729-994-9.

[85] M. Saleh and G. Murdoch. "In defence of gait analysis. Observation and measurement in gait assessment". In: *Journal of Bone and Joint Surgery* 1985.67 (), pp. 237–241.

[86] T. Schmalz, S. Blumentritt, and R. Jarasch. "Energy expenditure and biomechanical characteristics of lower limb amputee gait". In: *Gait & Posture* 16.3 (2002). PII: S0966636202000085, pp. 255–263. ISSN: 0966-6362.

[87] A. D. Segal, M. S. Orendurff, G. K. Klute, M. L. McDowell, J. A. Pecoraro, J. Shofer, and J. M. Czerniecki. "Kinematic and kinetic comparisons of transfemoral amputee gait using C-Leg and Mauch SNS prosthetic knees". eng. In: *Journal of rehabilitation research and development* 43.7 (2006). Journal Article Randomized Controlled Trial Research Support, U.S. Gov't, Non-P.H.S., pp. 857–870. DOI: 10.1682/jrrd.2005.09.0147. eprint: 17436172.

[88] R. E. Seroussi, A. Gitter, J. M. Czerniecki, and K. Weaver. "Mechanical Work Adaptions of Above-Knee Amputee Ambulation". In: *Archives of physical medicine and rehabilitation* 1996.77 (), pp. 1209–1213.

[89] H. B. Skinner and D. J. Effeney. "Gait analysis in amputees". eng. In: *American journal of physical medicine* 64.2 (1985). Comparative Study Journal Article Research Support, U.S. Gov't, Non-P.H.S. Review Comparative Study Journal Article Research Support, U.S. Gov't, Non-P.H.S. Review, pp. 82–89. ISSN: 0002-9491. eprint: 3887934.

[90] J. Uchytil, D. Jandacka, D. Zahradnik, R. Farana, and M. Janura. "Temporal-spatial parameters of gait in transfemoral amputees: Comparison of bionic and mechanically passive knee joints". eng. In: *Prosthetics and Orthotics International* 38.3 (2014). Comparative Study Journal Article Research Support, Non-U.S. Gov't, pp. 199–203. DOI: 10.1177/0309364613492789. eprint: 23824546.

[91] H. Warner, P. Khalaf, H. Richter, D. Simon, E. Hardin, and A. J. van den Bogert. "Early evaluation of a powered transfemoral prosthesis with force-modulated impedance control and energy regeneration". eng. In: *Medical engineering & physics* 100 (2022). Journal Article, p. 103744. DOI: 10.1016/j.medengphy.2021.103744. eprint: 35144731.

[92] R. L. Waters, J. Perry, D. Antonelli, and H. Hislop. "Energy cost of walking of amputees: the influence of level of amputation". In: *Journal of Bone and Joint Surgery* 1976 (), pp. 42–46.

[93] E. C. Wentink, V. G. H. Schut, E. C. Prinsen, J. S. Rietman, and P. H. Veltink. "Detection of the onset of gait initiation using kinematic sensors and EMG in transfemoral amputees". eng. In: *Gait & Posture* 39.1 (2014). Journal Article Research Support, Non-U.S. Gov't, pp. 391–396. ISSN: 0966-6362. DOI: 10.1016/j.gaitpost.2013.08.008. eprint: 24001871.

[94] M. W. Whittle. *Gait analysis. An introduction*. eng. 4th ed., reprinted. Edinburgh: Butterworth-Heinemann Elsevier, 2008. 255 pp. ISBN: 0750688831.

[95] D. A. Winter. *Biomechanics and motor control of human movement*. 4th ed. Hoboken N.J.: Wiley, 2009. xiv, 370. ISBN: 9780470398180.

[96] D. A. Winter. “Moments of force and mechanical power in jogging”. In: *Journal of Biomechanics* 16.1 (1983). PII: 0021929083900507, pp. 91–97. ISSN: 00219290. DOI: 10.1016/0021-9290(83)90050-7.

[97] D. A. Winter and S. E. Sienko. “Biomechanics of below-knee amputee gait”. In: *Journal of Biomechanics* 21.5 (1988). PII: 002192908890142X, pp. 361–367. ISSN: 00219290. DOI: 10.1016/0021-9290(88)90142-X.

[98] W. Zijlstra, A. W. Rutgers, A. L. Hof, and T. W. van Weerden. “Voluntary and involuntary adaptation of walking to temporal and spatial constraints”. In: *Gait & Posture* 3.1 (1995). PII: 0966636295908042, pp. 13–18. ISSN: 0966-6362. DOI: 10.1016/0966-6362(95)90804-2.

[99] Zuniga en, Leavitt LA, Calvert JC, Canzoneri J, and Peterson CR. *GAIT PATTERNS IN ABOVE-KNE AMPUTEES*. 1972. URL: https://pascal-francis.inist.fr/vibad/index.php?action=getrecorddetail&idt=pascal733572575.